ALLOSTERIC COMMUNICATION IN BINDING DOMAIN OF NICOTINIC ACETYLCHOLINE RECEPTOR

By
Levent TUNA
B.S., Chemical Engineering, Ege University 2003

Submitted to the Institute for Graduate Studies in
Science and Engineering in partial fulfillment of
the requirements for the degree of
Master of Science

Graduate Program in Chemical Engineering
Boğaziçi University
2006

ACKNOWLEDGEMENT

First, I thank my thesis supervisor Prof. Dr. Türkan HALİLOĞLU for her continuous and invaluable support. It was a great pleasure for me to be her student and study with her. Without her inspiring and thoughtful guidance I would have been lost in protein world.

I would also like to thank Asst. Prof. Şefika Banu ÖZKAN for not withholding her ideas and comments from me. Her gold worth recommendations helped me develop my thesis.

I thank Serkan KARADAĞ for all the support during the period of my work. I am greatly indebted to his great ability to solve any unsolvable problems concerning this thesis.

Besides my advisor, I would like to thank my capable and conscientious committee members: Prof. Dr. Viktorya AVIYENTE and Asst. Prof. Şefika Banu ÖZKAN for spending time on reading and evaluating my thesis.

Heavy Metal music, specially the band called MANOWAR has always been the best inspiration factor for me. Whenever I turned on the music, it reduced my stress and helped me work smoothly towards my thesis.

Last, but not least, I thank my family for their unconditional support and encouragement to complete this thesis. My father's instillation on making masters degree and my mother's never-ending support and effort to arrange me a better working environment made this thesis possible.

ABSTRACT

ALLOSTERIC COMMUNICATION IN BINDING DOMAIN OF NICOTINITIC ACETHYCHOLINE RECEPTOR

Allosteric interactions have been thought to be of great importance in regulating the gating mechanism of the receptors. The term *allostery* comes from the Greek words *allos*, "other," and *stereos*, "shape", meaning that action in one part of the molecule causes an effect at another site. Acetylcholine has been one of the first identified neurotransmitters. It is a chemical transmitter existing in the nervous system of many organisms including humans. In this work, allostery and allosteric pathways in the information transmission between Acetylcholine binding and the gate regions have been studied on three structures. These three structures are Acetylcholine Binding Protein, nicotinic Acetylcholine Receptor and the Ligand Binding Domain of nicotinic Acetylcholine Receptor without the transmembrane region. For this, combined computational methodologies have been employed. In understanding of the allostery; Gaussian Network Model (GNM) and Anisotropic Network (ANM) have been performed to study the fluctuations of residues and the correlation between them in various modes of motion. The results of the correlation analysis by GNM are elaborated using MCPOOL program. MCPOOL identifies allosteric pathways between a starting and a selected target region. These regions have been examined with respect to the dynamic mode shapes of GNM and ANM analyses and the conservation and the correlated mutational analysis. ANM has been applied to see three dimensional conformational changes of molecule in different modes. Changes in diameter of gate region in different modes of motion have been presented by HOLE program. Results suggest that Loop 2, Cys Loop and Loop 9 are mostly visited regions in the allosteric communications, which agree with experimental results and also suggest new regions that might be important. These regions overlap with the minimum points of the slowest mode shapes. The conservation and correlated mutations analyses shows that some of the mostly visited residues along the paths are either conserved or correlated during the evolution. The presence of the transmembrane domain in the calculations contributes to the pathways and the motion of the structure. Indeed, without the transmembrane regions, the ligand binding domain can not lead to a conformational change which contributes to the twisting motion of the receptor, which is an essential movement for the gating mechanism.

ÖZET

NİKOTİNİK ASETİLKOLİN RESEPTÖRLERİNİN HÜCREDIŞI BÖLÜMLERİNDEKİ ALLOSTERİK ETKİLEŞİMLER

Uzaktan etkileşimlerin reseptör kanallarının açılmasında büyük bir önemi olduğu düşünülmektedir. Allostery kelimesi molekülün bir tarafındaki etkinin molekülün bir başka yerine etki etmesi anlamına gelmektedir ve latincedeki allo "öteki" ve stereo "şekil" kelimelerinden türemiştir. Asetilkolin tanımlanmış ilk sinir hücreleri arası iletkendir. İnsanlar da dahil birçok organizmanın sinir sistemlerinde bulunurlar. Bu tezde asetilkolinin bağlandığı bölge ile kanalın en dar yeri arasındaki allosterik etkileşmiler incelenmiştir. Bu incelemeler asetilkolin bağlanma protein'i, nikotinik asetilkolin reseptörleri ve bu reseptörlerin hücre dışı kısımları için ayrı ayrı yapılmıştır. Bunun için bazı bilgisayarlı metotlar kullanılmıştır. Her aminoasitin birbirleri ile olan etkileşimlerini anlayabilmek için her üç yapıya da Gaussian ağ modeli (GNM) ve anizotropik ağ modeli (ANM) uygulandı. Bu etkileşimler MCPOOL isimli program ile analiz edildi. MCPOOL isteğe göre belirlenen iki bölge arasında yollar türeten ve bu bölgeler arasındaki uzaktan etkileşimleri gösteren bir programdır. Bu bölgelerin GNM ve ANM'in dinamik modlarında nerelere denk geldiklerine bakıldı. Bu bölgeler ayrıca korunmuşmu yoksa evrim boyunca mutasyona uğramışmı diye kontrol edildi. Yapıların üç boyutlu yer değişimlerini incelemek için ANM programı kullanıldı. Her üç molekül için de farklı modlardaki hareketler incelendi. Bu hareketler sonrasında kanalın açılıp açılmadığını anlamak için HOLE isimli program kullanıldı. Bütün sonuçlara göre Loop 2, Cys Loop ve Loop 9 bölgeleri allosterik etkileşimlerde en çok kullanılan yerler olarak görüldü ki buda daha önce yapılmış olan çalışmalarla örtüşmektedir. Bunların yanısıra bazı farklı bölgeler de önemli olarak görülmüştür. Bu bölgeler en yavaş hareketlerin olduğu modlarda minimum noktalarına karşılık gelmektedir. Korunmuşluk ve mutasyona uğrayıp uğramadıklarını incelemek için yapılan analizlerin sonucunda görülmüştürki allosterik etkileşimde önemli rol oynayan bölgelerin veya aminoasitlerin bir kısmı ya korunmuş yada mutasyona uğramış olarak göze çarpmaktadır. Hücre duvarı bölgesinin bulunması kanalın açılımı hakkında bazı yararlı bilgiler vermiştir. Hücre duvarı bölgesi olmadığı takdirde hücre dışı bölümü kendi başına kanalın açılmasını sağlayan dönme hareketini gösterememektedir.

TABLE OF CONTENTS

LIST OF FIGURES

LIST OF TABLES

LIST OF SYMBOLS / ABBREVIATIONS

C (i, j)	Normalized cross correlation function
gn	Minimum separation between residues
H	Internal hamiltonian
H	Hessian matrix
h	Elements of Hessian matrix
i	Residue index
j	Residue index
k	Residue index
k_B	Boltzmann constant
N	Number of residues
r_c	Cut off distance
T	Absolute temperature
u	Matrix containing eigenvectors
V	Potential function
W	Gaussian distribution function
Z	Sum of cross correlation values for possible pairs
ZN	Configurational integral
α	Alpha subunit
αγ	Alpha gamma subunit
αδ	Alpha delta subunit
β	Beta subunit
γ	Gamma subunit, and Hookean force constant
Γ	Kirchoff matrix
δ	Delta subunit
ε	Epsilon subunit
λ	Eigenvalue
3D	Three dimensional
5HT3	Subtype 3 of the 5-hydroxytryptamine

A	Alanine
ACh	Acetylcholine
AChBP	Acetylcholine binding protein
Ala	Alanine
ANM	Anisotropic network model
Arg	Arginine
Asn	Asparagine
Asp	Aspartic acid (Aspartate)
B10	Beta 10
C	Cysteine
CMA	Correlated mutation analysis
CMS	Congenital myasthenic syndrome
Cys	Cysteine
D	Aspartic acid (Aspartate)
DPPC	dipalmitoylphosphatidylcholine
E	Glutamic acid
F	Phenylalanine
G	Glycine
$GABA_A$	Gamma-amino butyric acid receptor type A
Gln	Glutamine acid (Glutamate)
Glu	Glutamic acid
Gly	Glycine
GNM	Gaussian network model
H	Histidine
His	Histidine
I	Isoleucine
Ile	Isoleucine
K	Lysine
L	Leucine
LBD	Ligand binding domain
Leu	Leucine
LGIC	Ligand gated ion channel
Lys	Lysine
M	Methionine

MD	Molecular dynamics
Met	Methionine
N	Asparagine
nAChR	Nicotinic Acetylcholine Receptor
P	Proline
PDB	Protein Data Bank
Phe	Phenylalanine
Pro	Proline
Q	Glutamine acid (Glutamate)
R	Arginine
S	Serine
Ser	Serine
T	Threonine
Thr	Threonine
TMD	Transmembrane domain
Trp	Tryptophan
Tyr	Tyrosine
V	Valine
Val	Valine
W	Tryptophan
Y	Tyrosine

1. INTRODUCTION

Nicotinic acetylcholine receptors (nAChR) are neurotransmitter receptors that function as transducers of various signals [1]. These receptors reside at the neuromuscular junctions, autonomic ganglia and at various sites in the central nervous system [2].These receptors are members of ligand gated ion channels (LGIC) where they mediate a rapid chemical transmission of electrical signals between nerve and muscle cells by opening a narrow path in response to the release of Acetylcholine (Ach) into the synaptic cleft [3].

Since all of the members of LGIC's contain disulphide bonded cystein residues in their extracellular domains, these LGIC's are also called as Cys-Loop receptors [4]. Some other members of LGIC superfamily are $GABA_A$ (Gamma-Amino Butyric Acid receptor type A), glycine receptors and serotonin (subtype 3 of the 5-hydroxytryptamine $5HT_3$) and [5]. Within the LGIC superfamily, the nAChR and $5HT_3$ are cation-selective channels while $GABA_A$ and glycine are anion-selective channels [6].

nAChR consists of five homologous subunits (α_2, β, δ, γ or ε) and contains three distinct domains which are called the ligand binding domain (LBD), transmembrane domain (TMD) and the intracellular domain (ID) (Figure 1.1). Each subunit is composed of around 370 residues and the length of the molecule from the top to the bottom is around 150 Å.

This thesis covers the analysis of three different molecules which are the nAChR of the electric organ of Torpedo Marmorata (PDB: 2bg9) [7], ligand binding domain of nAChR without the transmembrane domain, and the Acetylcholine Binding Protein (AChBP) (PDB: 1i9b) [8].

In the beginning of this thesis the full structure of nAChR didn't exist and the analyses had been made on AChBP. Later with the release of the full structure of nAChR, full structure has been analyzed. To see the differences and the similarities between AChBP and the LBD of nAChR, the LBD of nAChR is extracted from the full structure and considered to be an isolated structure, the third molecule. All of the analyses are made on these three structures which are AChBP, the full structure of nAChR and the LBD of nAChR.

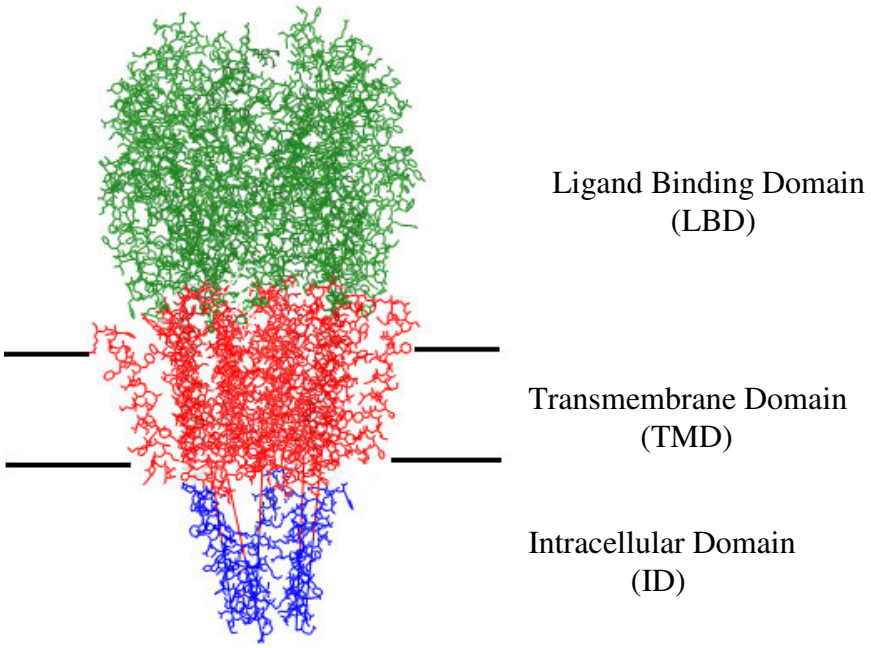

Figure 1.1. Graphical representation of nAChR from Torpedo Marmorata (PDB code: 2bg9). Green: Ligand binding domain (extracellular half), Red: Transmembrane Domain, Blue: Intracellular Domain [7].

Before the public release of the full structure of nAChR (PDB: 2bg9), AChBP (PDB: 1i9b) was supposed to be the extracellular domain of the Transmembrane Domain of nAChR since the actual extracellular half of the molecule was not resolved. Until the 3-D structure of nAChR is resolved, AChBP was analyzed as LBD of TMD of Torpedo Marmorata (PDB: 1OED) [9].

There is a great difference between the LBD of nAChR and AChBP. AChBP is formed by five identical subunits which makes it a homopentamer, while the subunits of LBD of nAChR are not identical. Another difference is that LBD of nAChR has got two binding pockets while AChBP contains five binding pockets which are located at the interfaces of subunbits at the extracellular domain.

1.1. Structure

1.1.1. Structure of AChBP (PDB: 1i9b)

Acetylcholine binding protein (AChBP) is a water-soluble protein with high similarity to the extracellular domains of ligand-gated ion channels. The protein is secreted from glial cells in the fresh-water snail, *Lymnaea Stagnalis,* from European fresh waters, where it modulates neuronal transmission [8]. It is composed of 5 homolog subunits and each subunit consists of 205 residues. AChBP is a homolog of the ligand binding domain of the pentameric ligand-gated ion-channels.

In the pentamer the only subunit contacts are at dimer interfaces. Each AChBP protomer consists of an α helix, two short 3_{10} helices, a core of twelve β-strands and twelve loops connecting the β-strands. In the ion channels, the transmembrane domains are at the bottom of the AChBP structure, starting at the end of β-strand β10. The upper part of the molecule is called N-termini and the lower part is called C-termini. In the LGICs the TMD lies at the end of the Beta 10 where it ends at the C-termini [8].

The alignment of the subunits along the AChBP molecule is shown in Figure 1.2.

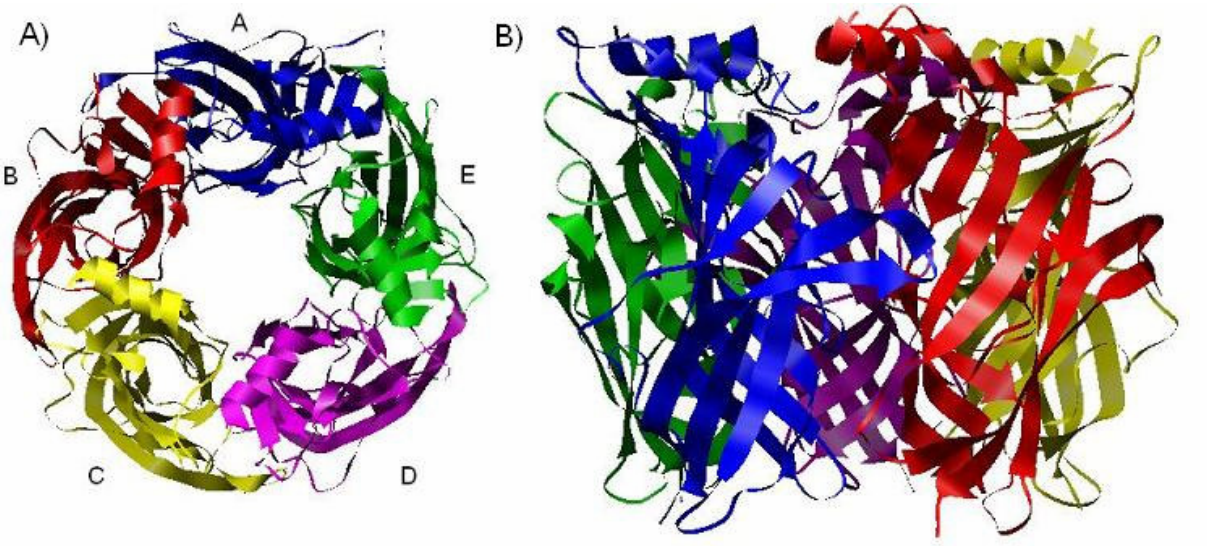

Figure 1.2. A) View of the AChBP from the top of the extracellular side, B) View of the AChBP from perpendicular to the pore axis.

There are many charged residues in the central pore of the pentamer which makes the central pore to be hydrophilic. On the subunit-subunit interfaces, there are cavities which are lined with the residues that are thought to be involved in the ligand binding. This region which is supposed to be the ligand binding sites of the molecule is about 30Å away from the C-termini. [8]

There are two types of binding residues which are called as the principle binding residues (TYR89, TRP143, HIS145, TYR185, CYS187, CYS188 and TYR192) corresponding to the loops, and the complementary binding residues (TRP53, GLN55, ARG104, VAL106, LEU112 and MET114) corresponding to the beta strands [8]. These binding residues are shown on Figure 1.3. The residues and corresponding regions of AChBP are given in APPENDIX A Table A.1.

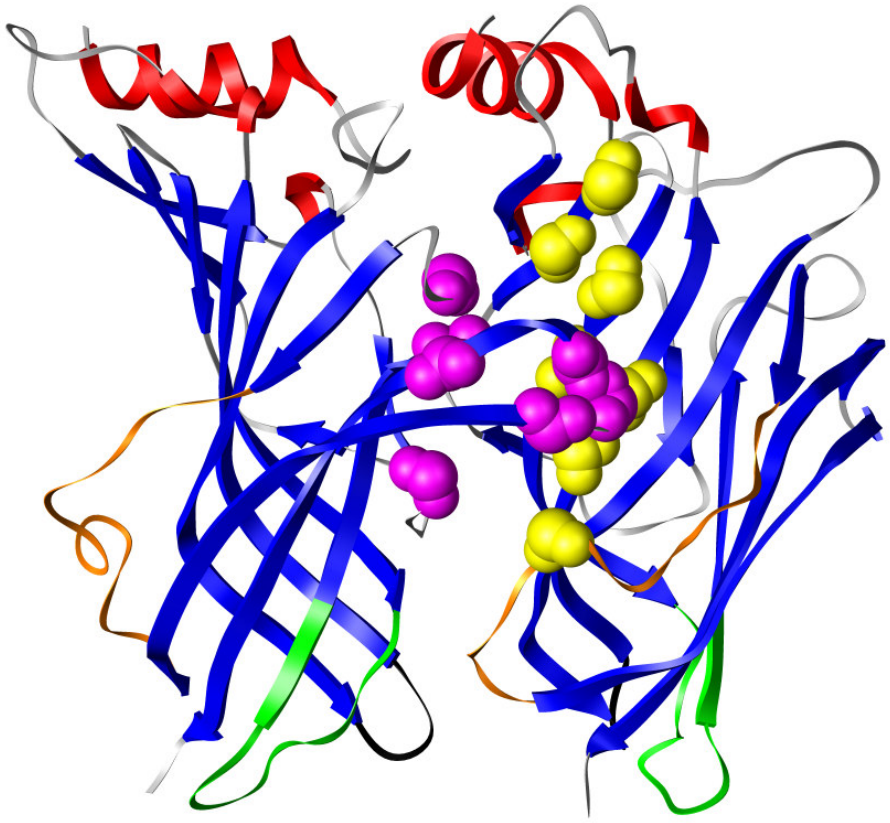

Figure 1.3. Representation of important regions of AChBP. Red: Alpha Helices, Blue: Beta Strands, Green: Cys Loop, Black: Loop2, Orange: Loop9, Magenta Balls: Primary Binding Site Residues, Yellow Balls: Complementary Binding Site Residues.

There is a Cys-Loop region in the molecule which lies between two disulphide bonded cysteine residues. This Cys-Loop is well conserved in the LGIC superfamily but not in AChBP. This Cys-Loop region is hydrophobic in the LGIC superfamily and it is located at the C-termini of the AChBP. Also this Cys-Loop region is located at the bottom of the LBD of receptors. This position of Cys-Loop and its hydrophobicity in the LGIC family may play a key role in the gating mechanism if a transmembrane domain exists and hence it may interact with TMD of the receptor.

1.1.2. Structure of nAChR (PDB: 2bg9)

The structure of nAChR of Torpedo Marmorata (PDB: 2bg9) is the closed structure of the receptor. nAChR consists of a beta subunit, a delta subunit, a gamma subunit and two identical alpha subunits (alpha-gamma & alpha-delta) which are named according to the neighbor with whom it makes a binding interface. All of these five homologous subunits are composed of approximately 370 residues and contain a LBD, a TMD and an ID.

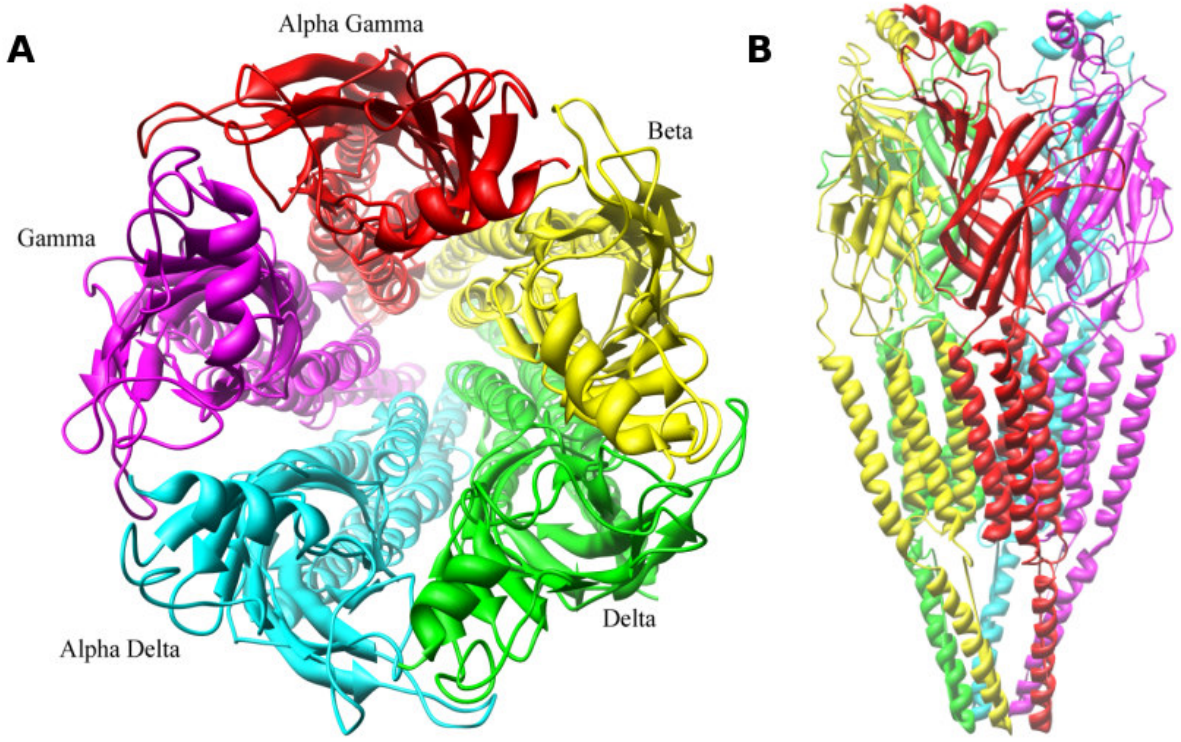

Figure 1.4. (A) A view of nAChR from the extracellular side. (B) A view of nAChR from membrane side. Red: Alpha-Gamma, Yellow: Beta, Green: Delta, Cyan: Alpha-Delta, Magenta: Gamma.

All subunits have a beta sheet dominated structure at the LBD and alpha-helix dominated structure at the TMD. The LBD consists of twelve beta sheets, twelve loops connecting these beta sheets and an alpha-helix segment at the N-termini. Residues belonging to the TMD come after the last residue of LBD where LBD and TMD are connected covalently.

The signature loop of LGICs, the cys loop, resides at the interface of ligand binding and transmembrane domains, along with the loop 2 (between beta1 and beta2). Another loop near the interface between the domains is the loop 9 which connects beta8 to beta9 [10]. There are two binding sites for ACh. These are located between the alpha subunits and their neighbours (alpha gamma–gamma, alpha delta–delta). The binding loop is formed by loop A (loop 5), loop B (loop 8), and loop C (loop 10) of alpha subunits and the Beta5 and Beta6 of adjacent subunits (gamma or delta) [7] but the main binding occurs on the Loop A, Loop B and Loop C regions of the LBDs of the alpha subunits.

The structure of the Alpha-Gamma subunit of the nAChR is given in Figure 1.5.

TMD of each subunit consists of four alpha-helical segments which are called M1, M2, M3 and M4. M2 is in the inner side of the TMD and forms the lumen of the pore [10, 6]. M4 is at the outer part of the TMD and it has contacts with the lipid. The other two alpha-helices M1 and M3 also have contacts with the lipid but not as much as M4 [10, 11, 12].

There is a gate region in the middle of the M2 helix which limits the ion flow in the closed state. The Loop between M2 and M3 helices which is called M2-M3 Loop or M2-M3 linker is thought to make interactions with the Loop 2, Cys Loop and Loop regions of LBD. It is thought that this interaction yields a signal transmission from the binding loops to the gate region in an allosteric mean [7, 9, 10].

The proposed gate in the transmembrane domain is thought to be formed by two constricting rings which lie at the α_{γ}LEU251 and α_{γ}VAL255. These two rings constitute a barrier to ion permeation as it forms the narrowest section along the nAChR [7]. This region widens after the binding of the agonist and lets the ions to pass, and it closes back as the agonist leaves the binding region. [13].

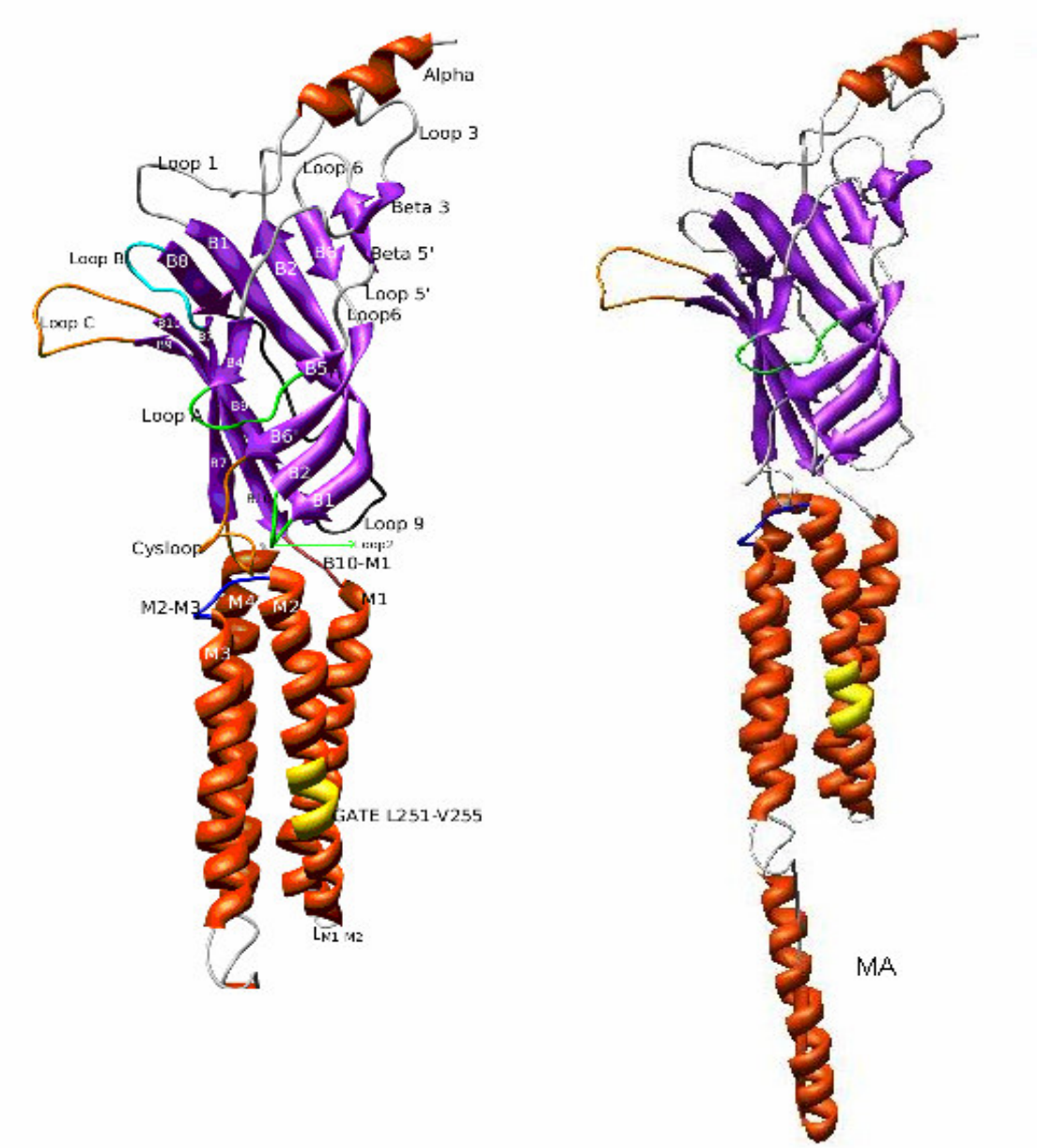

Figure 1.5: Overall structure of Alpha-Gamma subunit of nAChR.

In Figure 1.6, the interface between the LBD and TMD of nAChR shows the locations of M2-M3 linker, Cys Loop, Loop 2, Loop 9 and the other regions close to these regions.

There are missing residues in the ID of nAChR. The only existing region is the MA helices which are connected to the M4 helices. MA helices form an inverted pentagonal cone, which has five open spaces on the side. These open spaces are the only possible path for the ion flow [7]. Earlier kinetic studies established that nAChR can exist in at least three conformations with different functional properties, closed, open and desensitized [14].

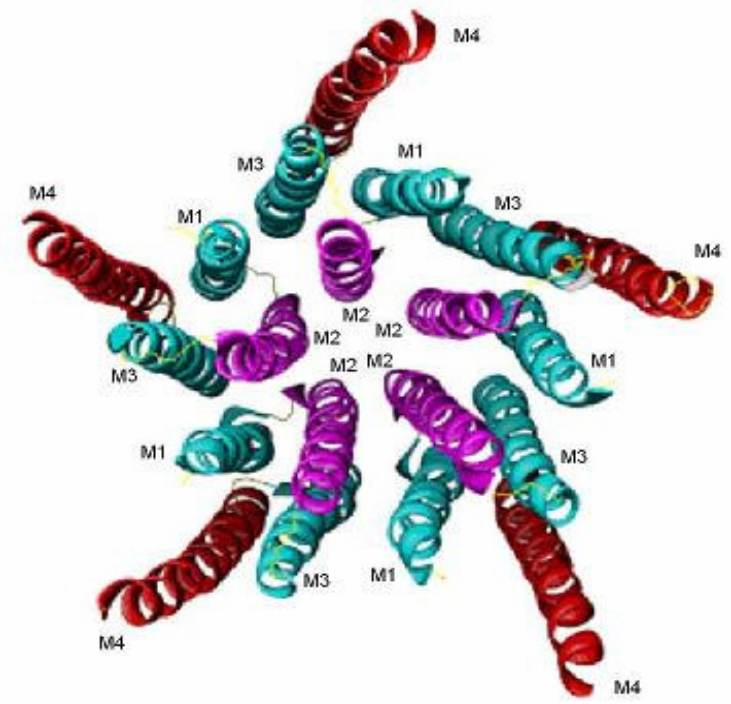

Figure 1.6. Transmembrane Domain of nAChR.

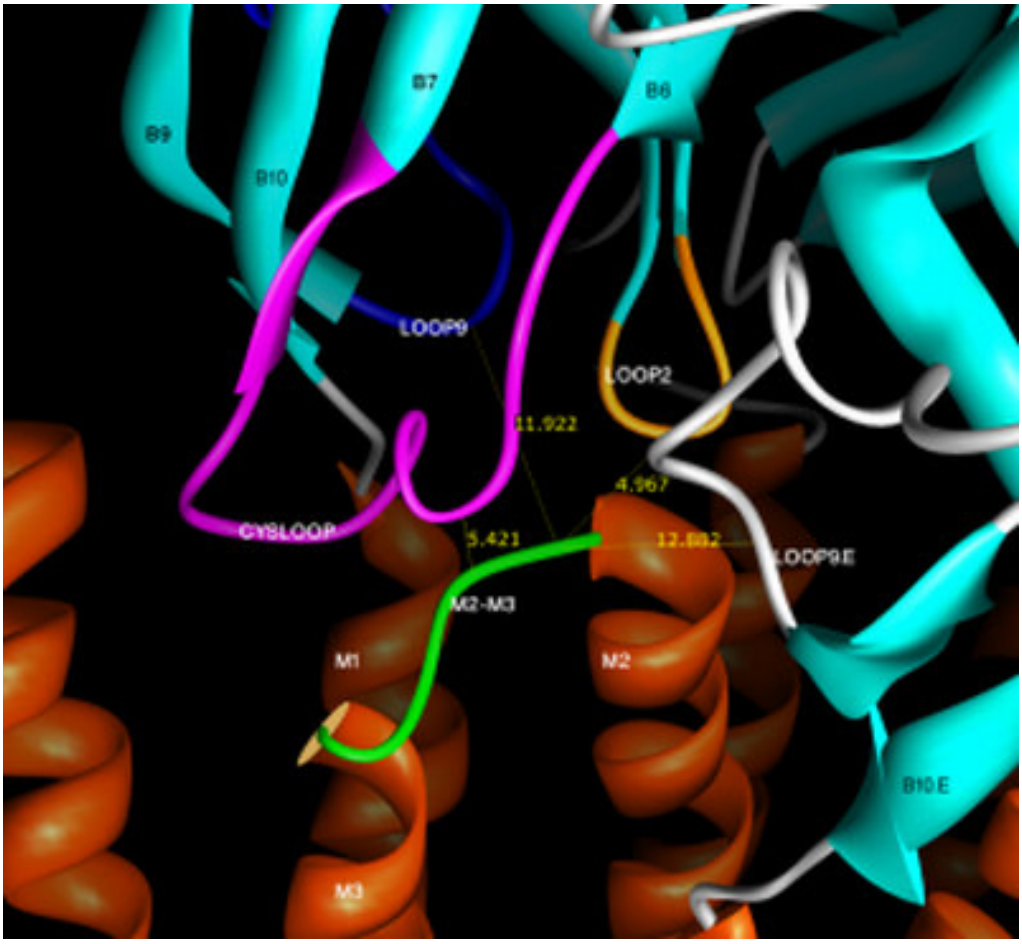

Figure 1.7. Interface between the LBD and TMD of nAChR.

1.2. Literature Survey

The basic mechanism that nAChR allows the cation flux into the cytoplasm is a stepwise motion in which individual interactions leading to an open channel are still unclear. Unwin et al. proposed that the binding of acetylcholine to the binding sites at the ligand binding domain triggers a conformational change at the alpha subunits, which is transmitted through the ligand binding domain to the transmembrane domain and the gate regions by a twist like motion, which in turn leads to an open channel [9]. This basic mechanism may be altered by mutations in the genes coding the structure of nAChR. The results of these alterations may be severe. Past studies have linked mutations in nAChR to several diseases [5].

Channel gating is the most important function of these receptors, without proper gating mechanism, due to mutations in the genes coding for nAChR [9], many congenital myasthenic syndromes (CMS) appear. A CMS is a an inherited disorder that causes muscle weakness (myasthenia) by affecting the connection between nerve cells and muscle cells, called the neuromuscular junction [Muscular Dystrophy Association; www.mdausa.org 2006]. Some of the deficiencies in AChRs, caused by the mutations, result in extended opening of the gate, while other result in the short-lived opening. It has been demonstrated that the cause of a CMS was the result of a mutation V285I in the M3 helix of alpha subunit [15]. Another cause of a CMS is the mutation at the cytoplasmic loop between the M3 and M4 helices of the β subunit [16].

Apart from nAChRs at the neuromuscular junction, many nAChRs function in the nerve cells in brain. Aberrations in these nAChRs are thought to be involved in many diseases including autosomal dominant nocturnal frontal lobe epilepsy, Alzheimer's disease, schizophrenia [17], Parkinson's disease, Crohn's disease [5].

The experimental studies of the nAChR in its membrane environment show that, there is a lipid belt region, which is closely associated with the nAChR, surrounding the AChR protein. This region is qualitatively different in terms of molecular mobility, and the lipid composition of the synaptic region has been reported to differ from that of the rest of the membrane in muscle cells [6]. There are experimental evidences that nAChR is effected by its lipid microenvironment, but the exact nature is still to be resolved [12].

Experiments with the membrane partition photoactivatable probes label M4 transmembrane helice extensively and M3 and M1 helices are also labelled [12] Photoaffinity experiments showed that gamma F292, L296, M295, and N300 faces lipid interface [18]. Mutation experiments are conducted on the lipid exposed residues of gamma M3 to elucidate the functional contributions of there lipid exposed residues on M3 subunit. These experiments have shown that an increase in the volume of hydrophobicity of these lipid – exposed residues will increase the nAChR function [15] Experiments done on the nAChR from the adult muscle cells indicate that 8' positions (alpha PHE284) of the M3 domains of all subunits contribute to channel gating [19].

The M4 domain is the least conserved among the transmembrane domains. It is the most hydrophobic and constitute to the outermost transmembrane domain [20]. Experimental mutation studies in which the therionine 422 was mutated to alanine, have shown that the hydrogen bond made by alphaT422 (a conserved residue) influences the opening and closing rates, and alpha T422 is essential for the proper gating [21, 22, 23]. Tamamizu et. al. [24] demonstrated that tryptophan mutations to residues L416 and I419 created an expression level less than 20 per cent of the wild type, while mutation of alpha V425 to tryptophan exhibited a significant increase in the open channel probability. Also Tamamizu et. al. suggested that I417 is important for the AChR folding, oligomerization.

Another mutational experimental study of the M4 helix demonstrated that mutations to the upper half of the M4 helices have a larger effect compared to those in the lower half. This mutation study also demonstrated that mutations at positions L410, M415, C418, T422, and F426 of alpha M4 helix affects gating [23] All of these mutatgenesis studies suggest that the M4 domain is essential for proper AChR activation [20].

The work done on $GABA_A$ receptor by Kash et. al. [25] supported the notion that cysloop and the loop region between M2 and M3 helices are important for gating. Also Kash et. al. [25] suggested that the work done by Unwin et. al. (a structural study which underlines the importance of cysloop and M2-M3 loop regions) is supported by their experiments [25, 3]. The work of Castillo et. al. demonstrated that M2-M3 loop in nAChR are involved in coupling agonist binding and gating [26].

In a recent experimental study by Lee et. al. [27], the principal pathway is thought to begin with loop C at the LBD and continue through Beta 10 strand to the M1 helix region where alpha Arg209 juxtaposes the alpha Glu45 (Loop 2). Glu45 and Val46 couples with Pro272 at the M2–M3 loop. Lee et. al. reported that mutations at alpha Arg209 impairs channel gating 46 fold. They also underlines the importance of Cys Loop and Loop 9 for the coupling of binding to gating [27] Bouzat et. al. proposed that Loop 9 from the adjacent subunit contacts Loop 2.Then, these Loop 2 and Cys Loop regions straddle M2-M3 loop suggesting a twisting motion which in turn twists the pore lining M2 domain to allow flow of cations [10].

Apart from experimental studies, nAhCRs have been the topic of many computational studies. These studies mainly include molecular dynamics (MD) and normal mode analysis (NMA).

Normal mode analysis conducted by Cheng et. [14] showed that cross correlation results point out a M2–M3 loop is correlated with Cys loop and Loop 2. Also, Cheng et. al. underline that NMA results favour that both the Cys loop and Loop2 undergo highly concerted movements with M2–M3 linker [14, 25]. Their NMA shows that first mode motions are dominated by twisting, second mode is dominated by symmetric expansion and third mode is dominated by asymmetric expansion motions. Taly et. al. reported that only the first mode of NMA produces a structural reorganization that result in a wide opening of the ligand binding and transmembrane domains [28].

MD studies conducted by Xu et. al. [29] on the transmembrane domain of nAChR in membrane showed that M4 helices convey the effects exerted by lipid surroundings into the M2 ring. MD studies, on the transmembrane domain of nAChR in a membrane mimicking environment, performed by Hung et. al. [30] pointed out that there is a hinge in the proximity of central hydrophobic gate. Also, their MD results underline a correlation of M2– M3 loop with the gate at the M2 helices. In addition, their results show that M2–M3 loop of alpha subunits (alpha gamma and alpha delta) exhibit highest fluctuations. Law et. Al. conducted MD simulations on the transmembrane and ligand binding domain of nAChR [31]. Their result state that motions of TMD and LBD are anti correlated. Law et. al. suggest that outer beta strands (Beta 9 – Beta10) form a lever that connects the binding site with the motions of

TM domain and that interaction of Loop2 with the M2–M3 loop pivoted by Cys Loop is important for gating [31].

This thesis covers many different analyses mainly made on AChBP and nAChR. At the beginning, there was only the AChBP and it was supposed to be the LBD of the transmembrane domain of nAChR. With the release of the refined structure of nAChR as a full structure, the analysis has been continued with the LBD of nAChR with and without the TMD. The similarities and differences between AChBP, LBD of nAChR and the LBD of nAChR with and without TMD with respect to the various properties in connection to gating have been the main focus in the present work. Three structures have been subjected to the analysis.

Firstly, to obtain the mean-square fluctuations of the residues (auto-correlations) and the correlation between the fluctuations of the residues (cross-correlations in the structure, the Gaussian Network Model (GNM) has been employed [32]. The cross-correlations have been elaborated by MCPOOL [33], which generates paths between any two arbitrary residues or regions using the cross-correlation values. These paths allows us to see the allosteric interactions between residues.

Since GNM is a one-dimensional model, it doesn't show the directions of displacements. For this, Anisotropic Network Model (ANM) has been employed to generate the conformations that display the fluctuations from the average structure in various modes of motion [34]. To see the behavior of the pore in a set of slowest modes of motion, whether the radius of pore tightens or widens at different conformations, the software HOLE is employed [35].

To see the structural and/or functionally important residues, conservation analysis has been carried out using the Consurf server [36, 37]. Conservation score of each residue is taken from this server and checked if any of the well conserved residues contribute to the gating mechanism. For the probability that some of the important residues could have been correlated during the evolution, correlated mutations analyses have also been conducted using "Analysis of Correlated Mutations" server [38]. Finally, to see the shortest and most visited regions along the paths that have been generated by MCPOOL [39] using the results of cross-correlation analysis, the PAJEK program has been used [40]. PAJEK analyzes the generated

paths and gives graphical outputs showing the most frequently used steps along the paths. The starting point and target point is connected with lines and dots. Each dot displays the mostly visited regions along the paths and lines connecting the points show where a region goes mostly.

2. METHODS

2.1. GNM

Gaussian network model is a coarse grained one dimensional elastic network model where the fluctuations are thought to be isotropic. Residues are thought to be connected to each other with harmonic springs. Since GNM assumes fluctuations to be isotropic, fluctuations are described with their amplitudes on a one dimensional scale and that the protein is in its native equilibrium state. Interactions of individual atoms are coarse grained using a Virtual bond model.

Each individual residue is represented by backbone carbon atoms (C^{α}) in this model and the interactions between different residues are not specific. All backbone atoms are assumed to undergo Gaussian fluctuations about their equilibrium values [41]. If the distance between two backbone atoms is less than a certain cut-off distance (r_c). the backbone atoms are considered to be interacting and in contact.

This analysis decomposes this network of interactions, represented by a Kirchoff matrix, a matrix representing the contacting pairs, [41] and a harmonic potential. The decomposition results in the eigen values and the eigen vectors of the system. The smallest non-zero eigen values define the slowest modes of motions while the highest eigen values define the fastest modes of motions.

Slow modes represent a global motion, while fast modes represent the isolated motions of individual backbone atoms [41]. The work done on GNM identifies the residues, which are active in the fast modes, as key players upholding the stability of the folded molecule [41]. The local minima in the slow mode fluctuations are thought to be stable regions, with minimum global fluctuation [42]. These minimum fluctuating regions act as hinges, a static point, in between two more fluctuating (mobile). Therefore they are usually referred to as hinges.

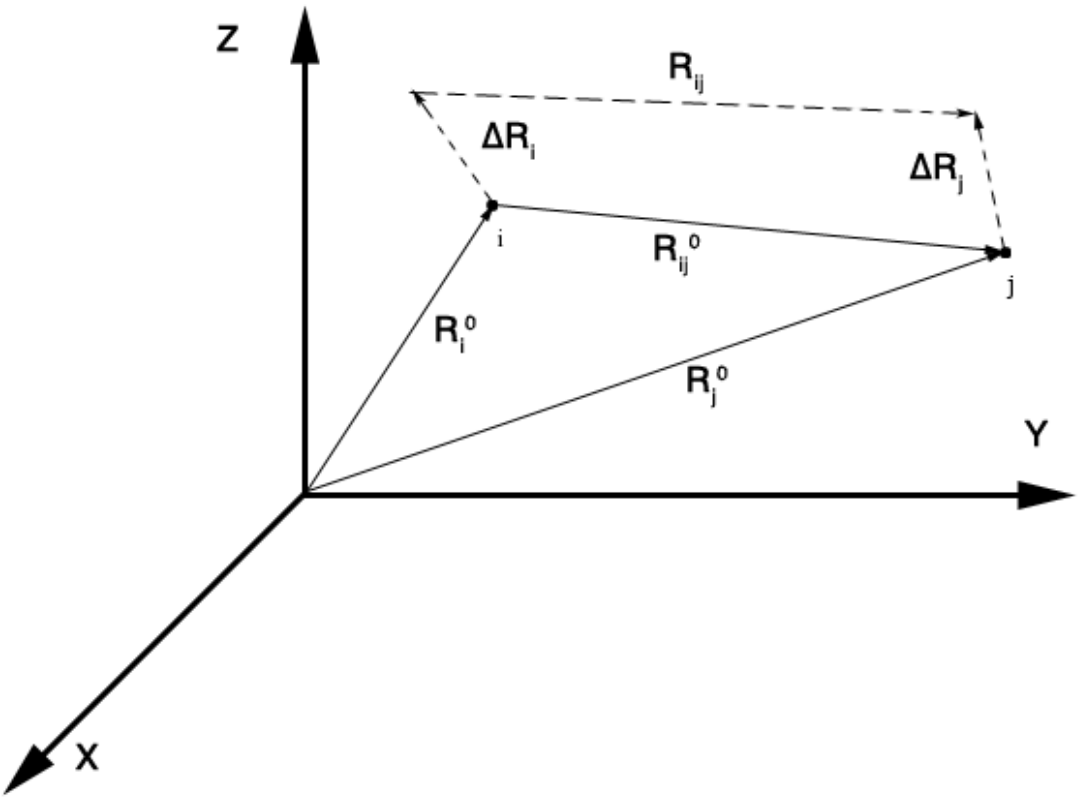

Figure 2.1. Representation of equilibrium positions R_i^0 and R_j^0 of the backbone atoms of i^{th} and the j^{th} residues. ΔR_i : instantaneous fluctuation of i^{th} residue, ΔR_j : instantaneous fluctuation of j^{th} residue, R_{ij} : instantaneous fluctuation separation.

The fluctuations of backbone atoms are assumed to obey a Gaussian distribution, shown by Equation 2.1

$$W(\Delta R_i) = \exp\left(-3(\Delta R_i)^2 / 2\langle(\Delta R_i)^2\rangle\right) \qquad where \quad 1 \le i \le N \qquad (2.1)$$

Where $\langle(\Delta Ri)^2\rangle$: mean square fluctuation of the i^{th} residue,

N : total number of residues.

The total potential for a molecular system of N residues can be written using the pairwise as shown in Equation 2.2

$$V_{tot} = \sum_i \sum_j V(R_i, R_j) = \sum_i \sum_j (1/2)\gamma(\Delta R_{ij} \cdot \Delta R_{ij}) \qquad where \quad 1 \le i < j \le N \qquad (2.2)$$

In potential equation, V_{tot} is calculated for all i and j pairs. In this equation γ represents the Hookean force constant assumed for all interacting pairs regardless of the chemical or physical nature of the interacting pair, ΔR_{ij} can be calculated by Equation 2.3

$$\Delta R_{ij} = R_{ij} - R_{ij}^{0} \tag{2.3}$$

Where ΔR_{ij} is the fluctuation in the distance vector relative to the equilibrium separation R_{ij}^{0}. The separation between sites i and j (R_{ij}) can be calculated by Equation 2.4

$$R_{ij} = R_i - R_j \tag{2.4}$$

R_i and R_j are the positions of ,i^{th} and j^{th} sites, respectively [42]. In Equation 2.2 the term γ is used for all interactions, without considering the individual chemical or physical properties of pairs. In equation 2.2 the summations are only valid for interacting pairs for which equilibrium separation is less than a cut-off distance R_c, ($R_{ij}^{0} < R_c$). The fluctuations of the distance separating the residues are represented by ΔR_{ij} (Figure 1.1) can be rewritten as Equation 2.5

$$\Delta R_{ij} = \Delta R_i - \Delta R_j \tag{2.5}$$

where ΔRi represents the fluctuation of the i^{th} residue (Figure 1.1).

The Kirchoff matrix is a symmetric and a sparse matrix, which represents the connectivity of a biomolecular system [42]; Kirchoff matrix can also be named as the connectivity matrix.

$$\Gamma_{ij} = \begin{Bmatrix} -1 i \neq j R_{ij} \leq r_c \\ 0 i \neq j R_{ij} \geq r_c \\ -\sum_{i \neq j} \Gamma_{ij} \; i = j \end{Bmatrix} \tag{2.6}$$

Equation 2.6 summarizes how connectivity matrix is obtained. In this equation Γ is the connectivity matrix. R_{ij} represents the distance between the i^{th} and j^{th} backbone carbon atom.

r_c is the cut off distance, is maximum distance allowed for connected i^{th} and j^{th} residues (10Å). After obtaining the connectivity matrix eigen values and eigen vectors are calculated and connectivity matrix is inverted.

Kirchoff matrix (Γ) can be used to write the total potential in a compact manner using Equations 2.1 and 2.2.

$$V_{tot} = H = (\gamma/2) tr\left[\Delta R^T \Gamma \Delta R\right] \tag{2.7}$$

The ΔR term in Equation 2.7 represents the matrix of instantaneous fluctuations of ΔR_i of all residues, ($1 \leq i \leq N$). ΔR is a (Nx3) matrix whose i^{th} row is the transpose of ΔR_i. H is the internal Hamiltonian represents the total potential of a biomolecular system [42]. The average fluctuations of interacting residues in a molecular system are found from Equation 2.8 replacing the inverse of Kirchoff matrix,

$$\left\langle \Delta R_i \cdot \Delta R \right\rangle = \frac{1}{Z_N} \int \left(\Delta R_i \cdot \Delta R_i\right) \exp\left\{-\frac{H}{k_B T}\right\} d\{\Delta R\} = \left(\frac{3k_B T}{\gamma}\right) \left[\Gamma^{-1}\right]_{ij} \tag{2.8}$$

Z_N is the configurational integral which can be written as Equation 2.9

$$Z_N = \int \exp\{H k_B T\} d\{\Delta R\} \tag{2.9}$$

where k_B is the Boltzmann constant, T is the absolute temperature and $d\{\Delta R\}$ represents the integration over all residue fluctutations. The average fluctuation of interacting pairs can be found using Equation 2.8, this equation can further be simplified using the eigen vectors and eigen values obtained by decomposition of Kirchoff matrix along with equation 2.8 and 2.9 [41].

$$\begin{aligned} \left\langle \Delta R_i \cdot \Delta R_i \right\rangle_k &= \left(3k_B T / \gamma\right) \left[\lambda_k^{-1} \mathbf{u}_k \mathbf{u}_k^T\right]_{ii} \\ &= \left(3k_B T / \gamma\right) \lambda_k^{-1} \left[\mathbf{u}_k\right]_i \left[\mathbf{u}_k\right]_i \end{aligned} \tag{2.10}$$

Eqution 2.10 shows the mean square fluctuations associated with the k^{th} mode where λ_k is the k^{th} eigen value. The ($3\ k_B\ T/\ \gamma$) represents the harmonic potential constant obtained by Gaussian distribution assumption. The term u_k represents the eigen vectors (u_k is the k^{th} eigen vector). The individual modes (k) of autocorrelations can be calculated using the eigen value and the corresponding eigenvector. The smallest non-zero eigen value can be used to calculate the lowest mode and individual modes can be calculated using the corresponding eigen value. The contribution of several modes together, is calculated by

$$\left[\Delta R_i \cdot \Delta R_i\right]_{n,ni} = \frac{\sum_{k=n,ni>n}^{ni} \left[\Delta R_i \cdot \Delta R_i\right]_k \lambda_k^{-1}}{\sum_{k=n,ni>n}^{ni} \lambda_k^{-1}} \tag{2.11}$$

In Equation 2.11 n and ni represent the range of modes to be taken into account. The normalized cross correlations of i^{th} and j^{th} (C(i,j)) nodes can be calculated using Equation 2.10 for i^{th} and j^{th} pairs

$$C(i,j) = \frac{\left\langle \Delta R_i \cdot \Delta R_j \right\rangle}{\left[\left\langle \Delta R_i \cdot \Delta R_i \right\rangle \left\langle \Delta R_j \cdot \Delta R_j \right\rangle\right]^{1/2}} \tag{2.12}$$

Cross correlations are normalized using the individual auto correlations (Equation 2.10). Normalization with respect to auto correlations yields Equation 2.12. Cross correlations represent the extent of correlation between the motions of i^{th} and j^{th} residues. Cross correlation values range from -1 to 1. Positive values describe that i^{th} and j^{th} residues move in the same direction, while negative values mean that they move in opposite directions. Small absolute values of cross correlations represent a weak correlation between residues.

Equation 2.12 can be used to calculate the contributions of individual or several modes together by Equation 2.13 which is essentially the same as equation 2.8 without the ensemble averages.

$$C(i,j)_{n,ni} = \frac{\left[\Delta R_i \cdot \Delta R_j\right]_{n,ni}}{\left[\left[\Delta R_i \cdot \Delta R_i\right]_{n,ni} \left[\Delta R_j \cdot \Delta R_j\right]_{n,ni}\right]^{1/2}} \tag{2.13}$$

Slow modes, representing the global motions of the backbone atoms are defined by the smallest non-zero eigenvalues. In the slow mode fluctuations, the minima points are referred as hinges and they are thought to be stable and less mobile than the other residues. On the other hand fast modes represent the isolated motions of the backbone atoms and are defined by the highest eigenvalues. The peak points on the fast mode motions are referred as kinetically hot residues.

In the GNM analysis, autocorrelations are calculated using Equation 2.11 and cross correlations are calculated using equation 2.13. Results of GNM analyses are elaborated to see the correlations between residues. Slow and fast mode fluctuations are drawn and the results of other calculations such as conservation, correlated mutations and MCPOOL analysis are plotted into these figures. The results of GNM analyses are also used in MCPOOL section to find coupled correlations.

2.2. ANM

An extension of the Gaussian Network Model, called the Anisotropic Network Model [34], makes it possible to determine the directions of the resiudes and/or regions of a molecule on the three dimensional scale for different possible conformations that the molecule may have. In GNM, the directions of residues are controlled by the harmonic potentials but in ANM, because the displacements are both on X, Y and Z coordinates, the coordinates of fluctuation vector are controled by the Gaussian dynamics. So the potential including the fluctuations at X, T and Z directions becomes;

$$V = \frac{1}{2}\gamma\left(R_{ij} - R_{ij}{}^{0}\right)^2 \tag{2.14}$$

Substituting R_{ij} into Equation 2.14,

$$V = \frac{1}{2}\gamma\left\{\left[\left(X_j - X_i\right)^2 + \left(Y_j - Y_i\right)^2 + \left(Z_j - Z_i\right)^2\right]^{1/2} - R_{ij}{}^{0}\right\} \tag{2.15}$$

Where; γ = force constant, $R_{ij}{}^{0}$ and R_{ij} = seperation vector of residue i and j and X, Y and Z = components of seperation vectors.

The counterpart of Kirchoff Matrix used in the ANM calculations is called the Hessian Matrix, which is a square matrix of second partial derivatives of the potential. If the second derivative of Equation 2.14 is taken for X only and for two different components such as X and Y, the resulting derivatives become;

$$\frac{\partial^2 V}{\partial X_i^{\,2}} = \frac{\gamma (X_j - X_i)^2}{R_{ij}^{\,2}} \tag{2.16}$$

$$\frac{\partial^2 V}{\partial X_i \partial Y_j} = -\frac{\partial^2 V}{\partial X_j \partial Y_i} = -\frac{\gamma (X_j - X_i)(Y_j - Y_i)}{R_{ij}^{\,2}} \tag{2.17}$$

For the residues around the i^{th} residue, Equations 2.16 and 2.17 become;

$$\frac{\partial^2 V}{\partial X_i^{\,2}} = \gamma \sum_j \frac{(X_j - X_i)^2}{R_{ij}^{\,2}} \tag{2.18}$$

$$\frac{\partial^2 V}{\partial X_i \partial Y_i} = \gamma \sum_j \frac{(X_j - X_i)(Y_j - Y_i)}{R_{ij}^{\,2}} \tag{2.19}$$

Where j under the summation sign stands for summation over all of the surrounding residues where $R_{ij}^{\,0} < r_c$. Using the Equations 2.17-2.19 the Hessian Matrix can be formed where hessian matrix is expressed as Equation 2.20. Each individual H_{ij} in the Hessian matrix are calculated from equation 2.21. For the case of i=j, H_{ii} matrices form the diagonal elements of the Hessian Matrix.

$$\mathcal{H} = \begin{bmatrix} H_{11} & H_{12} & . & . & H_{1N} \\ H_{21} & & & & H_{2N} \\ . & & & & . \\ . & & & & . \\ H_{N1} & . & . & . & H_{NN} \end{bmatrix} \tag{2.20}$$

$$H_{ij} = \begin{bmatrix} \frac{\partial^2 V}{\partial X_i \partial X_j} & \frac{\partial^2 V}{\partial X_i \partial Y_j} & \frac{\partial^2 V}{\partial X_i \partial Z_j} \\ \frac{\partial^2 V}{\partial Y_i \partial X_j} & \frac{\partial^2 V}{\partial Y_i \partial Y_j} & \frac{\partial^2 V}{\partial Y_i \partial Z_j} \\ \frac{\partial^2 V}{\partial Z_i \partial X_j} & \frac{\partial^2 V}{\partial Z_i \partial Y_j} & \frac{\partial^2 V}{\partial Z_i \partial Z_j} \end{bmatrix} \quad (2.21)$$

For the case of dealing on the one direction only, the diagonal elements of Equation 2.21 are calculated by Equation 2.18 and the off-diagonal elements of Equation 2.21 are calculated by Equation 2.19. And these Equations 2.18 and 2.19 form the diagonal elements of Equation 2.20, while the off-diagonal elements of Equation 2.20 are calculated by Equation 2.17 which correspond to H_{ij}'s. Hence the counterpart of Kirchoff Matrix in the ANM is shortly $\mathcal{H}/\gamma$ and its decomposition extract 3N-6 eigen values and 3N-6 eigen vectors for the individual modes. There are 6 zero eigenvalues in ANM while there was only one in the GNM.

In the ANM calculations, ten slowest non-zero eigen values and corresponding eigen vectors which also correspond to the respective modes are taken into consideration. One plus and one minus conformations are derived over the original conformation of the molecules and these new conformations are added to the original conformation. To see the movements clearly, the new found minus and plus conformations are exaggerated by multiplying them with an arbitrary constant and the resulting conformations are observed by using the Visual Molecular Dynamics (VMD) program.[43].

To analyze how the conformation and the radius of the molecule changes at both minus and plus conformations, the HOLE program has been applied [35].

2.3. Multiple Sequence Alignment

The starting step for both conservation and correlated mutations analysis was search for homologous sequences for our molecule. For this, the multiple sequence alignments were carried out. Multiple sequence alignment is an approach [44] that compares multiple DNA or amino acid sequences and aligns them to highlight their similarities.

For this purpose 100 homologous sequences (up to 35 per cent similarity) were taken for each of the subunits of our molecule by using EXPASY BLAST [45]. With the default values on the site and excluding the fragment sequences, the search for homologous sequences was carried out on Swiss-Prot database. After the blast is run and the homologous sequences are found, these sequences are given to the version 1.83 of Clustal W, by using the default parameters, to obtain multiple sequence alignments.

These steps have been carried out for both five subunits of nAChR and thus five multiple sequence alignments for each subunit have been obtained. And these alignments were used for the analysis of conservation and correlated mutation.

2.4. Conservation Analysis

Conservation is the degree to which a specific residue is found at a specific site in related sequences of a family of nucleic acids, proteins etc. [36]. If that specific residue is found at that specific site throughout the sequence family this residue at this site is conserved. Conservation can also be considered as a scale of the resistance to evolutionarily mutations. These conserved residues are often found to be functionally or structurally important residues [37].

Conservation analysis was performed using the web interface of version 3.0 of "Consurf" [36, 37]. The default parameters were kept but the MSA file retrieved from ClustalW server was used. Consurf returns a conservation score, ranging from a negative value to a positive value, for each residue. This score corresponds to the evolutionary rate of the residue [37], a negative rate translates into a more conserved residue.

Also, Consurf presents another scale (a colour scale) to represent the conservation scores. This colour scale ranges from 1 to 9. Only most conserved residues are rated 9 and most variable residues are rated 1.

Another feature of Consurf is the confidence interval. This interval represent the range for which the conservation score and the colour number can take on. Therefore, in this work only the residues with colour number confidence interval with 9 – 9 are considered as highly conserved residues.

An important thing about conservation analyses is that the conservation scores are normalized along each subunit. This normalization process makes it impossible to compare two different subunits with each other.

2.5. Correlated Mutations

Correlated mutations refer to the coupled mutation of two residues, for which the mutation of the second residue compensates for the loss of function caused by the first mutation [38, 46]. These couples could be formed near neighbours or distant neighbours. These distant couples may reflect an allosteric regulation mechanism [47].

Correlated mutation analysis was carried out using the "Analysis of Correlated Mutations" server [38]. The default parameters were used along with the MSA from the ClustalW server. The results were graphed using the Dot and Dotty programs [48].

2.6. MCPOOL

MCPOOL interprets the outputs of GNM calculations. It analyzes the cross correlation values of residue pairs and discriminates the values according to the given minimum correlation value. In MCPOOL analyses, the correlation values of above 0,5 are taken into consideration [39]. After MCPOOL realizes which residue pairs have correlation value of greater than 0,5, it starts to generate residue-residue steps similar to the basis of Monte Carlo chain generation method. Each residue may be cross correlated with hundreds of other residues.

The starting region or residue is given by the user and according to this starting point Mcpool seeks residues which have cross correlation value of minimum 0.5 with the starting residue. Then these correlation values are normalized by the total value of these correlation values. So each residue obtains a value between zero and one. Each normalized value is added to the previous one and thus the cross correlation values of each residue lie adjacently between one and zero. The main purpose of this normalization process is to give each residue a range which will be used in the pathway generation similar to the Monte Carlo chain generation.

After the normalization and selecting the ranges for each residue, MCPOOL generates random numbers between zero and one. Number corresponding to the values obtained from the normalization procedure show which residue is selected in the next step. Next random gerneration procedure yields another number, hence another residue. This procedure continues until the path reaches to the preselected target region or the path reaches to a total number of steps which was limited by a desired number. If a path reaches to the desired target region that path is called connected path.Furthermore if that path doesn't use any residue out of the starting subunit it is called internal connected path. If a path uses at least one residue of the other subunits than the starting subunit, this path is called external path. In the analyses of Mcpool, 100,000 paths are generated for maximum of 10, 20 and 30 steps.

The minimum correlation value is allowed to be 0,5 for each residue pair. For the AChBP molecule the starting point of these calculations are the principle binding residues and the target regions are selected to be the Cys Loop, Loop 2 and Loop 9 regions. For the molecule of nAChR, the starting point is the binding loops which are named as Loop A, Loop B and Loop C, while the target region is selected to be the gate region in the transmembrane region.

The outputs of MCPOOL show the most visited regions and residues along the connected paths and categorize the connected paths as internal connected paths and external connected paths. The residues that are visited at the most are presented with respect to the fluctuations in the average of the slowest two modes and in the average of the fastest 30 modes. The most visited regions are further elaborated with the software PAJEK [40].

3. RESULTS AND DISCUSSION

3.1. GNM Calculations

GNM calculations were performed for AChBP, nAChR and the LBD of nAChR to compare the differences and similarities in dynamic fluctuations. The fluctuations at two ends of dynamic spectrum, in the slowest and fastest modes, and the correlation between the fluctuations in the slowest modes are analyzed for each of the molecules in turn.

3.1.1. Fluctuations in the Slowest Modes

The slowest modes, with the low frequency fluctuations, are the most cooperative modes of motion of a structure and significantly overlap its functionally important fluctuations (32). The mimina of the slowest mode shape point to the hinge sites, which are mechanistically important regions, mechanistic hotspot of the structure. The maxima, on the other hand, describe the regions that display high amplitude of motion and these regions could be associated with binding sites. Here, the distributions of the mean-square fluctuations in the average of the slowest two modes are analyzed and presented in Figures 3.1-3.3.

Figures 3.1 to 3.3 display the fluctuations in the average of the two slowest modes of AChBP, LBD of nAChR and the full structure of nAChR respectively. Since AChBP is a homopentamer and all of its subunits are identical, only the alpha-gamma subunit is shown here.

The subunits of LBD of nAChR and the full structure of nAChR are not identical. So each figure will be discussed separately but only the figures of Alpha-Gamma subunit will be shown in this section. The other figures can be seen in Appendix B, Figure B.1 to Figure B.6.

Loop2, Cys Loop and Loop9 which are thought to be important regions in the allosteric system of gating mechanism, are shown on the graph and positions of the principle binding residues are shown by arrows.

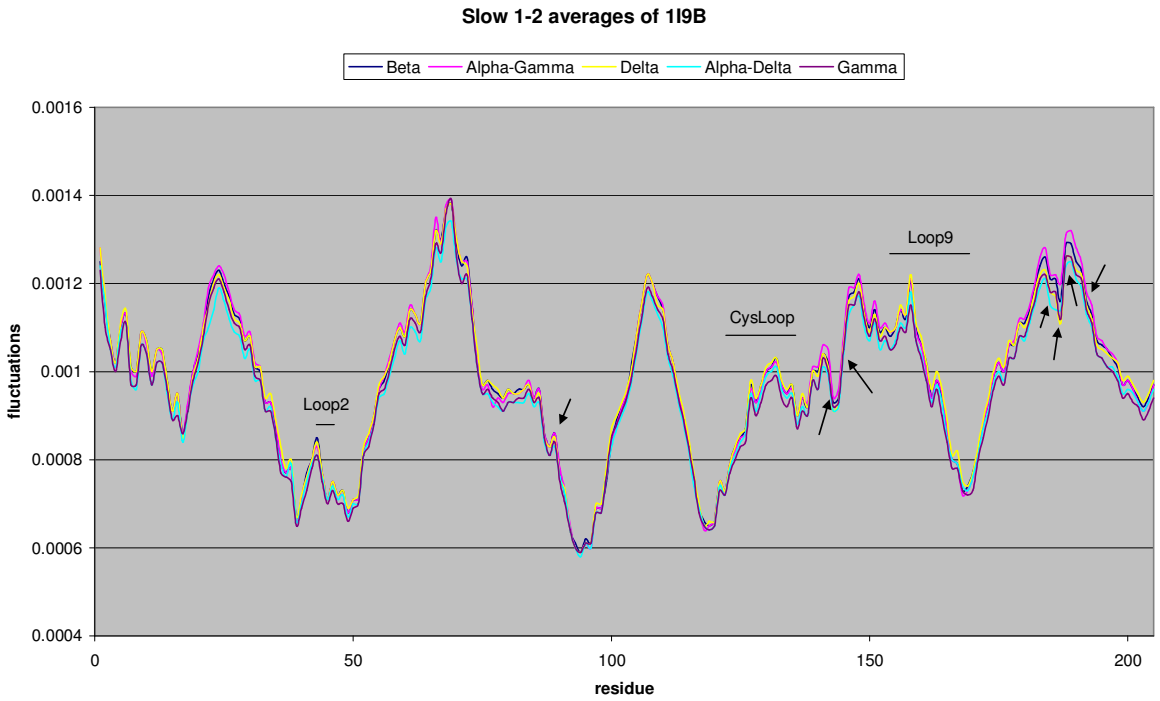

Figure 3.1. Slow 1-2 averages of each subunit of AChBP. Dark Blue: Alpha-Gamma, Pink: Beta, Yellow: Delta, Turquoise: Alpha-Delta, Violet: Gamma. Arrows point the binding residues of the AChBP molecule.

As expected, the shapes of the average of the slowest two modes are similar for all five units of the AChBP, which is a pentamer. The last residues of Loop 2 and Loop 9 seem to act as a hinge point as they contribute to some minimum points on the Figure 3.1. However, Cys Loop seems to be relatively mobile as the other loops do. The principle binding residues seems to be mobile, which would be important for the recognition of Acetylcholine.

The fluctuations of residues of Alpha-Gamma subunit of LBD in nAChRin the average of slowest two modes are presented in Figure 3.2. The binding residues are not presented for clarity in the figure. The regions of the binding loops are shown instead. Figures for other subunits are given in Appendix B, Figure B1 to Figure B3.

As the subunits of LBD of nAChR are different from each other, the slow 1-2 average figure of each individual subunit is different except the alpha subunits. This difference is mainly on the fluctuations values, but the shape is similar in all. When a subunit shows minima, the other subunits almost have minima on that region too. In opposition to Figure 3.1 of AChBP, Loop 2 corresponds to a minimum point in the LBD of nAChR. But this situation

is not valid for Delta and Alpha-Delta subunits. Similar to this, only the Beta and Gamma subunits have minima while the other three subunits have a maximum point at Loop C.

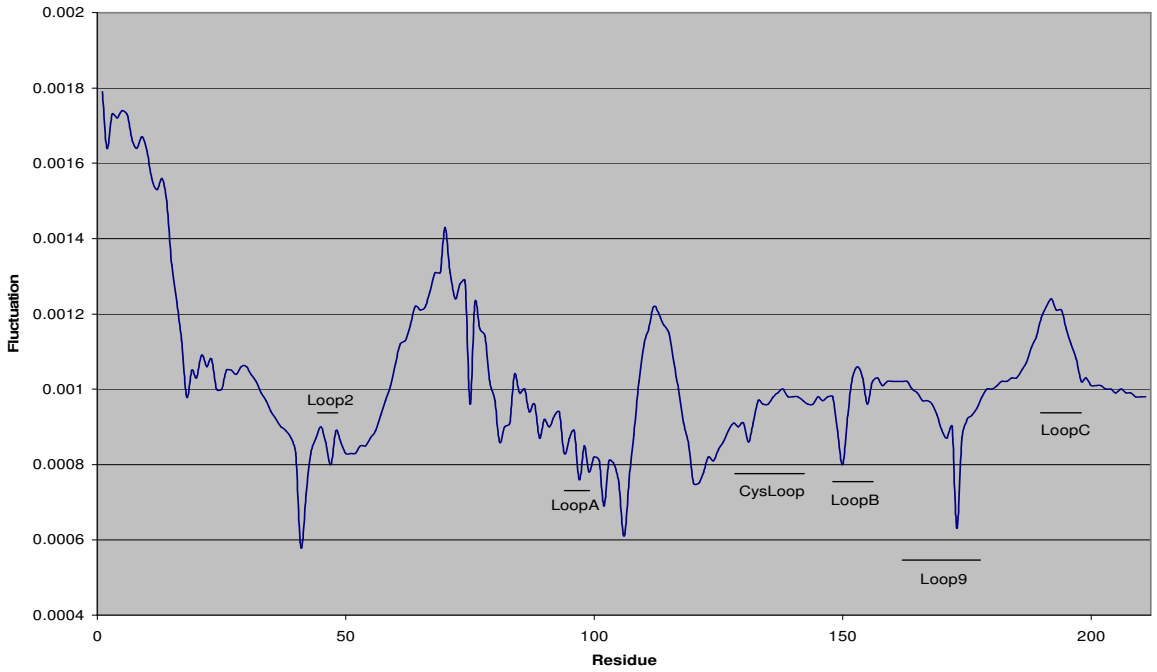

Figure 3.2. Fluctuations of Ligand Binding Domain of nAChR for Alpha-Gamma Subunit in the average of the slowest two modes.

The binding loops Loop A and Loop B are at minima, while the other binding loop Loop C displays high amplitude of motion. Few residues of Cys Loop and Loop 9 correspond to the minimum values but the residues of Loop 2 don't correspond to the minimum regions. This shows that if some residues of Cys Loop and Loop 9 have residues at minimum fluctuations while some of their other residues are mobile, it may be considered that these loops move over points which may act as hinge point letting the Cys Loop and Loop 9 to move. This motion may agree with the expression that these loops straddle over the M2-M3 region of TMD [10].

For the case of full structure of nAChR containing both LBD and TMD, Figure 3.3 displays the slow 1-2 average fluctuations. Loop 2 and Cys Loop regions of the nAChR display hinge behavior, which is not the case with AChBP and with the LBD of nAChR as a isolated structure. This is apparently due to the absence of transmembrane region.

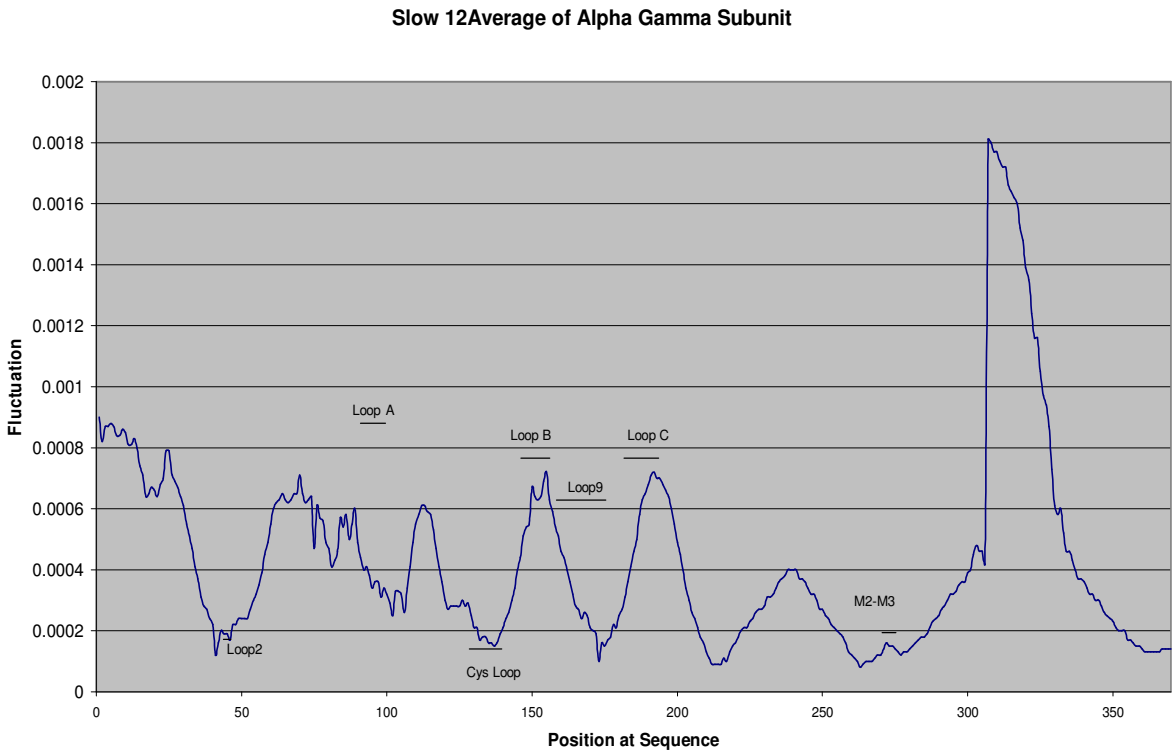

Figure 3.3. Slow 1-2 average of Alpha-Gamma subunit of nAChR.

When the TMD is attached to the LBD, the molecule seems to modify its structural fluctuations and these loops seem to act as hinge points leading the structure to move around these loops. These loops may be pivot regions letting the molecule to make motions separately. Figures of the other subunits of nAChR are given in APPENDIX B, Figure B4 to Figure B6. In the ANM section, the motions of each residue on the three dimensional scale will be discussed.

3.1.2. Fluctuations in the Fastest Modes

The fluctuations in the fastest modes of are analyzed. The average of the fastest 30 modes, i.e. modes with the 30 highest frequencies, are analyzed and presented here. These highest frequency fluctuations reflect the localized motion. The peaks in these modes are referred as kinetically hot residues.

Figures 3.4 to 3.6 show the fast 30 average fluctuations of AChBP, LBD of nAChR and the full structure of nAChR respectively. Since AChBP is a homopentamer and all of its subunits are identical, only the alpha-gamma subunit is shown here. But the subunits of LBD

of nAChR and the full structure of nAChR are not identical. Thus, each figure will be discussed separately but only the figures of Alpha-Gamma subunit will be shown in this section. The other figures can be seen at Appendix B.

Loop2, Cys Loop and Loop9 which are thought to be important regions in the allosteric system of gating mechanism, are shown on the graph and positions of the principle binding residues are shown by arrows.

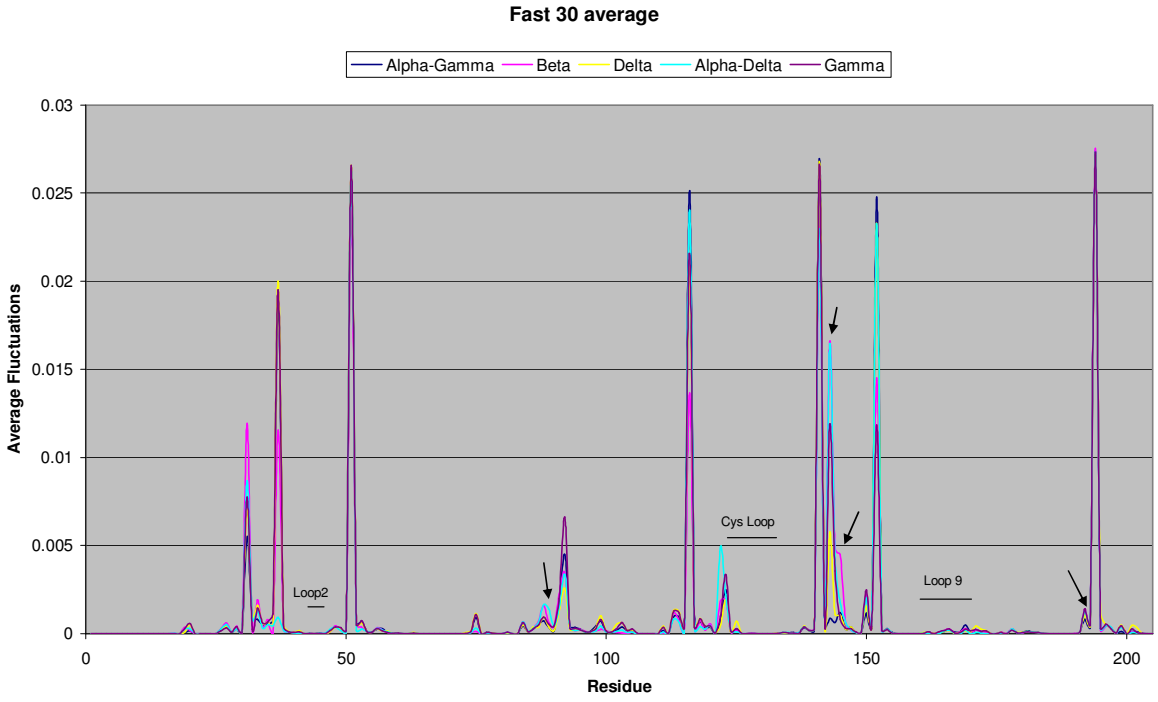

Figure 3.4. Fluctuation in the average of 30 fastest modes for each subunit of AChBP. Dark Blue: Alpha-Gamma, Pink: Beta, Yellow: Delta, Turquoise: Alpha-Delta, Violet: Gamma.

As seen from the Figure 3.4, the fast 30 average fluctuations of each individual subunit of AChBP are the same, as the molecule is a homopentamer. It shows that the principle binding residues of AChBP are located on the hot spots while the regions which are considered to be important at the gating mechanism (Loop2, Cys Loop and Loop 9) don't appear on the hot spots. Some other regions containing hot spots are beta 1, Loop 5 which is a binding loop at nAChR, Loop 8 which is another binding loop at nAChR and the beta 10 region. This beta 10 region is in contact with Cys Loop and Loop 2.

The LBD of nAChR which may be thought as the counterpart of AChBP is not a homopentamer as AChBP. So the fast average figures of each individual subunit should be different from each other just like the slow 1-2 average figures were. Instead of showing the principle binding residues, where principle binding residue fact belongs to AChBP, the binding loops are located on the fast mode fluctuations of LBD of nAChR in Figure 3.5.

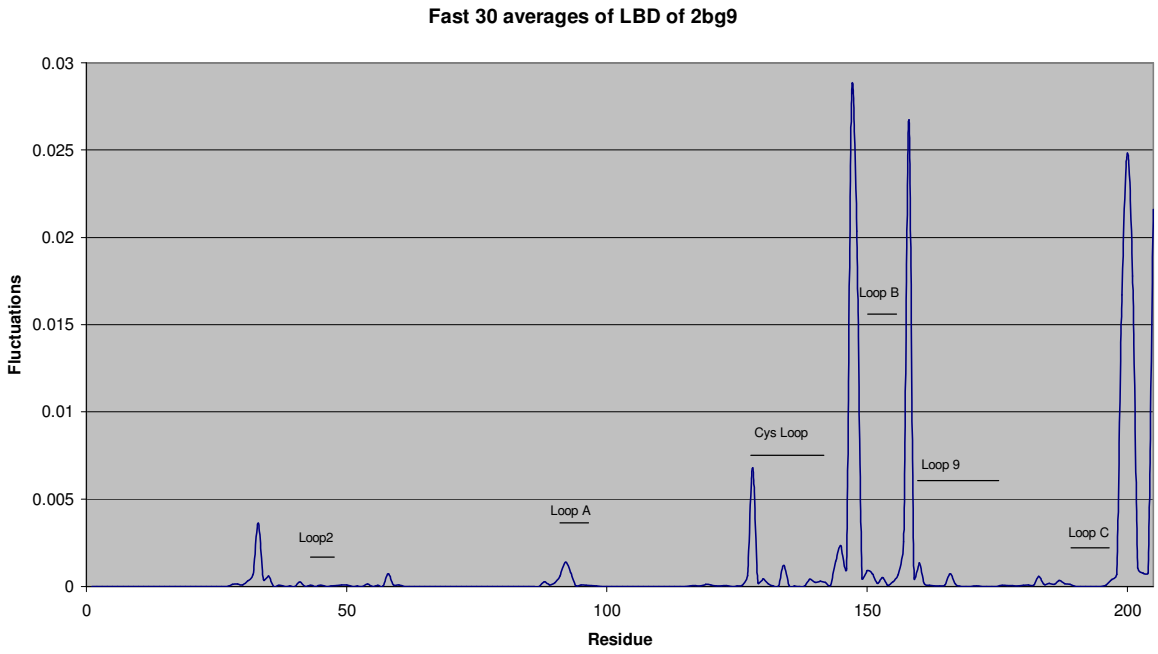

Figure 3.5. Fluctuations in the average of fastest 30 modes of LBD of nAChR for Alpha-Gamma Subunit.

Similar to Figure 3.4, Cys Loop, Loop 2 and Loop 9 do not correspond to the hot spots in Figure 3.5, i.e., the high frequency fluctuating residues, for the alpha-gamma subunit. Beta, Delta and alpha-delta subunits have maximum points in the Loop 2 region and beta and delta subunits also have maximums (hot spots) at the Cys Loop region. Also, Beta, Delta and Alpha-Delta subunits have peaks in the fast mode fluctuations at Loop 9. There also one hot spot in the beta 1 region and two hot spots in the beta 10 regions.

In Figure 3.4 it was observed that the principle binding residues correspond to the hot spots, but in the fast 30 average fluctuation figure of alpha-gamma subunit of LBD of nAChR, the binding loops do not have any residues corresponding to hot spots. Only, Loop A has got a residue corresponding to a hot spot but this is not so obvious. The other alpha subunit, Alpha-Delta subunit, doesn't have any binding loop at the hot spots even not at the Loop A.

but the other subunits have some hot spots at different binding loops. All of these binding loops have hot spots at the Beta subunit. Delta subunits Loop A region also contains a residue corresponding to a hot spot. One of the residues in the Loop B region of Gamma subunit corresponds to a hot spot (See APPENDIX B, Figure B.7 to Figure B.9).

When TMD is attached to LBD, the fluctuations in the average of 30 fastest modes are presented in Figure 3.6.

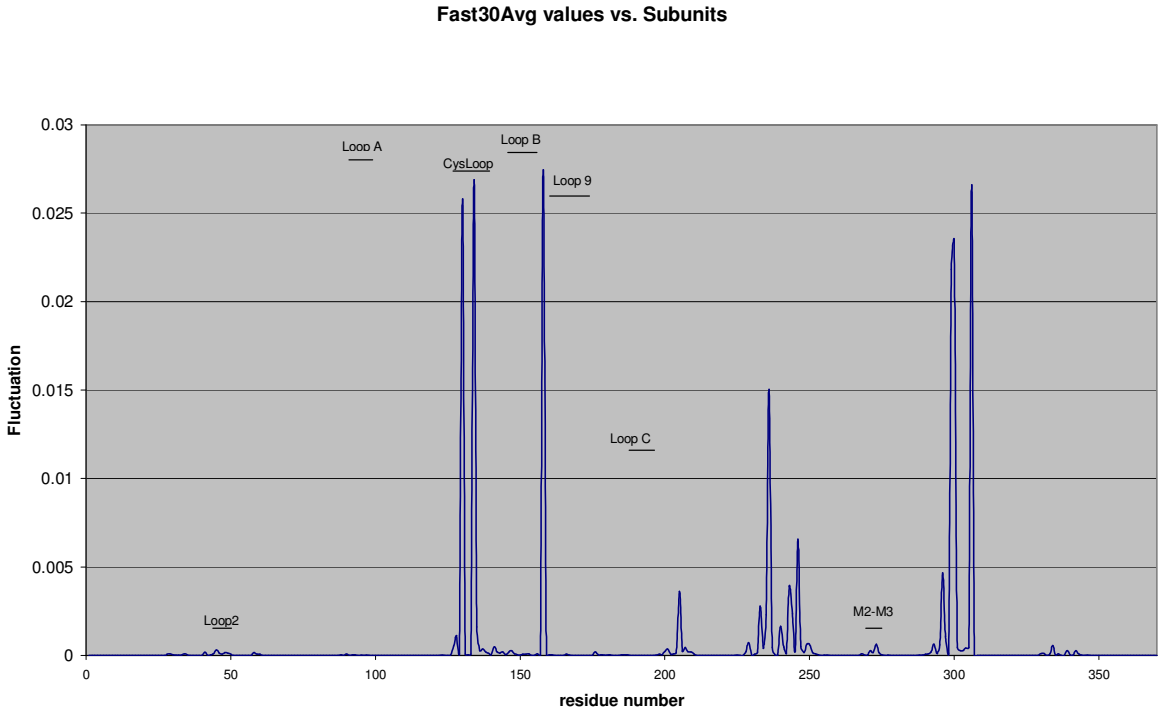

Figure 3.6. The fluctuations in the average of the fastest 30 modes of Alpha-Gamma Subunit of the full structure of nAChR.

For the fluctuations of nAChR in the average of 30 fastest modes, Alpha-Gamma subunit contains some residues at the Cys Loop region that correspond to the hot spots. Also a small hot spot peaks is seen at the M2-M3 linker of TMD. There are some hot spots observed at the TMD but most of these hot spots correspond to the lower part of nAChR. Also there is a hot spot at the Beta 10 region of Alpha-Gamma subunit. Beta 10 is between Loop 9 and the binding loop Loop C. This beta 10 region covers a hot spot at each of the individual subunits. There are absolutely some differences between the subunits. Delta and Alpha-delta don't have any residues in the Cys Loop region that corresponds to a hot spot. And there are not any residues at the M1 region of Delta subunit corresponding to a hot spot.

The hot spots at Cys Loop can only be seen when a TMD is attached to the LBD. Cys Loops of AChBP and LBD of nAChR do not have hot spots while one or two residues near this Cys Loop correspond to hot spots. Also many of the principle binding residues of AChBP are on hot spots while none of the binding loops are on the hot spots in nAChR. The hot spots seen on the Beta 10 regions are similar in all of the three structures. The other subunits are shown in APPENDIX B, Figure B.10 to B.12.

3.1.3. Cross Correlations

The correlations between the fluctuations in the slowest 10 modes are presented here. The interactions between two subunits are investigated. Generally the analyses are focused on the Alpha-Gamma subunits and the figures are plotted for Alpha-Gamma subunits. The figures of the other subunits are given in Appendix B.

The slowest 10 modes correspond to 17 per cent of dynamics in AChBP, 29 per cent of dynamics in LBD of nAChR and 20 per cent of the dynamics in the full structure of nAChR. The results suggest how residue pairs fluctuate in a given topology of the structure. The residue pairs may be positively or negatively correlated and these correlations are shown in different colors. The positive values indicating the positive correlations, between 0 and 1, are shown in different tones of red while the negative values indicating the negative correlations, between -1 and 0, are shown in different tones of blue where the darker the color, the greater the correlation between those residue pairs.

In this section cross correlation results of the average of first ten modes are analyzed for AChBP, LBD of nAChR and for the full structure of nAChR respectively. Figure 3.7 is the cross correlation map of AChBP structure including all of the subunits.

Since 1i9b is a homopentamer, interactions between alpha-gamma subunit and beta subunit are the same with the interactions between beta subunit and delta subunit and so on. The intramolecular correlations of each individual subunit are the same with each other. It can also be seen from the graph that the picture is almost the same on the x = y diagonal on the subunit basis.

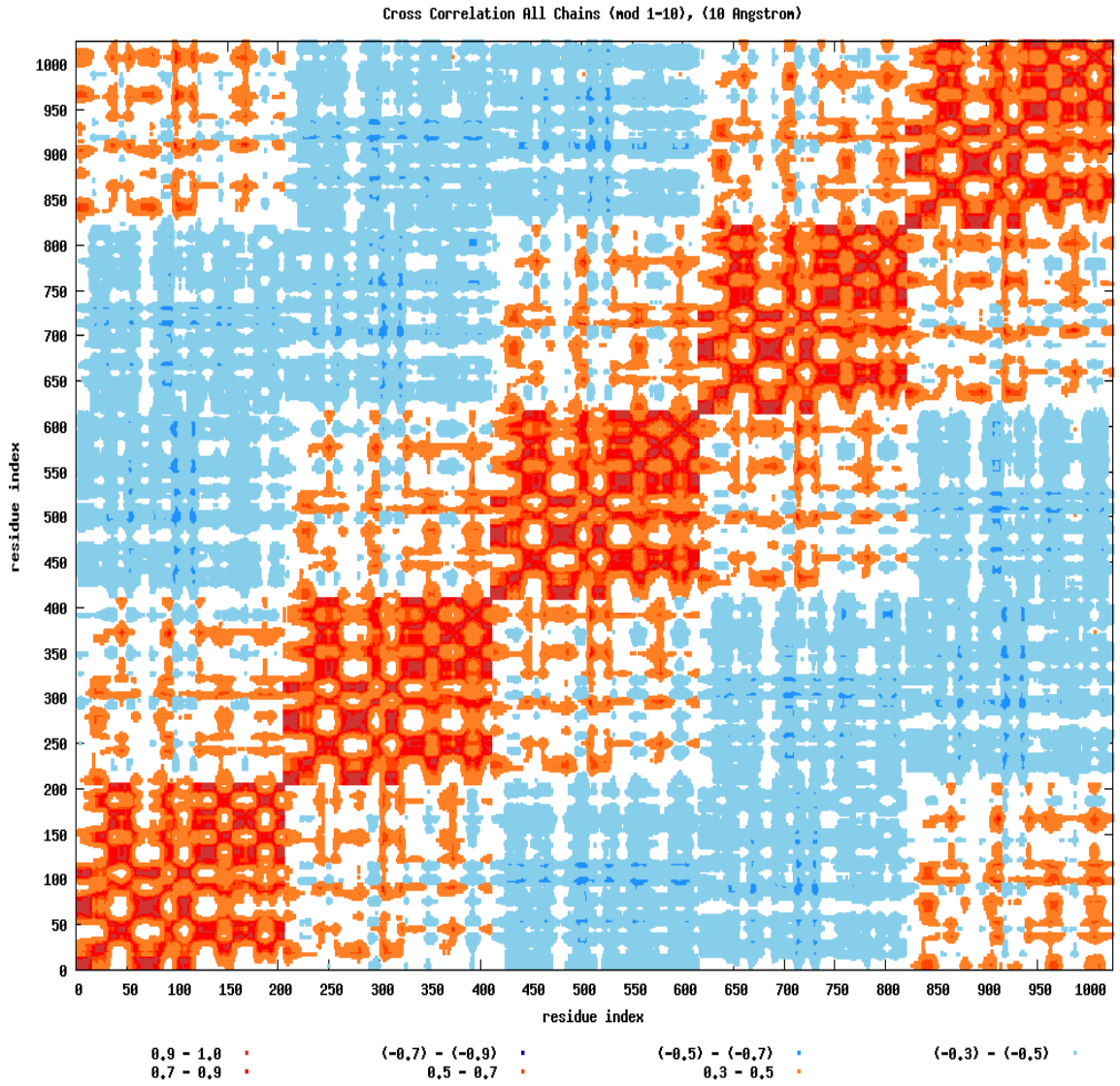

Figure 3.7. Cross correlation map showing all of the five subunits of AChBP.

Figure 3.7 shows that each subunit is positively correlated with its neighbors and negatively correlated with non-neighboring subunits. Since 1i9b is a homopentamer and contains five binding region, one at each interface, it is plausible that the positive correlations are at the neighboring subunits where the residues are close to each other. Negative correlations occur between the non-neighboring subunits where long distances may obstruct positive correlations.

The residues within each subunit are highly positively correlated within themselves. The regions at the lower part of the AChBP, C-termini, seem to be coupled with each other. Loop2, Cys Loop, Loop 9 and Beta 10 regions are close to each other in the space and these regions are positive correlated. Almost all of the binding residues of AChBP have positive

correlations with Loop 1, Beta 2, Beta 7 and beta 8 regions. Loop 2, Cys Loop and Loop 9 also have some positive correlations with binding residues. Loop 2, Cys Loop and Loop 9 regions also have positive correlations with Beta 1 and Beta 2 regions. Beta 1 and Beta 2 regions appear like as the spine of the AChBP molecule. Since they are positively correlated with binding residues and with the some other regions such as Loop 2, Cys Loop and Loop 9, they may act like a bridge between the binding residues and the C-termini of the AChBP molecule.

It was proposed that Loop 2 and Cys Loop of one subunit and Loop 9 of the adjacent subunit are correlated and when these regions come together they straddle the M2-M3 linker of the transmembrane region [10]. But AChBP doesn't have a transmembrane domain region. However, in Figure 3.8, the cross correlations between the A and B subunits show that Loop 9 of subunit B is positively correlated with Loop 2 and Cys Loop regions of subunit A.

The black rectangles in Figure 3.8 show the positive correlation of Loop 2, Cys Loop and Loop 9 regions. It is seen that Loop 2 and Cys Loop of Subunit A is positively correlated with the Beta 10 region of subunit B. Beta 10 is the end of the subunit and in the presence of a TMD, it connects LBD to TMD. Loop 2 and Cys Loop are on the near side of subunit B and show positive correlation with Beta 10. But Loop of subunit A do not have positive correlation with Beta 10 region of subunit B. Loop 9 is on the other side of the subunit and it is not close to the Beta 10 region of subunit B.

The other positively correlated regions are as; Loop 1, Beta 3, Loop 4, Loop 8, Loop 10 and Beta 10 regions of subunit A of AChBP are positively correlated with the alpha helix, Beta 2, Loop 3, Beta 3, Beta 5' (contains two complementary binding residues), Beta 6 (contains two complementary binding residues) and Loop 9 regions of subunit B. And the Loop5, Loop 8 and Loop 10 regions of subunit B is negatively correlated with subunit A.

In Figure 3.8, the intersections of yellow and green rectangles show the correlation between the principle binding residues of subunit A and the complimentary binding residues of subunit B. It is seen that the principle binding residues of subunit A of AChBP are positively correlated with complimentary binding residues of subunit B of AChBP.

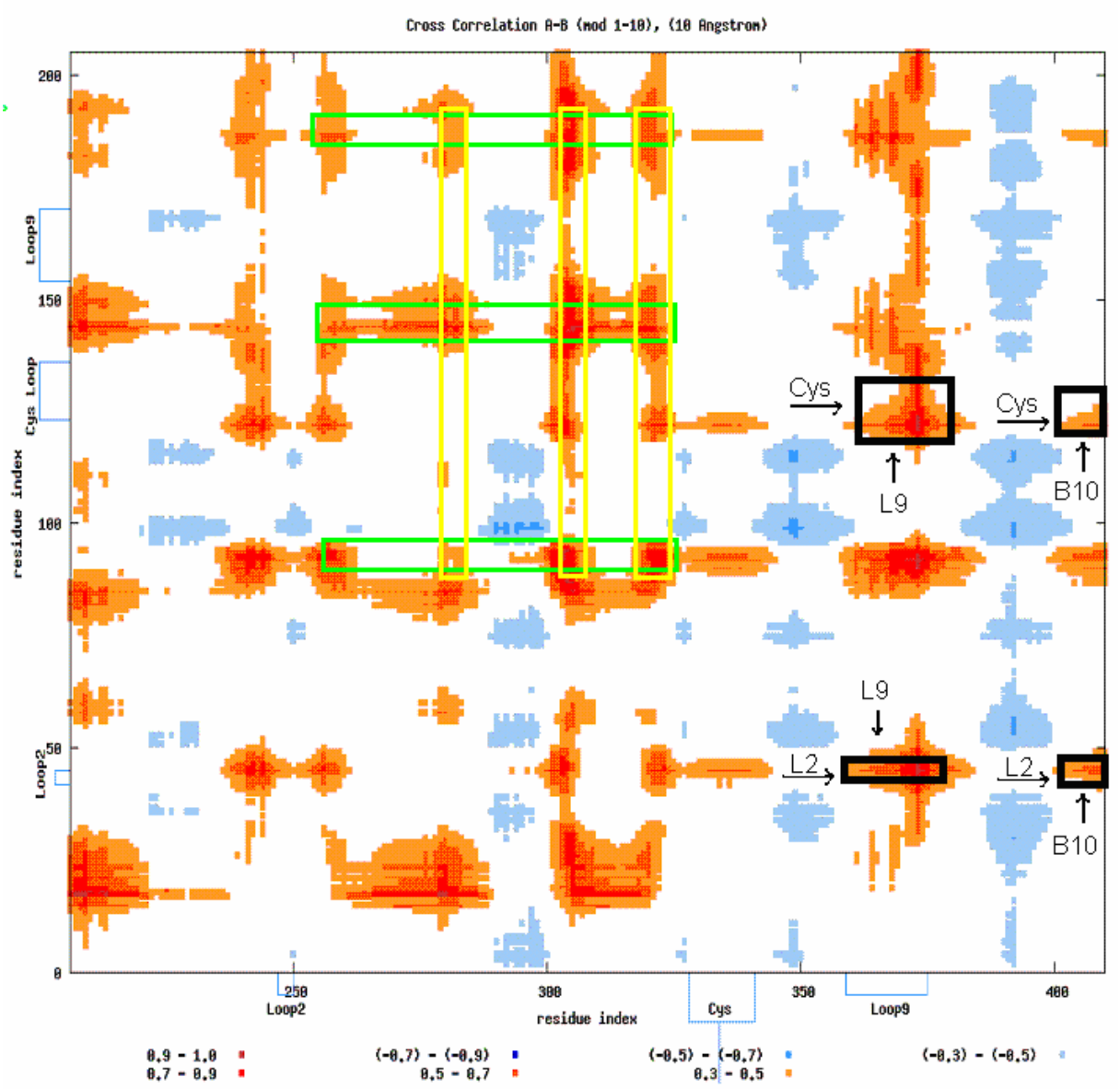

Figure 3.8. Cross correlation map of subunit A and subunit B of AChBP. X axis: Subunit B, Y axis: Subunit A. Green and Yellow rectangles represent the principle binding residues of subunit A and the complimentary binding residues of subunit B respectively.

In the subunit B, the region between the residues 294 and 300 correspond to Loop A of subunit B. The residues between 349 and 354 correspond to the Loop B of subunit B while the residues between 390 and 393 form Loop C regions. These regions contain principle binding residues. Figure 3.8 show that these binding regions of subunit B are positively correlated with the binding regions of subunit A. Since AChBP is a homopentamer the correlations between any two adjacent subunits are all the same.

For the non-neighbor interactions of subunit A and subunit C and subunit D, there aren't any positively correlated regions in the overall correlation map of AChBP. The entire correlation map is covered with negative correlations (APPENDIX B, Figure B.13 and Figure B.14.).

For the other neighbor of subunit A, subunit E stands on the clockwise side of subunit A just like the subunit A stands at the clockwise side of subunit B when viewed from the top of the extracellular side. For the subunit E-subunit A interaction, Loop 2 and Cys Loop of subunit A reside far to Loop 9 of subunit E. However, if it was subunit E-subunit A interaction, it would be the same with the subunit A-subunit B interaction which has already been discussed above. The interactions of subunits are given in the APPENDIX B, Figure B.15.

When these cross correlation evaluations are carried out for the LBD of nAChR without TMD, the cross correlation map totally changes as shown in Figure 3.9. There are 1025 residue in the AChBP molecule but there are 1053 residues in the LBD of nAChR when TMD is extracted. In addition, AChBP is a homopentamer while LBD of nAChR is not a homopentamer.

In the cross correlation maps of AChBP it was seen that each subunit is positively correlated with its two neighboring subunits. But in the cross correlation maps of LBD of nAChR, in Figure 3.9, the subunits do not necessarily make positive correlations with both of their neighboring subunits.

In opposition to the cross correlation maps of AChBP (Figure 3.7), the LBD of nAChR seems to be separated into two clusters according to Figure 3.8. Beta and Delta subunits form one cluster while the other three subunits form the second cluster. The formation of these two clusters increases the amount of negatively correlated regions. Subunits of LBD of nAChR have positive correlation with their neighbors standing at the counter clockwise side (when viewed fro mthe top of the extracellular side). Only Gamma subunit has got positive correlations with both neighboring subunits.

The intramolecular correlations of each individual subunit are almost the same with a similarity of 99 per cent. The intramolecular correlations are made up of positive correlations.

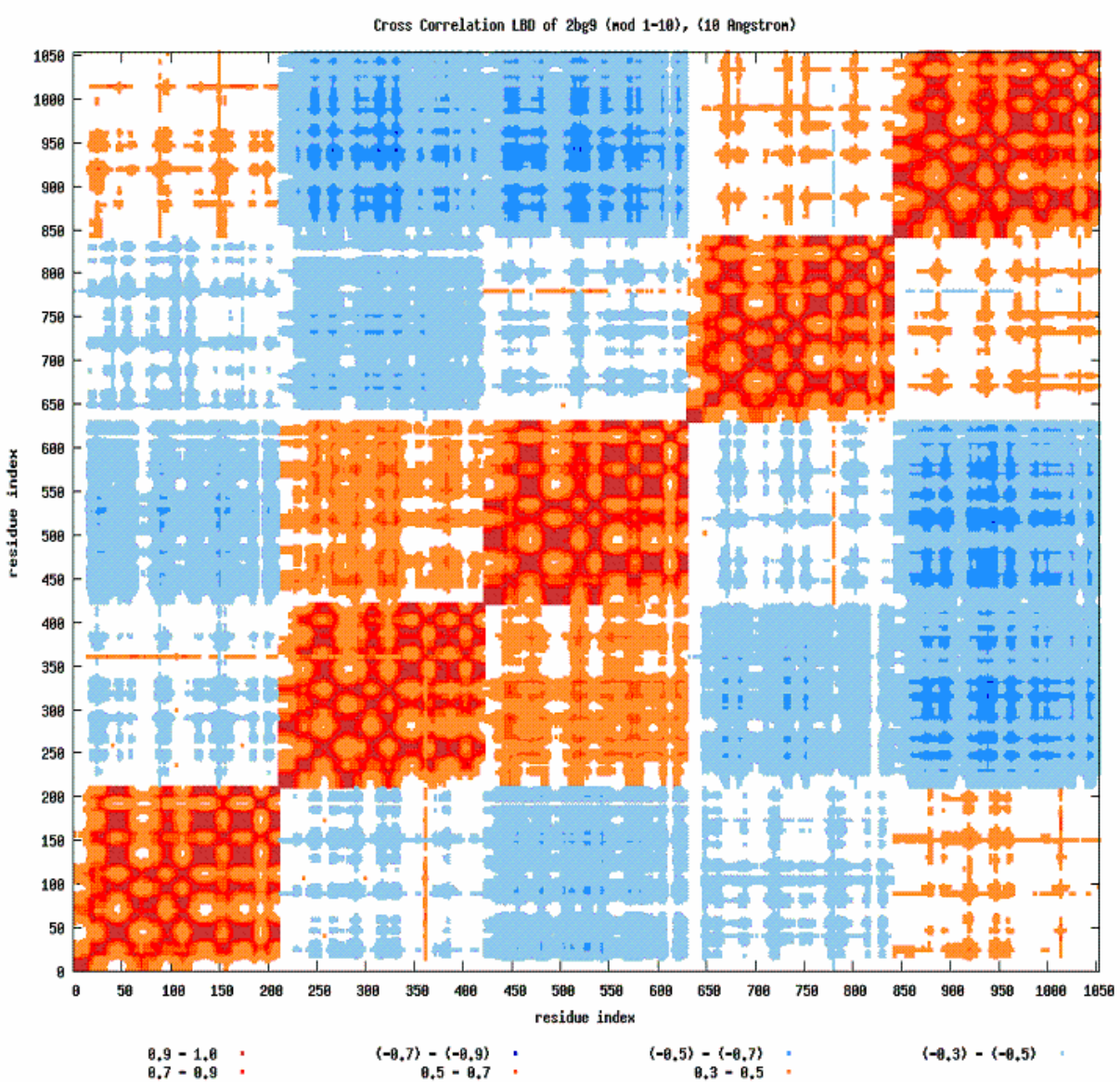

Figure 3.9. Cross correlation map showing all of the five subunits of the LBD of nAChR without the TMD.

Alpha-Gamma and Delta subunits of LBD of nAChR are positively correlated with their neighbor subunits which are located at the counter-clockwise side (from the view of the extracellular side) and they are negatively correlated with their other neighbors. On the other hand, Beta and Alpha-Delta subunits of LBD of nAChR are positively correlated with their neighbor subunits which are on the clockwise direction while they are negatively correlated with their subunits which are at the counter-clockwise direction when viewed from the extracellular side. All of the mentioned directions are from the view of the top of the extracellular side and will be from this view in the following sections. Only the Gamma subunit is positively correlated with its both neighboring subunits. On the negatively

correlated neighbors of each individual subunit there is only one region showing positive correlation, which is the Loop B region.

Loop B is a binding region at the LBD of nAChR. There are five binding regions in AChBP but there are only two binding regions in LBD of nAChR. One of these binding sites of LBD of nAChR is at the interface of Alpha-Gamma and Gamma subunits and the other binding site is at the interface between Alpha-Delta and Delta subunits.

Figure 3.9 shows that Alpha-Gamma is negatively correlated with Beta subunit, but Loop B region of Beta subunit is positively correlated with Alpha-Gamma subunit in the LBD of nAChR. The same situation is also valid between Delta and Alpha-Delta subunits. The Delta subunit is negatively correlated with Alpha-Delta subunit but the Loop B region of Alpha-Delta subunit is positively correlated with Delta subunit. Also this Figure 3.9 is symmetric on the x=y axis.

The names of the subunits in the AChBP were named as A, B, C, D and E lining on the counter-clockwise order [8]. But in the LBD of nAChR the subunits are labeled in the opposite direction [3]. For example, subunit B is on the counter-clockwise direction of subunit A in the AChBP molecule but Beta subunit is on the clockwise direction of Alpha-Gamma subunit in the LBD of nAChR. So the subunit A–subunit B interaction of AChBP corresponds to the subunit A–subunit E interaction in the LBD of nAChR.

Among the binding loops of Alpha-Gamma subunit of the LBD of nAChR, only Loop B is slightly positively correlated with the Loop 2, Cys Loop and Loop 9 regions of Gamma subunit of the LBD of nAChR. This Loop B region is positively correlated with each region of Gamma subunit. The other binding loops, Loop A and Loop C have positive correlations with Gamma subunit except the Loop 2, Cys Loop and Beta 10 regions of Gamma subunit in the LBD of nAChR.

The Loop 2 and Cys Loop regions of Alpha-Gamma subunit are close to Loop region of Gamma subunit in space. Loop 9 region of Alpha-Gamma subunit is close to the Loop 2 and Cys Loop regions of Beta subunit in the LBD of nAChR. Loop 2 and Cys Loop of Alpha-Gamma subunit is positively correlated with the Loop 9 region of Gamma subunit in the LBD of nAChR as seen in Figure 3.10.

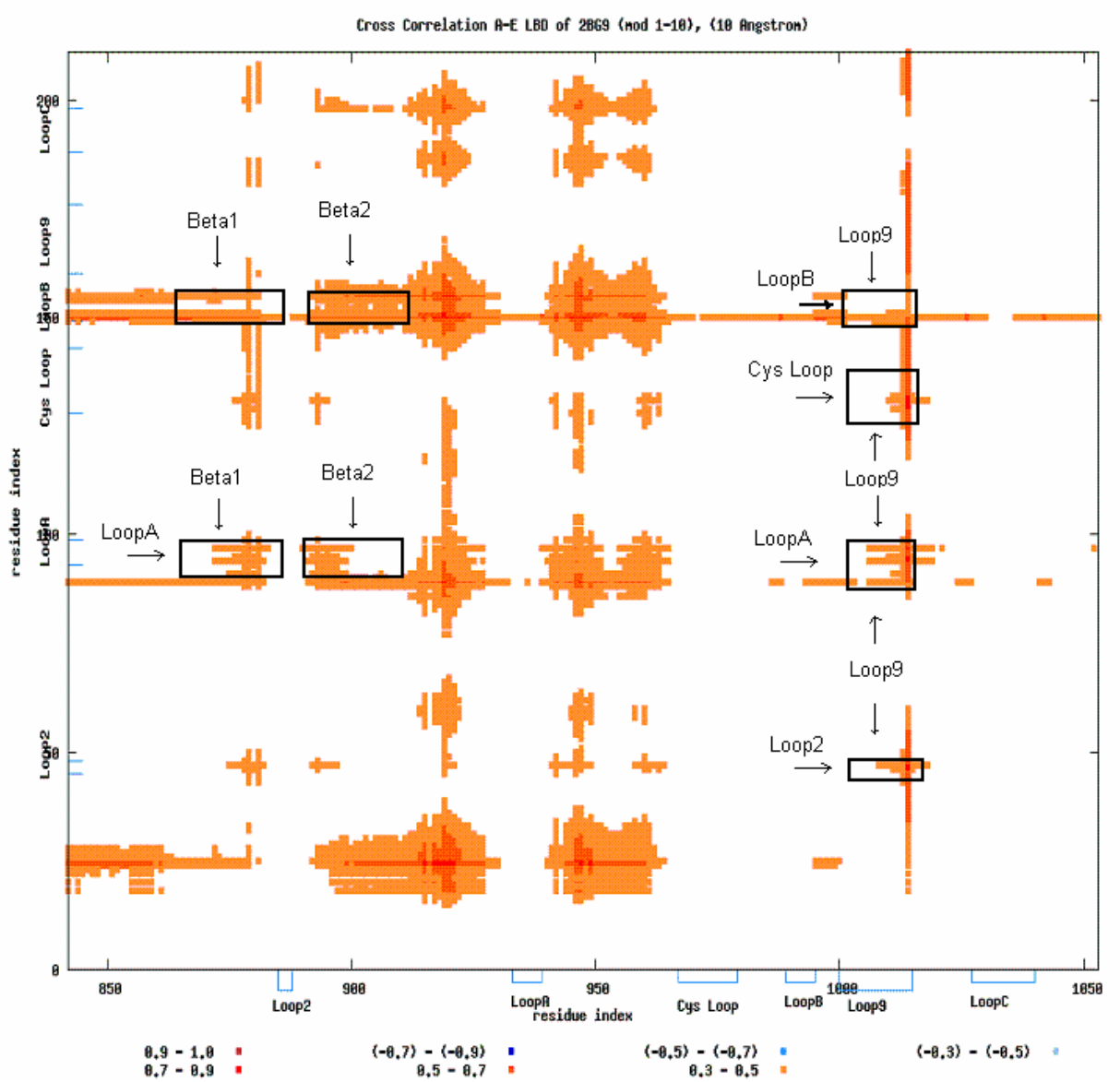

Figure 3.10. Cross correlation map of Alpha-Gamma and Gamma subunits of LBD of nAChR.

Figure 3.10 shows that two binding loops of Alpha-Gamma subunit, Loop A and Loop B, are positively correlated with the Beta 1, Beta 2 and Loop 9 regions of Gamma subunit of LBD of the nAChR. The latter regions are specially showed because these regions will appear at the MCPOOL results in section 8.

One can see a contrast between Figure 3.10 and Figure 3.8. For the AChBP, it was shown that the Loop 2 and Cys Loop regions of subunit A are close to Loop 9 region of subunit B and these regions were positively correlated. But in the case of LBD of nAChR

when no TMD exist, Loop 2 and Cys Loop regions of Alpha-Gamma subunit are close to Loop 9 region of Gamma subunit in space and these regions are positively correlated.

When we look at the correlations between Loop2 and Cys Loop regions of Alpha-Gamma subunit and the Loop 9 region of Beta subunit, there are only one or two positively correlated residues APPENDIX B, Figure B.16.

The correlations between non-neighboring subunits are totally negative correlations in LBD of nAChR. There aren't any positive correlations between non-neighboring subunits as it was seen in AChBP molecule. Also the correlations between two alpha subunits are negative. On the other hand Beta and Delta subunits are highly positively correlated with each other.

In GNM outputs for the LBD of nAChR, Figure 3.9 shows that Alpha Gamma subunit is positively correlated with its neighbor on the counter-clockwise side (Beta subunit). But Alpha-Delta subunit is positively correlated with its neighbor on the clockwise direction (with Gamma subunit). This behavior of the subunits make the molecule to be splitted into two clusters as mentioned before. Loop B and Loop C regions of Alpha-Delta subunit aren't positively correlated with any of the regions of Gamma subunit. But the Loop B and Loop C regions of Gamma subunit are positively correlated with all regions of Alpha-Delta region. Also each of the binding loops of Gamma subunit are positively correlated with the Beta 10 region of Alpha-Delta subunit APPENDIX B, Figure B.17.

As shown on Figure 3.7 and Figure 3.9 the alpha subunits of AChBP and the LBD of nAChR behave differently. When Alpha-Gamma subunit correlates positively with Gamma subunit, Alpha-Delta subunit correlates negatively with Delta subunit. However, the binding regions are thought to be at these two interfaces. One is at the interface between Alpha-Gamma and Gamma subunits and the other is at the interface between the Alpha-Delta and Delta subunits [3]. Since the subunits around these interfaces show different correlations the molecule may not move cooperatively. One subunit may go one way while the other subunit move to the opposite side. These three dimensional movements will be discussed in section 3.2.

GNM calculations have also been carried out for the full structure of nAChR. When a TMD exists under LBD, the total number of negative correlations decrease. The correlations

between the subunits become more positive and the amount of the positive correlations increases. Each of the subunits makes positive correlations with their both neighbors but these positive correlations are not as much as the subunits of AChBP. The LBD of nAChR when there is TMD forms two clusters as it was the case when there wasn't a TMD. The correlations between subunits are shown in Figure 3.11.

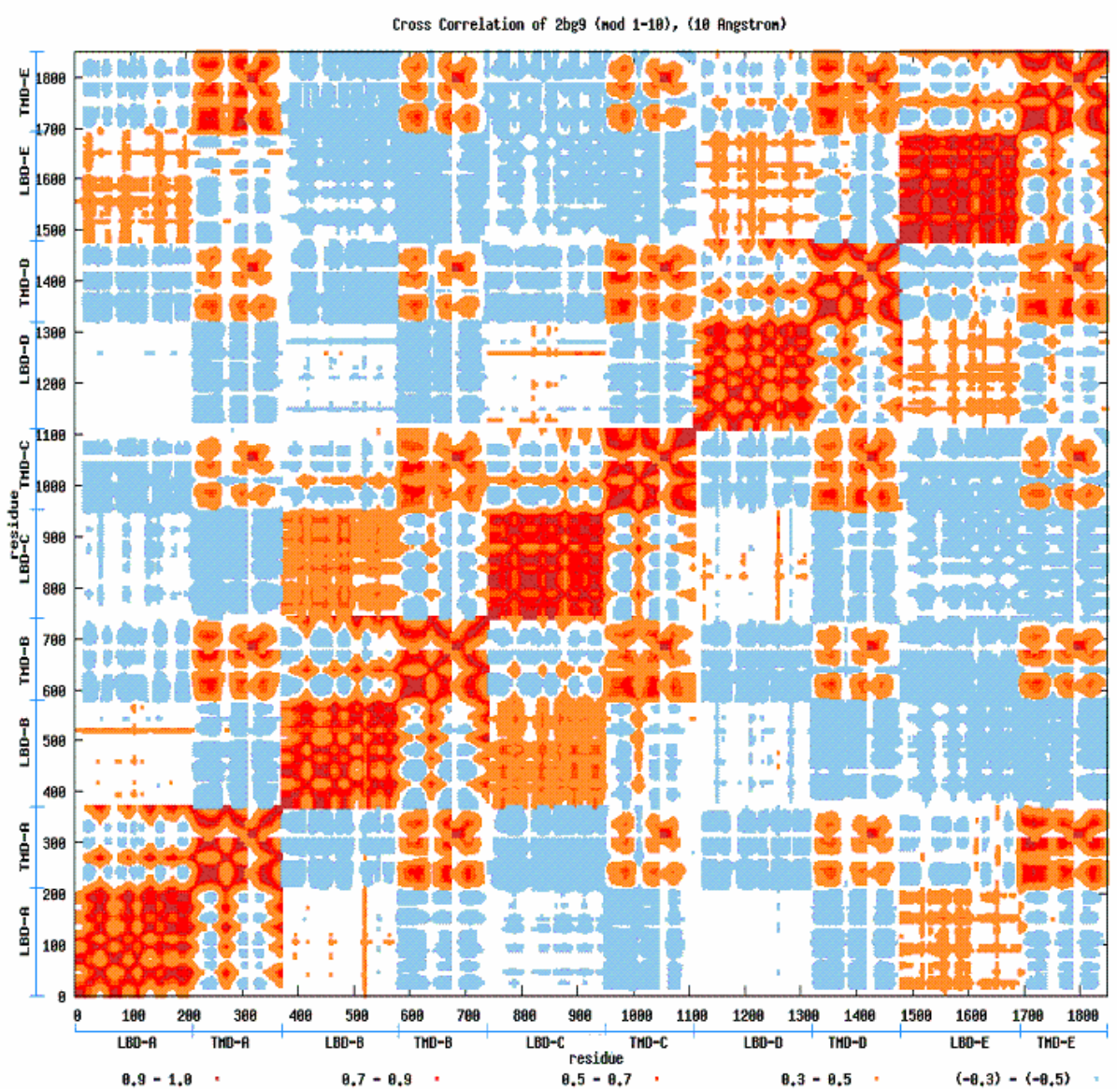

Figure 3.11. Cross correlation map showing all of the five subunits of the full structure nAChR.

In the GNM analysis of LBD of nAChR without TMD, there are 1053 residues in the system. When the full structure of nAChR is analyzed, there are 1849 residues. The increase

in the total residue number of the system changes some cross correlations as seen in Figure 3.11.

The correlations between the transmembrane sections of each subunit in the nAChR are totally positive. LBDs are positively correlated with the TMD of their own subunit. All of the transmembrane regions are positively correlated with each other. One residue may not have positive correlation with any residues located at the TMD of another subunit. Since it is positively correlated with the residues of its own TMD, the residue at the TMD can be positively correlated with the other residue located at the TMD of the other subunits. In the MCPOOL section, section 3.8, these positive correlations will be used to connect positively correlated residues to seek if there are any possibilities to go from one residue to another one.

In Figure 3.11, Alpha-Gamma subunit seems to have more positive correlations with Gamma subunit than it has with Beta subunit. And the other alpha subunit, Alpha-Delta subunit seems to have more positive correlations with Gamma subunit too.

Loop B region of Beta subunit is positively correlated with the gate region and LBD of Alpha-Gamma subunit (see APPENDIX B, Figure B.18.). In addition, Alpha-Gamma subunit is positively correlated with the Gamma subunit as seen from Figure 3.12. The total amount of positively correlated residues are much more than the positive correlations observed between these Alpha-Gamma and Gamma subunits while LBD of nAChR was extracted from the full structure. However, LBD of Alpha-Gamma is not positively correlated with the LBDs of its non-neighboring subunits.

The correlations between Alpha-Gamma and Gamma subunits of nAChR are shown in Figure 3.12. The LBDs and TMDs are positively correlated within themselves. The LBD of Gamma subunit has some positive correlations with TMD of Alpha-Gamma. However, LBD of Alpha-Gamma has got positive correlation with the TMD of Gamma only at the M2-M3 Loop.

Loop 2 and Cys Loop regions of Alpha-Gamma subunit has positive correlations with Loop 9 region of Gamma subunit. Loop B of Alpha-Gamma subunit seems to be positively correlated with the M2-M3 Loop of Gamma subunit. This result also agrees with the cross correlation studies of Andrew McCammon et al [14]. In addition, Loop 9 region of Gamma is

positively correlated with the M2-M3 Loop of Alpha-Gamma subunit. In Figure 3.12, Beta 10 regions are showed within the green rectangles.

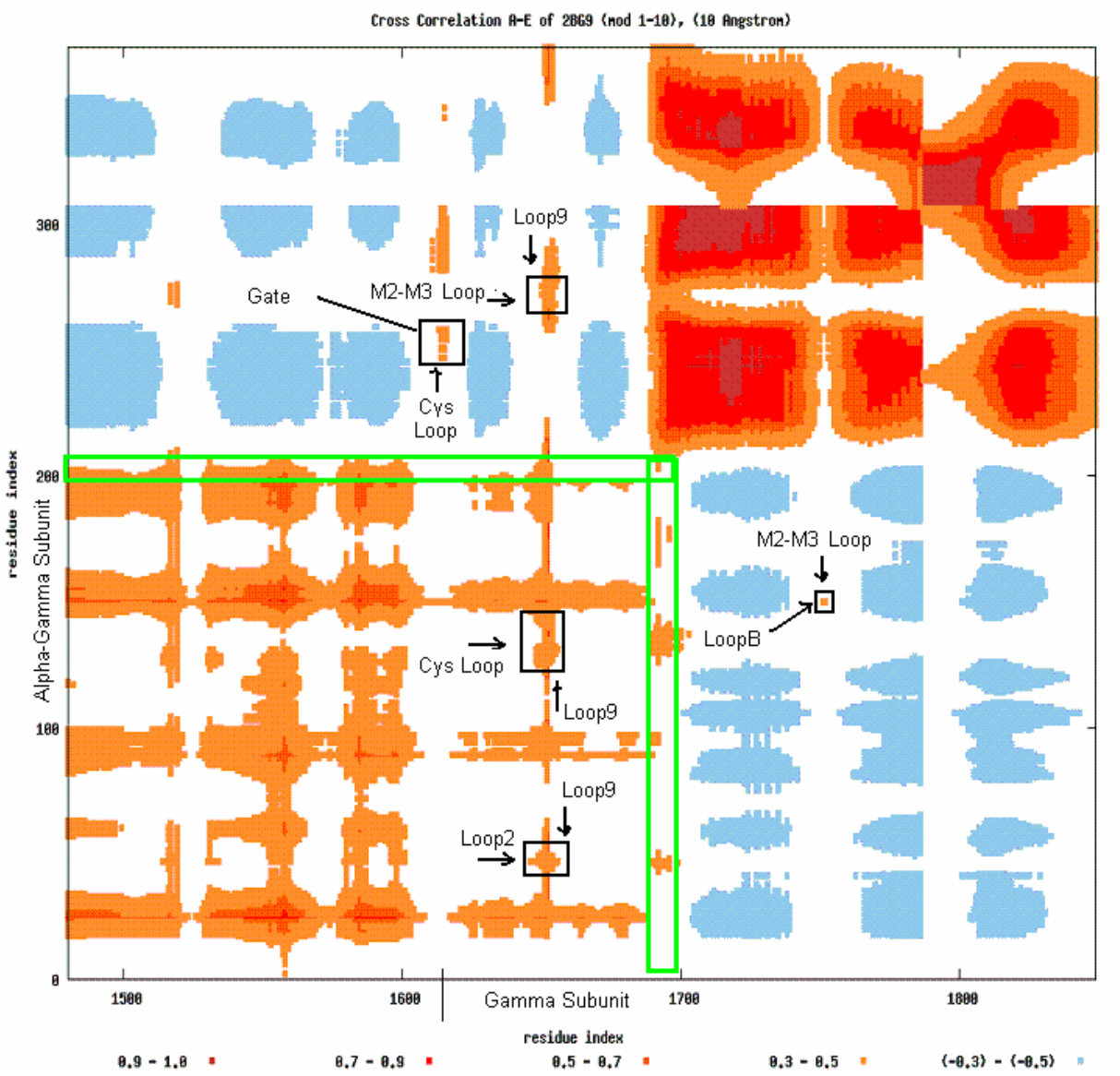

Figure 3.12. Cross correlation map of Alpha-Gamma and Gamma subunits of nAChR. Green rectangle: positions of Beta10 and Beta10-M1 regions.

In the absence of TMD, when LBD of nAChR is studied separately, these Beta 10 regions do not seem to have positive correlations with any other regions. But in the presence of a TMD, Beta 10 region of Gamma subunit makes positive correlations with Loop2, Cys Loop and Loop 9 regions of Alpha-Gamma subunit and vice versa. Won Yong Lee and Steven M. Sine suggested in one of their studies that [27], after the binding of an agonist Loop

C caps the binding site. They suggest that this capping motion is propogated through the interface of LBD and TMD through the Beta 10 region [27].

Cys Loop region of Gamma subunit is positively correlated with the Gate region of Alpha-Gamma subunit as seen in Figure 3.12. This Cys Loop of Gamma subunit is also positively correlated with the upper half of M2 and M3 regions of the Alpha-Gamma subunit. In addition, the Loop 9 region of Gamma subunit seems to be positively correlated with the upper half or the M4 region of Alpha-Gamma subunit.

The ligand binding domains of both Alpha-Gamma and Gamma subunits are highly positively correlated with each other. Mainly, Loop A, Loop B and Loop C regions of Alpha-Gamma subunit are positively correlated with alpha-helix, Loop 1, Beta 1, Beta 2, Beta 3, Beta 5' and Beta 6 regions in addition the Loop 9 and Beta 10 regions of Gamma subunit.

The Beta 1, Beta2, Loop 2, Cys Loop, Binding Loops and Loop 9 are highly correlated with each other. Also in the cross correlation figures of the full structure of nAChR the Beta 10 region appears to be positively corrlated with the regions mentioned above. Also it is seen that the binding loops are positively correlated with Loop 2, Cys Loop and Loop 9 regions and these regions are also positively correlated with gate regions if TMD is connected with LBD.

The LBD at the full structure of nAChR shows some similar correlations with the LBD of nAChR when no TMD exists. But the existence of a TMD leads the molecule make more positive correlations. But in the case of AChBP the molecule shows much more differences with respect to the LBD of the nAChR.

Correlations between the subunits are different for AChBP and nAChR. In the case of AChBP all of the subunits make the same correlations because it is a homopentamer. But in the case of nAChR, even a TMD exists or not, the molecule is partitioned into two clusters. The correlations between Beta and Delta subunit are strongly positive. These clusters are shown in Figure 3.13.

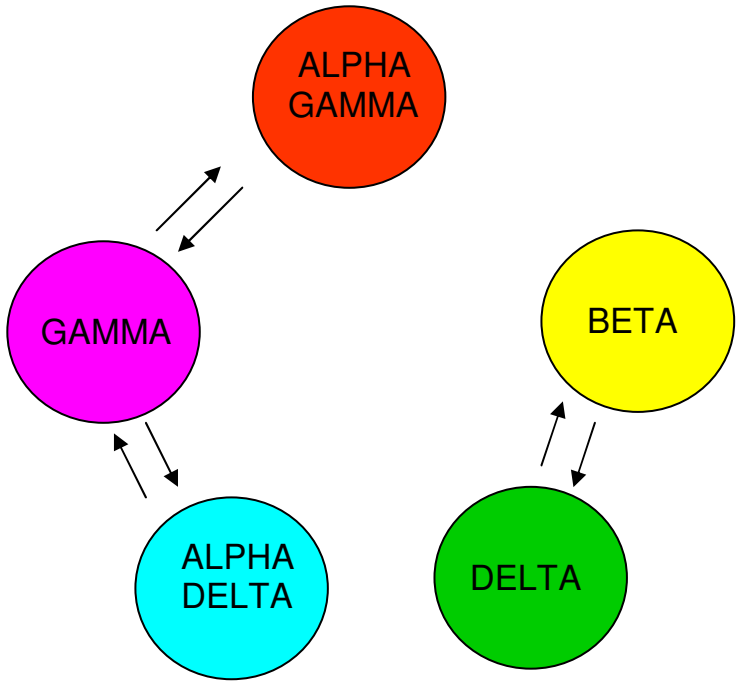

Figure 3.13. View of the subunits from extracellular side. Arrows represent the positive correlations. Directions of the arrows mean that the subunit at the starting side of the arrow is positively correlated with the subunit showed by the end of that arrow.

3.2. ANM Calculations

Using ANM, the conformations that describe the fluctuations from the average structure, which is the X-ray structure here, in the slowest modes of motion are presented and analyzed here for AChBP, the LBD of nAChR while TMD is extracted and for the full structure of nAChR.

To see the transitions from one conformation to the other conformation, the vectors that describe the direction of the fluctuations are rescaled by multiplying them with an arbitrary constant and then these new rescaled vectors are added and extracted from the original average conformation to get two conformations, which will be referred as positive and negative conformations respectively from this on.

In the slowest modes of motion, eight slowest modes by ANM have been elaborated. These conformations are visualized on VMD software to study the behaviors reflected by these modes [43].

3.2.1. ANM Analyses for AChBP

The slowest first mode displays a breathing motion of AChBP as shown in Figure 3.14. All of the subunits, except the Alpha-Gamma subunit, move through in and out of the pore. Alpha-Gamma subunit in AChBP moves parallel to the pore axis, which means that this subunit doesn't expand as much as the other subunits.

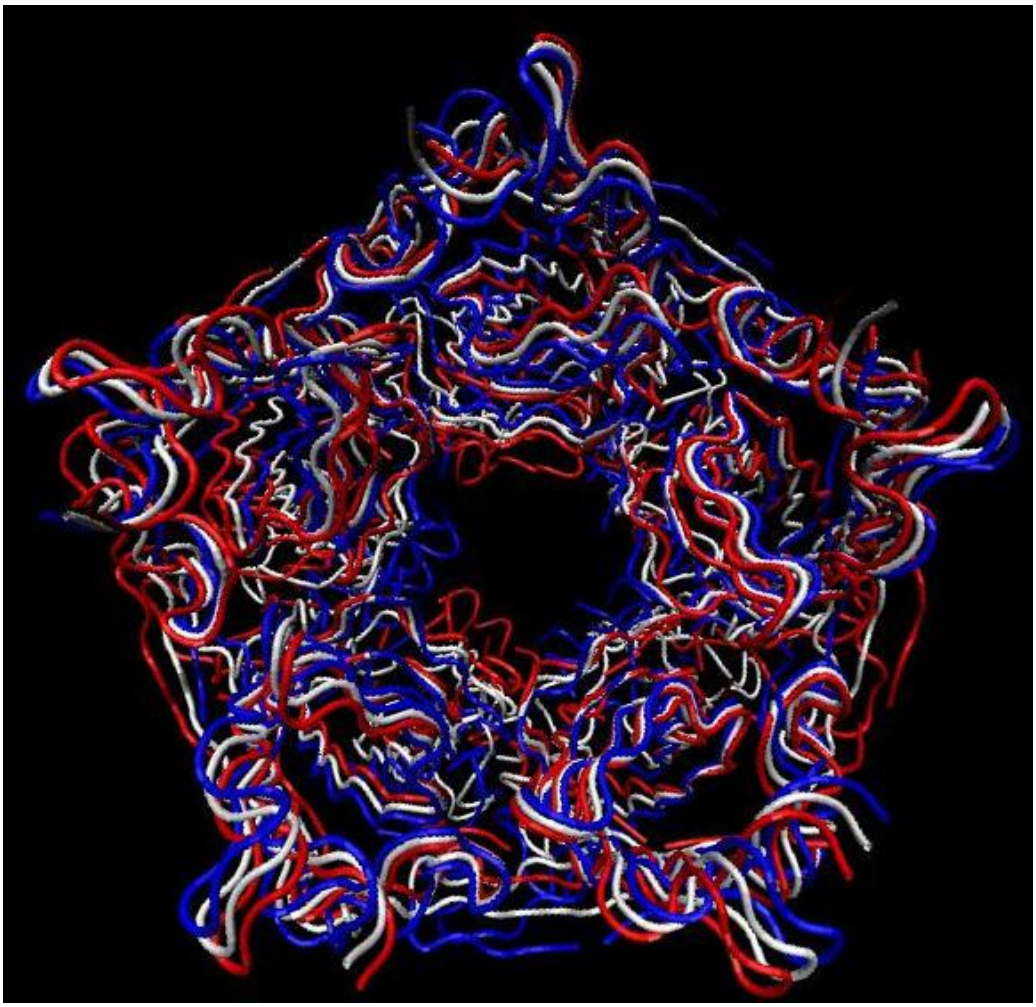

Figure 3.14. Graphic representation of AChBP for the first mode of ANM. White: Original conformation, Blue: Negative conformation, Red: Positive conformation.

If we take a close look at Figure 3.14, it can be seen that when positive conformation of one subunit moves into the channel pore, the positive conformations of other four subunits move outwards. For example, if we follow the blue conformation (negative conformation) in the figure, the negative conformation in the lower left part seems that it has moved to the clockwise direction of the original average conformation but the negative conformation in the

lower right part seems that it has moved to the counter-clockwise direction of the original average conformation. If it was a twisting motion, the motion of each conformation should have been in the same direction.

A similar breathing motion is also observed in the slowest second mode. When two Alpha subunits (Alpha-Gamma & Alpha-Delta) move towards the pore axis, Gamma and Beta subunits moves outwards. Delta subunit neither moves inward the pore nor moves outwards the pore. It sways parallel to the pore axis.

The slowest third mode also displays a breathing motion, but this time the channel stretches more than that is observed in the first two modes. Despite the breathing motion of the molecule, Alpha-Delta subunit twists on its own axis. Each time it twists, it takes one of its adjacent subunit inwards the channels pore while the other neighbor subunit is taken outwards.

The slowest fourth mode also shows a breathing motion in which the stretching of the molecule is smaller than the observed one in the third mode. Delta and Gamma subunits move inwards the channel while Alpha-Delta subunit moves outwards. Meanwhile, Alpha-Gamma and Beta subunits twist on their own axis's slightly

Slowest fifth mode displays a breathing motion and is very similar to the one observed in previous slowest modes. The upper part of the molecule (N-terminal) seems to be more mobile than the lower part (C-terminal) of the molecule. Actually it can be said that the lower hardly moves and the Alpha-Delta subunit is the least mobile along the five subunits.

So far the movements of the subunits are observed to be similar. The actual behavior of the system is identical but the subunits differ in each individual mode. When one subunit moves in a one way, the other subunit makes the same movement in the other mode and this is valid for the first five slowest modes. The main reason of this situation is the homopentamer structure of the AchBP.

At the sixth mode of ANM calculations for AChBP molecule, the molecule seems to be separated into two portions where Beta and Delta subunits form a couple and the other three subunits (Alpha-Gamma, Alpha-Delta and Gamma) form another. These couples seem

to move together where Beta and Delta moves outward from the channel while Alpha-Gamma, Alpha-Delta and Gamma subunits move inwards the channel.

Seventh mod is similar to the first mode behavior. When Delta, Alpha-Delta and Gamma move inwards the channel Alpha-Gamma moves outwards and Beta moves parallel to the channel pore axis. The upper part of Alpha-Delta is the most mobile while the upper part of Beta is the least.

There is an impressing motion in the eighth mode where the molecule makes a twisting motion (Figure 3.15) on the contrary of breathing motion that has been observed at the previous modes. The upper part (N-terminal) and the lower part (C-terminal) moves in the opposite directions. The alpha helices of the molecule seem to close on the adjacent subunit that may be a sign of closing over the binding region.

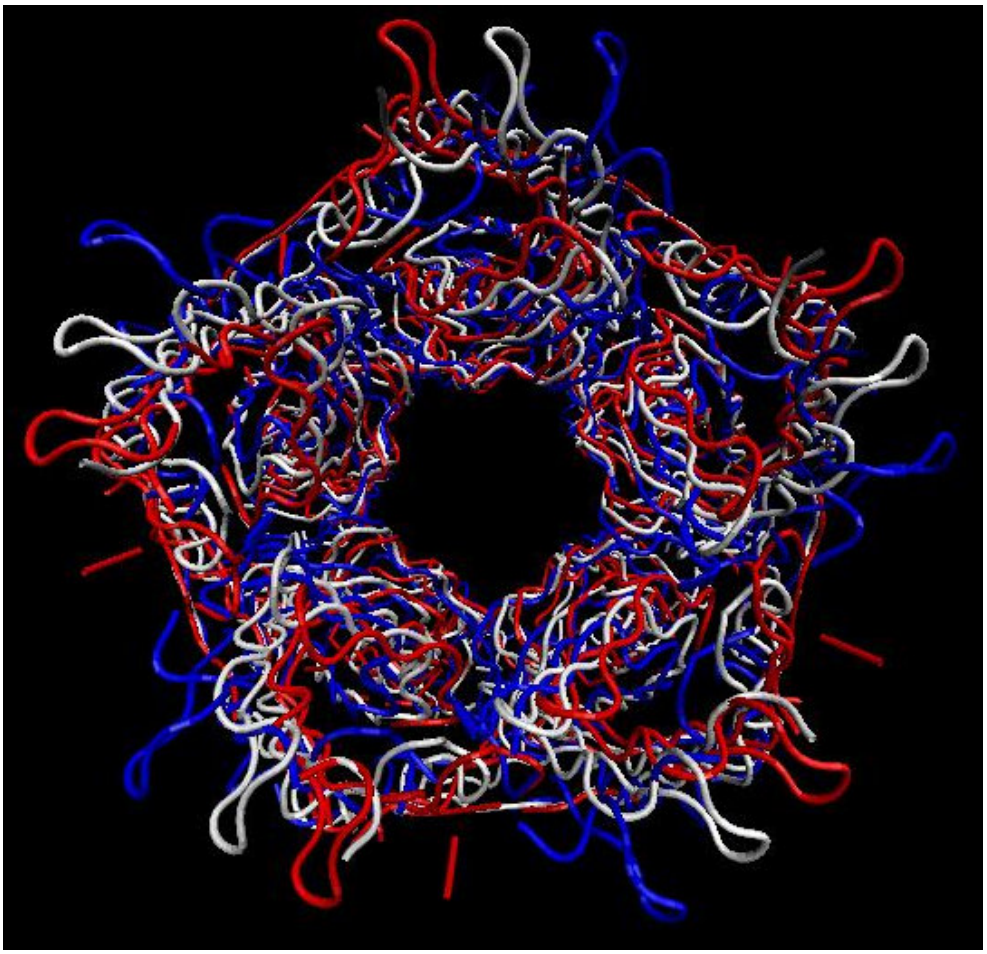

Figure 3.15. Graphic representation of AChBP for the eighth mode of ANM. White: Original conformation, Blue: Negative conformation, Red: Positive conformation.

3.2.2. ANM Analyses for LBD of nAChR without TMD

When LBD of nAChR is taken as a separate molecule and analyzed to observe conformational changes in the slowest, the following observations are held:

In the slowest first mode, the molecule oscillates from the central point which means that when the upper half of the molecule moves one side, the other half moves to the other side. In other words the molecule sways from one side to the other side keeping the middle of the molecule as a pivot point. Unlike AChBP, a breathing motion doesn't occur in this molecule when the LBD of nAChR is supposed to be alone without the TMD.

The behavior observed in the second slowest mode of AChBP has also been observed in the second slowest mode of LBD of nAChR. When the LBD of nAChR is taken as a separate molecule, the beta and delta subunits move cooperatively. When these subunits move one side (for example into the channel pore) the alpha subunits move to the other side (in this case through out of the pore axis) leading the molecule to make a breathing motion.

Even though a twisting motion has been observed for the subunits (not for the molecule) of AChBP in the third slowest mode, none of the subunits of LBD of nAChR does this motion in this mode. Its alpha-gamma and gamma subunits move in the opposite direction of beta and alpha-delta subunits. The beta and alpha-delta subunits move cooperatively instead of beta and delta subunits in the case of the second slowest mode of LBD of nAChR.

The forth slowest mode is a little bit different than the fourth motion of AChBP. Actually the behavior of the molecule is similar to the motions observed at the third slowest mode of LBD of nAChR. But this time the alpha-gamma and gamma subunits move towards each other by a small twisting movements. These two subunits close over each other and when they close they move inwards the channel pore by pushing alpha-delta and beta subunits out of the channel pore.

In the fifth mode of LBD of nAChR, the alpha-delta subunit turns around itself and every time it turns it pushes the adjacent subunits. When it moves to clockwise direction, it pushes the gamma subunit into the pore and when alpha-delta moves in the counter-clockwise direction it pushes the delta subunit into the pore. Meantime, the delta subunit moves

cooperatively with the alpha-gamma subunit and the gamma subunit moves cooperatively with the beta subunit.

At the sixth slowest mode, the molecule seems to be separated into two portions where Beta and Delta subunits form a couple and the other three subunits (Alpha-Gamma, Alpha-Delta and Gamma) form another. These couples seem to move together where Beta and Delta moves outward from the channel while Alpha-Gamma, Alpha-Delta and Gamma subunits move inwards the channel.

In the seventh slowest mode, the upper halves of each subunit are more mobile than the lower halves. Also the mobility of alpha-gamma, beta and delta subunits are greater than the mobilities of alpha-delta and gamma subunits. In this seventh slowest mode of nAChR a very small breathing motion reigns the molecule.

In the eighth slowest mode, there is a breathing motion. No twisting motion occurs in this mode as it has been observed in the eighth slowest mode of AChBP. The Beta and Delta subunits move cooperatively forming a couple while these subunits move in the opposite directions of alpha subunits. In this eighth slowest mode of LBD of nAChR, the alpha delta subunit moves as a rigid body moving from one side to other side. The upper part and the lower part of the subunit move together on the same direction.

3.2.3. ANM Analyses for the full structure of nAChR

A twisting motion is observed in the first mode. Each subunit closes onto the adjacent subunit at the LBD and the most closure is seen at the alpha subunit. The LBD rotates in the opposite direction to the transmembrane domain leading the molecule to make a twisting motion. Figure 3.16 shows such twisting motion of the nAChR molecule.

If we take a close look at the Figure 3.16, it is seen that the positive conformations of each subunit, for an example, are on the clockwise direction of the original conformation. This shows that all of the subunits move towards the same direction. But in the case of breathing motion the conformations of each subunit are on different sides just as showed in Figure 3.14.

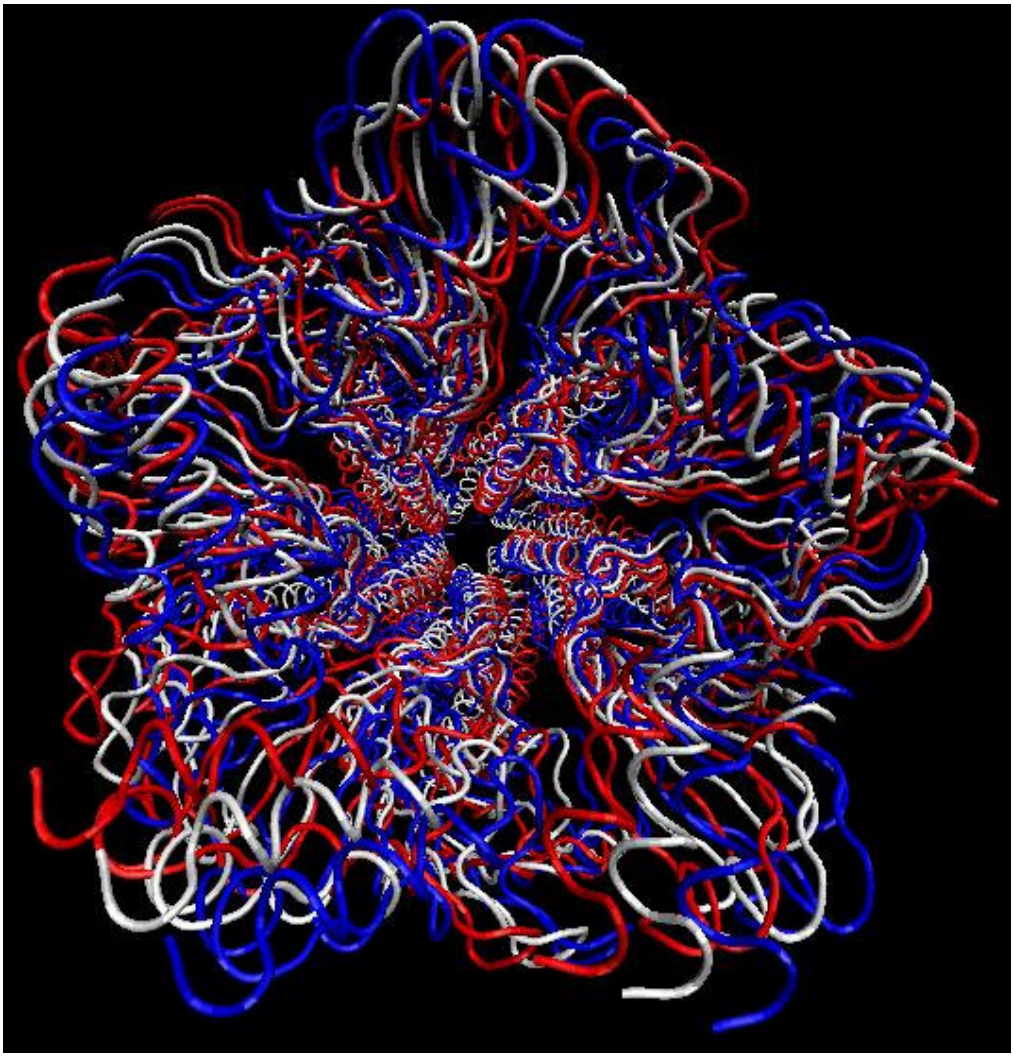

Figure 3.16. Graphic representation of nAChR for the first mode of ANM. White: Original conformation, Blue: Negative conformation, Red: Positive conformation.

In this motion, Cys Loop and Loop2 straddle M2-M3 loop of transmembrane domain and push it in the opposite direction of the ligand binding domain while Loop 9 of adjacent subunit moves away from M2-M3 Loop.

In the third slowest mode, no breathing motion is observed. The whole molecule bends cooperatively within each domain but domains move to opposite directions. This bending motion means that while transmembrane moves through one side, the other two domains (ligand binding and cytoplasmic) move through the opposite side. It is also seen that the cytoplasmic region is the most mobile region among the molecule.

In the fourth slowest mode, the full structure of nAChR is more mobile than the motions observed at the previous modes. This time both alpha subunits move inwards the pore while the other three subunits move outwards which shows that the alpha subunits act together. Although the ligand binding domain is very mobile, transmembrane domain seems to be more stable.

In the fifth slowest mode, Alpha-Gamma and Delta subunits move outwards, Beta subunit moves inwards and in the mean time Alpha-Delta and Gamma subunits get closer to the channel by spinning on the opposite directions. But all of these motions observed in the fifth slowest mode of nAChR are carried out cooperatively on the subunit basis which means the ligand binding and transmembrane domains move as a whole rigid body.

For the sixth slowest mode, a breathing motion is observed. Gamma subunit closes over Alpha-Gamma subunit, Alpha-Gamma subunit closes over Betasubunit, and Delta subunit closes over Alpha-Delta subunit while Beta and Alpha-Delta subunits move outwards the channel. But even these regions of ligand binding domain move this much, the mobility of transmembrane domain are less than the mobility of ligand binding domain.

In the seventh slowest mode, the negative conformation of seventh mode is similar with the negative conformation of the slowest fist mode. The twisting motion can be seen in this mode too. Cys Loop and Loop2 move together and the Loop9 of adjacent subunit gets close to this two loops. These regions form a mobile socket which covers M2-M3 linker leading it to be pushed in the opposite direction of ligand binding domain.

In the eighth slowest mode of nAChR molecule, the subunits twist around themselves. But this twisting motions do not make the whole molecule twist. For example, the ligand binding domain of Delta subunit turns around itself but doesn’t close over Alpha-Delta subunit.

Same spinning motion is valid for Beta subunit but it spins through the other side of Delta subunit instead of closing over Delta. Both alpha-Gamma and Alpha-Delta subunits spin around themselves to close over Gamma subunit. The transmembrane domain also seems to be more mobile than the motions it has in the other modes.

So far the movements of each subunit in the molecule have been investigated. In most of the modes of AChBP except the eighth mode, a breathing motion dominates the molecule and for all of the modes of LBD of nAChR the breathing motion is observed. But when a TMD is attached to the LBD as it is in the full structure of nAChR, the first mode shows a total twisting motion where the LBD and the TMD move in the opposite directions.

Since the first modes have more contribution and significance on the total motions that the molecule may show, the twisting motion of the first mode of nAChR carries a big importance showing that the molecule twists the M2-M3 linker by the help of cys loop, Loop2 and Loop9 regions of LBD.

Up to now only the relative motion characteristics of each individual subunit have been analyzed for eight different modes but nothing has been said if these motions can lead to any changes in the pore radius. To evaluate the changes in the pore volume, HOLE program [35] is used.

3.3. HOLE Analyses

The conformations that describe the fluctuations from the average structure in the slowest 10 modes by ANM were further analyzed with respect to the changes in the pore radius with the fluctuations. For this, the software HOLE was utilized [35]. HOLE calculates the radius of of the pore at any point, thus find the narrowest regions and how the radius' of those putative regions change throughout the pore.

To this aim, Table 3.1 displays the differences between the positive and negative conformations of AChBP, LBD of nAChR without the transmembrane region, and the full structure of nAChR in a given mode at the narrowest region.

The narrowest part of AChBP pore is situated at the lower part of the molecule, namely at the C-terminal region. The radius of this region is calculated as 6.761 Å in unperturbed, native average conformation. None of the 10 modes led to the conformations that have a greater radius value than the latter, except the negative conformations in the sixth and eighth modes.

Table 3.1. Minimum radius values of AChBP, the LBD of nAChR as a separate structure and the full structure of nAChR at their narrowest sections. (-conf) shows the value of minimum radius at the negative conformation, (+conf) shows the value of minimum radius at the positive conformation.

	AChBP			LBD of nAChR			nAChR		
Mod #	(- conf)	original	(+ conf)	(- conf)	original	(+ conf)	(- conf)	original	(+ conf)
Mod 1	6.311	6.761	4.655	5.128	4.787	4.548	2.727	2.171	2.576
Mod 2	5.364	6.761	5.341	4.896	4.787	4.615	2.359	2.171	2.266
Mod 3	4.242	6.761	4.049	4.721	4.787	4.829	2.602	2.171	2.517
Mod 4	4.446	6.761	3.919	4.661	4.787	4.362	2.053	2.171	2.45
Mod 5	6.747	6.761	4.141	5.032	4.787	4.403	2.127	2.171	2.465
Mod 6	6.971	6.761	4.338	4.698	4.787	4.658	2.598	2.171	2.522
Mod 7	4.611	6.761	6.708	4.599	4.787	5.159	2.618	2.171	2.692
Mod 8	7.162	6.761	6.370	4.210	4.787	4.597	2.328	2.171	2.397
Mod 9	5.328	6.761	5.662	4.557	4.787	4.487	2.152	2.171	2.513
Mod 10	6.396	6.761	6.253	4.331	4.787	4.408	1.942	2.171	2.274

Similar observation was also held for the LBD of nAChR. The minimum radius of the LBD of nAChR seems to be 4.787 Å which is smaller than the minimum radius value encountered in AChBP. Since the coordinates of LBD of nAChR aren't subject to any changes, the narrowest part of the LBD of nAChR is the same even if TMD exists or not. So it can be said that the narrowest section of the LBD of nAChR is 4.787 with and without TMD, The narrowest section of the full structure of nAChR becomes the MA region and the gate region. The reasons of the difference between the narrowest sections of AChBP and the LBD of nAChR may be the existence of a transmembrane region at the nAChR and the difference of the structures of the AChBP and the LBD. The shape and some characteristics of the AChBP and the LBD of nAChR may be similar but the alignment of residues is not, which means that the sequences of AChBP and LBD of nAChR are not the same, which may be another reason of this difference of minimum value of the narrowest part.

Minimum radius of the molecule (LBD of nAChR where the TMD is excluded) seems to be greater than its value of the original conformation only at the positive conformations of the third and seventh mode and the negative conformations of the first, second and fifth

modes. All of the other conformations of the other modes yield smaller minimum radius. The absence of the TMD makes the molecule to be more compact. When LBD is free of TMD, it moves easier than it does when a TMD is attached. The TMD tightens the overall structure and hence making the two separate domains of nAChR move cooperatively.

The most significant result suggested by Table 3.1 is that whatever the value of the minimum radius at the LBD is, it never decreases below the minimum radius value of the full structure of nAChR which is at the gate and MA region. The minimum radius of nAChR is 2.171 Å, which corresponds to the intracellular domain of nAChR.

The second narrowest region of nAChR is the gate regions of the molecule, which is more important than the intracellular domain as the gate region is the main restrictive part along the molecule for the transmission of the signals. The signals don't need to pass through the middle of the intracellular domain, because there are some large gaps around this intracellular region and the signals can pass through these gaps instead [7].

It can also be seen from Table 3.1 that the value of radius at the narrowest region of nAChR broadens for positive conformations of each different mode. And most of the modes yield wider pore radius at the negative conformations too. The minimum radius of the gate region is around 2.60 Å, which is also smaller than the values of the positive and negative conformations of both AChBP and LBD of nAChR. With the positive and negative conformations, the narrowest region shifts from ID to the gate region of TMD. Thus, the narrowest region along the full molecule of nAChR will remain the gate region as seen in Figure 3.17, where hole profile of the full structure of nAChR is displayed. Figure 3.17 shows such shifting situation for the first mode of ANM results.

Figure 3.17 shows that the narrowest region at original conformation of nAChR is the lower part of ID which is also called as MA region. But according to the results of ANM calculations, gate region seems to be the narrowest region for both positive and negative conformations. It is also possible to see that the MA region has got a large amount of movement at both positive and negative conformation. Even the narrowest region of LBD is wider than the radius of gate region

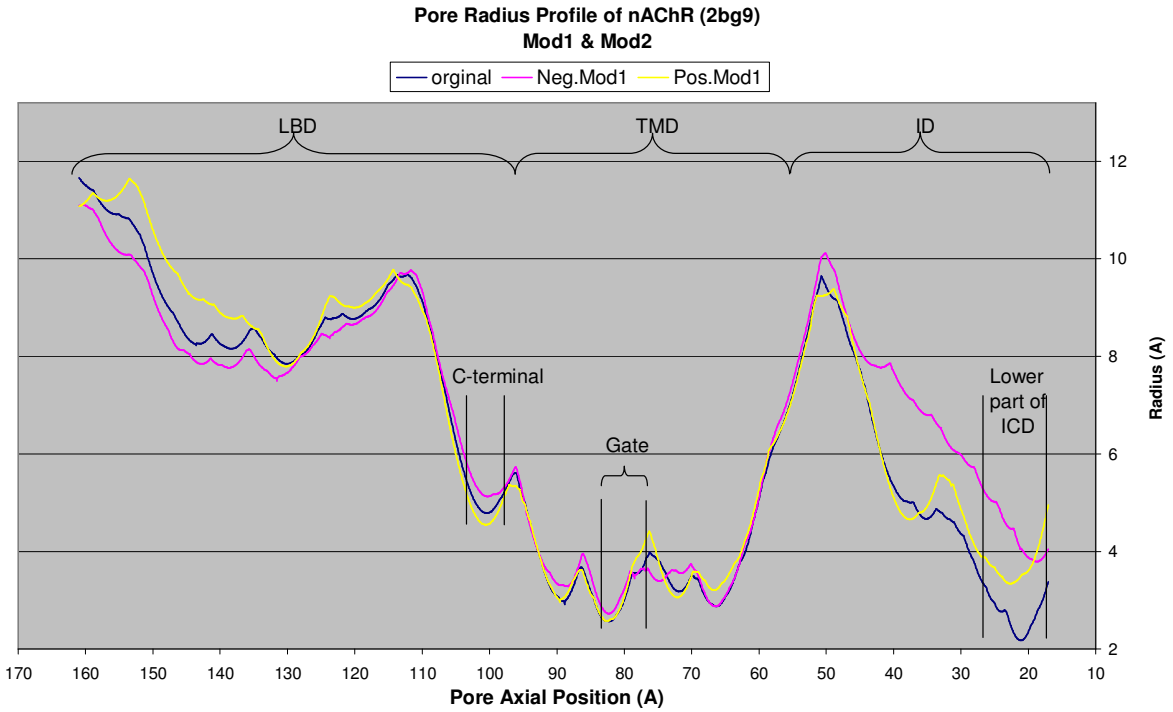

Figure 3.17. Pore radius's along the full structure of nAChR. Dark Blue: The original conformation of nAChR, Yellow: positive conformation of nAChR at the first mode, Pink: negative conformation of nAChR at the first mode.

3.4. Conservation Analysis

For the identification of functionally important residues, we have recoursed to the conservation analysis using the Consurf server [36]. After obtaining the conservation scores of each residue, only the most conserved ones which correspond around per cent 10 of the total residues are taken into consideration.

This section will show the results of conservation analysis applied for AChBP and for the full structure of nAChR. Also, the most conserved residues will also be shown in the MCPOOL section (section 3.6).

The negative values of the conservation scores means show the conserved residues. The smaller the conservation score is, the higher the conservation of that residue is. Different conservation scores of each individual residue and regions can be used to see the differences between the residues and/or regions. But the conservation scores of each residue are normalized within the individual subunits to make the overall average conservation score of

the subunit to be zero. This means that the conservation scores of different subunits cannot be compared using these conservation values.

Figure 3.18 displays the conservations of each region of the AChBP. Since AChBP is a homopentamer the conservation scores of each subunit is the same. Therefore, conservation scores of only one subunit will be shown.

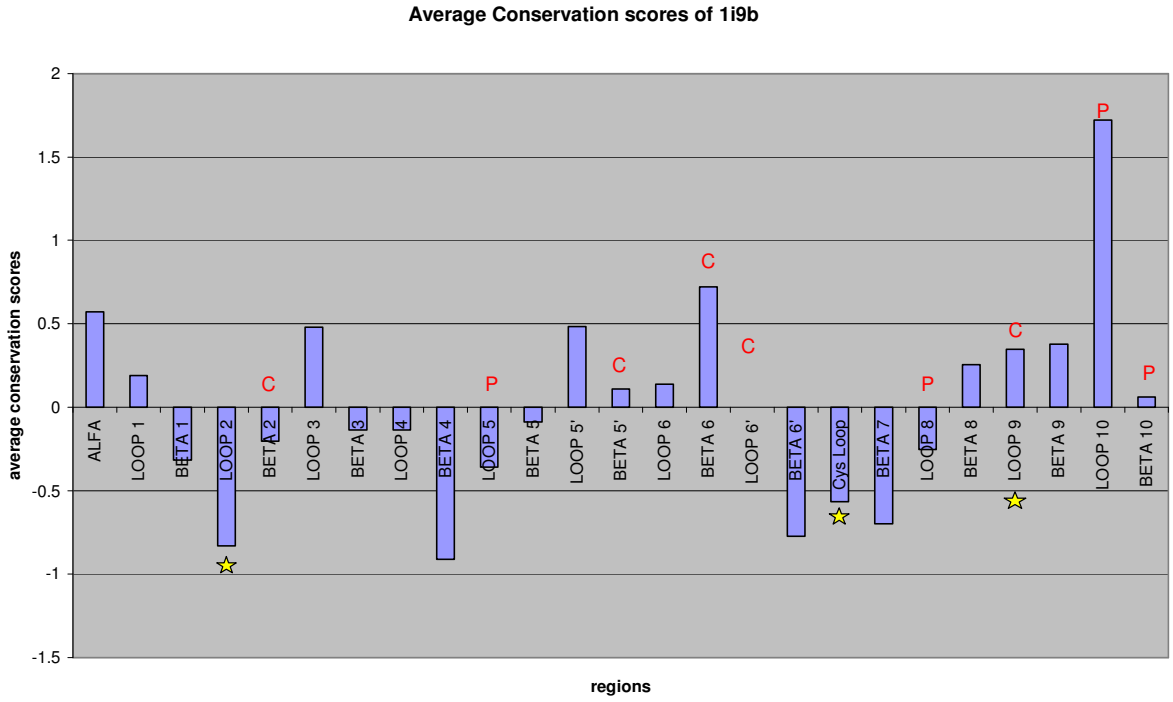

Figure 3.18. Average conservation score of each subunit belonging to the Acetylcholine Binding Protein (AChBP). P: regions which contain principle binding residues, C: regions which contain complimentary binding residues, Yellow Star: Regions which are thought to be important at the gating mechanism [10].

For the gating mechanism of AChBP, it was proposed that each subunit consists of principal and complementary binding residues [8]. It was also proposed that the principal binding residues of one subunit and the complementary binding residues of adjacent subunit forms the binding cavity for Acetylcholine [8]. Loop 2 and Cys Loop appear to be well conserved but Loop 9 is not conserved along the AChBP molecule. Also only two of seven complementary residues are conserved while four of seven principle binding residues seem to be conserved along the molecule. But Loop 10 and Beta 10 which contain principle binding residues seem to be not conserved.

The conservation scores of each subunit along the alpha-gamma subunit of nAChR are shown in Figure 3.19. The conserved regions of AChBP and LBD of nAChR are similar.

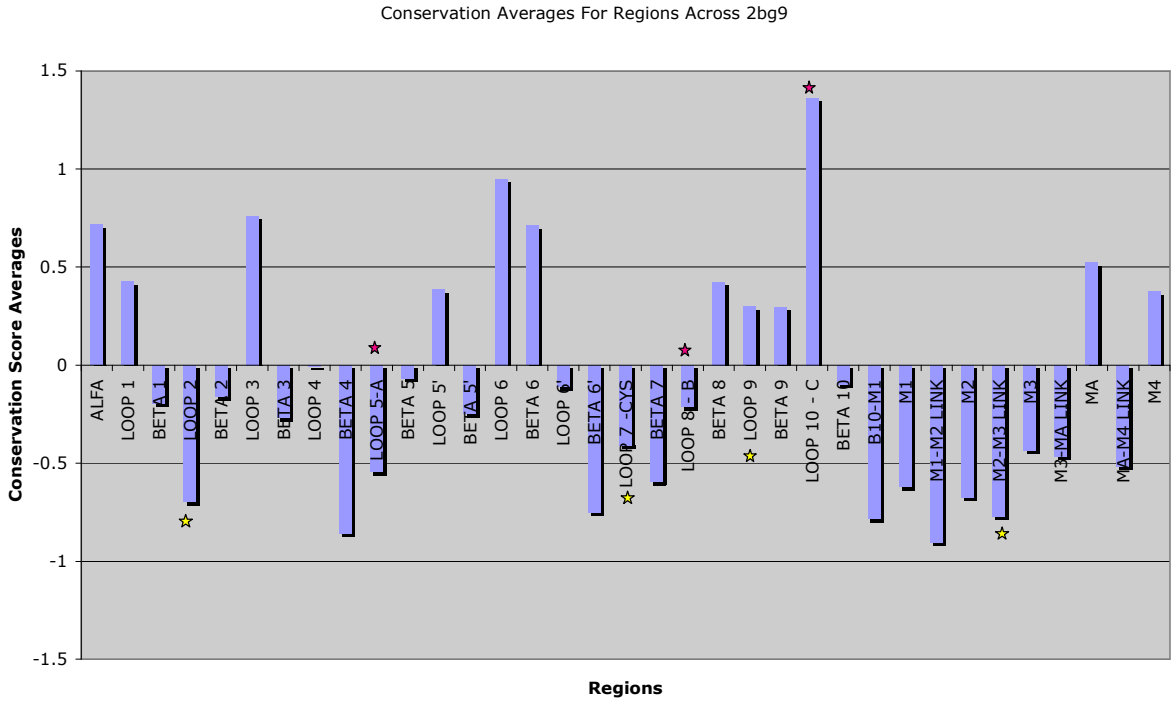

Figure 3.19. The conservation score averages for each individual region across nAChR over five subunits. Red stars show the binding loops [7]. Yellow stars are the regions which are supposed to be important regions for the gating mechanism [10].

Figure 3.19 is generally in agreement with Figure 3.18 except for some regions. For example Loop10 is not conserved at AChBP and nAChR even it consists of binding residues in it. Figure 3.19 also shows that the transmembrane domain of nAChR is more conserved than Ligand binding domain even though the MA region seems to be not conserved yet its whole sequence is still unknown.

An impressing result of Figure 3.18 and 3.19 is that Loop 9 is conserved for neither AChBP nor nAChR. Also these yellow starred regions are in contact with each other in the molecule and the high conservation scores of these loops may suggest us that the gating signal is transmitted mainly along these Loop2, Cys Loop and M2-M3 Loop of Transmembrane region. And also the high conservation score of Beta10-M1 region which couples the Ligand binding domain and Transmembrane domain may add more importance to this region.

Since the conservation outputs of Consurf server [36] are normalized the differences of conservation levels of each individual subunits cannot be compared. However, the conservation scores of subunits for different subunits are given in Figure 3.20 to get some insight.

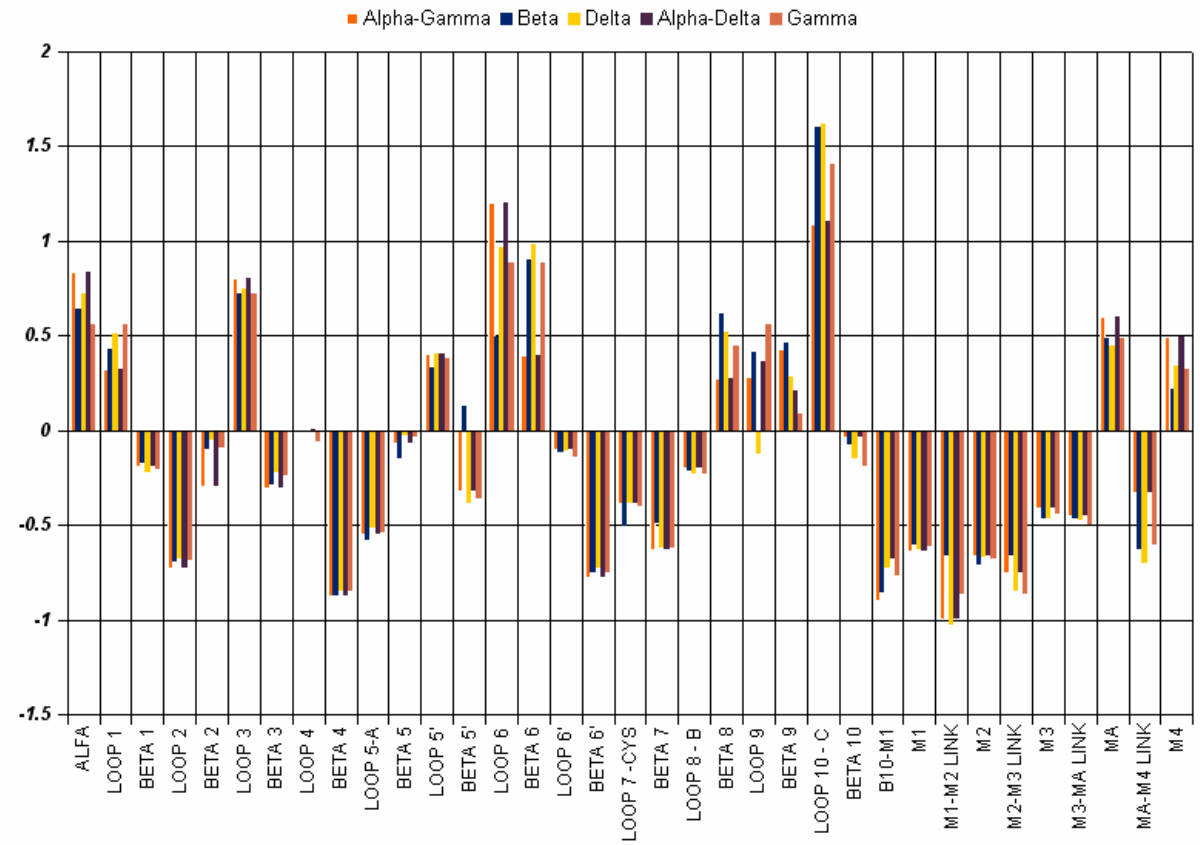

Figure 3.20. Conservation scores of each region for each subunit of nAChR.

Even though it is not possible to compare the subunits with each other using the results of Consurf, Figure 3.20 shows that the same regions of different subunits show similar conservations. There are only two exceptions. In the Beta subunit, the Beta 5' region seems to be not conserved while the Beta 5' regions of the other subunits are conserved. The other exception arises at the Loop 9 region. The Loop 9 region of Delta subunit seems to be conserved while the Loop 9 regions of the other subunits aren't.

One of the differences between the AChBP and the nAChR is the Beta 10 region. Beta 10 is conserved in the nAChR but it isn't conserved in the AChBP. At the beginning, Beta 10 of AChBP wasn't considered to be the region which connects the Transmembrane and Ligand binding domains since it was a putative Ligand binding domain of 1OED without any

transmembrane domain. So, it was not considered to be an important region at the very beginning, but after the discovery of the real Ligand binding domain of nAChR, it started to gain more importance.

TMD of nAChR is more conserved than LBD of nAChR. Even though the conservation values are normalized to make the overall average of the conservation scores zero, the average conservation scores of the LBD of nAChR is around 0.1. But the low conservation of TMD with a value of -0.14 makes the overall conservation score average to be zero. But the point is that the LBD of nAChR becomes less conserved, when the analysis is carried out together with the sequence of TMD as attached to LBD.

3.5.Correlated Mutations

To understand how the residues behaved during the evolution, "Analysis of Correlated Mutations" server has been used [38]. This server has been run to compare the results of correlated mutation analysis for each individual subunits of AChBP, LBD of nAChR and for the full structure of nAChR.

Similarities and differences between the results of these molecules have been checked. After obtaining the results of this sever, the correlated residue pairs are investigated and some figures showing these pairs are drawn. These residues are then analyzed together with the conservation analysis and MCPOOL calculations (to be discussed later) to give us some insight about possibilities of being important residues.

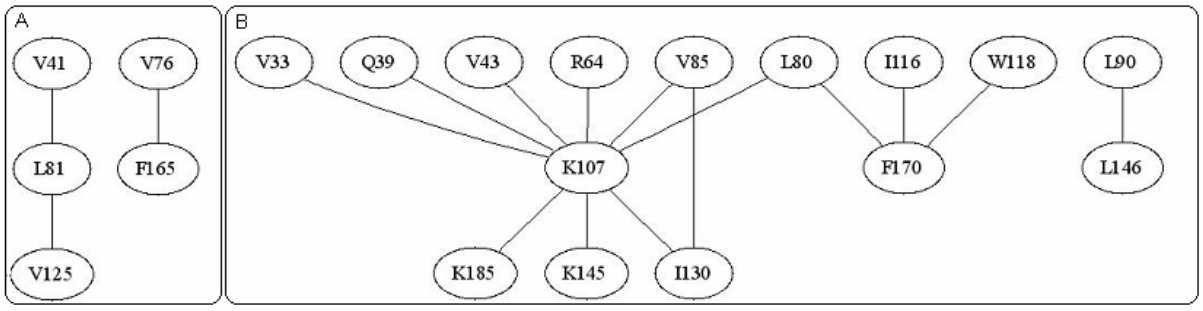

Figure 3.21. Schematic representation of correlated mutation pairs obtained form "Analysis of Correlated Mutations" server. A: residue pairs having correlated mutation at AChBP, B: residue pairs having correlated mutation at Ligand Binding Domain of nAChR

In Figure 3.21, each connected circles represent the residue pairs having correlated mutation which are obtained from “Analysis of Correlated Mutations” server. The letter in each circle stands for the name of residue and the number represents which residue it is. This figure shows that Ligand Binding Domain of nAChR has more correlated pairs than AChBP.

If we take a close look at this Figure 3.21, it can be seen that only five residues of alpha-gamma subunit of AChBP have correlated mutations while LBD of nAChR has got 15 correlated residues. None of these residues are the binding residues. The correlated residues of the Alpha-Gamma subunit of AChBP are in the Beta1, Beta 3, Loop 4, Cys Loop and Loop 9 regions. And the correlated residues of the Alpha-Gamma subunit of LBD of nAChR are scattered through Beta 1, Loop 3, Beta 3, Loop4, Beta 4, Beta5’, Beta 7, Cys Loop, Beta 9 and Loop 9 regions.

Both of these molecules have one correlated residue in their Cys Loop regions (VAL125 of AChBP and ILE130 of the LBD of nAChR). Also PHE165 of AChBP and PHE170 of the LBD of nAChR are in the Loop 9 regions. There are 15 correlated residues in the LBD of nAChR. Four of these 15 residues are on the loops while the other eleven are on the beta sheets. The residues belonging to loops are ARG64 (Loop 3), VAL85 (Loop 4), ILE130 (Cys Loop) and PHE170 (Loop 9). It is also seen from Figure 3.21 that LYS107 (Beta5’) of the Alpha-Gamma subunit of LBD of nAChR has got many correlated mutation pairs. But this residue has never been thought to be an important residue up to now.

Since AChBP is a homopentamer the correlated mutation analyses for each subunit yields the same residues. But the correlated residues of the LBD of nAChR differ from subunit to subunit as seen in Figure 3.22.

Since both alpha subunits are identical, the correlated mutation pairs of Alpha-Gamma subunit are the same with the correlated mutation pairs of Alpha-Delta subunit. Gamma subunit seems to have the least amount of residues having correlated mutations which are LEU49 (Beta 2) and VAL89 (Beta 4). Correlated residues of Beta subunit are spreaded through the Beta 1, Beta 3, Beta 6, Loop 9, Loop 10 (Loop C) and Beta 10 regions. Correlated residues of Delta subunit appear at Beta 1, Beta 2, Beta 3, Beta 6, Cys Loop and Loop 9 regions.

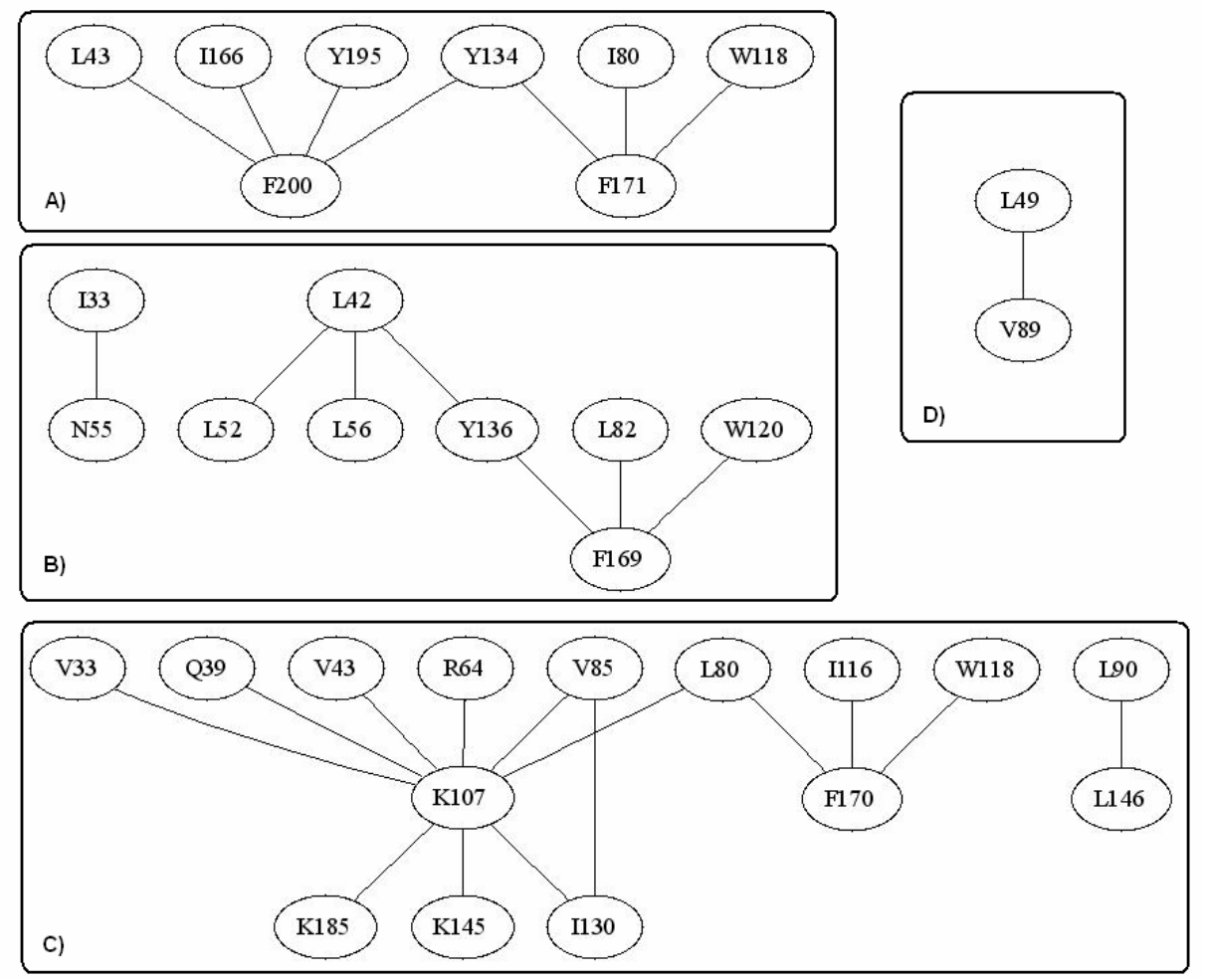

Figure 3.22: Schematic representation of correlated mutation pairs of LBD of nAChR obtained form "Analysis of Correlated Mutations" server. A: Beta subunit, B: Delta Subunit, C: Alpha-Delta subunit, D: Gamma subunit

Among the five subunits of LBD of nAChR, LYS107 located in the Loop 9 region of the alpha subunits make the most correlated mutation pairs. The other residues having much correlated mutation pairs are the PHE200 (Beta 10) and PHE171 (Loop9) of Beta subunit, LEU42 (Beta1) and PHE169 (Loop9) of Delta subunit and the PHE170 (Loop9) of the Alpha subunits having three correlated mutation pairs. All of these residues of Loop 9 regions are their counterparts in those subunits which mean that PHE170 of Alpha subunit is the counterpart of PHE169 of Delta subunit. This shows that, this residue of this position is mutated among the evolution which is not one of the most conserved residues on the molecule.

Also only the Beta subunit have residues involved with correlated mutations (TYR195) in its binding loop Loop C whereas the other subunits do not have any correlated residue in the binding regions. Also all of the subunits except the Beta subunit have correlated residues in Cys Loop and Loop 9 regions.

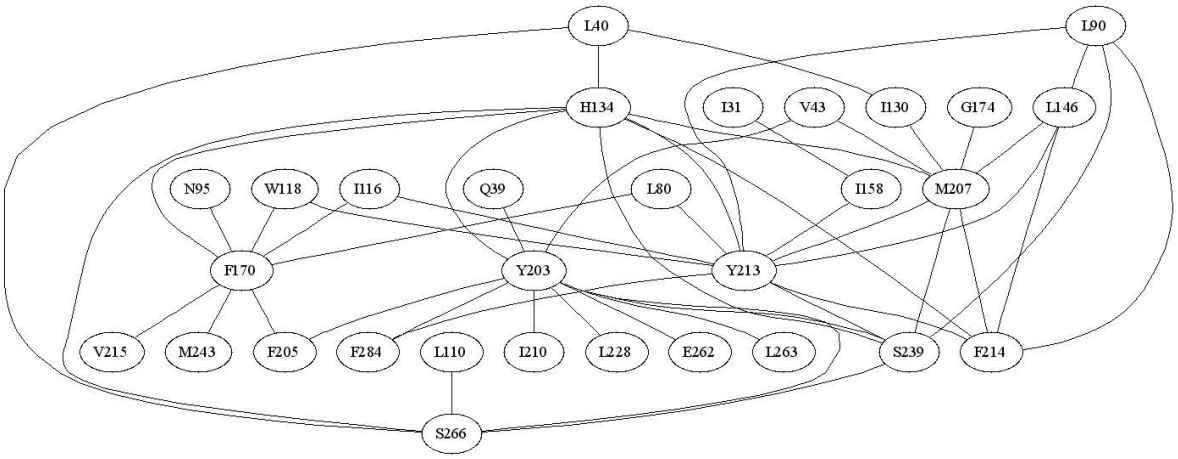

Figure 3.23. Schematic representation of correlated mutation pairs of the Alpha-Gamma subunit in the full structure of nAChR obtained from the "Analysis of Correlated Mutations" server.

As the total amount of the residues inside the molecule increases, the correlated mutations increase (Figure 3.23). More possibilities of making correlated mutation pairs yield tens of correlated mutation pairs. Alpha subunits have got 30 residues having correlated mutations where TYR203 (Beta 10) is correlated with 11 of these 30 residues; Beta subunit has got 32 correlated residues where ILE204 (Beta 10) is correlated with 8 of these32 residues; Delta subunit has got 39 different correlated residues where PHE202 (Beta 10) is correlated with 22 of these residues and Gamma subunit has got 16 correlated residues where PHE203 (Beta 10) is correlated with 9 of these residues. So it can be said that the correlations of these residues affect many of the other residues. Figures of such correlated pairs are shown in APPENDIX B, Figure B.19 to Figure B.21.

Some of the correlated mutations form loops between residues. For example PHE170 (Loop 9) is correlated with HIS134 (Cys Loop), HIS134 is correlated with TYR203 (Beta 10), TYR203 is correlated with PHE205 (Beta 10) and PHE205 is correlated with PHE170. This is only one of the examples.

From the correlated mutation analyses of nAChR, it is seen that only Beta and Delta subunits have residues having correlated mutations in the MA and M4 regions. Also these Beta and Delta subunits have got correlated residues in the gate regions. In one study of Auerbach [23], he showed that the mutations in the upper half of the M4 region have larger effect than on the lower part.

The results here suggest a measure for the cooperativity within the subunits as the calculations were carried out with the subunit sequences. Nevertheless, the intersubunit cooperativity can be addressed as seen in sections GNM and ANM.

3.6. MCPOOL Analyses

So far the correlations between the fluctuations and the conformations that describe the fluctuations from the average structure in the slowest and fastest modes have been discussed along the conservation and correlated mutational analysis. Here, MCPOOL [39], which finds pathways between any two arbitrary locations at any desired length using the correction maps, will combine all of the data. The residues that are mostly visited along these paths and the location and the importance of these residues will be discussed.

For AChBP, the principle binding residues are chosen as a starting point and Cys Loop, Loop 2 and Loop 9 are given as target locations as these regions are thought to be involved for gating mechanism [8, 10]. For the Ligand binding domain of nAChR, the target locations remained the same but the starting points are taken as Loop A, Loop B and Loop C that are thought to contain binding residues of nAChR. As for full structure of nAChR, the target point is set as the gate region that is located at the transmembrane region while the starting points are again Loop A, Loop B and Loop C.

The motivation for the generation of the paths is able to account for the allosteric communication between LBD and TMD. For the case of only Ligand binding domain analysis, this allosteric communication is thought to be between the binding regions and Cys Loop, Loop 2 and Loop9 as these regions are thought to play key role in the signal transmission from the binding regions to the gate regions [3]. For this, 100,000 paths have been generated starting from the given region at a given maximum number of steps. This doesn’t mean that those paths should arrive to the preselected region at given maximum

number of allowed steps. One path can reach to the target region at three steps while another path can never reach to target region even at 30 steps. After the generation of the paths, the paths are analyzed whether they reached to the target regions at a given number of steps. These allowed maximum numbers of steps are selected to be 10, 20 and 30.

First analysis of MCPOOL output is to search for the connected paths between the starting and the target regions among the total generated paths in a given number of steps. It has been seen that as the allowed number of steps of the connectedness increases, the number of connected paths found in the pool of paths increases. After several runs of the program for different allowed maximum number of steps and total number of generated paths, it has been decided to generate 100.000 as the total number of generated paths has no significant effects on the results. Nevertheless, the number of allowed step sizes for the connectedness is an important parameter on the results. Thus, the analyses have been carried out for a set of number of allowed steps as 10, 20 and 30.Table 3.2 shows how these connected paths are distributed.

Table 3.2: Number of connected paths reaching to each individual subunit along AChBP. First column shows maximum allowed length of the steps used in the path generation. Second column shows the starting. Third column shows the target region. Fourth to eighth columns show the number of connected paths between the starting subunit and the target of the subunit

# of steps	Starting Subunit	Target	Alpha-Gamma	Beta	Delta	Alpha-Delta	Gamma
10 steps	Alpha-Gamma	Cys Loop	19334	10607	1051	244	2998
		Loop 2	7447	3511	309	190	2423
		Loop 9	23769	20533	2134	223	2364
20 steps	Alpha-Gamma	Cys Loop	27892	18176	4163	2231	7851
		Loop 2	12309	7493	1742	1500	5774
		Loop 9	32241	28167	5720	1943	6584
30 steps	Alpha-Gamma	Cys Loop	31654	22203	6836	4398	10967
		Loop 2	15360	10364	3618	3251	8443
		Loop 9	35365	31361	8038	3628	8919

Table 3.2 shows that as the number of allowed step size increases, the total amount of connected paths increases. For example, to understand the table 10607 out of 100,000 generated paths start from the binding residues of AChBP located in the Alpha-Gamma subunit and arrive to the Cys Loop of Beta subunit in maximum 10 steps. Another example is; 18176 out of 100,000 generated paths starts from the binding residues of Alpha-Gamma subunit of AChBP and arrive to the Cys Loop region of Beta subunit in maximum 20 steps.

Table 3.2 shows that the total amount of paths that reach to the target regions either by using internal connected paths or external connected paths. In the case of using external paths which mean that the path has been using the residues of non-starting subunit, the paths tend to use their neighbors more than their non-neighbor subunits. So, the paths starting from any subunit of AChBP mostly uses its neighbor which is on the clockwise direction (named as the positive side) when viewed from the extracellular side. For example, if the starting region is on the Alpha-Gamma subunit, the most used subunit along the four of the other subunits is the Beta subunit and if the starting region is on the Beta subunit, the most used subunit along the other four subunits is the Delta subunit and so. But what is the ratio of these external connected and internal connected paths?

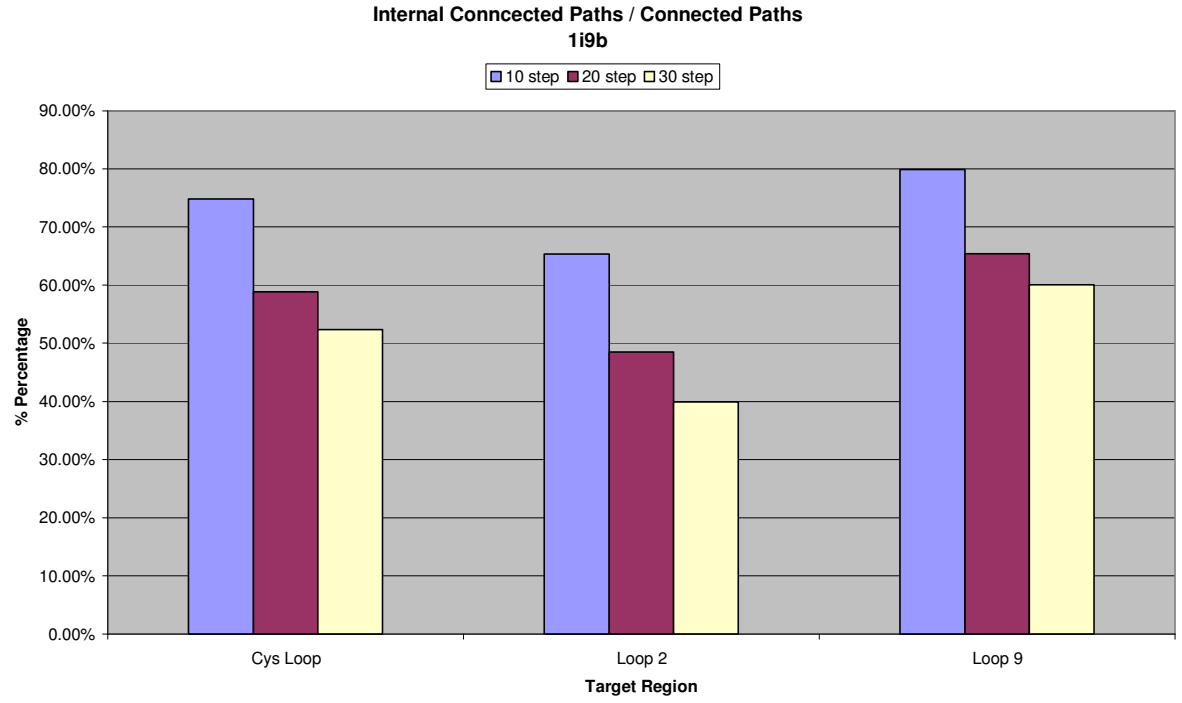

Figure 3.24: The ratio of internal paths to the total connected paths generated for AChBP.

As seen from the figure, the paths starting from any subunit of AChBP tend to use only the residues of their own subunit for short paths, but as the length of the path increase, the amount of external subunit usage increases. But even for the paths in 30 step length, the amount of internal connected paths reaching to either Cys Loop or Loop 9 is greater than the amount of the external connected paths. This may be because of the short distance between these regions and high amount of residue contents of these regions.

Table 3.3. Number of connected paths reaching to each individual subunit along nAChR.

# of steps	Starting Subunit	Target	Alpha-Gamma	Beta	Delta	Alpha-Delta	Gamma
10 steps	Alpha-Gamma	Gate	1581	737	482	523	1055
	Beta	Gate	589	1240	998	518	451
	Delta	Gate	338	742	735	413	244
	Alpha-Delta	Gate	588	517	810	1752	967
	Gamma	Gate	947	537	463	793	1277
20 steps	Alpha-Gamma	Gate	4256	2600	2012	2282	3483
	Beta	Gate	2084	3355	2940	2026	1808
	Delta	Gate	1609	2613	2644	1747	1378
	Alpha-Delta	Gate	2340	2256	2808	4507	3215
	Gamma	Gate	3153	2154	2077	2707	3675
30 steps	Alpha-Gamma	Gate	6799	4604	3941	4293	5909
	Beta	Gate	3769	5492	4980	3771	3303
	Delta	Gate	3190	4791	4666	3414	2800
	Alpha-Delta	Gate	4442	4211	4965	7118	5604
	Gamma	Gate	5382	3989	3895	4835	6082

First column shows maximum allowed length of the steps used in the path generation. Second column shows the starting subunit containing the binding loops. Third column shows the target region. Fourth to eighth columns show the number of connected paths between the starting subunit and the target of the subunit shown on the column

The same MCPOOL analyses were carried out for the full structure of nAChR. This time there is a TMD attached to the LBD and there is an ID attached to the TMD. So we can select the gate region as the target and check how these paths are distributed. Starting from the binding loops of each individual subunit and going to gate region of any subunit, the analyses yielded the following table.

This table shows the amounts of connected paths along the 100.000 generated paths. As the number of steps used in the paths increase, the amount of connected paths increases. But as the length of the path increases, the significance of that path decreases. 5 per cent of the total generated paths can go to the selected target while we limit the maximum length of a path to be 10 steps, 15 per cent for 20 steps, and 25 per cent for 30 steps. The paths starting from Alpha Delta and Alpha Gamma subunits can go to any gate region with greater amounts than non-alpha subunits can and these alpha subunits use their own subunit more than the other subunits do.

The internal and external connected path analyses have also been investigated for the full structure of nAChR where LBD, TMD and ID are altogether. Because Loop A, Loop B and Loop C are considered to be the binding loops of nAChR, these regions have been selected as the starting points of the paths and the middle of M2 helix of TMD which is considered to be the gate region of nAChR is selected as the target region.

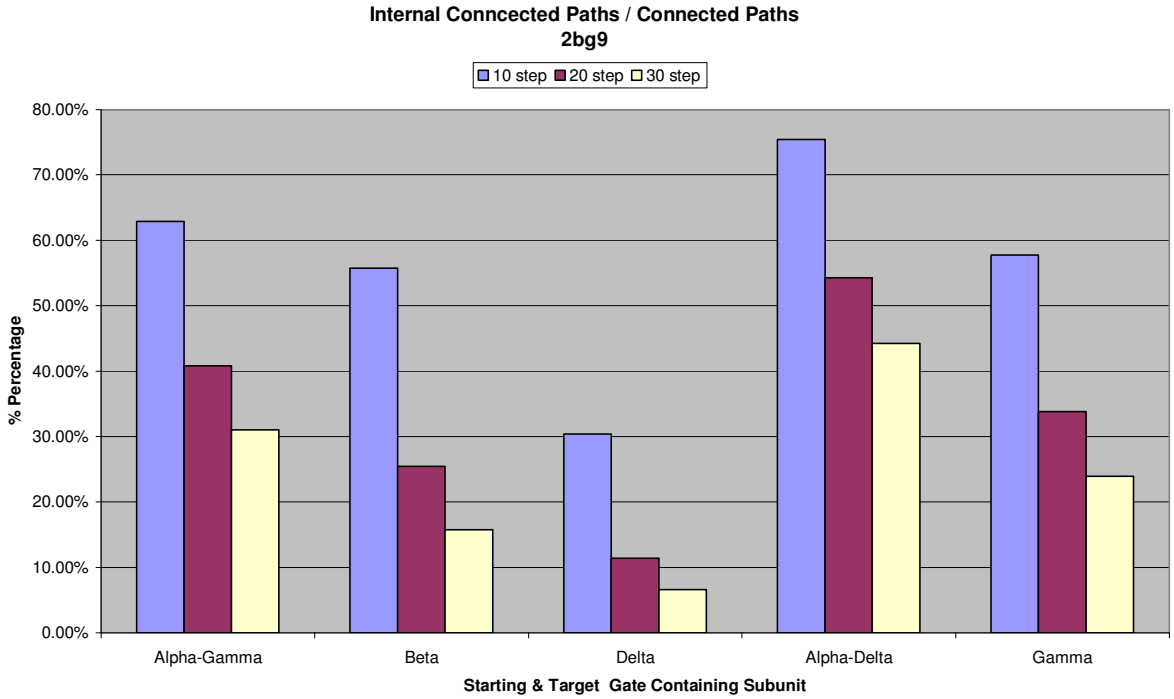

Figure 3.25: The ratio of internal paths to the total connected paths generated for nAChR.

In Figure 3.25., X axis shows the subunit which contains the target gate region and Y axis shows the percentage of internal connected path usage over the total connected paths.

Figure 3.25 shows the percentage of internal connected paths usage. As seen from the figure, for the shorter paths, the internal connected path percentage is greater than the external connected path percentage which means that short paths do not need to leave the starting subunit. And it is seen that the alpha subunits have the greatest percentages of using the internal connected paths.

It is known that only the alpha subunits of nAChR contain binding loops, on the other hand it is seen from Figure 3.25 that the paths starting from the binding regions of alpha subunits tend to use the residues which are on their own subunit more than using the residues of other subunits. Besides, an allosteric signal should be transmitted from the binding region to the gate region for the channel to open and let the ions pass. Combining all these data, the high amount of total connected and internal connected path reveals the importance of alpha subunits and contributes to their importance of being the actual actuator of the signal transmission.

When the LBD of nAChR is considered to be alone, this molecule behaves like it does on the full structure. But this time the target is not the gate region. Similar to the targets selected at the AChBP, Cys Loop, Loop 2 and Loop 9 has been chosen as the target regions. Alpha subunits seem to use their own subunits more than that the other subunits do and even at the long paths the internal connected path usage is greater than the external path usage. But this is reasonable while the distance between the starting and target regions is smaller than the distance in the full structure.

The amount of internal connected path usage in the AChBP is smaller than the amount of internal connected paths in the LBD of nAChR and there is a bigger difference between the internal connected path usage ratios of subunits. For example the internal connected path amount at the alpha subunits of AChBP is around 60-70 per cent while this amount is around 95 per cent at the alpha subunits of LBD of nAChR. But the distance is short for these cases. When the TMD is also taken into consideration, the amount of internal connected path usage decreases to the values of 50 per cent. Also, when LBD is alone the total amount of the connected paths is around five times more than the connected paths of nAChR. So it is seen that most of the generated paths can reach to the Cys Loop, Loop 2 and Loop 9 regions.

After realizing that it is easy and highly possible to reach Cys Loop, Loop 2 and Loop 9 regions, it has been analyzed if these regions exist on the paths starting from the binding region and going to the gate of nAChR. To this aim, each individual step on the connected paths has been analyzed. If a residue belonging to TMD comes after any residue of the LBD on the connected paths, these two residues are analyzed to see which region of LBD is correlated with the TMD. The results show that the Cys Loop and Loop 9 regions of LBD are the most used regions when a path jumps from LBD to TMD. Loop 2 region cannot be seen at the top of the list but this is mainly because of the low residue content of Loop 2. But on the residue basis instead of region basis, the residues of Loop 2 seem to be more involved on the transmission from the binding domain to the transmembrane domain then the other residues. Another highly used region is beta1 strand of LBD. On the other hand, LBD is more correlated with the upper part of TMD than it is with the lower part.

All of these regions have been analyzed and evaluated as the most used regions and some of the shortest and mostly used paths have been demonstrated at the PAJEK section (to be shown later). Even on those figures, Cys Loop and Loop 9 seem to be the most used regions at the LBD.

The results of Mcpool are elaborated with respect to the fluctuation behavior of residues at two ends of dynamic spectrum, the conservation of residues and correlated mutation of residue pairs.

3.6.1. Combined Analyses for AChBP

Figures 3.26 to 3.28 display the fluctuations in the slowest two modes for AChBP with the conserved residues and residues in the pairs of the correlated mutations. The most visited residues on the paths starting from the binding residues and going to Cys Loop, Loop 2 and Loop 9 are also labeled on the figures.

The general representations of the figures are all the same. The paths generated by MCPOOL are analyzed for the paths which reach the target in maximum of 10, 20 and 30 steps.

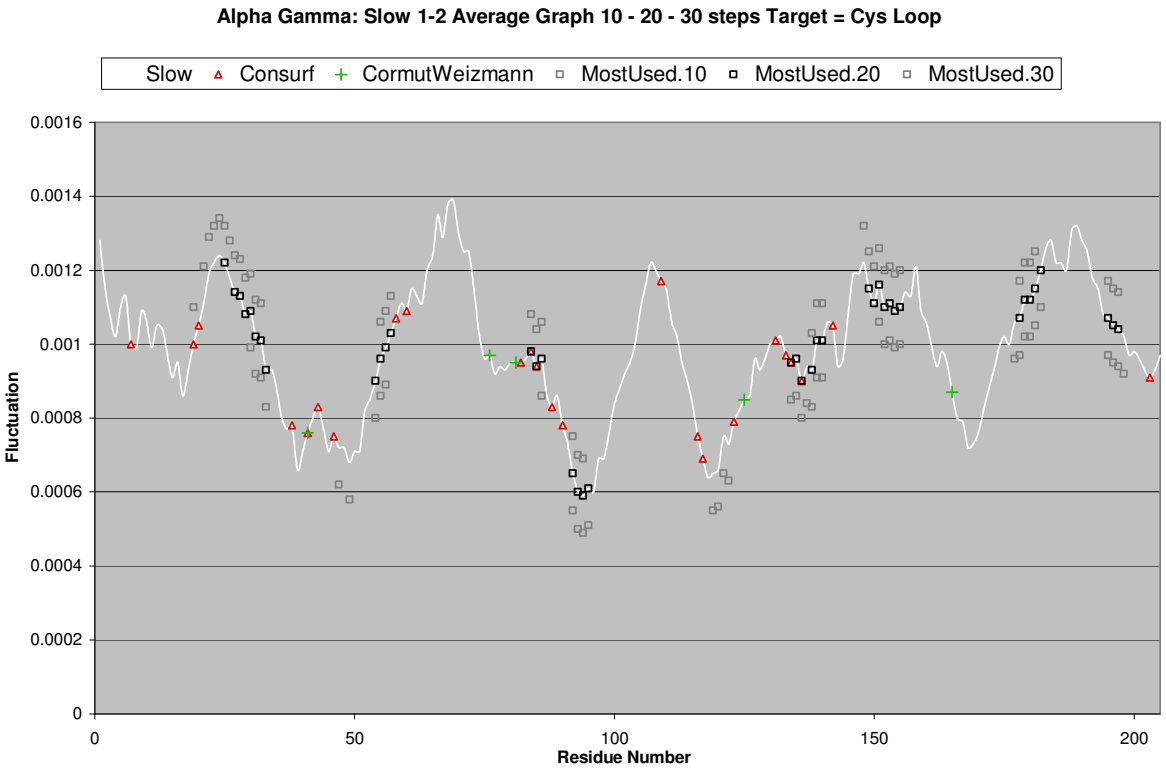

Figure 3.26. Fluctuations of alpha-gamma subunit of AChBP in the average of slowest two modes.

In Figure 3.26., the white line represents the slow 1-2 average fluctuations. Grey boxes below the white line shows the most used 40 residues at the paths with maximum allowed step size of 10, the black boxes on the white lines show the most used 40 residues at the paths with maximum allowed step size of 20, grey boxes above the white line show the most used 40 residues at the paths with maximum allowed step size of 30. Red triangles on the while line shows the most conserved residues and the green plus signs on the white line shows the pairs having correlated mutations.

In Figure 3.26, the preset target is Cys Loop of any subunits in the AChBP molecule. The most visited residues along the shorter paths (maximum of 10 steps) correspond to the beta 2, loop 5, beta 6', beta 7, beta 8, beta 9 and beta 10 regions. Beta 2 is kind of a spine in the molecule starting from the lower part of the molecule and going through the upper part of the molecule. Beta 10 is in contact with the Cys Loop.

On the paths with up to 20 steps, the most visited residues are similar to the residues that have been observed for the paths with maximum 10 steps. These most visited residues mainly correspond to beta 1, beta 2, loop 4, loop 5, beta 7, beta 8, beta 9 and beta 10. And on the paths containing maximum of 30 steps, the most used residues correspond to beta 1, beta 2, loop 4, and beta 8 beta 9 and beta 10.

Also from Figure 3.26, it is seen that some of the conserved residues along the AChBP molecule are also most visited residues along the paths but these conserved residues are spreaded along the subunit. On the other hand the residues having correlated mutations do not seem to appear on the important regions.

When the target regions are selected as Loop 2 region, Figure 3.27 shows the most visited residues along the paths;

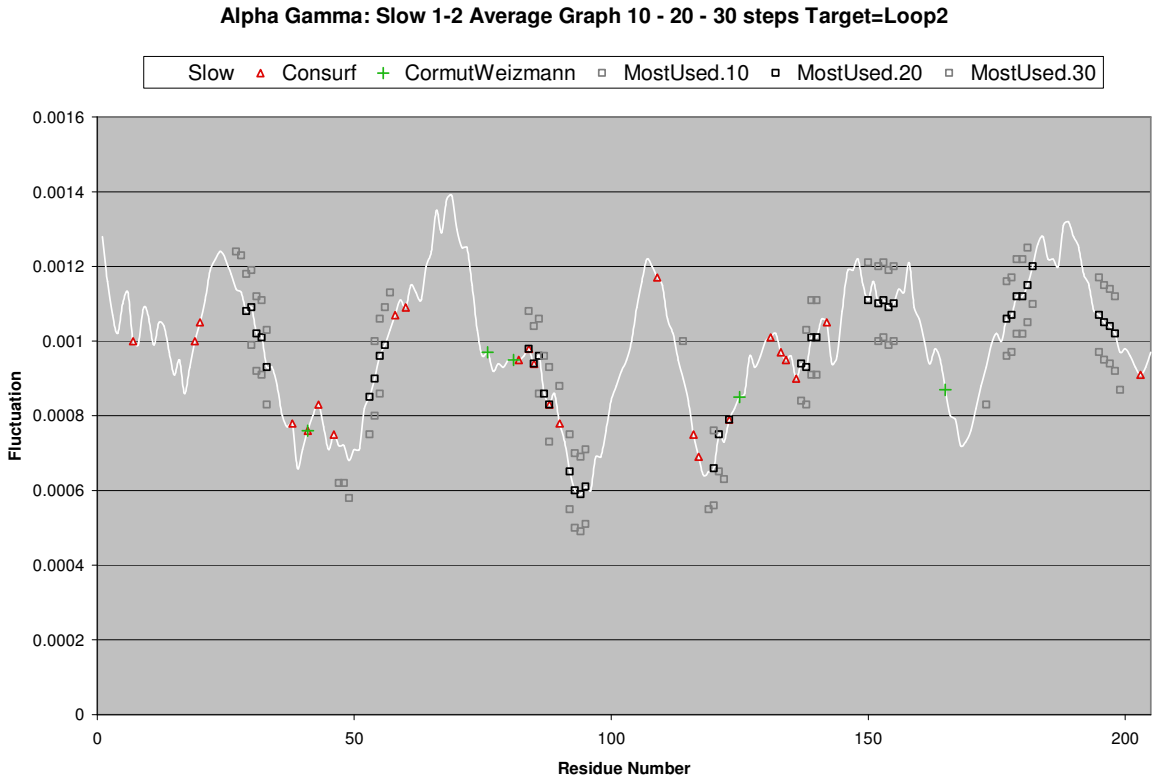

Figure 3.27. Slow 1-2 average fluctuations of alpha-gamma subunit of AChBP.

In Figure 3.27 the preset target is the Loop 2 of any subunits in the AChBP molecule. The most visited residues along the shorter paths (maximum of 10 steps) correspond to the

beta 1, beta 2, loop 5, beta 6', beta 7, beta 8, beta 9 and beta 10. On the paths with up to 20 steps, the most visited residues mainly correspond to beta 1, beta 2, loop 4, loop 5, beta 7, beta 8, beta 9 and beta 10. And on the paths containing maximum of 30 steps, the most used residues correspond to beta 1, beta 2, loop 4, beta 8 beta 9 and beta 10.

The third preset target for the MCPOOL analysis along the AChBP molecule is the Loop 9 region. Figure 3.28 shows the most used residues along the paths;

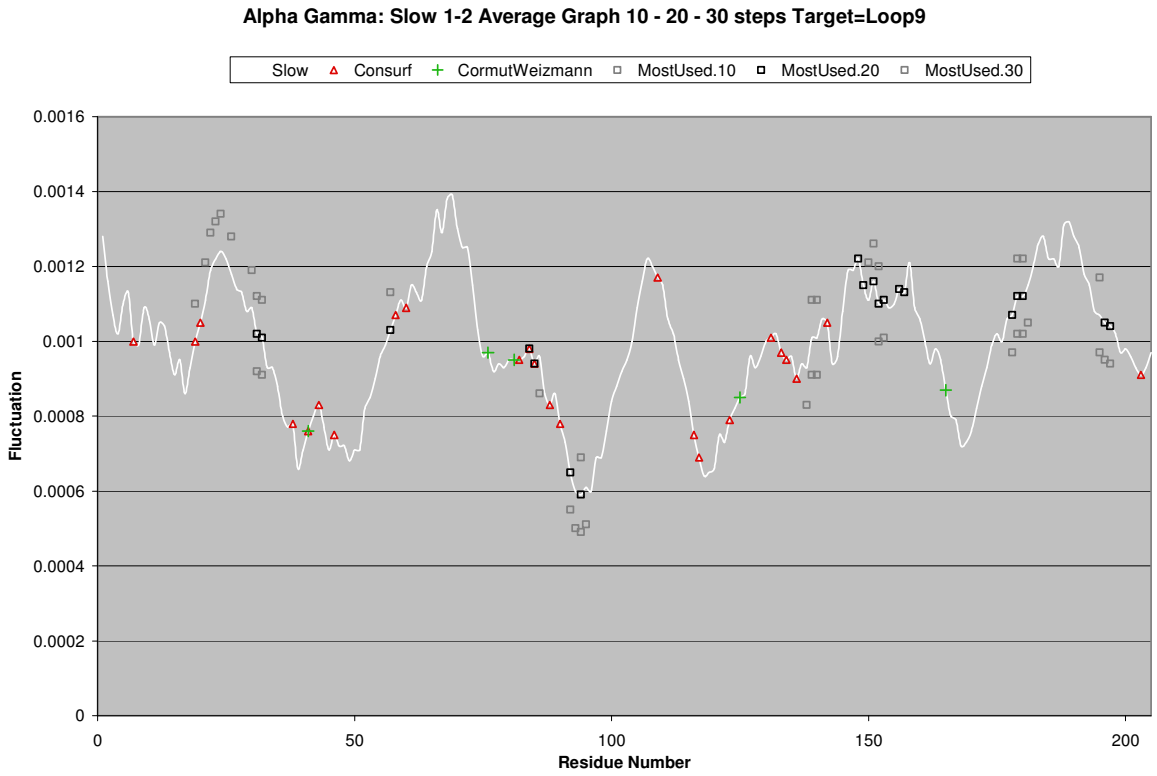

Figure 3.28. Slow 1-2 average fluctuations of alpha-gamma subunit of AChBP.

In Figure 3.28 the preset target is the Loop 9 of any subunits. The most visited residues along the shorter paths (maximum of 10 steps) correspond to the beta 1, beta 2, loop 5, beta 6', beta 7, beta 8, beta 9 and beta 10.

On the paths with up to 20 steps, the most visited residues mainly correspond to beta 1, beta 2, loop 4, loop 5, beta 7, beta 8, beta 9 and beta 10. And on the paths containing maximum of 30 steps, the most visited residues correspond to beta 1, beta 2, loop 4, beta 8, beta 9 and beta 10.

3.6.2. Combined Analyses for the LBD of nAChR without TMD

When TMD does not exist in the nAChR molecule, the LBD of nAChR contains one starting point and three target regions for each subunit. The starting regions of each subunit are the binding loops which are Loop A, Loop B and Loop C whereas the target regions are the Loop 2, Cys Loop and Loop 9 regions of each subunit. These analyses are performed for all of the subunits of the LBD of nAChR but only the results of Alpha-Gamma subunit are displayed here. The other figures are listed in APPENDIX B, Figure B.22 to Figure B.27. Figure 3.29 to 3.31 display the slow 1-2 average fluctuations of the Alpha-Gamma subunit.

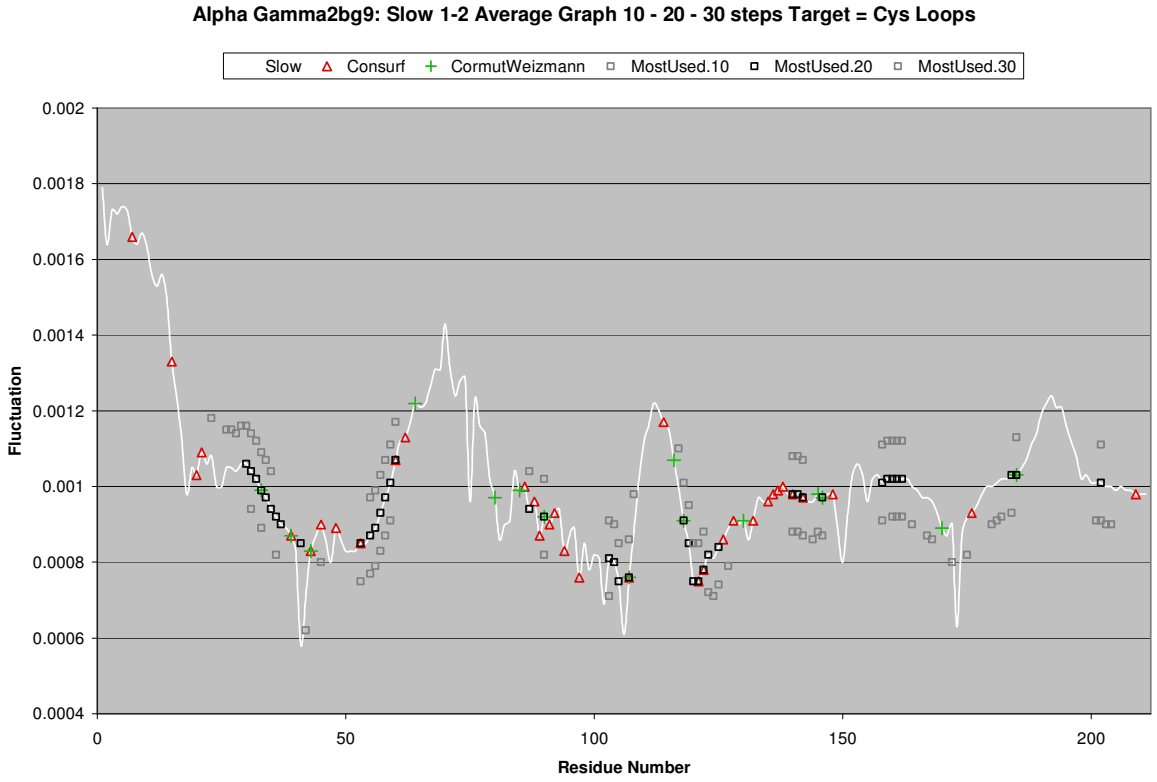

Figure 3.29. Slow 1-2 average fluctuations of alpha-gamma subunit of the LBD of nAChR.

Grey boxes below the slow 1-2 fluctuations curve represent the most visited residues along the paths which are composed of maximum 10 steps. The black boxes right onto the slow 1-2 average fluctuations curve are the most visited residues along the paths which are composed of maximum 20 steps. And the grey boxes above the slow 1-2 average fluctuations curve are the most visited residues along the paths which are composed of maximum 30 steps.

The red triangles and the green plus signs on the slow 1-2 average fluctuations curve represent the most conserved and correlated residues respectively

In Figure 3.29, the most visited residues are on the paths which start from the binding loops of Alpha-Gamma subunit and go to any Cys Loop region of any subunit. And the most visited residues are the residues of the Alpha-Gamma subunit. The Cys Loop region seems to be well conserved but this region do not appear on any hinge point of the slow 1-2 average fluctuations. The most visited residues on the paths which are composed of maximum 10 steps seem to appear at the Beta 2, Beta 7, Loop 9, Beta 9 and Beta 10 regions. There is only one residue belonging to the Loop 2 region which is also one of the most conserved residues (GLU45). Also one of the most visited in residue in these paths is ASN53 (Beta2) which is also well conserved. According to figure (MC5) LEU90 (Beta4) is also one of the most visited residue and it seems to be correlated during the evolution whereas the neighboring residues ASP89 and VAL91 are well conserved. LYS145 and LEU146 of the Beta 7 region and the VAL33 of Beta 1 are the other most visited residues and these residues have correlated mutations along the subunit.

When the paths are allowed to search for more steps, some of the most visited residues are the same with the residues found on the paths which are composed of maximum 10 steps. Residue of Beta 1, Beta 2, Beta 5', Beta 6' and some residues from Loop 9 and Beta 9 are the most visited residues on the paths of maximum 20 steps. Only four residues of the Beta 1 region are most visited residue at the paths of maximum 10 steps. But nine residues of the Beta 1 region seem to be most visited residues on the paths of maximum 20 steps. On the other hand, residues of Beta 9 and Beta 10 are most visited residues on the paths of maximum 10 steps, but only one or two of these residues (TRP184 and LYS185 of Beta9 and THR202 of Beta10) appear on the most visited residues of paths containing maximum 20 steps. VAL33 (Beta1), LEU90 (Beta4), LYS107 (Beta 5'), LEU146 (Beta7) and LYS185 (Beta9) seem to be the most visited residues along the paths of maximum 20 step and these residues also have correlated mutation pairs.

If the paths are allowed to visit more residues, the most visited residues change for a few cases by comparison to the most visited residues seen on the paths of maximum 20 steps. On the paths of maximum 30 steps, there are some residues of Loop 1 region which do not appear on the paths of maximum 10 and 20 steps. Residues of Loop 5' are also most visited

residues along the paths of maximum 30 steps but these residues do not appear to be mostly visited residues for the paths of maximum 10 steps.

There are some mostly visited residues in all of the paths whatever the length of the paths is. When the most visited 40 residues are listed, 16 of them appear on both maximum of 10, 20 and 30 step paths. These residues are generally in Beta 1, Beta 2, Beta 4, Beta 7, Beta 8, Loop 9 and Beta 10 regions. Residues of Loop 2 are visited for shorter paths which contain four or five steps. The main difference between short (2 to 10 steps) and the long paths (10 to 30 steps) is the usage of inner sheets (residues between 1 and 127) and outer sheets (residues from 143 to 211) [3]. Shorter paths visit the residues of outer sheet more than the long paths. Outer sheet interacts with the adjacent subunit. One the alpha helix regions are the least visited regions in all of the paths whatever the number of step is.

For the shorter paths (1 to 10 steps), some residues of Beta 1, Beta 2, Loop 9, Beta 9 and Beta 10 are mostly visited for all of the subunits. For longer paths (10 to 30 steps), Loop 1 region of Alpha-Gamma, Delta and Gamma subunits are on the mostly visited regions list while the other subunits do not have mostly visited residues in Loop 1 region.

But these analyses are residue based analysis. The most visited residues are plotted on the figures. But each region consists of different number of residues. For example Loop2 contains four residues whereas Loop region contains around 17 residues. This residue based analysis enables us to see the most visited residues but on the analysis of most visited regions this Loop 2 region disappears from the most visited regions list.

For the analyses of most visited residues along the paths going to the Loop 2 regions, Figure 3.30 is drawn. Figure 3.30 displays the most visited residues for different length of paths (maximum of 10, 20 and 30 steps) and the most conserved residues and the residues having correlated mutations are also shown.

From comparison of Figure 3.29 and Figure 3.30, the most visited residues along the connected paths seem to be very similar. But the target regions aren’t plotted on the figures, so none of the residues of Cys Loop are shown on Figure 3.29. But in Figure 3.30 the short paths (1 to 10 steps) residues of Cys Loop region seems to be visited so many times along the

paths going to Loop 2 region of the LBD of nAChR. These residues are either well conserved or have correlated mutations.

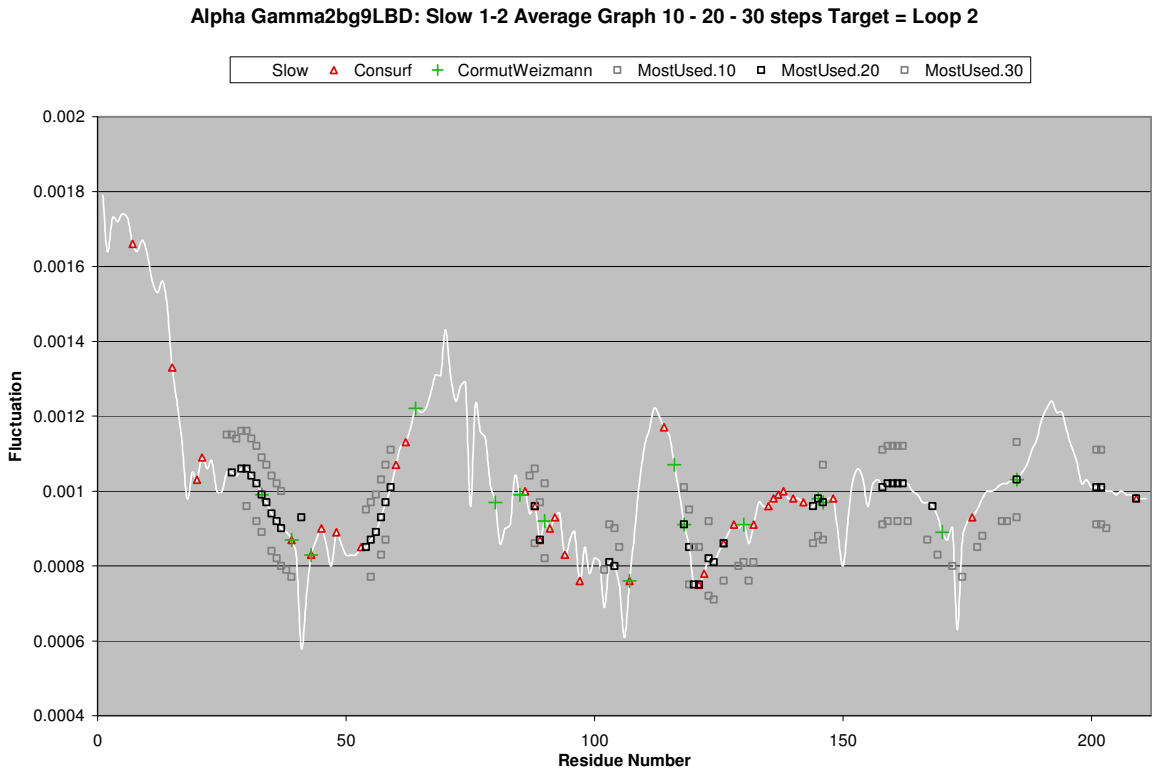

Figure 3.30: Slow 1-2 average fluctuations of alpha-gamma subunit of the LBD of nAChR.

Also, the paths reaching to the Loop 9 regions are similar to the paths reaching to the Cys Loop and Loop 2 regions. In all of the cases, no matter which region is selected to be the target region, as the number of maximum allowed step is increased, the paths tend to visit the residues of inner sheet more than the residues of outer sheet. But the inner and outer sheet usage slightly changes in the paths of Delta and Alpha-Delta subunits.

Each bracket shows the Target regions and each column under the target columns are the maximum allowed step number along the paths. Numbers in table represent the number of the most visited residues along the connected paths. Lines inside the brackets separate the subunit as inner and outer sheets. Residues before the Cys Loop belong to the inner sheet and the residues after the Cys Loop belong to the outer sheet [3].

Table 3.4 displays the most visited residues along the paths starting from the binding loops of Alpha-Gamma subunit of LBD of nAChR and going to the Cys Loop, Loop 2 and Loop 9 regions of each subunit.

Table 3.4: Most visited residues along the paths in the LBD of nAChR.

Target = Cys Loop		
10 Step	20 Step	30 Step
31	28	23
33	29	26
36	30	27
42	31	28
45	32	29
51	33	30
52	34	31
53	35	32
55	36	33
56	37	34
57	53	35
58	54	36
59	55	55
90	56	56
103	57	57
123	58	58
124	59	59
125	60	60
127	87	87
143	90	88
144	103	90
145	104	103
146	105	104
158	107	105
160	118	107
161	119	108
162	120	117
164	121	118
167	122	119
168	123	120
172	125	121
175	146	122
180	158	146
181	159	158
182	160	159
184	161	160
201	162	161
202	184	162
203	185	185
204	202	202

Target = Loop 2		
10 Step	20 Step	30 Step
30	27	26
32	29	27
33	30	28
35	31	29
36	32	30
37	33	31
38	34	32
39	35	33
55	36	34
57	37	35
58	54	36
88	55	37
90	56	54
119	57	55
123	58	56
124	59	57
126	88	58
129	89	59
130	103	87
131	104	88
132	118	89
144	119	90
145	120	102
146	121	103
158	123	104
159	124	105
161	126	118
163	144	119
167	145	120
169	146	121
172	158	123
174	159	146
177	160	158
178	161	159
182	162	160
183	168	161
185	185	162
201	201	185
202	202	201
203	209	202

Target = Loop 9		
10 Step	20 Step	30 Step
28	23	20
29	26	22
31	27	23
32	28	26
34	29	27
35	30	28
37	31	29
39	32	30
43	33	31
51	34	32
53	35	33
54	36	34
55	37	36
56	53	54
57	54	55
58	55	56
88	56	57
90	57	58
103	58	59
119	59	60
120	87	86
121	88	87
122	89	88
123	90	89
124	103	90
126	104	103
128	105	104
143	118	105
145	119	107
146	120	108
158	121	117
159	122	118
180	145	119
181	146	120
183	158	121
184	159	122
201	184	146
202	185	158
203	201	159
204	202	201

Red numbers in first bracket mean that, those residues are the most visited residues along the paths going to Cys Loop regions whatever the number of used step is. Green numbers in the second bracket mean that, those residues are the most visited residues along the paths going to the Loop 2 regions whatever the number of used step and the blue numbers in the third bracket mean that, those residues are the most visited residues along the paths going to the Loop 9 regions whatever the number of used step is. The numbers highlighted with yellow represent the mostly used residues on the paths wherever the target region and whatever the number of step of the path is.

Table 3.4 shows that whatever the length of the step is and wherever the target region is selected, ARG55, ARG57 and GLN58 of Beta 2, LEU146 of Beta 7 and the ILE158 of Beta 8 are the most visited residues. Another result of this table is that the shorter paths (1 to 10 steps) tend to visit the residues of outer sheet more than the residues of inner sheet where the longer paths (10 to 30 steps) tend to visit the residues of inner sheet. Table 3.4 does not include the residues of binding loop as it is the starting point and the residues of Loop 2, Cys Loop and Loop 9 regions as they are the target regions.

Table 3.5. Most visited residues along the paths of LBD of nAChR

Alpha-Gamma	Beta	Delta	Alpha-Delta	Gamma
55-ARG	35-LEU	29-GLU	33-VAL	33-LYS
57-ARG	36-THR	35-LEU	34-GLY	54-TRP
58-GLN	37-LEU	36-SER	36-GLN	55-ILE
146-LEU	39-SER	59-ASP	55-ARG	88-ASP
158-ILE	40-LEU	90-PRO	56-LEU	157-LEU
	53-SER	91-ASP	57-ARG	158-GLN
	56-LEU	92-ILE	90-LEU	
	103-THR	147-LYS	103-ASN	
	124-TYR	148-PHE	119-THR	
		160-MET	120-PRO	
		200-VAL	121-PRO	
			122-ALA	
			146-LEU	
			158-ILE	
			159-SER	
			187-TRP	
			201-ILE	
			202-THR	

For the most visited residues along the paths starting from the other subunit four subunits of the LBD of nAChR, Table 3.5 gives some insight. Residues shown in Table 3.5 are the counterparts of yellow highlighted residues shown in Table 3.4.

Table 3.5 displays that most visited residues found for each path whatever the number of step and wherever the target is. 18 residues of Alpha-Delta subunit are visited mostly on the paths and these residues seem to be the most visited residues for the arrival to the desired region after the path starts from the binding regions. And all of the other residues are crucial for the generated paths to be able to reach the target regions.

3.6.3. Combined Analyses of the full structure of nAChR

When nAChR is analyzed as a full structure with its TMD attached to the LBD, it contains one starting point and one target region for each subunit. The starting region of each subunit are the binding loops which are Loop A, Loop B and Loop C whereas the target regions are the gate regions of each subunit. These analyses are performed for all of the subunits of the nAChR but only the results of Alpha-Gamma subunit are displayed here. The other figures are listed in APPENDIX B, igure B.28 to Figure B.30.

Figure 3.31 displays the slow 1-2 average fluctuations of the Alpha-Gamma subunit.Grey boxes below the slow 1-2 fluctuations curve represent the most visited residues along the paths which are composed of maximum 10 steps. Black boxes right onto the slow 1-2 average fluctuations curve are the most visited residues along the paths which are composed of maximum 20 steps. And the grey boxes above the slow 1-2 average fluctuations curve are the most visited residues along the paths which are composed of maximum 30 steps. The red triangles and the green plus signs on the slow 1-2 average fluctuations curve represent the most conserved and correlated residues respectively.

In Figure 3.31, the preset target is the gate region of any subunits in the full structure of nAChR molecule. The most visited residues along the shorter paths (maximum of 10 steps) correspond to Loop 2, Cys Loop, Loop9, Beta9 and Beta 10 regions at the extracellular side. The loop connecting extracellular and transmembrane domains, named as the Beta10-M1 loop here, is also one of the most visited regions. In TMD, the most visited residues are at the top parts of the helices which places are close to the extracellular side.

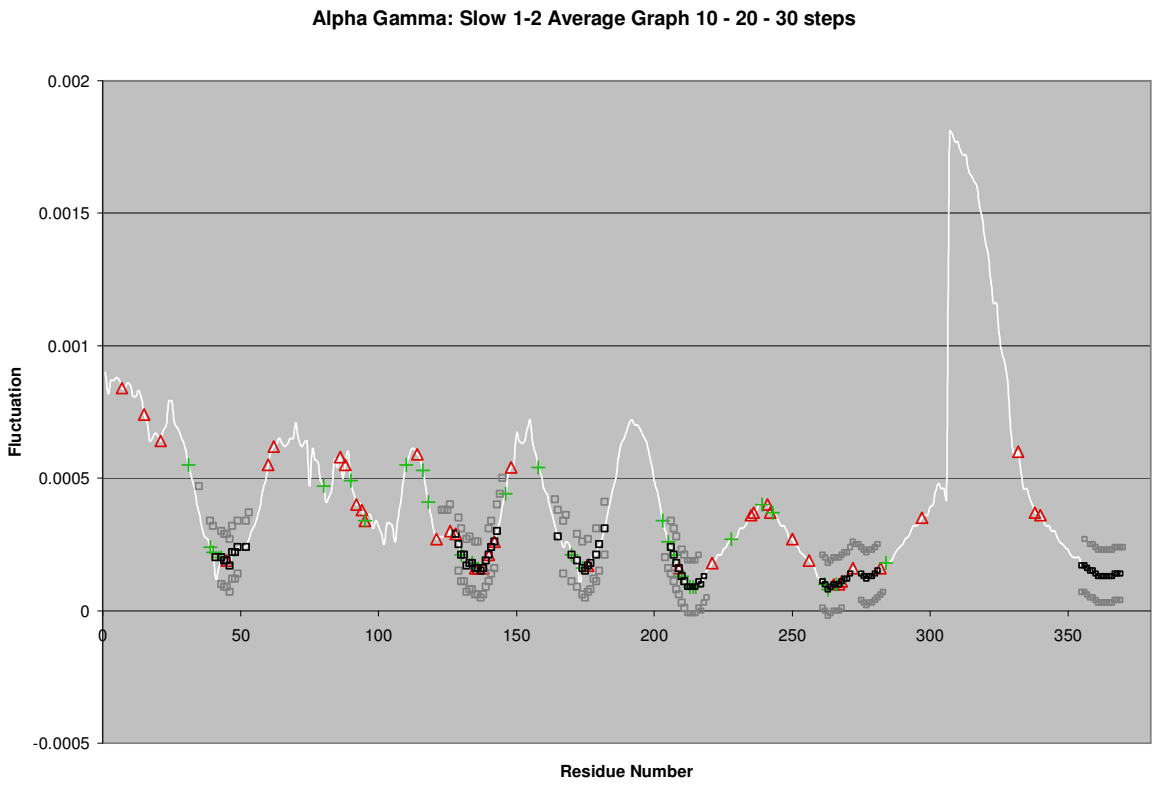

Figure 3.31. Slow 1-2 average fluctuations of the Alpha-Gamma subunit of nAChR.

All of the most visited residues in LBD are close to each other in space and these regions are supposed to be the actuator regions of the gating mechanism [8, 10]. In Figures 3.26 to 3.30, the target regions were selected to be Loop 2, Cys Loop and Loop 9 regions supposing these regions as important regions. In Figure 3.31 it is seen that these regions really appear on the most visited regions on the paths heading to the gate regions. These regions appear at the hinge point of the slow 1-2 average fluctuations. The most visited residues shown in Figure 3.31 are either well conserved or have correlated mutations. Also, in spite of M4's distant location from the inner interface between LBD and TMD, the upper part of M4 seems to be highly visited along the connected paths. But this M4 region does not seem to be highly visited for the long paths of the Delta subunit. This region was studied by Auchbach to see its effects on the gating mechanism and they claim that mutation on some of the residues of M4 affects gating mechanism [23].

Alpha-helix region of each subunit is the least visited region among the whole molecule for each of the subunits. Loop 2, Cys Loop and Beta 10 regions are mostly visited

for all of the subunits of nAChR.Also the upper halves of the helices of TMD are mostly visited during the paths reaching to the gate region.

In the full structure of nAChR, the most visited residues are in Loop 2, Cys Loop, Beta 10 and in the upper halves of the helices of TMD. Also some short paths seem to visit Loop 9 regions but not as much as they visit Loop 2 and Cys Loop regions. In the LBD of nAChR and AChBP analyses these Loop 2, Cys Loop and Loop 9 regions were selected to be the target regions and it was observed that Beta 1, Beta 2 and Beta 10 regions were mostly visited along the paths. Also from the GNM section it was shown that the transmembrane region is highly correlated within itself and with the other transmembrane regions. Also the analyses of MCPOOL shows that there are so many visited regions in the upper parts of the helices of the TMD. These data show that after the coupling of the ligand, binding regions transmit the signal to the lower part of the extracellular side using the Beta 1, Beta 2 and Beta 10 regions. The signal then comes to either Loop 2 or Cys Loop. Residues of M2-M3 Loop are mostly visited. Then the upper halves of the helices of the TMD regions are highly visited. But these are the most used residues and this is not the actual order of the transmission. As the order of the steps remains unknown this is only a theory which may be in agreement with the previous studies of various researchers [3, 5, 10, 25, 27]. But this theory will be checked in the PAJEK section because PAJEK will show the steps involved in the transmission of signal from the binding regions to the target regions. It will also show where a residue goes and which residue was visited before that one.

3.7. PAJEK Visualizations

In section 3.6, the most visited residues and regions on the paths identified in the network of cooperative fluctuations of the structure have been discussed. Such regions are presented with respect to the fluctuations in the average of the slowest two modes in Figures 3.26 to 3.31 with the conserved residues and residues having correlated mutations labeled. Here, we further present how the two end points may connect, when we have a starting and target regions, with these most visited residues.

As there are too many paths connecting these end points, graphic representations of the most used paths are presented below for AChBP, LBD of nAChR and full structure of

nAChR. For the AChBP the starting point is selected to be the principle binding residues and the end points are selected to be the Cys Loop, Loop 2 and Loop 9 regions.

For LBD of nAChR the starting points are selected to be the binding loop Loop 8 (Loop B) and the end point is selected to be the Cys Loop, Loop 2 and the Loop 9 regions. For the full structure of nAChR the starting point is Loop B again but the end point is the gate region this time. From the PAJEK figures it is seen that almost all of the most used residue and region outputs of MCPOOL appear on the figures.

For PAJEK analyses, each path was analyzed individually. Since each path is composed of its own individual steps, these steps were investigated and categorized for each path and this data was given to PAJEK. PAJEK analyzes the Mcpool outputs and looks at each visited step. When a residue goes to another residue it is considered to be a step and PAJEK takes these data from MCPOOL.

After calculating the usage value of each step, it points each individual residue and starts connecting the residues according to the usage of those steps. There may be thousands of different steps, but in the PAJEK calculations only the strongly connected residues are taken into consideration. Strongly connected residue means that, those steps are used so many times on the total paths. The numbers standing on the lines show how many times that step has been used totally.

Results of MCPOOL and PAJEK don't need to be exactly the same since the analyses of these methods are different (to be described on the following pages). Figures 3.32 to 3.34 display the most used steps along the paths. The figures are listed as starting from the binding loop and ending at the Cys Loop, Loop 2 and Loop 9 respectively.

According to the results of MCPOOL, the most visited regions on the paths belonging to AChBP were found to be Beta10, Beta1, Beta9, Beta2 and Loop9 Here, PAJEK displays how these regions are involved in the most used pathes between the given end points These regions remain on the analysis of most used path search as visualized in Figure 3.32. Even though none of these regions are close to Cys Loop along the sequence, they are close to each other in space and they display correlated fluctuations.

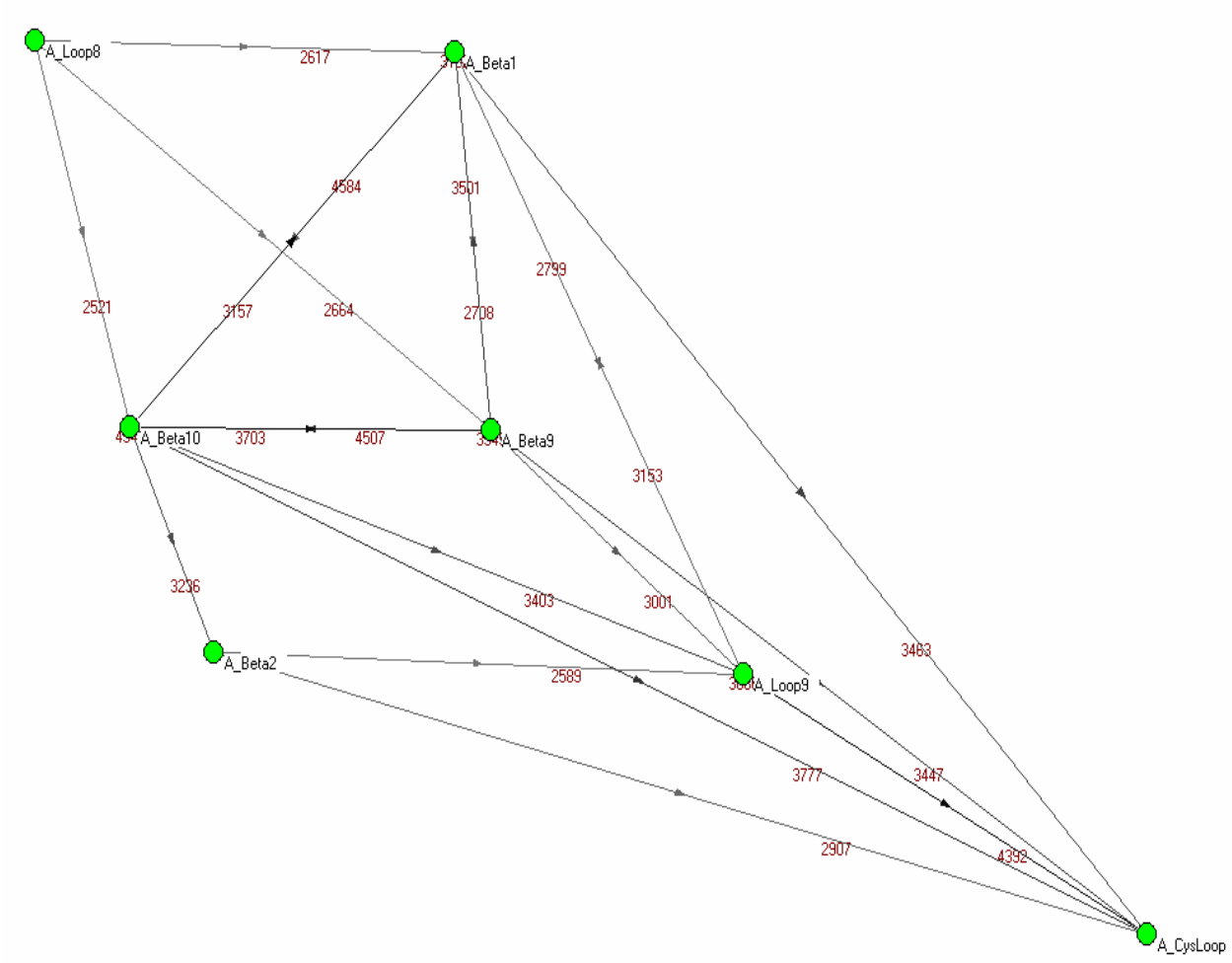

Figure 3.32. Graphic representation of the most visited steps along the paths which start from the Loop B of alpha-gamma subunit of AChBP and go to the Cys Loop of the same subunit.

Figure 3.33 displays the most used regions on the paths starting from Loop 8 and arriving at Loop 2 to see how these most used regions behave. Loop 2 is also considered to be an important region as an actuator of the gating mechanism. Each green dot stands for the most visited residues. The values on the lines of connected dots are the number of generation of those steps and the arrows on each line shows which way do those lines go through

In MCPOOL section the most used residues were indicated but in this PAJEK section the most used steps are shown. There are hundreds of residues along the molecule and MCPOOL calculates the usage of each residue along the paths bu this doesn't mean that the most used residues are connected on the paths. The most visited residue doesn't mean that these residues must follow each other on the paths. However, PAJEK shows the most used steps. When the end point is selected to be the Loop 2 region of AchBP, the figure becomes;

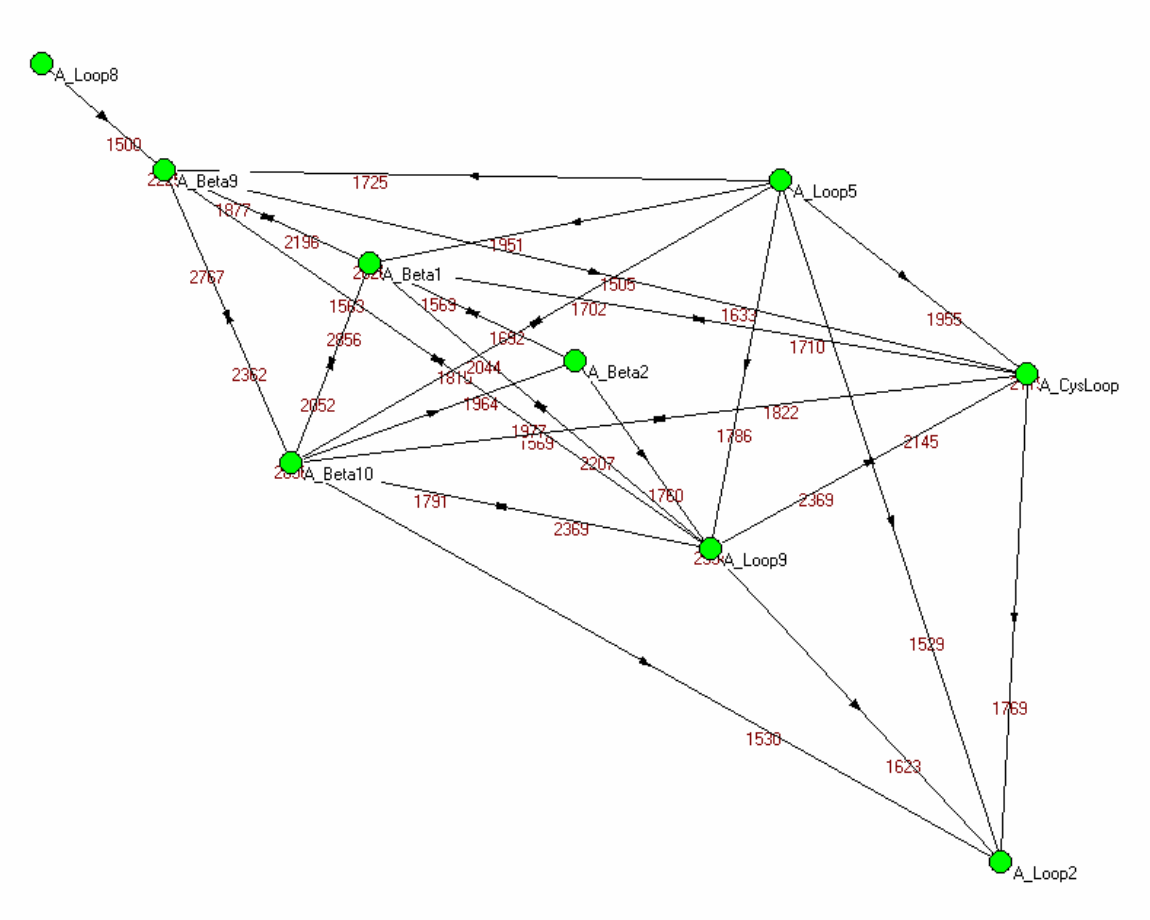

Figure 3.33. Graphic representation of the most used paths which start from the Loop 8 (Loop B) of alpha-gamma subunit of AChBP and go to the Loop 2 of the same subunit. Each green dot stands for the most used regions.

For example, if PAJEK shows a step that has been used 2000 times along the paths, it means that one residue of that step is connected with the other residue of that step for 2000 times. But if MCPOOL says a residue is visited 2000 times, this doesn't mean that this residue is visited 2000 times after the residue shown on the PAJEK output. So, combining both results of MCPOOL and PAJEK it is seen that there is an agreement within these results. Beta1, Loop 9, Beta9 and Beta10 regions were observed to be the most visited four regions by the analysis of MCPOOL. These regions are also found in the PAJEK calculations in addition to Cys Loop, Beta 2 and Loop 5. These Cys Loop, Loop 2 and Loop 9 regions were considered to be involved in gating mechanism [10] either by actuating or helping the signal to be transmitted. These data also show that they are coupled and they are of great importance for each other in the name of signal transmisson.

It has been mentioned above that the shortest and the most frequently used regions on the paths from binding loop to cys loop or loop2 to be in agreement with the regions that we have found in the MCPOOL. Similar situation holds true for the paths arriving to loop9 region too. But this time loop 2 is not seen neither in the shortest nor the most frequent paths. The Loop B don't make any direct connections with Loop 2 and the connections of Loop s with other residues are weak. Also the other binding loops connect with Loop 2 weakly. So this Loop 2 region do not appear on the paths that starte from the binding loop of A and arrives to the Loop 9. One of the reasons of this situation may be the low residue content of Loop 2.

In Figure 3.33 it was seen that a path goes via loop 9 to loop2. However, on the paths which start from the Loop B of AchBP and go to the Loop 9 of AchBP, Loop 2 region does not appear on the PAJEK figures This may lead us to think that on the way to the lower parts of the molecule, maybe to a gate region if a transmembrane region is present, loop9 is visited before loop 2 on the paths. Similarly, Loop2 do not appear on the paths to the cys loop while we see Cys Loop on the paths to loop 2. This may also lead us to think that on the paths down to the lower parts of the molecule, cys loop is visited before loop 2. These two statements may imply that if a signal is transmitted from binding loops to the transmembrane domain, since Cys Loop and Loop 9 comes before Loop on the paths, these Cys Loop and Loop 9 regions may be the actual allosteric transmitter. Also due to the close position of Loop 2 to Cys Loop and Loop 9 and the buried position of Loop 2 at the bottom of the LBD, Loop 2 may be highly affected by the motions of Cys Loop and Loop 9.

Since AchBP is a homopentamer, only three pajek outputs show the paths involved in only Alpha-Gamma subunit is presented. Each subunit is the same and the most visited regions and the paths are almost the same. In the case of Ligand Binding Domain of nAChR, since each subunit is different from each other, the PAJEK calculations were carried out for each subunit separately. In Figures 3.32 to 3.34, the starting point was the Loop8 (Loop B) region of AchBP. Here, as LBD of nAChR contains three binding loops which are referred as Loop A, Loop B and Loop C, the paths starting from Loop A, Loop B or Loop C and going to Cys Loop, Loop 2 or Loop 9 are analyzed. The results will be presented only for the paths of Alpha-Gamma subunit. There are some differences on the paths starting from the non-alpha subunits. One of the biggest difference is the amount of the step usages. In the MCPOOL section it was shown that the alpha subunits can reach to the target regions more than the non-

alpha subunits. The figures of other subunits will be given in APPENDIX B, Figure B.31. to Figure B.42 in detail. Another difference is on the most visited regions.

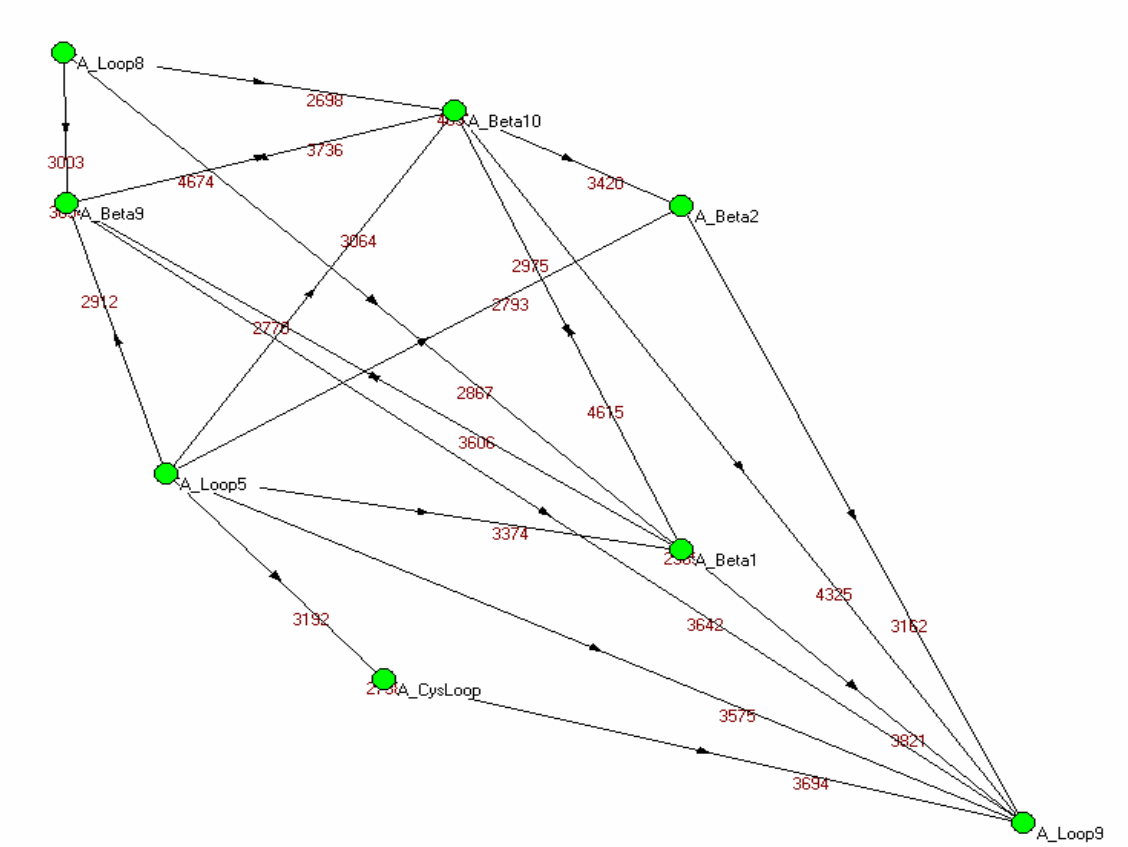

Figure 3.34. Graphic representation of the most used and shortest paths which start from the Loop 8 (Loop B) of alpha-gamma subunit of AchBP and go to the Loop 9 of the same subunit.

Figures 3.35 to 3.37 will show the most connected regions and the most visited regions on the paths starting from the binding loop Loop 8 to the Cys Loop, Loop 2 and Loop 9 of the LBD of nAChR respectively.

Figure 3.35 shows the most visited regions along the paths originated from the Loop 8 and reached to the Cys Loop of LBD of nAChR. Most of the regions appeared in the Figures 3.32 to 3.34 of AchBP are seen here too. This implies that the LBD of nAChR behaves similar to AChBP even though AChBP is not a real ligand binding domain of a receptor. There are six vertices shown on this figure where four of them (Loop9, Beta 1, Beta 2 and Beta 10) are at the top of most used regions according to MCPOOL analysis. In addition to MCPOOL two other regions (Beta 9 and Loop 10) are shown to be the most visited regions where Loop 10 is a binding loop (Loop C), and Beta 9 connects Loop 9 and the Loop C (Loop

10). But this doesn't mean that these two regions do not appear on the MCPOOL results. Because MCPOOL lists only the four most visited regions. So the fifth and sixth most visited regions may be these regions.

The other alpha subunit, Alpha-Delta, has got five vertices on its pajek output APPENDIX.B, Figure B.37, four of which are the four mostly used regions (Beta 1, Beta 2, Loop 9 and Beta 10) according to MCPOOL. Also these regions are the same with the regions that has been used at the paths of Alpha-Gamma subunit. Similarly, the Beta and Gamma subunits use the same regions of their own subunit, but at different proportions. Since each subunit is different and only the alpha subunits contain binding regions, the amount of connected path is different for each starting subunit. The only difference arises for Delta subunit. Loop 1 of Delta subunit seems to be visited frequently on the paths starting from the binding loops of Delta and reaching to the Cys Loop but this region cannot be seen on the PAJEK graphs due to the principles of PAJEK calculations mentioned above. So we may think that if Loop 1 is on the most used regions list of MCPOOL but doesn't appear on the PAJEK figures, it is not involved at the paths that we are really interested.

In section 3.6, it was shown that the longer paths visit the residues of the inner sheet more than the outer sheet. But the Cys Loop is between this inner and outer sheets and it is located at the bottom of the extracellular domain. If a binding occurs and if the signal is to be transmitted through the Cys Loop from binding residues it should be mainly from the residues of outer sheet. And Loop 1 is located at the inner sheet. This may show that as the number of allowed maximum step of the generated path increases, the steps are involved at the inner sheet and make loops within some residues. That's why the Loop 1 region seem the be visited many times but the important thing is the transmission ot the signal through the Cys Loop, not through the Loop 1.

Since the main purpose of these analysis is to find out which regions are the most visited regions and which region to region connections occur frequently for the transmission of signal from binding loops to C-terminal of the molecule, we must deal with the outputs of PAJEK. A region may be used so many times on the total paths but it doesn't mean that this region is involved on the gating. And the results of pajek shows us the regions that we mentioned before.

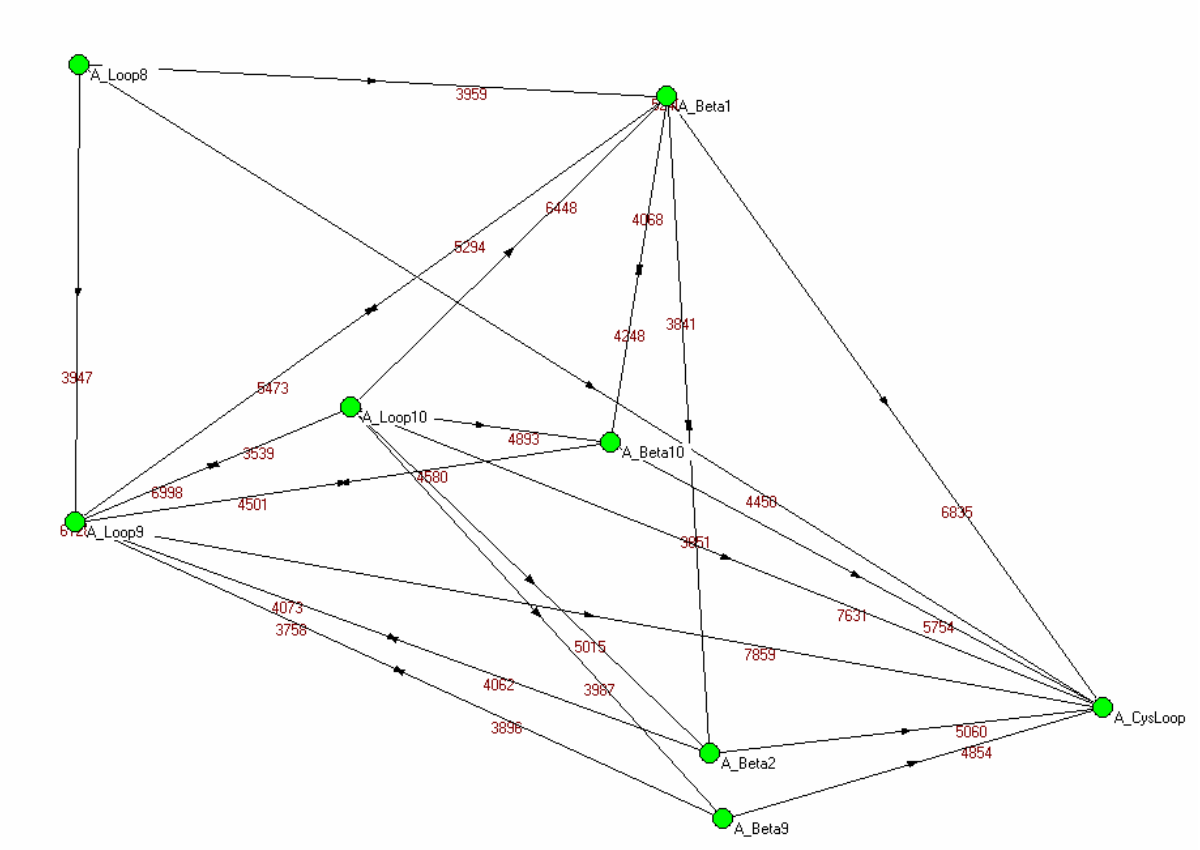

Figure 3.35. Graphic representation of the most visited paths which start from the Loop B of alpha-gamma subunit of LBD of nAChR and go to the Cys Loop of the same subunit.

Similar to the analysis that have been made for the paths from binding regions of LBD of nAChR to Cys Loop region, both of the most used regions of MCPOOL results appear on the Figure 3.36.

There are some small differences between Figure 3.35 and Figure 3.36. For the paths going to Cys loop it is seen from Figure 3.35 that there the connection between Loop 8 and Cys Loop occurs 4450 times. This value means that this step is used 4450 times on the total connected paths.

In Figure 3.36 the paths which start from Loop 8 split into two parts. One part is the Loop 8 to Loop 9 step and the other is Loop 8 to Beta 1 step. Figure 3.36 shows that the Loop 8 to Loop 9 step occurs 2117 times and Loop 8 to Beta 1 step occurs 2123 times. Even we add the values on these two separate branches it doesn't make 4450.

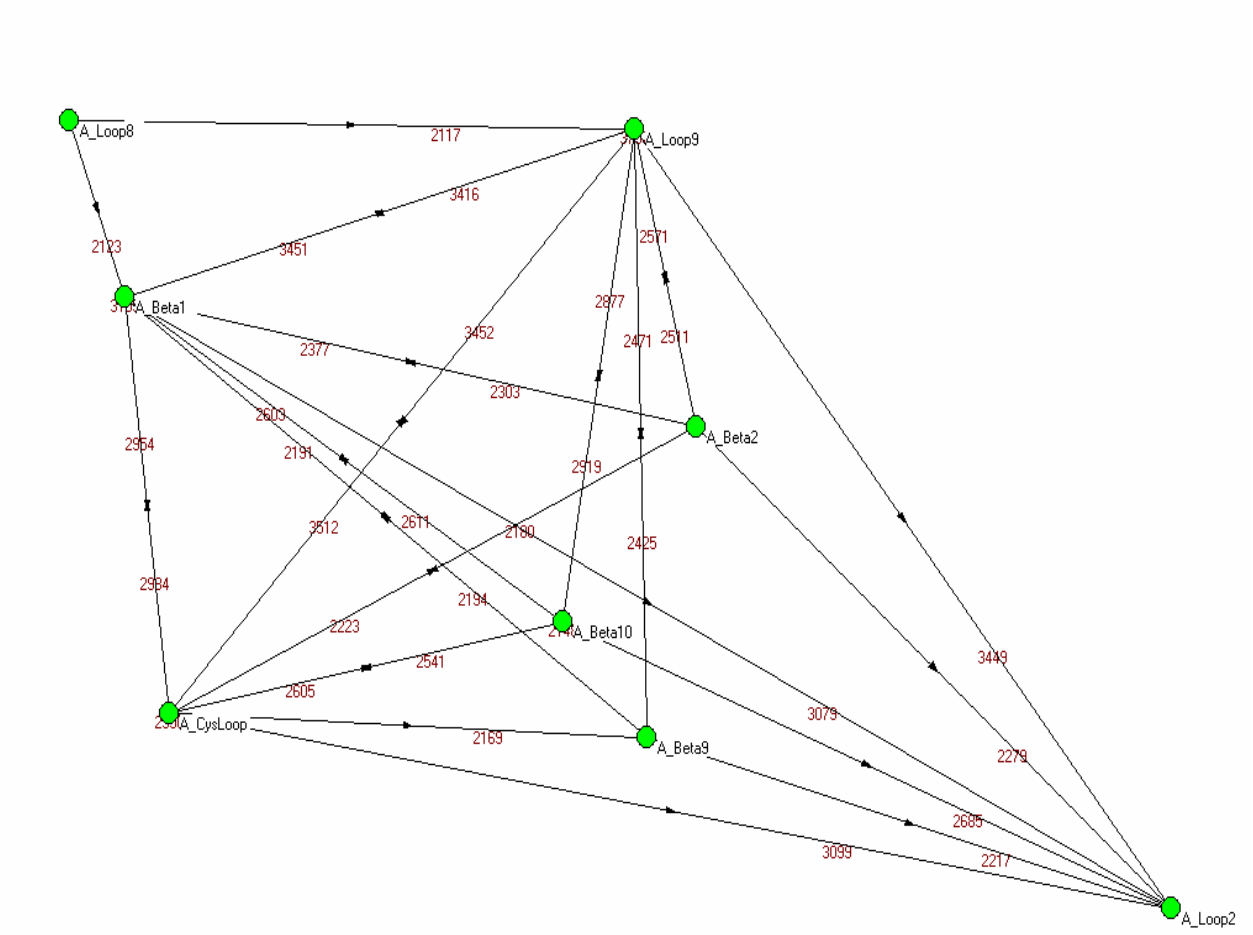

Figure 3.36. Graphic representation of the most used and shortest paths which start from the Loop B of alpha-gamma subunit of LBD of nAChR and go to the Loop 2 of the same subunit.

Figure 3.36 also shows that there aren't direct connections between Loop 8 and Loop 2. the main reason of this is that only the most frequent steps are taken into consideration. For to this aim the steps which are connected with a value of lower than 2000 were discarded. But the value of Loop 8 to Loop 2 step occurs 1580 times. Therefore no direct connections can be seen on Figure 3.36.

Another difference is on the total amount of the values entering to the target regions. From Figure 3.35 and Figure 3.36 it is seen that the occurance of Cys Loop of the most frequent steps is greater than the occurence of Loop 2 on the most frequent steps. For the case of Cys Loop this number is almost three-fold of the total value on the lines entering to Loop2. But one detail is that the total number of residues in Loop 2 is around one-third of the number of residues present in Cys Loop.

The results of MCPOOL show that Loop 1 of the LBD of nAChR is one of the most visited regions along the paths starting from the binding loops and going to the Cys Loop of LBD of nAChR. But this Loop 1 region does not appear on the PAJEK figures. The biggest reason is the limitations on the PAJEK figures. Since only the most frequent steps are obseved, Loop 1 of LBD of nAChR does not appear on the Figure 3.36.

However, all of the other subunits have got the same regions on the MCPOOL and pajek outputs. Neverthelles, Beta and Delta subunits have got less paths reaching on target than the other subunits.

Figure 3.37 displays the most frequent steps involved in the paths starting from the Loop 8 of LBD of nAChR and going to Loop 9 region. On the analysis of these paths, much of the results of MCPOOL and PAJEK are the same. In the Figure 3.35 and 3.36, Loop 1 was discussed . Loop 1 seems to be one of the most used regions for the paths originating from the Delta subunit and going to Cys Loop, Loop 2 and/or Loop 9. But for the paths going to Loop9 region of alpha-gamma subunit of LBD of nAChR, as the number of allowed steps reaching to Loop 9 is increased, the probability of Loop 1 to be on the most visited list increases.

When the allowed maximum step number is set to be high, MCPOOL continues to generate paths until the path length be 30. If the paths reach to the desired target at the 30^{th} step, all of the 30 steps are taken into consideration in PAJEK analysis. If the generated steps are repeated because of the low probability of going from one residue to another residue, some residues or regions may seem to be highly involved on the connected paths even if they don’t have a significant effect on the allosteric mechanism.

So, almost all of the paths to the Loop 9of LBD of nAChR use Loop 1 region as much as they use Beta 1 or Beta 2. But on the pajek analysis we are dealing with most frequent steps and this eliminates most of the paths containing Loop 1 region. On the other hand, if there are these many paths which can reach to target at three or four steps, the presence of Loop 1 on the paths, which reach to target on ten or twenty steps doesn’t make sense.

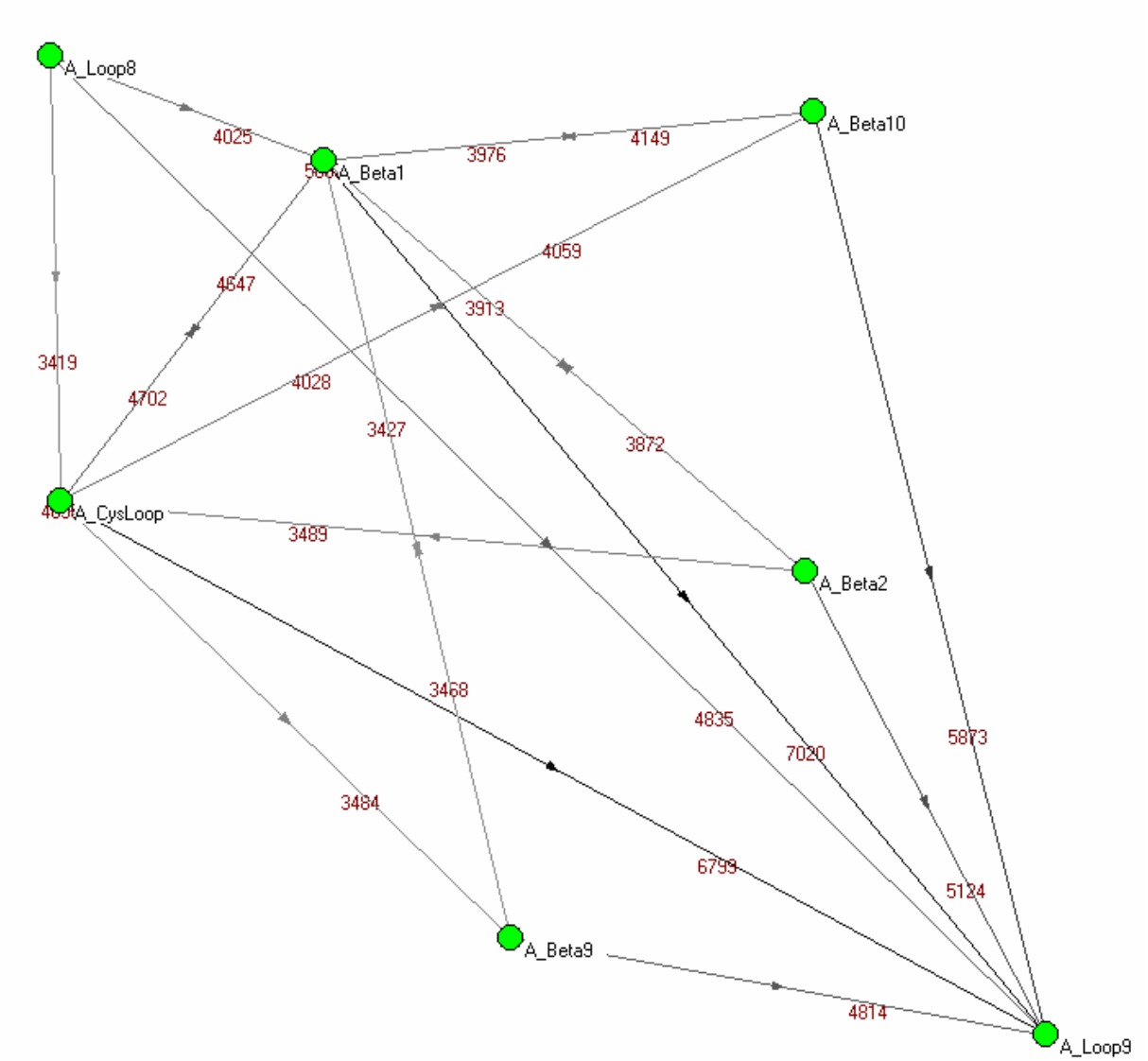

Figure 3.37. Graphic representation of the most used and shortest paths which start from the Loop B of alpha-gamma subunit of LBD of nAChR and go to the Loop 9 of the same subunit. Each green dot stands for the most used regions. The values on the lines of connected dots are the number of generation of those steps and the arrows on each line shows which way do those lines go through.

So far many PAJEK outputs have been discussed and it is seen that mostly the same regions are appear on the PAJEK figures which were drawn for the aim of reaching to Cys Loop, Loop 2 or Loop 9 from the binding regions. But how about if there was a transmembrane region attached to these molecules?

So far we always talked about the paths arriving to Cys Loop, Loop 2 and/or Loop 9, supposing that these regions are of great importance for gating mechanism [10]. To check this

theory, we took nAChR under consideration to see if these regions are located on the pajek figures. If so, it can be said that these regions are important for the allosteric transfer of the signal from binding sites to the gate region of the molecule.

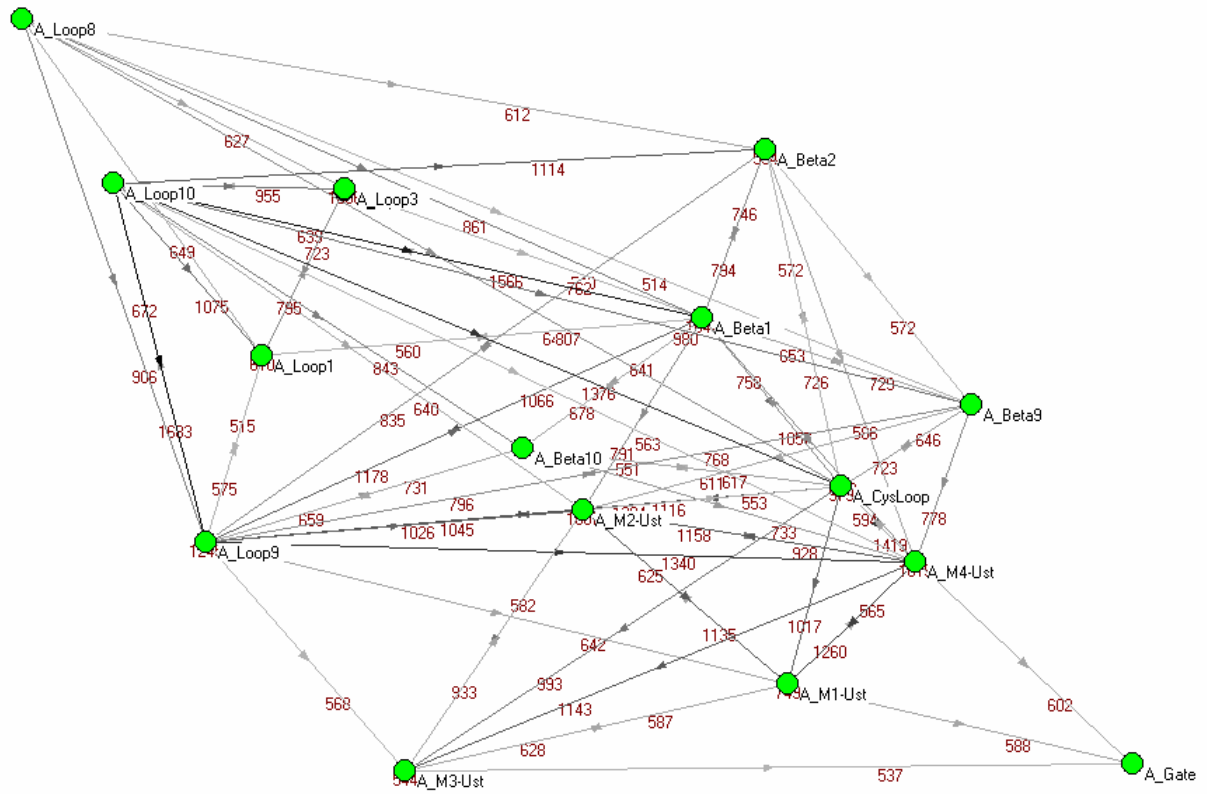

Figure 3.38. Graphic representation of the most used and shortest paths which start from the Loop B of alpha-gamma subunit of nAChR and go to the Gate of the same subunit.

Figure 3.38 displays the most frequent steps along the paths starting from the binding loop Loop 8 (Loop B) of full structure of nAChR and going to the gate region located at the transmembrane domain. This figure may seem complicated but it is plausible since nAChR has got around 60 per cent more regions than both AchBP and the Ligand Binding domain of the whole molecule. Previous MCPOOL results showed us that the upper regions of transmembrane domain are the most used regions along the TMD and the pajek output of this nAChR shows these regions to be either the shortest or the most used regions while reaching to gate regions after starting from the binding region. PAJEK outputs of other subunits are given in APPENDIX B, Figure B.43 to Figure B.46.

As expected, Cys Loop and Loop 9 can be seen on this figure and surprisingly Loop 1 too. While working on the ligand binding domain of nAChR without the TMD, Loop 1

haven’t been seen on any of the PAJEK figures. So it wasn’t considered to be an important region. But when the TMD is attached to LBD, Loop 1 region seems to carry more importance than it does on AChBP or LBD of nAChR. But no direct connections are seen between Loop 1 and the gate regions. It maybe because that Loop 1 is at the N-terminal of LBD while gate region is placed at the middle of TMD.

For both of the AChBP, nAChR and the LBD of nAChr molecules, the Beta 1 and Beta 2 regions of LBD seem to be mostly visited regions. And also according to the results of MCPOOL section these regions are the must regions if a path is expected to reach the selected target. The upper halves of the TMD seem to be more visited on the paths through the gate. Actually it would be meaningless to go through the lower part and then go to the gate.

In the end of the MCPOOL section the most visited residues were listed for the paths of starting from the binding regions and going to the gate regions of nAChR. And it was said that the order of the steps in the paths are unknown. In this section the most frequent steps showed that the binding loops visit the Cys Loop, Loop 2 and Loop 9 regions and sometimes they visit the Beta 1 and Beta 2 regions as mentioned at the end of the MCPOOL section. Then, these regions interact with the upper halves of the transmembrane helices. And finally these signals coming from the upper halves of the helices gather at the gate region. After the binding of the ligand to the extracellular region of the nAChR molecule, a conformational change occurs and this change yields a twisting motion.

4. CONCLUSION

nAChR receptors have been important material for the researchers for a couple of decades. Among the Ligand Gated and Voltage sensitive classes of ion channels, nAChR is the most studied ion channel from the Ligand Gated ion Channel family. Later studies revealed the full structure of nAChR molecule but before the public release of the full structure of nAChR, many different transmembrane channels were studied with different Ligand Binding Domains such as Acetylcholine Binding Protein. It has been subject to many different studies as its shape and configuration is similar to LBD of the nAChR. Also, since the defective opening or closing mechanisms of such ion channels lead to serious diseases, the exact gating mechanism of the nAChR has been a prior study for many researchers. In this thesis many different calculations are performed to understand the gating mechanism of the channel. And to understand the intrinsic behaviors of the molecule, the LBD of nAChR is considered as a separate molecule. In addition, the structural behavior of AChBP is investigated.

The cross correlation analyses of these three molecules yielded different results. The homopentamer structure of AChBP showed exactly the same results for each individual subunit. But this is not the real expected behavior, as the real ligand binding domain of nAChR is not homopentamer. There are five binding regions in the AChBP whereas there are two binding regions in the LBD of nAChR which are located at the Alpha subunits of nAChR. But the importance or difference of these Alpha subunits of AChBP couldn't have been designated due to the homopentamer structure of AChBP. But in the case of LBD of nAChR study, the subunits appeared to behave different where the molecule appeared to split into two clusters. But in the presence of TMD, the full structure showed real opening motion of the gate region. Cys Loop, Loop 2 and Loop regions of the LBD interact with each other and move cooperatively to straddle the M2-M3 linker of the TMD. Cys Loop is less mobile in the full structure of the nAChR than it is in the other two structures. It behaves as a hinge point between the LBD and TMD of nAChR. Also some residues of the Cys Loop region of nAChR are observed to be kinetically hot residues. But when no TMD exist, the residues of Cys Loop region do not correspond to any kinetically hot residues. In addition, the M2-M3 loop is also a stable region which acts as a hinge point in the full structure of nAChR but it

moves enough to form a couple with the Cys Loop and Loop 2 regions of the Ligand Binding Domain. The upper regions of the helices of the transmembrane domain are more involved in the gating mechanism than the lower part of the transmembrane region. And these regions of each subunit are highly correlated with each other. When the investigations are made on the effects of ligand binding to the signal transmission to the gate regions of the other subunits, it is seen that the paths jump to the TMD of the starting subunit first and then goes to the other subunit through the transmembrane regions.

On the search for allosteric pathways through the target regions, Cys Loop, Loop 2 and Loop 9 regions are important regions for the transmission of the signal from the ligand binding to transmembrane region. Also the Beta 10 region of the extracellular domain, which is covalently bonded to the transmembrane domain, is an important region for the transmission of the signal after the activation of the molecule by an agonist. Signals come to these regions either directly or by a second region. These secondary regions are mostly the Beta 1 and Beta 2 regions for each of the three structures. These regions are located in the molecules as if they are the spines of the molecules; hence these regions affect the behaviors and motions of the molecule. Also some of the residues of these regions are either conserved or correlated among the evolution which makes those residues more important.

When LBD of nAChR is studied as a separate structure, it showed breathing motions just like the AChBP. But the presence of the TMD caused the molecule to make a twisting motion. The wideness of the pore is determined by the side chains of the residues of gate regions. As the molecule twists, the side chains of the residues recede and the interactions between these side chains diminish. Also, since the outer part of the transmembrane domain of the nAChR is in contact with the lipid layer, it would be easier for the molecule to twist than to expand.

Both the LBD of nAChR and the AChBP molecules tightens for the positive and negative conformations but the gate region of nAChR broadens. The LBD of the molecule is squeezed and this shrinking of the LBD leads the TMD to widen by the twisting motion pivoted from the LBD to TMD interface.

APPENDIX A: STRUCTURAL DATA

Table A.1. Residue index of AChBP.

Res. #	Res. Name	Region	Res. #	Res. Name	Region	Res. #	Res. Name	Region	Res. #	Res. Name	Region
1	PHE		53	TRP	Beta 2	105	VAL	Beta 5'	157	GLU	Loop 9
2	ASP	Alpha	54	GLN	Beta 2	106	VAL	Beta 5'	158	ASN	Loop 9
3	ARG	Alpha	55	GLN	Beta 2	107	SER	Loop 6	159	SER	Loop 9
4	ALA	Alpha	56	THR	Beta 2	108	ASP	Loop 6	160	ASP	Loop 9
5	ASP	Alpha	57	THR	Beta 2	109	GLY	Loop 6	161	ASP	Loop 9
6	ILE	Alpha	58	TRP	Beta 2	110	GLU	Beta 6	162	SER	Loop 9
7	LEU	Alpha	59	SER	Beta 2	111	VAL	Beta 6	163	GLU	Loop 9
8	TYR	Alpha	60	ASP	Loop 3	112	LEU	Beta 6	164	TYR	Loop 9
9	ASN	Alpha	61	ARG	Loop 3	113	TYR	Beta 6	165	PHE	Loop 9
10	ILE	Alpha	62	THR	Loop 3	114	MET	Loop 6'	166	SER	Loop 9
11	ARG	Alpha	63	LEU	Loop 3	115	PRO	Loop 6'	167	GLN	Loop 9
12	GLN	Alpha	64	ALA	Loop 3	116	SER	Beta 6'	168	TYR	Loop 9
13	THR	Alpha	65	TRP	Loop 3	117	ILE	Beta 6'	169	SER	Loop 9
14	SER	Alpha	66	ASN	Loop 3	118	ARG	Beta 6'	170	ARG	Loop 9
15	ARG	Loop 1	67	SER	Loop 3	119	GLN	Beta 6'	171	PHE	Beta 9
16	PRO	Loop 1	68	SER	Loop 3	120	ARG	Beta 6'	172	GLU	Beta 9
17	ASP	Loop 1	69	HIS	Loop 3	121	PHE	Beta 6'	173	ILE	Beta 9
18	VAL	Loop 1	70	SER	Loop 3	122	SER	Beta 6'	174	LEU	Beta 9
19	ILE	Loop 1	71	PRO	Loop 3	123	CYS	Cys Loop	175	ASP	Beta 9
20	PRO	Loop 1	72	ASP	Loop 3	124	ASP	Cys Loop	176	VAL	Beta 9
21	THR	Loop 1	73	GLN	Beta 3	125	VAL	Cys Loop	177	THR	Beta 9
22	GLN	Loop 1	74	VAL	Beta 3	126	SER	Cys Loop	178	GLN	Beta 9
23	ARG	Loop 1	75	SER	Beta 3	127	GLY	Cys Loop	179	LYS	Beta 9
24	ASP	Loop 1	76	VAL	Beta 3	128	VAL	Cys Loop	180	LYS	Beta 9
25	ARG	Loop 1	77	PRO	Beta 3	129	ASP	Cys Loop	181	ASN	Beta 9
26	PRO	Loop 1	78	ILE	Loop 4	130	THR	Cys Loop	182	SER	Beta 9
27	VAL	Beta 1	79	SER	Loop 4	131	GLU	Cys Loop	183	VAL	Beta 9
28	ALA	Beta 1	80	SER	Loop 4	132	SER	Cys Loop	184	THR	Beta 9
29	VAL	Beta 1	81	LEU	Loop 4	133	GLY	Cys Loop	185	TYR	Beta 9
30	SER	Beta 1	82	TRP	Loop 4	134	ALA	Beta 7+ Cys	186	SER	Loop 10
31	VAL	Beta 1	83	VAL	Loop 4	135	THR	Beta 7+ Cys	187	CYS	Loop 10
32	SER	Beta 1	84	PRO	Loop 4	136	CYS	Beta 7+ Cys	188	CYS	Beta 10
33	LEU	Beta 1	85	ASP	Loop 4	137	ARG	Beta 7	189	PRO	Beta 10
34	LYS	Beta 1	86	LEU	Beta 4	138	ILE	Beta 7	190	GLU	Beta 10
35	PHE	Beta 1	87	ALA	Beta 4	139	LYS	Beta 7	191	ALA	Beta 10
36	ILE	Beta 1	88	ALA	Beta 4	140	ILE	Beta 7	192	TYR	Beta 10
37	ASN	Beta 1	89	TYR	Loop 5	141	GLY	Beta 7	193	GLU	Beta 10
38	ILE	Beta 1	90	ASN	Loop 5	142	SER	Beta 7	194	ASP	Beta 10
39	LEU	Beta 1	91	ALA	Loop 5	143	TRP	Loop 8	195	VAL	Beta 10
40	GLU	Beta 1	92	ILE	Loop 5	144	THR	Loop 8	196	GLU	Beta 10
41	VAL	Beta 1	93	SER	Loop 5	145	HIS	Loop 8	197	VAL	Beta 10
42	ASN	Beta 1	94	LYS	Loop 5	146	HIS	Loop 8	198	SER	Beta 10
43	GLU	Loop 2	95	PRO	Loop 5	147	SER	Loop 8	199	LEU	Beta 10
44	ILE	Loop 2	96	GLU	Beta 5	148	ARG	Loop 8	200	ASN	Beta 10
45	THR	Loop 2	97	VAL	Beta 5	149	GLU	Loop 8	201	PHE	Beta 10

46	ASN	Loop 2	98	LEU	Loop 5'	150	ILE	Beta 8	202	ARG	Beta 10
47	GLU	Beta 2	99	THR	Loop 5'	151	SER	Beta 8	203	LYS	Beta 10
48	VAL	Beta 2	100	PRO	Loop 5'	152	VAL	Beta 8	204	LYS	
49	ASP	Beta 2	101	GLN	Loop 5'	153	ASP	Beta 8	205	GLY	
50	VAL	Beta 2	102	LEU	Beta 5'	154	PRO	Loop 9			
51	VAL	Beta 2	103	ALA	Beta 5'	155	THR	Loop 9			
52	PHE	Beta 2	104	ARG	Beta 5'	156	THR	Loop 9			

APPENDIX B: ADDITIONAL FIGURES

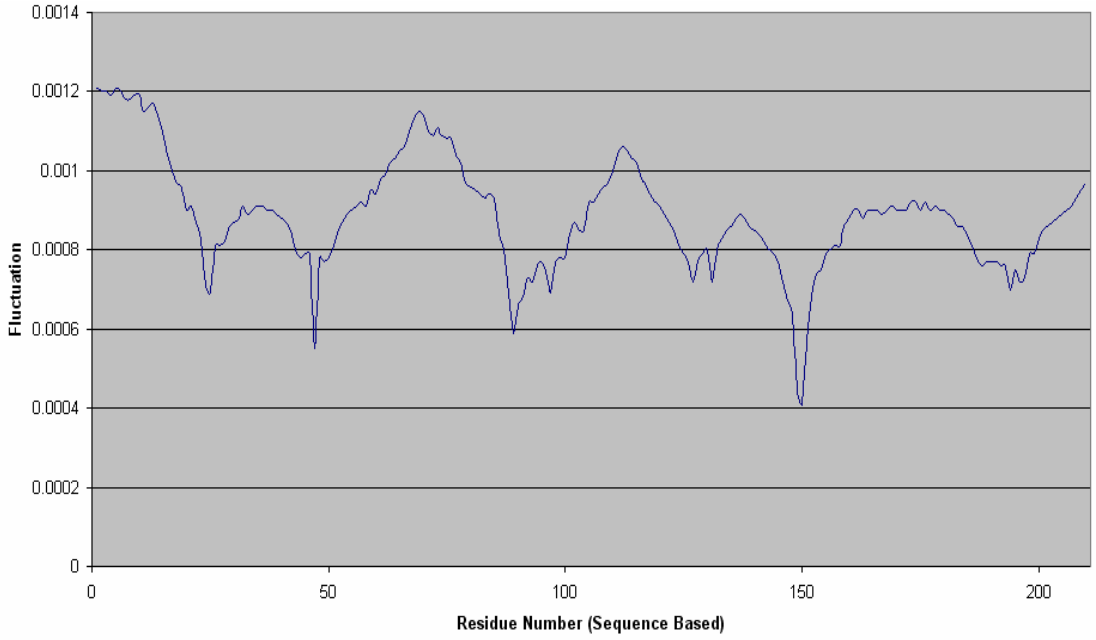

Figure B.1. Fluctuations of Beta subunit of LBD in nAChR in the average of slowest two modes

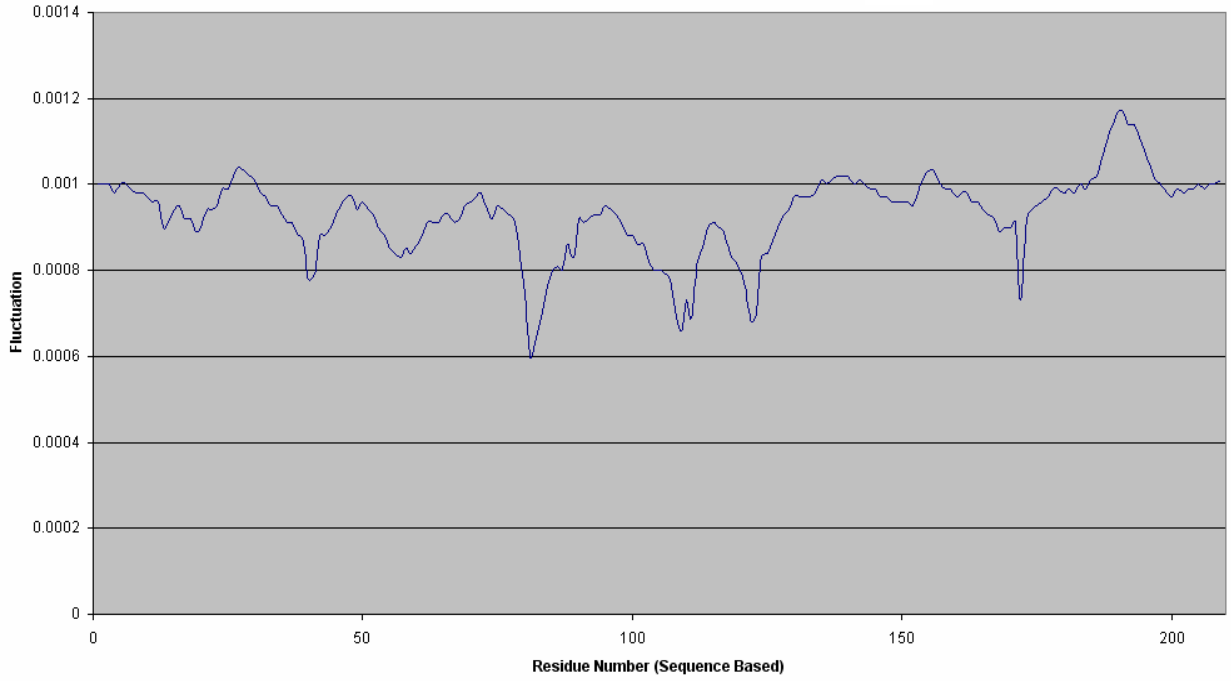

Figure B.2. Fluctuations of Delta subunit of LBD in nAChR in the average of slowest two modes

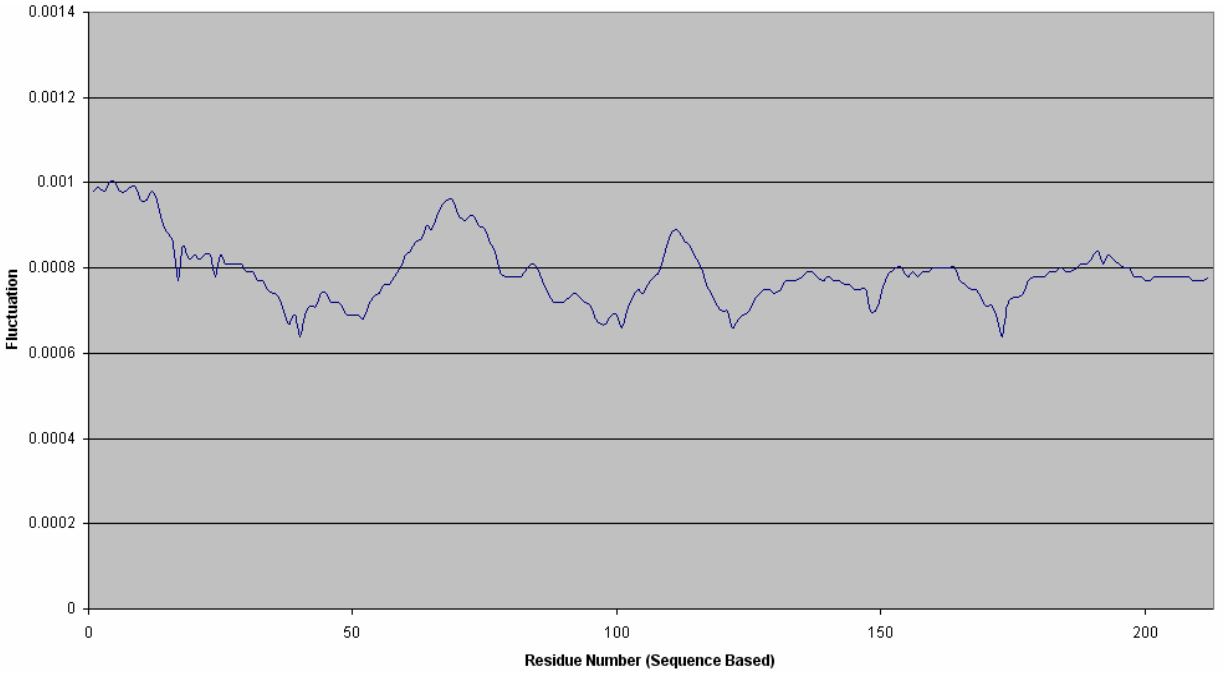

Figure B.3. Fluctuations of Gamma subunit of LBD in nAChR in the average of slowest two modes

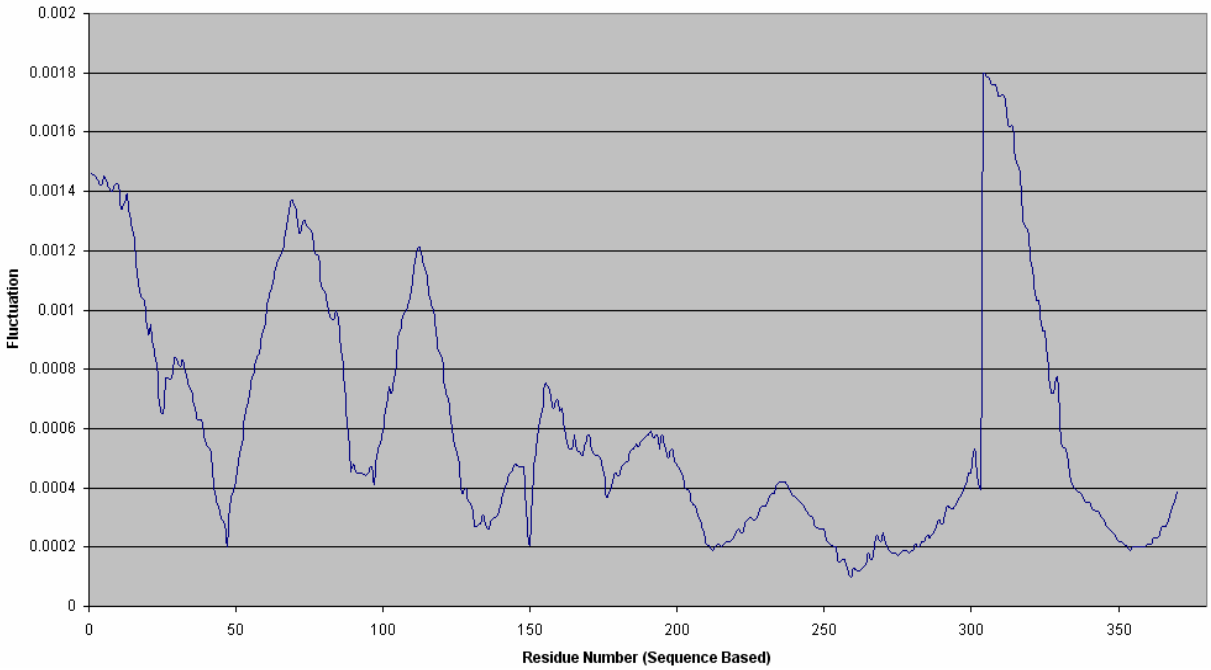

Figure B.4. Fluctuations of Beta subunit of nAChR in the average of slowest two modes

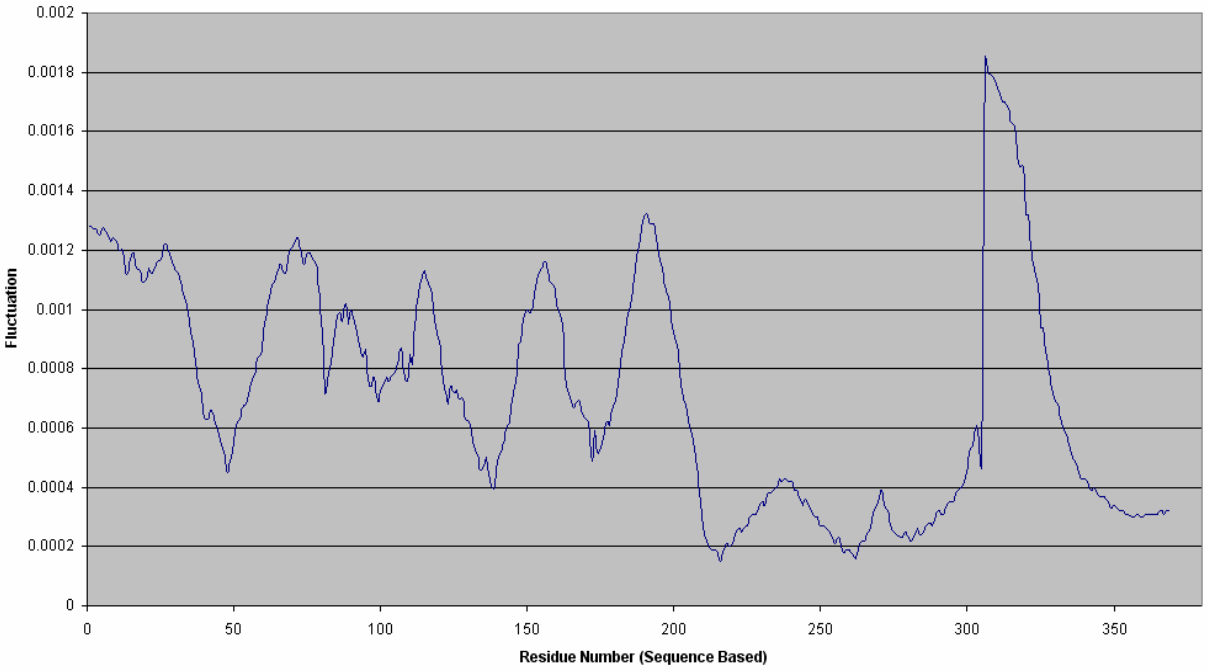

Figure B.5. Fluctuations of Delta subunit of nAChR in the average of slowest two modes

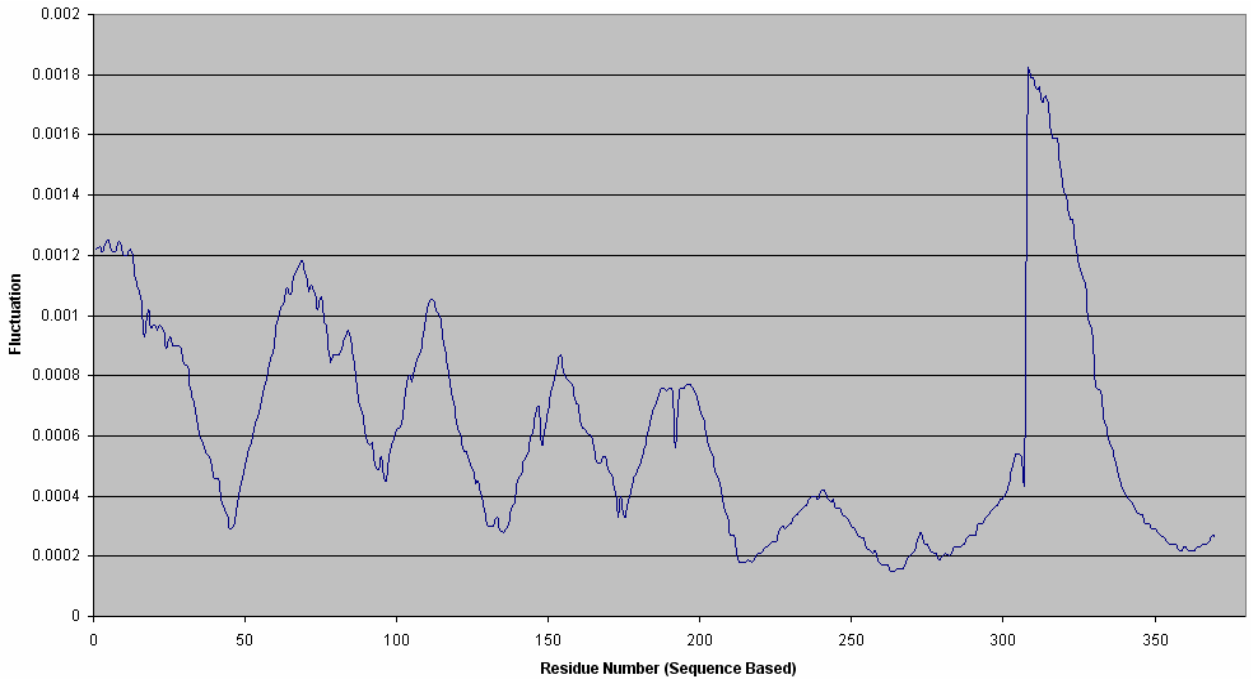

Figure B.6. Fluctuations of Gamma subunit of nAChR in the average of slowest two modes.

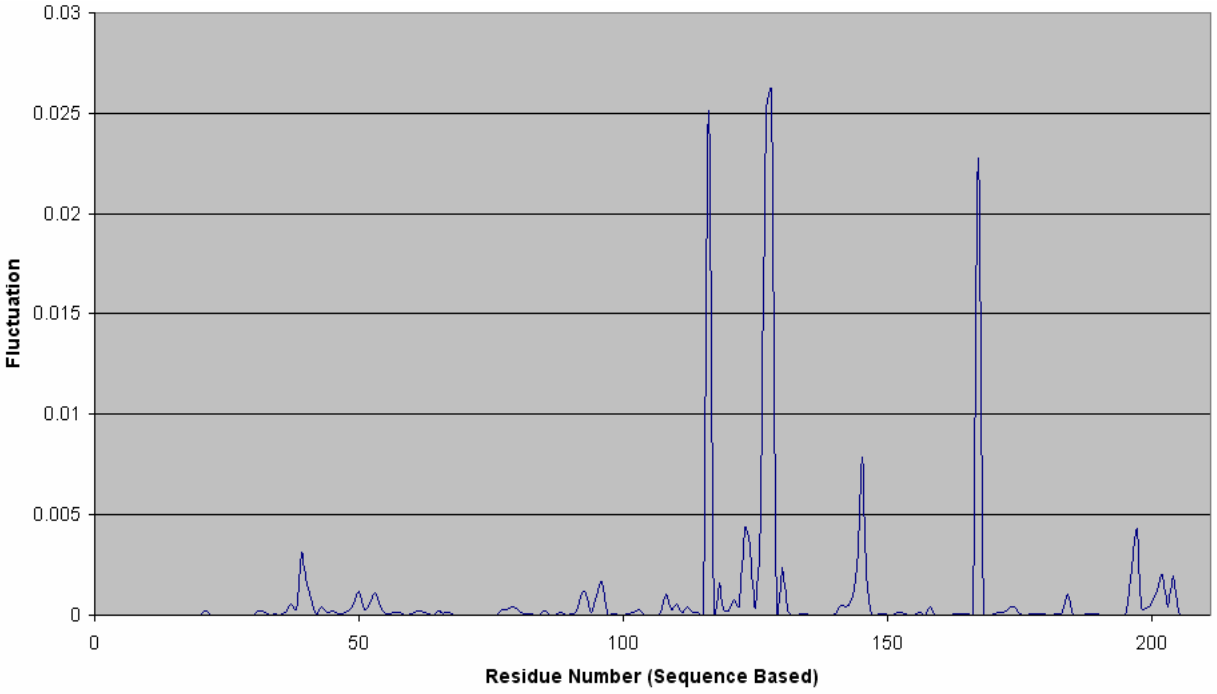

Figure B.7. Fluctuations of Beta subunit of LBD of nAChR in the average of fastest thirty modes

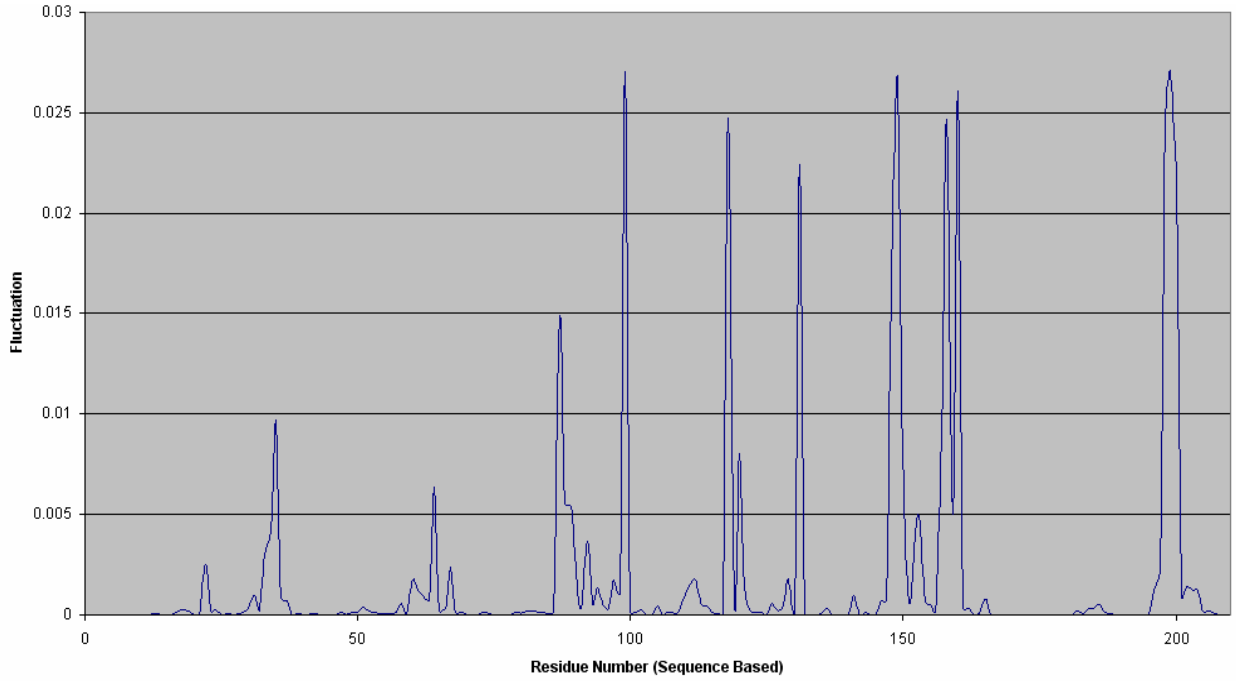

Figure B.8. Fluctuations of Delta subunit of LBD of nAChR in the average of fastest thirty modes

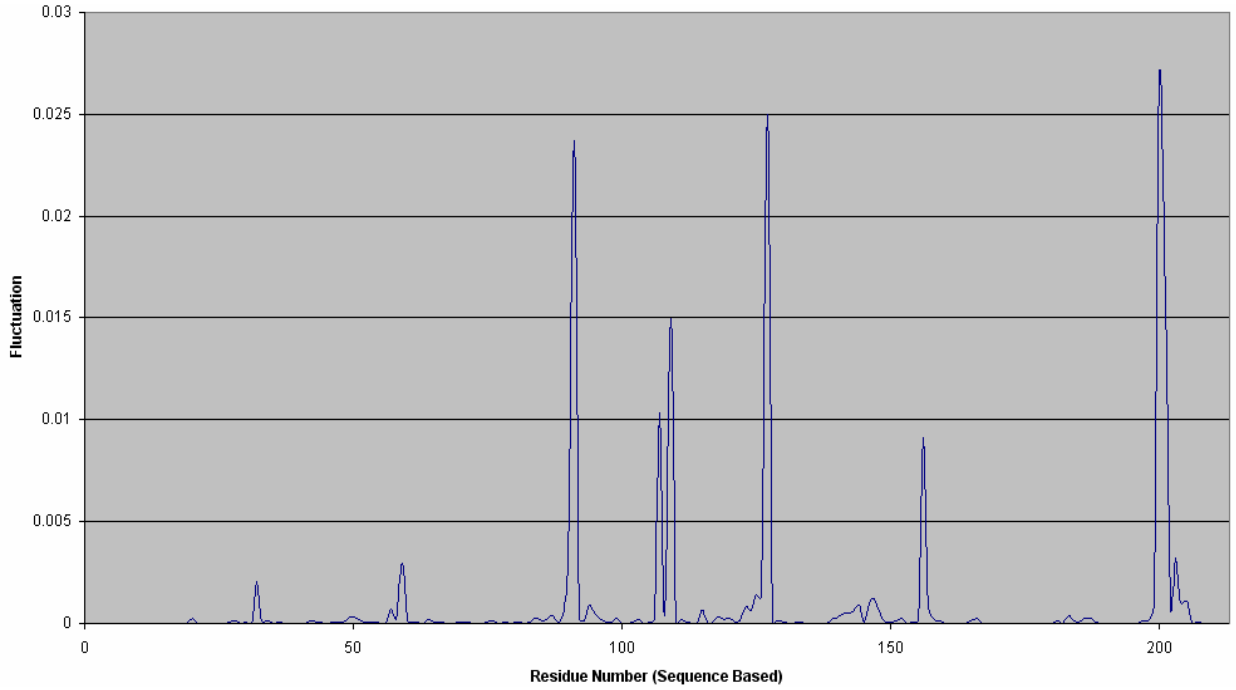

Figure B.9. Fluctuations of Gamma subunit of LBD of nAChR in the average of fastest thirty modes.

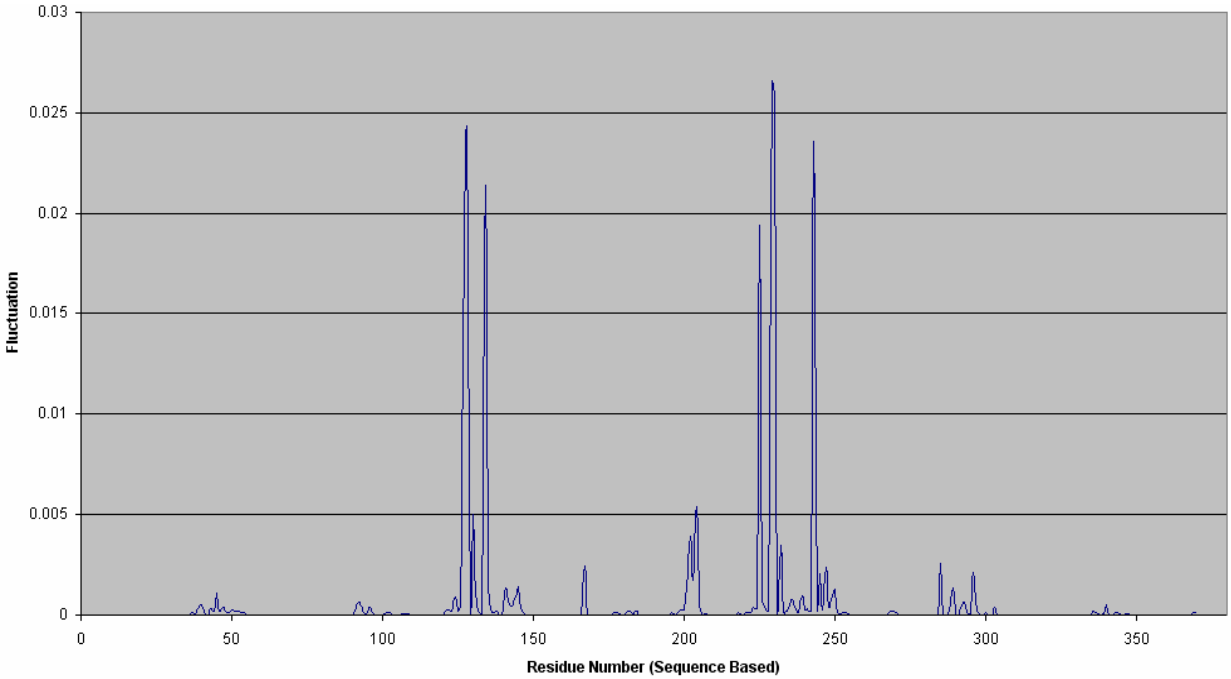

Figure B.10. Fluctuations of Beta Subunit of nAChR in the average of the fastest 30 modes

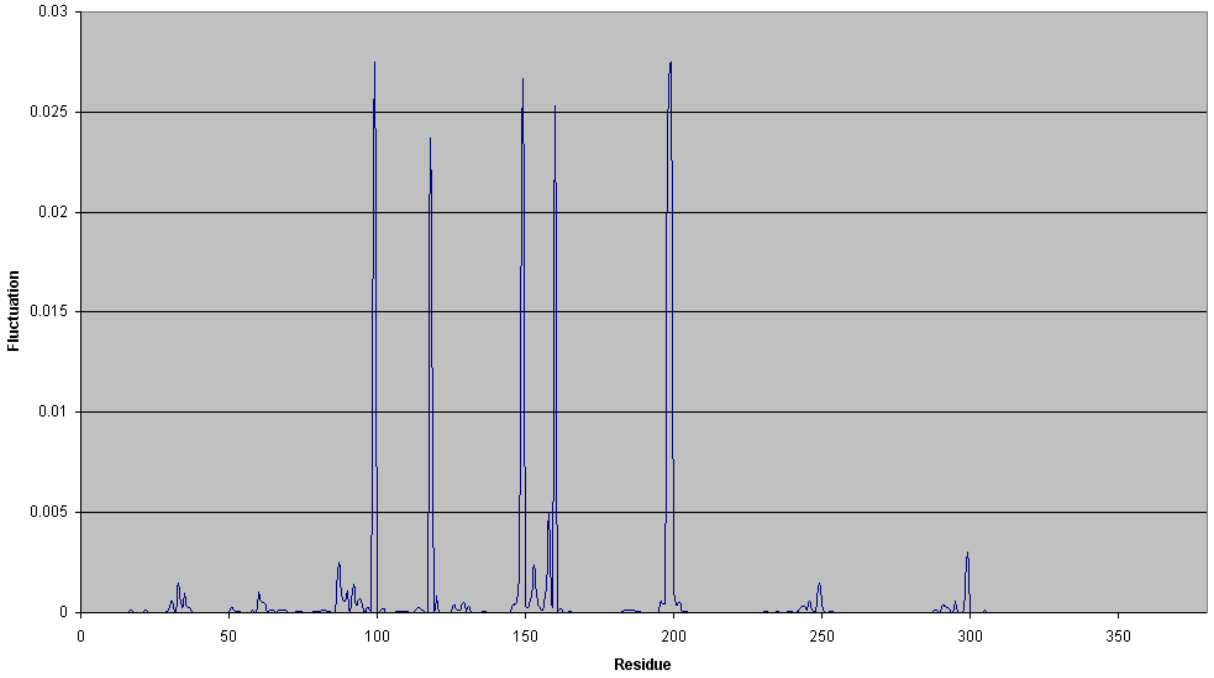

Figure B.11. Fluctuations of Delta Subunit of nAChR in the average of the fastest 30 modes

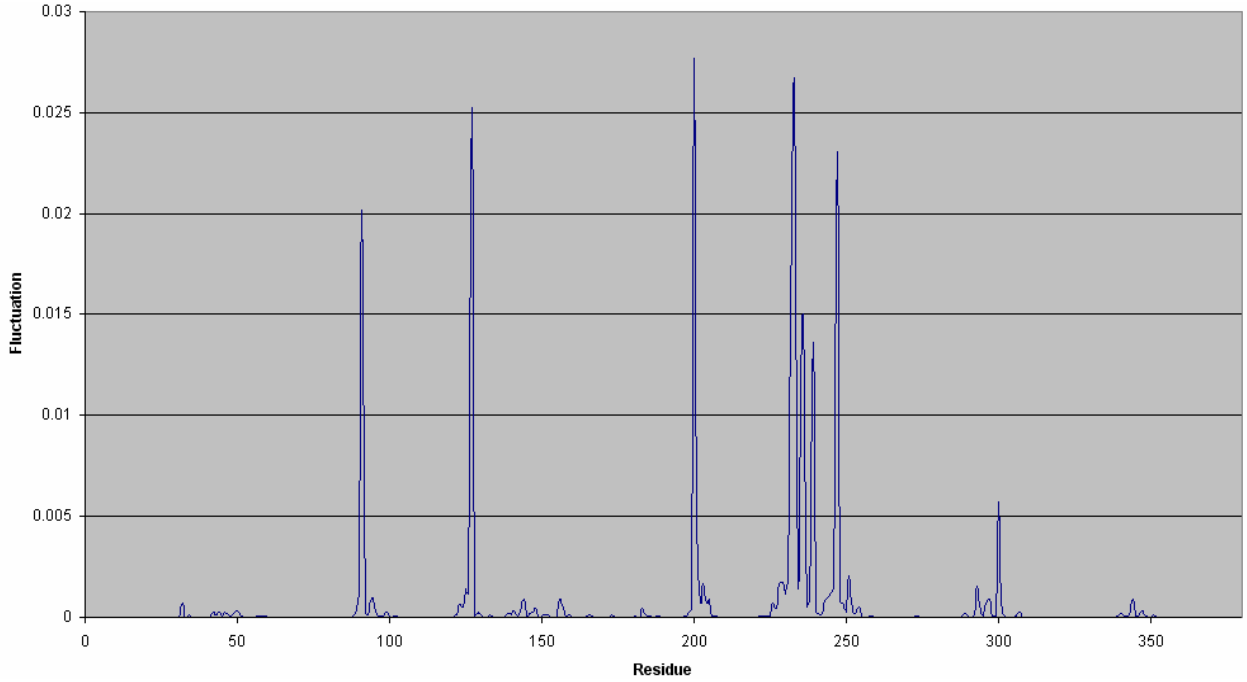

Figure B.12. Fluctuations of Gamma Subunit of nAChR in the average of the fastest 30 modes

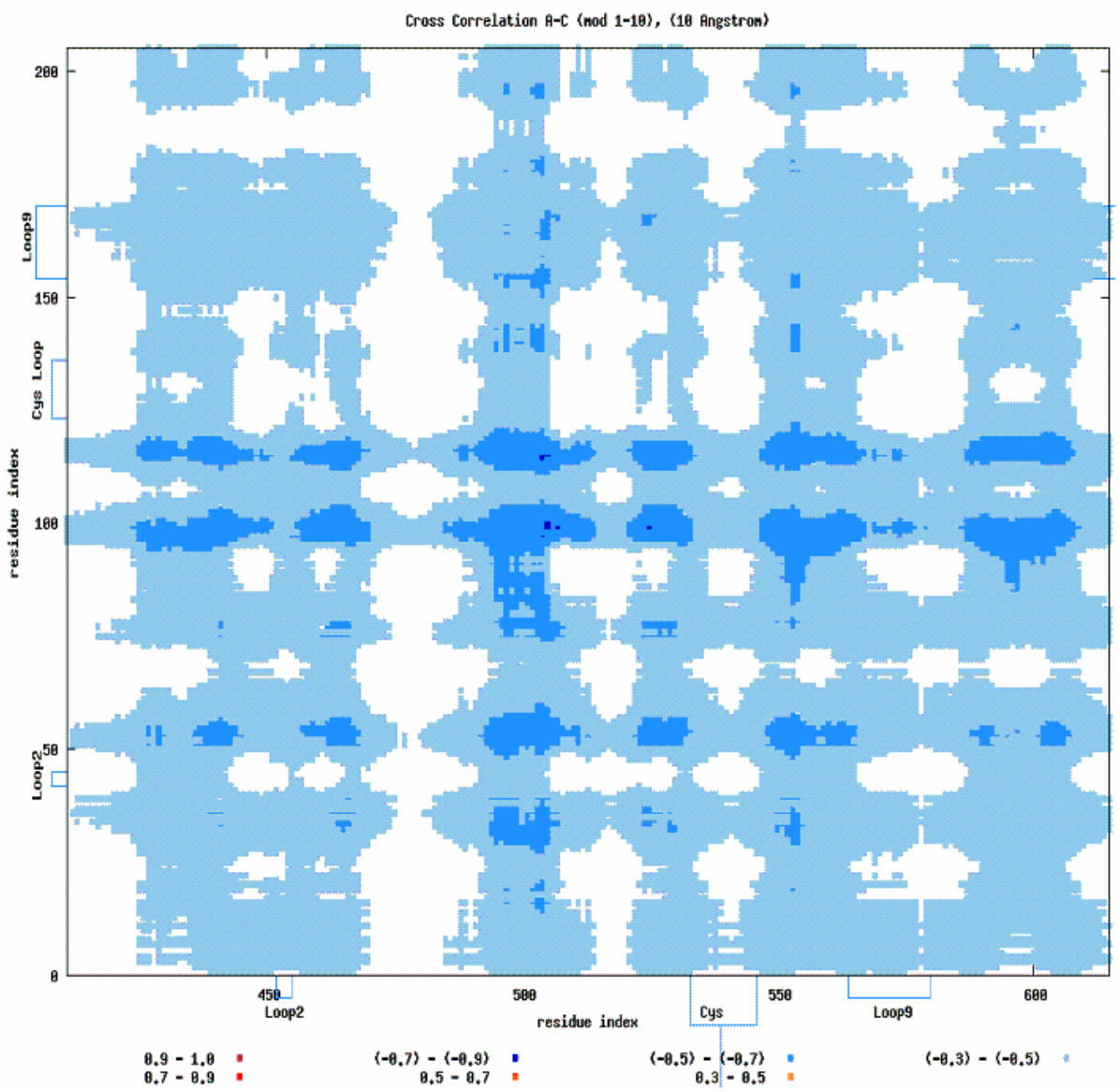

Figure B.13. Cross correlation map of subunit A and subunit C of AChBP.

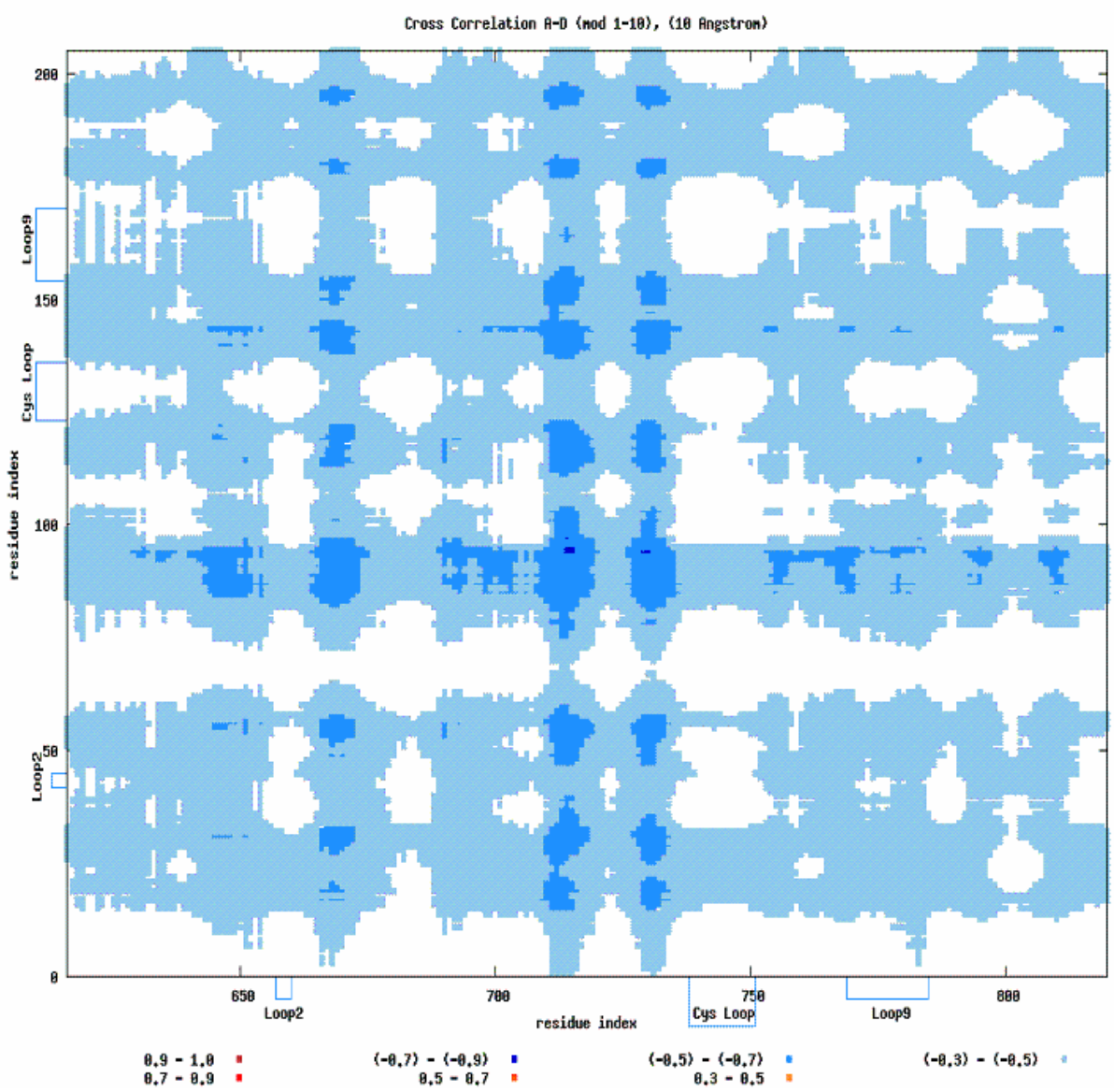

Figure B.14. Cross correlation map of subunit A and subunit D of AChBP.

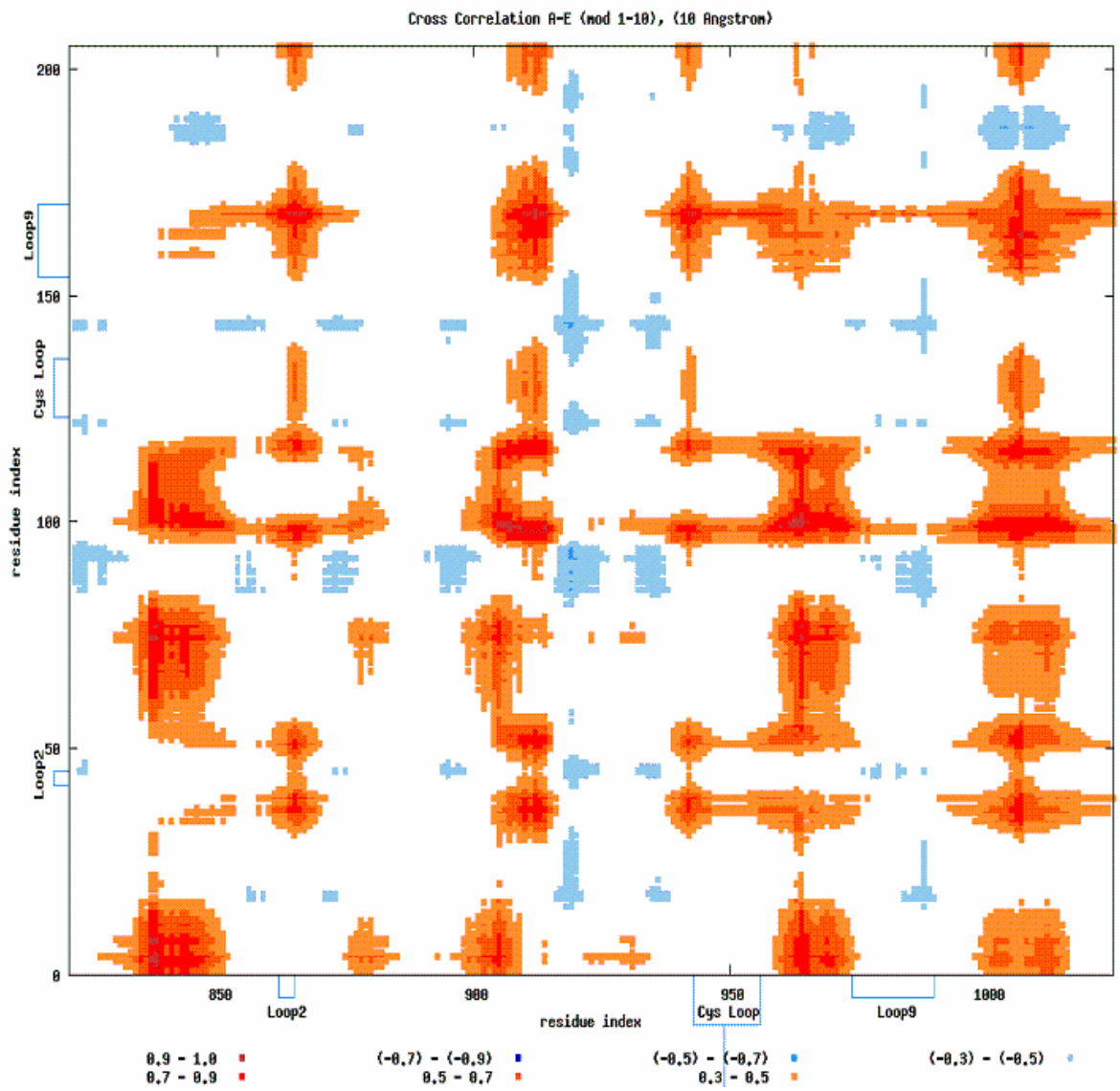

Figure B.15. Cross correlation map of subunit A and subunit E of AChBP.

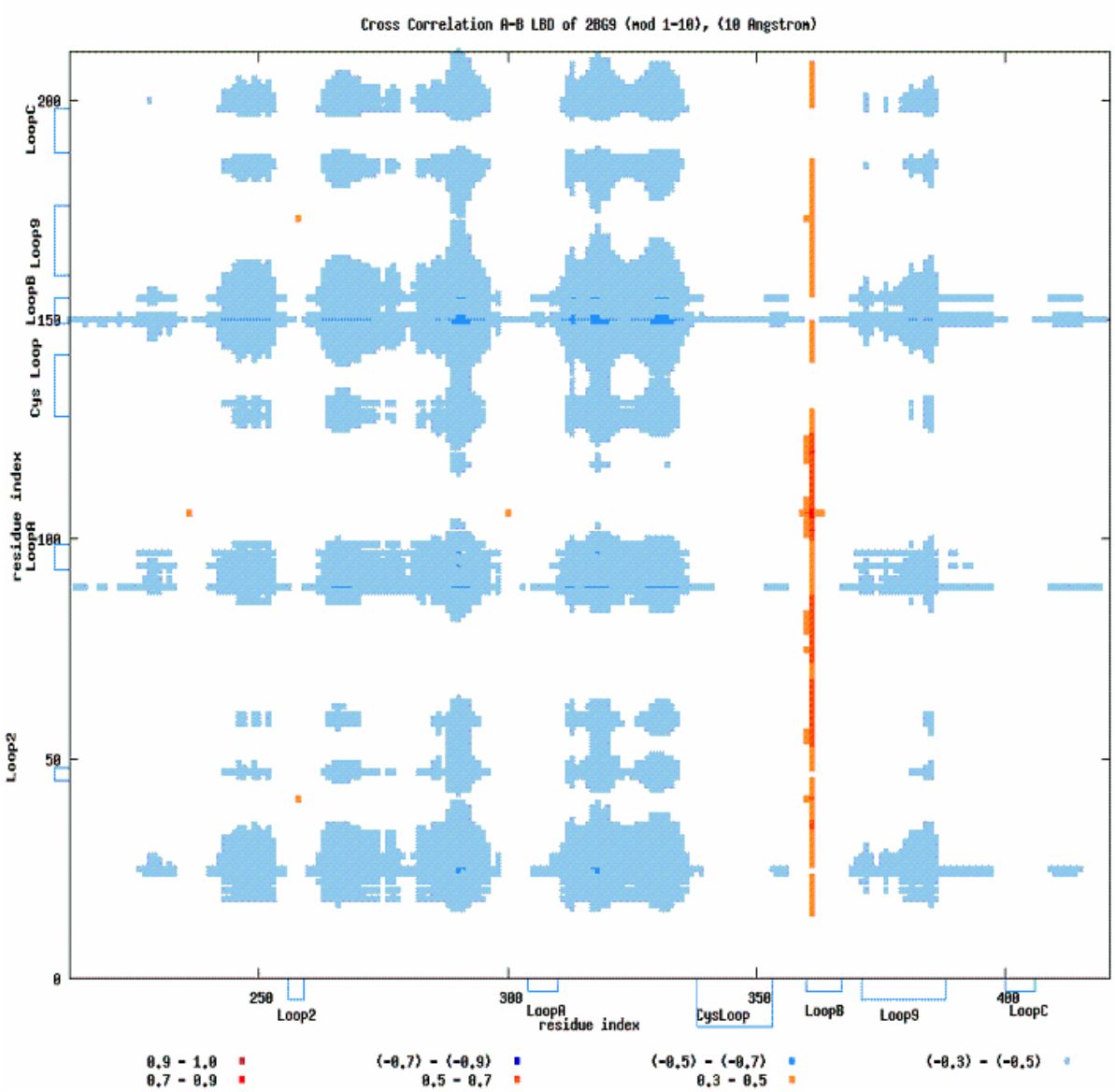

Figure B.16. Cross correlation map of subunit Alpha-Gamma and Beta subunits of LBD of nAChR.

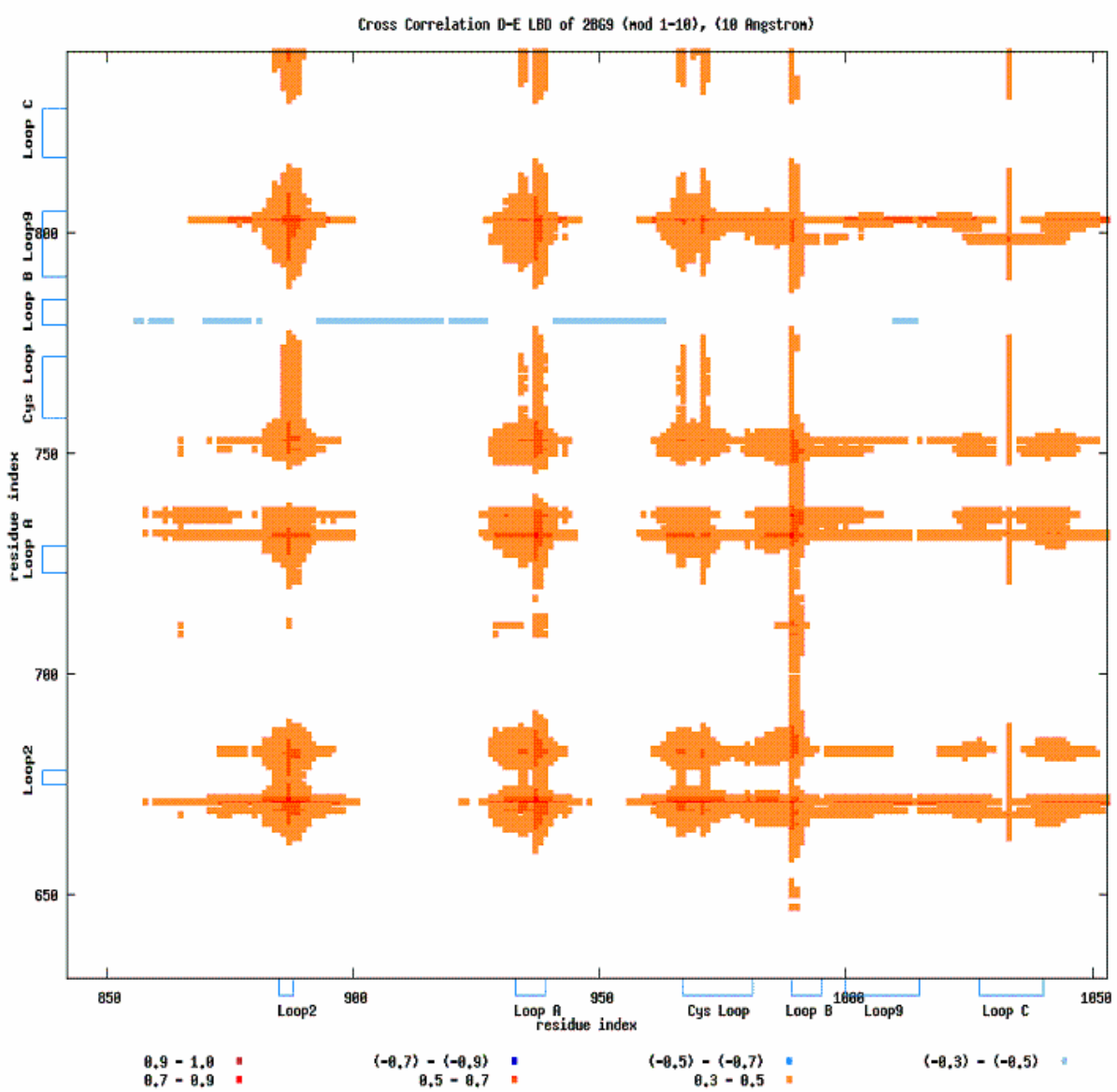

Figure B.17. Cross correlation map of subunit Alpha-Delta and Gamma subunits of LBD of nAChR.

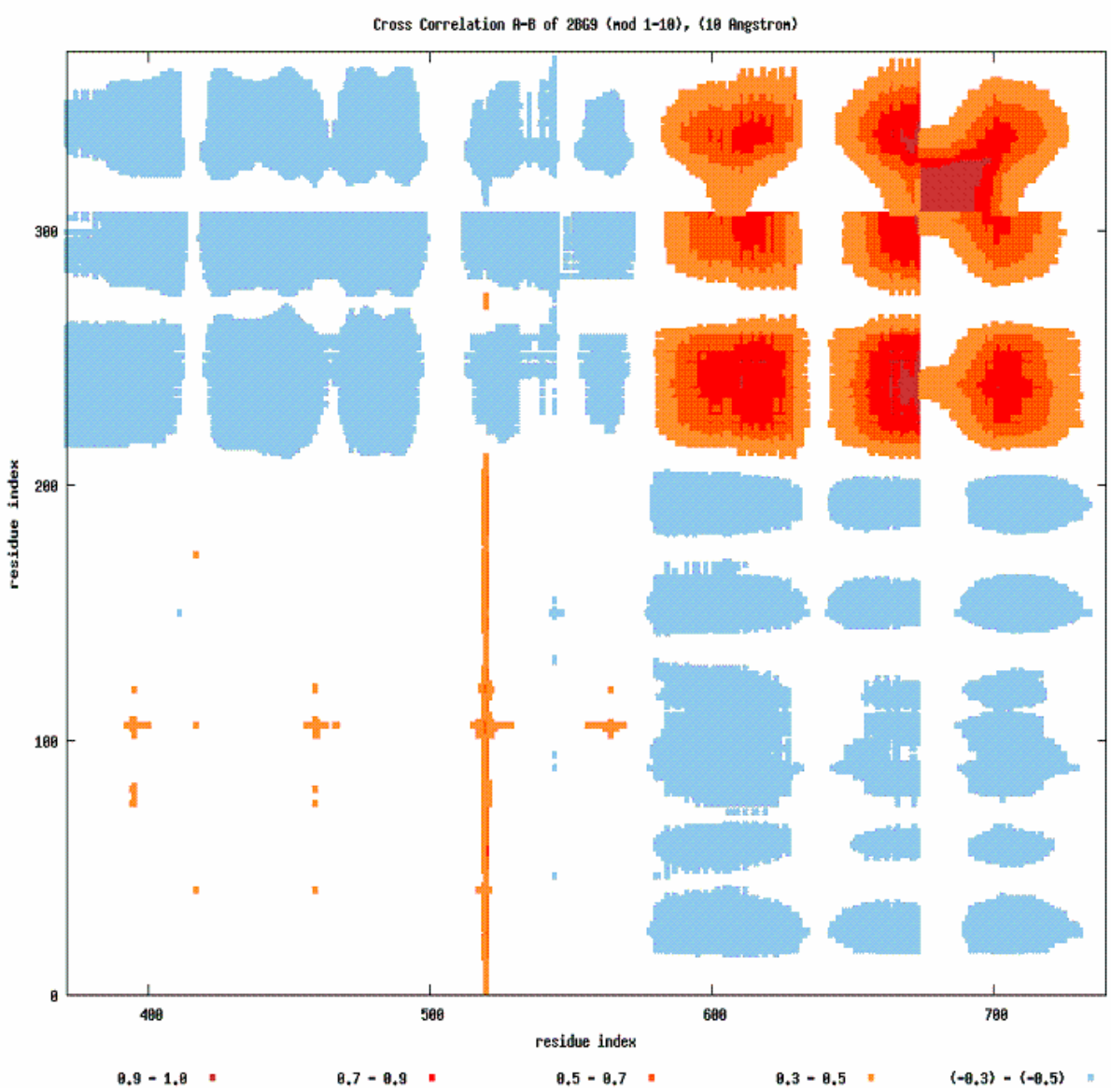

Figure B.18. Cross correlation map of subunit Alpha-Gamma and Beta subunits of nAChR.

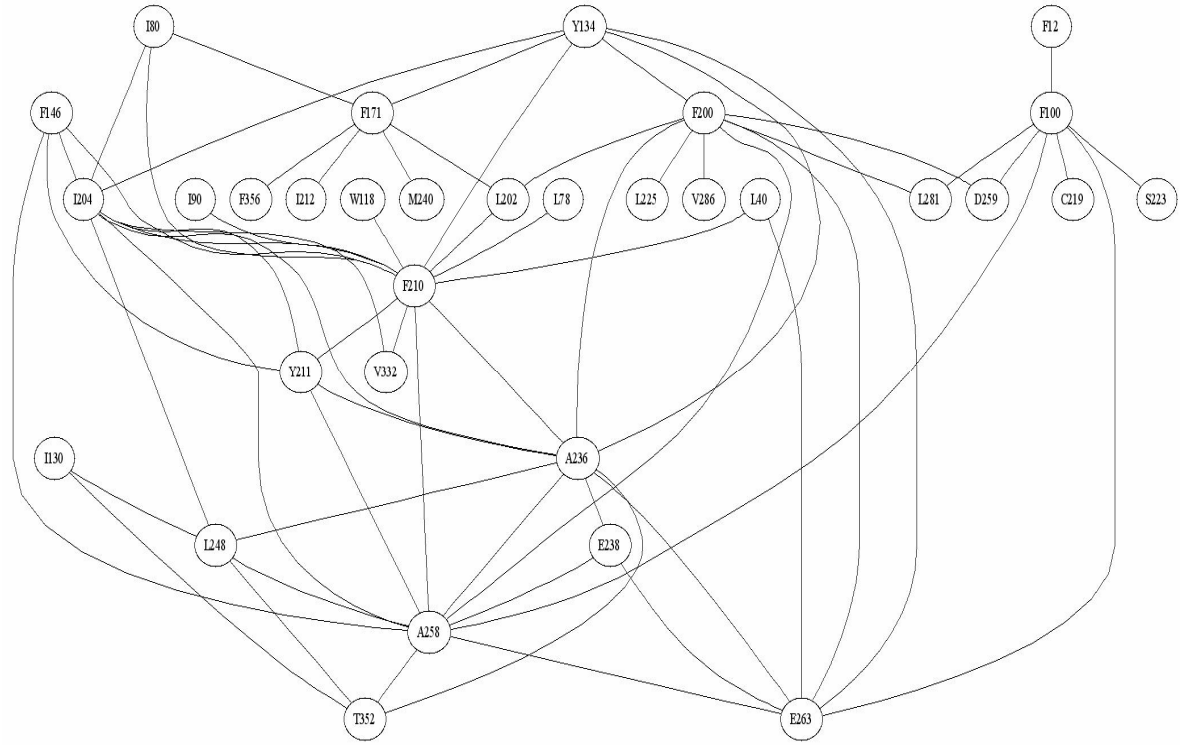

Figure B.19. Schematic representation of correlated mutation pairs of the Beta subunit in the full structure of nAChR

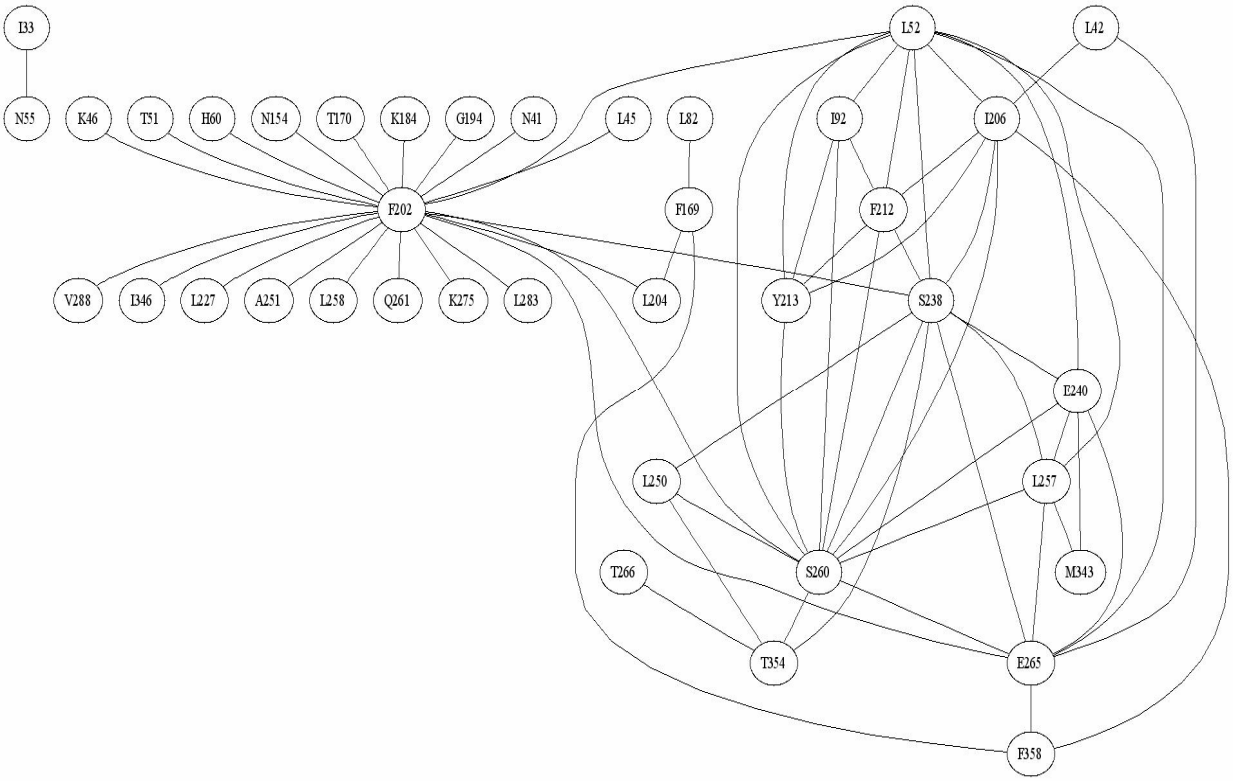

Figure B.20. Schematic representation of correlated mutation pairs of the Delta subunit in the full structure of nAChR

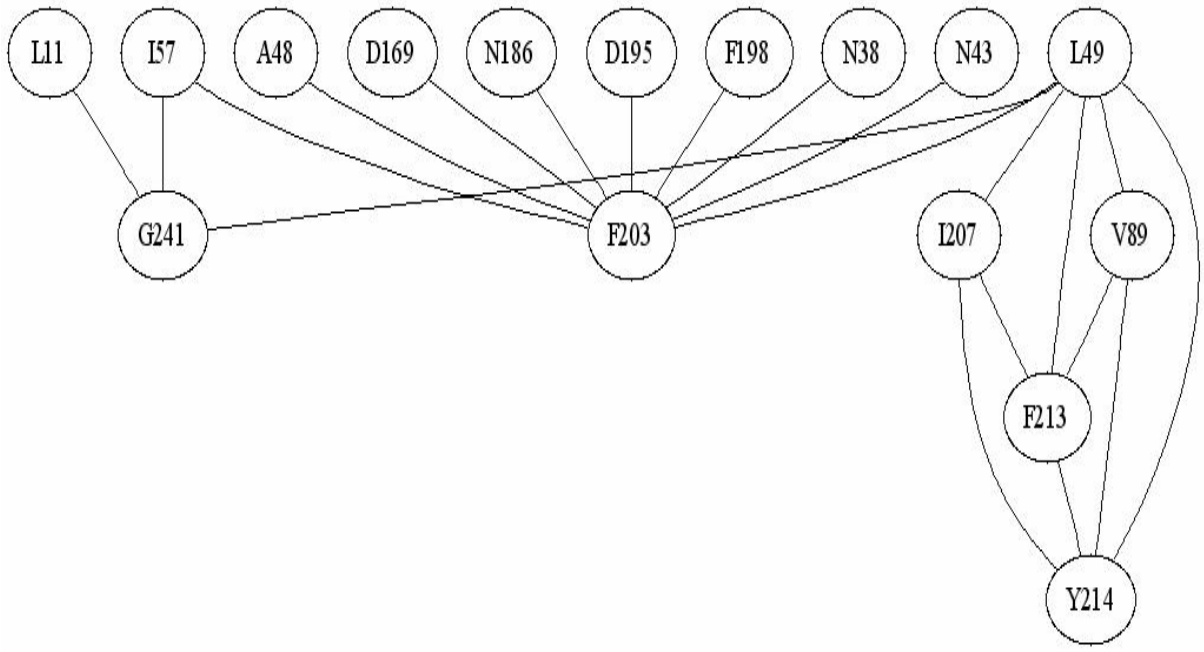

Figure B.21. Schematic representation of correlated mutation pairs of the Gamma subunit in the full structure of nAChR

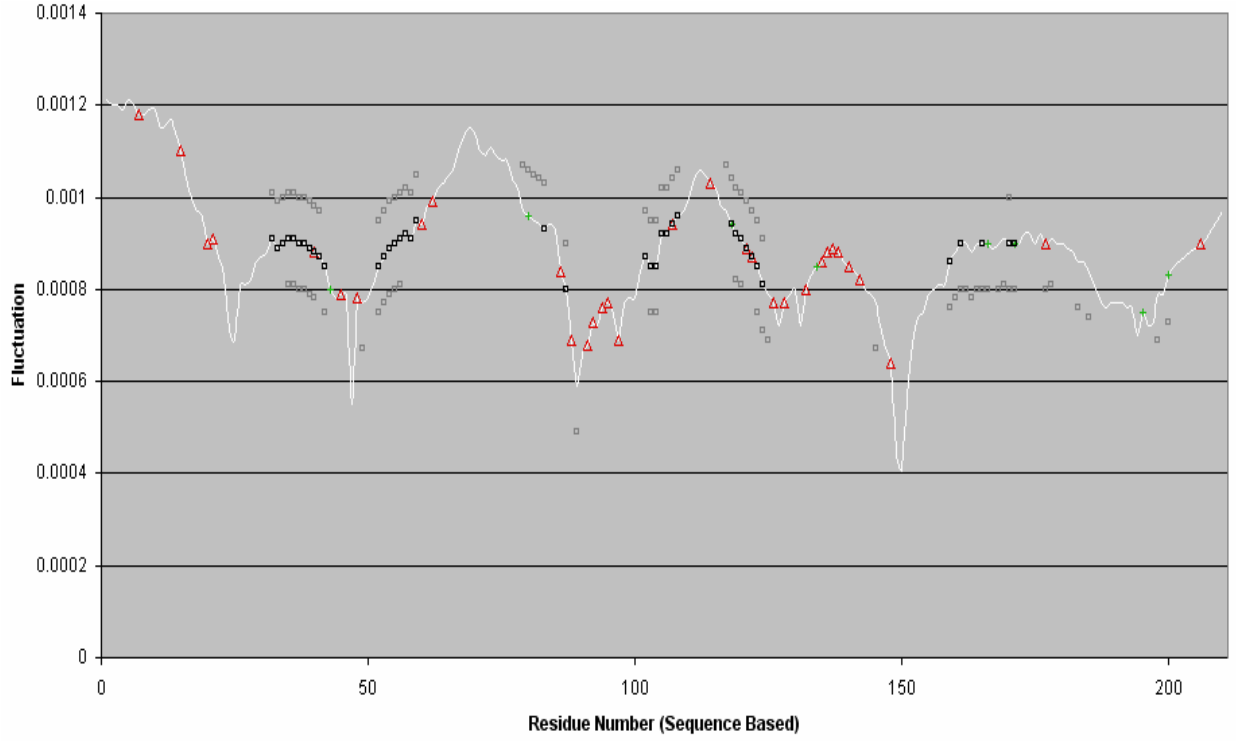

Figure B.22. Slow 1-2 average fluctuations of Beta subunit of the LBD of nAChR.

Target = Cys Loop

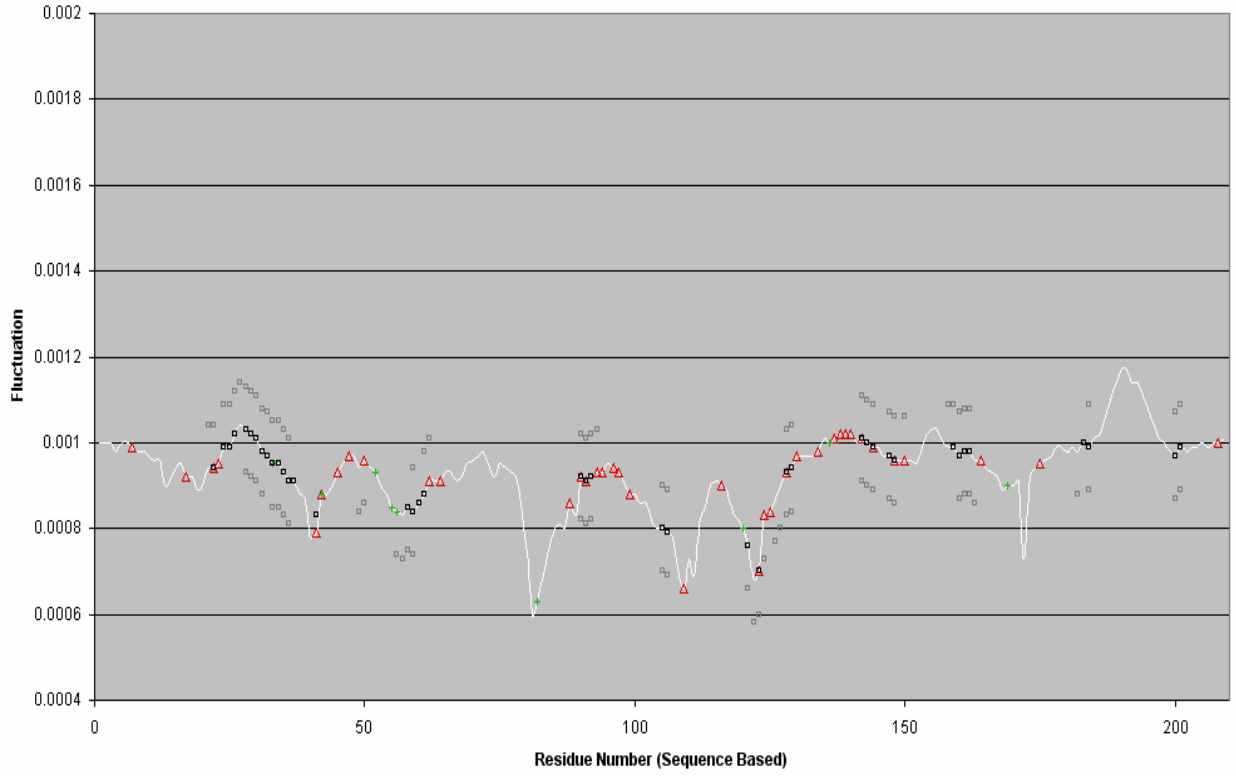

Figure B.23. Slow 1-2 average fluctuations of Delta subunit of the LBD of nAChR.

Target = Cys Loop

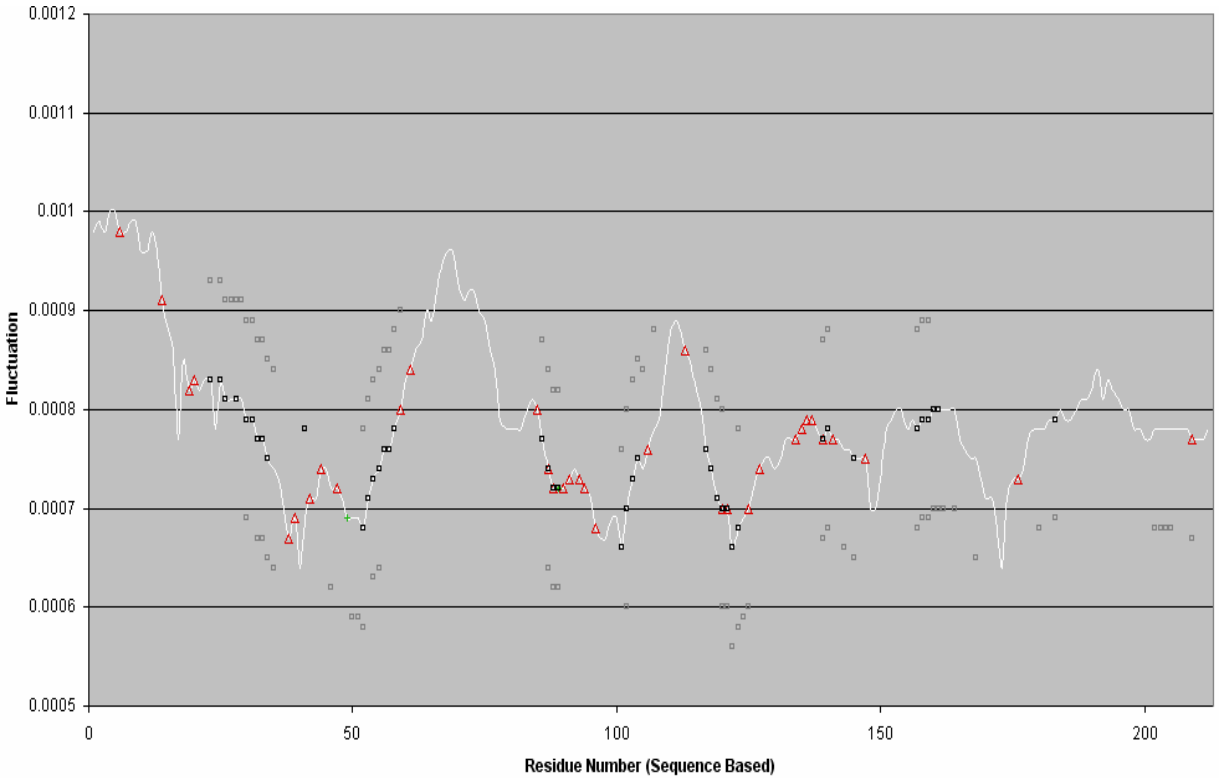

Figure B.24. Slow 1-2 average fluctuations of Gamma subunit of the LBD of nAChR.

Target = Cys Loop

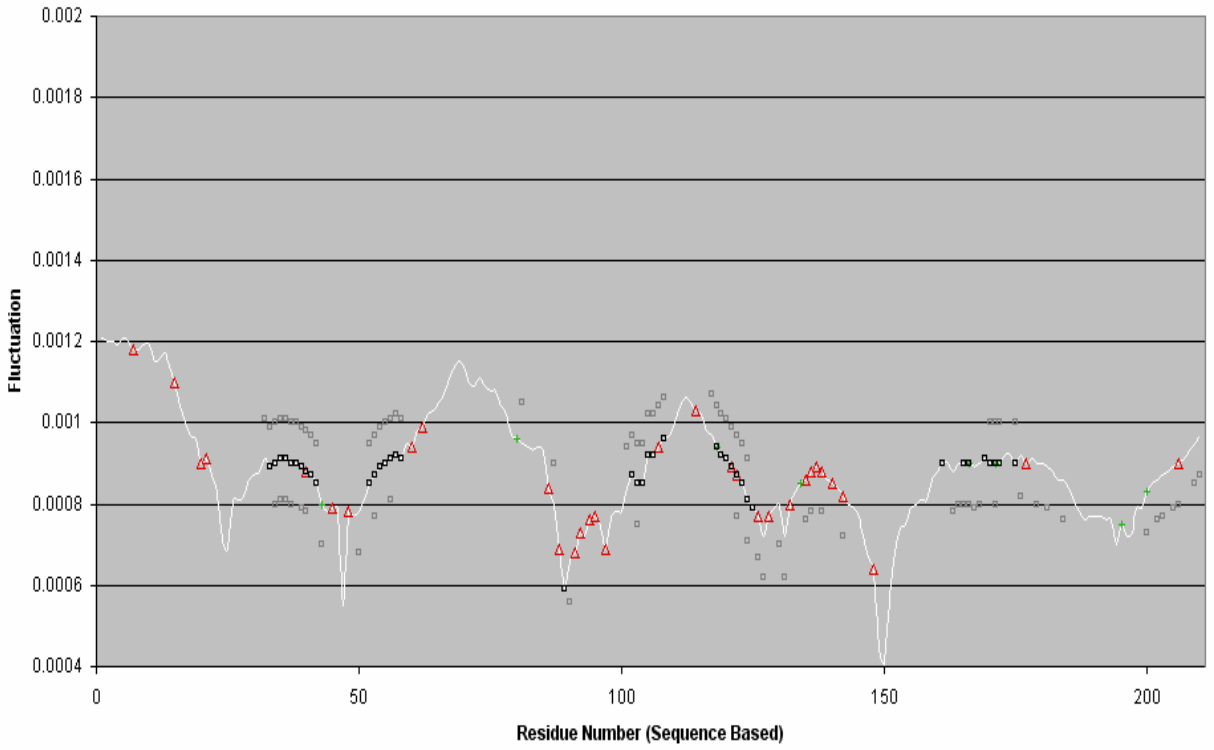

Figure B.25. Slow 1-2 average fluctuations of Beta subunit of the LBD of nAChR.

Target = Loop 2

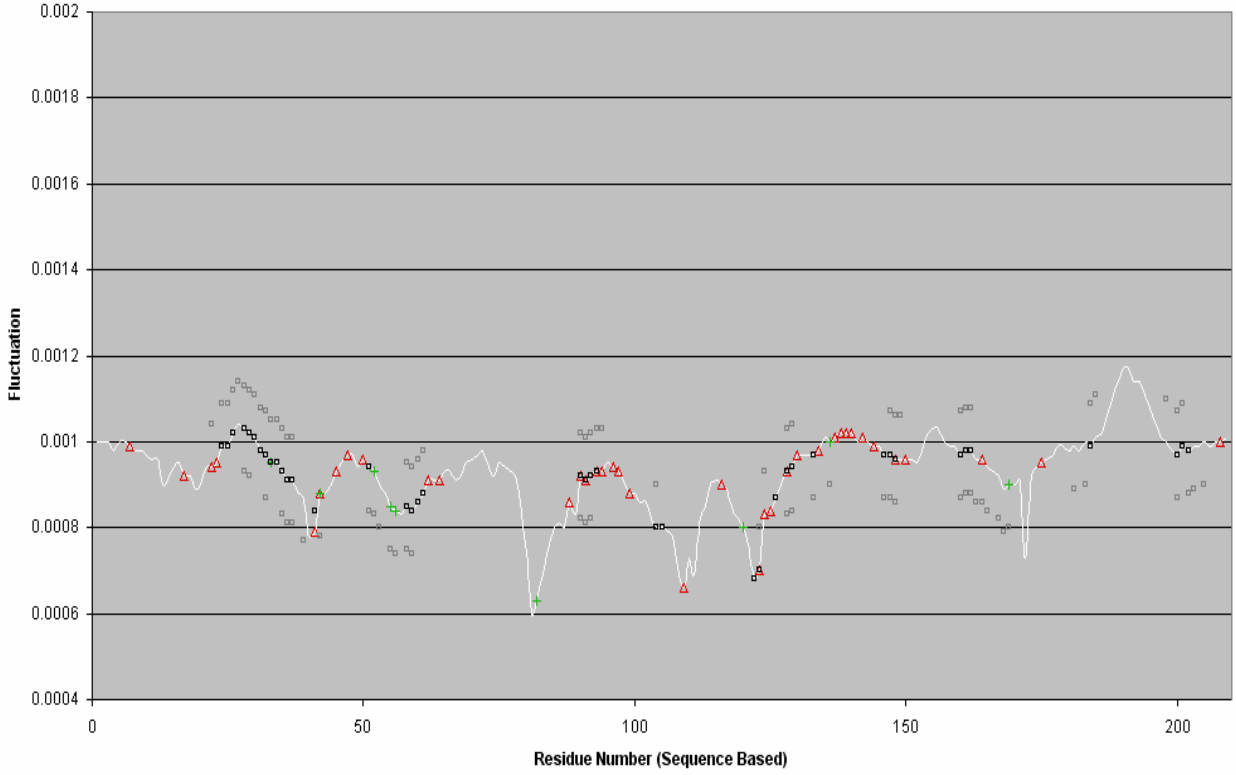

Figure B.26. Slow 1-2 average fluctuations of Delta subunit of the LBD of nAChR.

Target = Loop 2

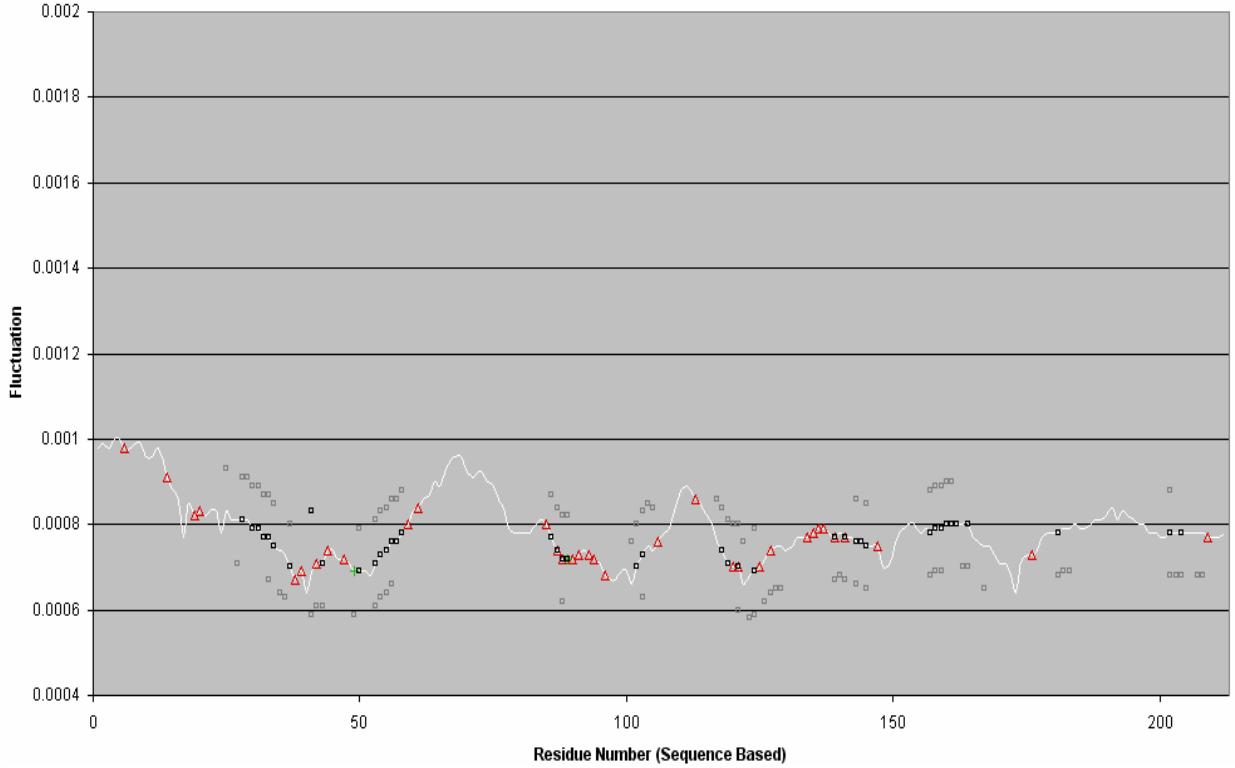

Figure B.27. Slow 1-2 average fluctuations of Gamma subunit of the LBD of nAChR.

Target = Loop 2

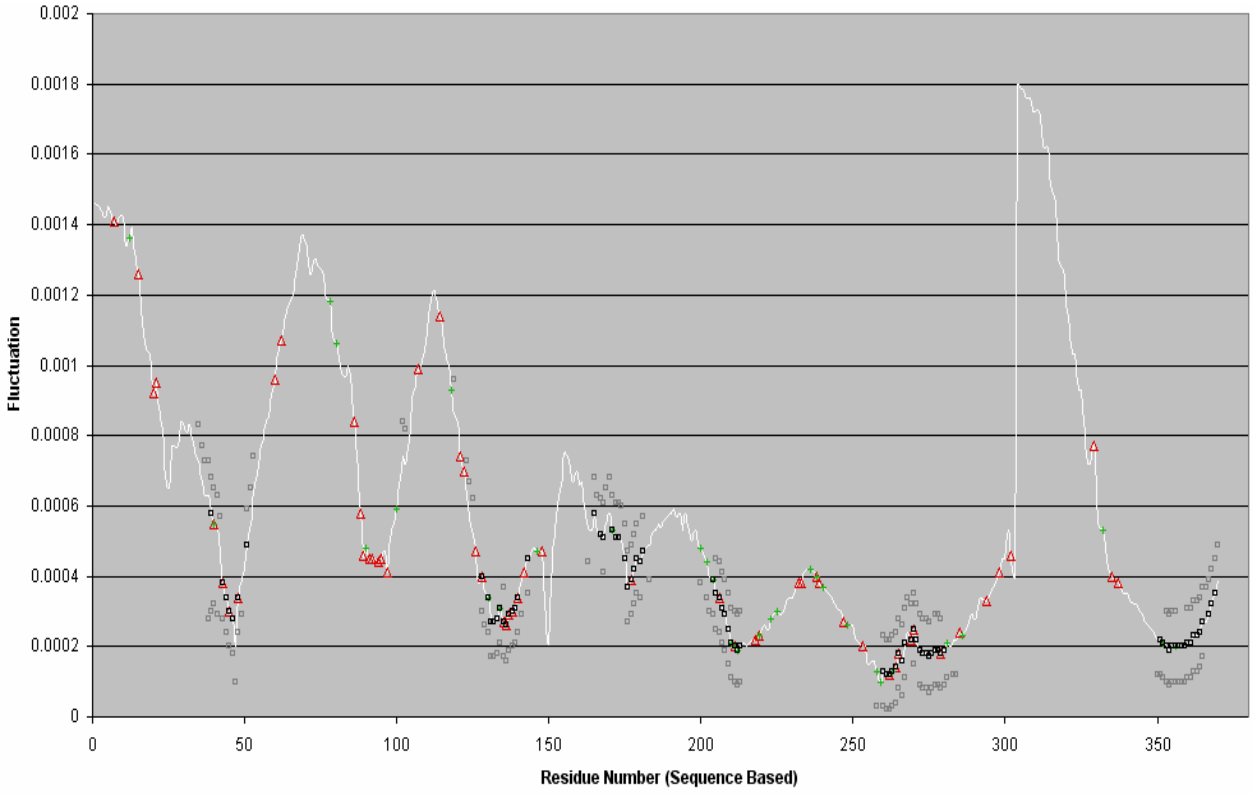

Figure B.28. Slow 1-2 average fluctuations of the Beta subunit of nAChR. Target = Gate

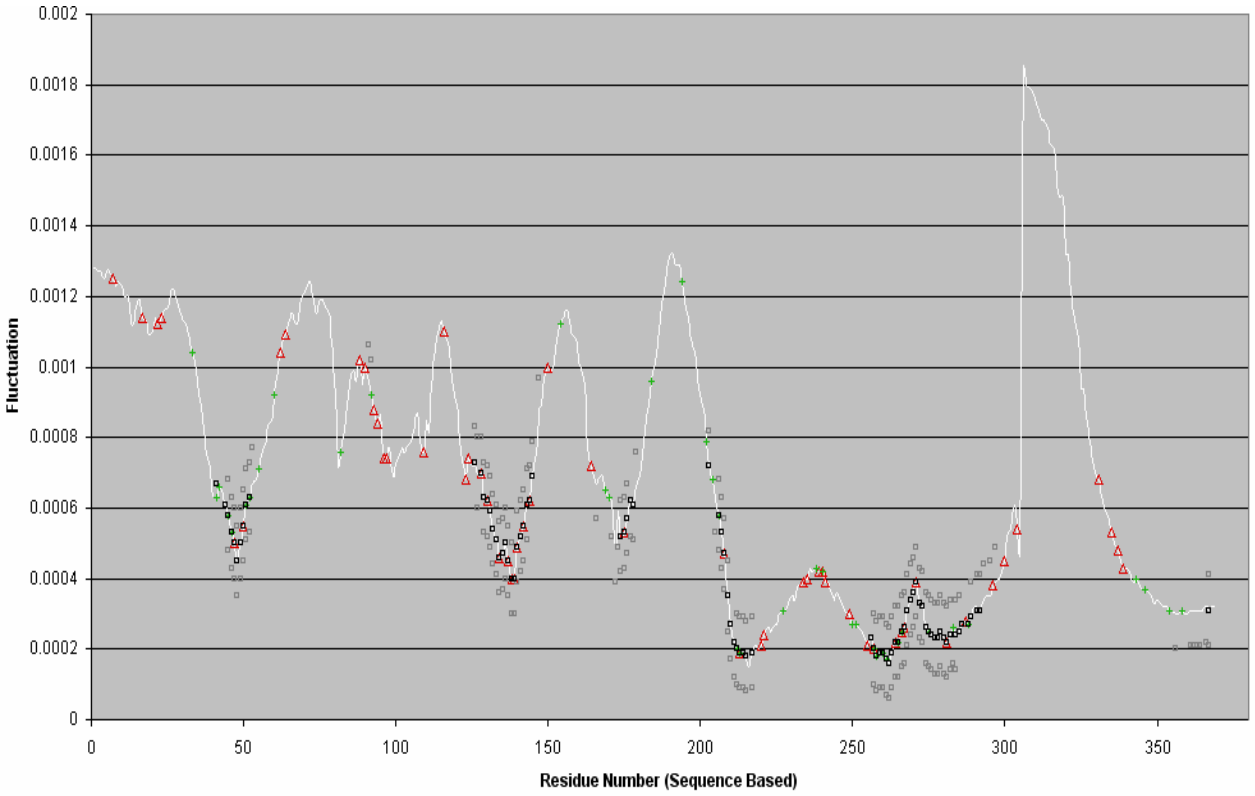

Figure B.29. Slow 1-2 average fluctuations of the Delta subunit of nAChR. Target = Gate

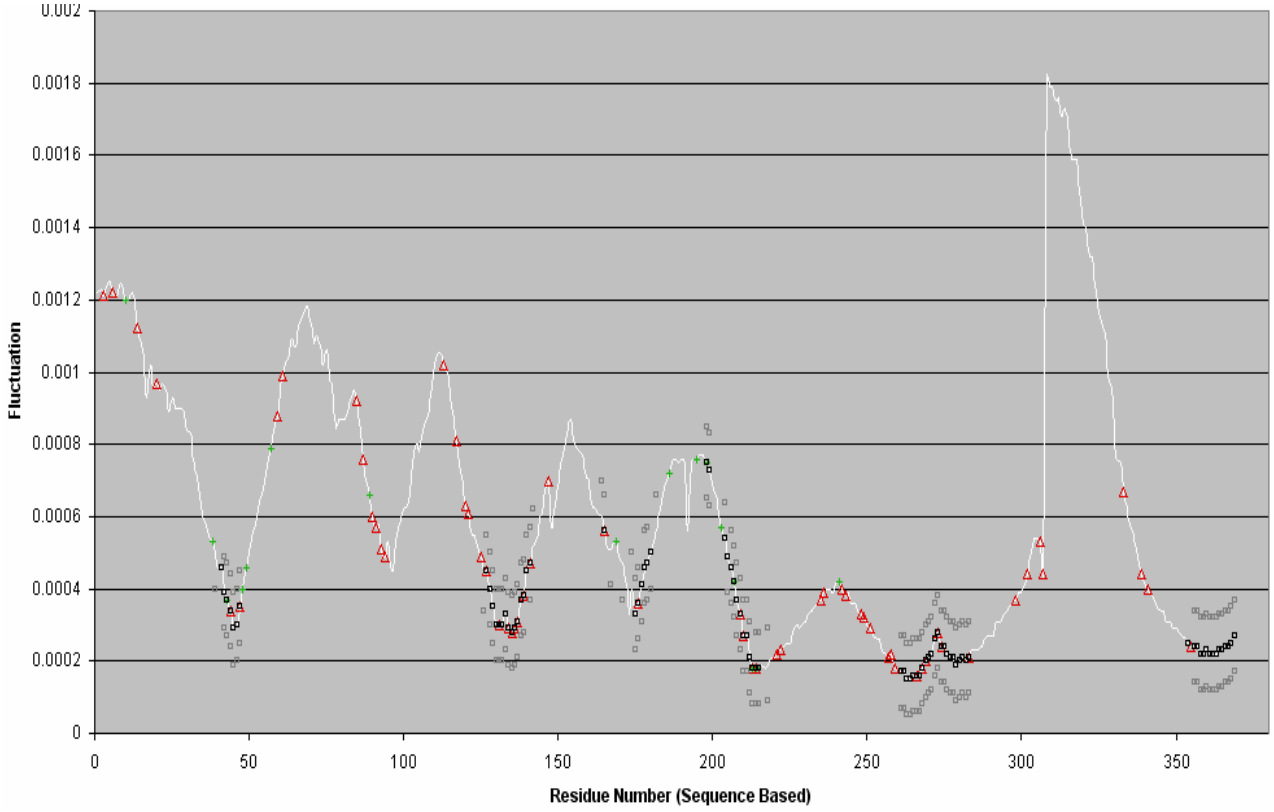

Figure B.30. Slow 1-2 average fluctuations of the Gamma subunit of nAChR. Target = Gate

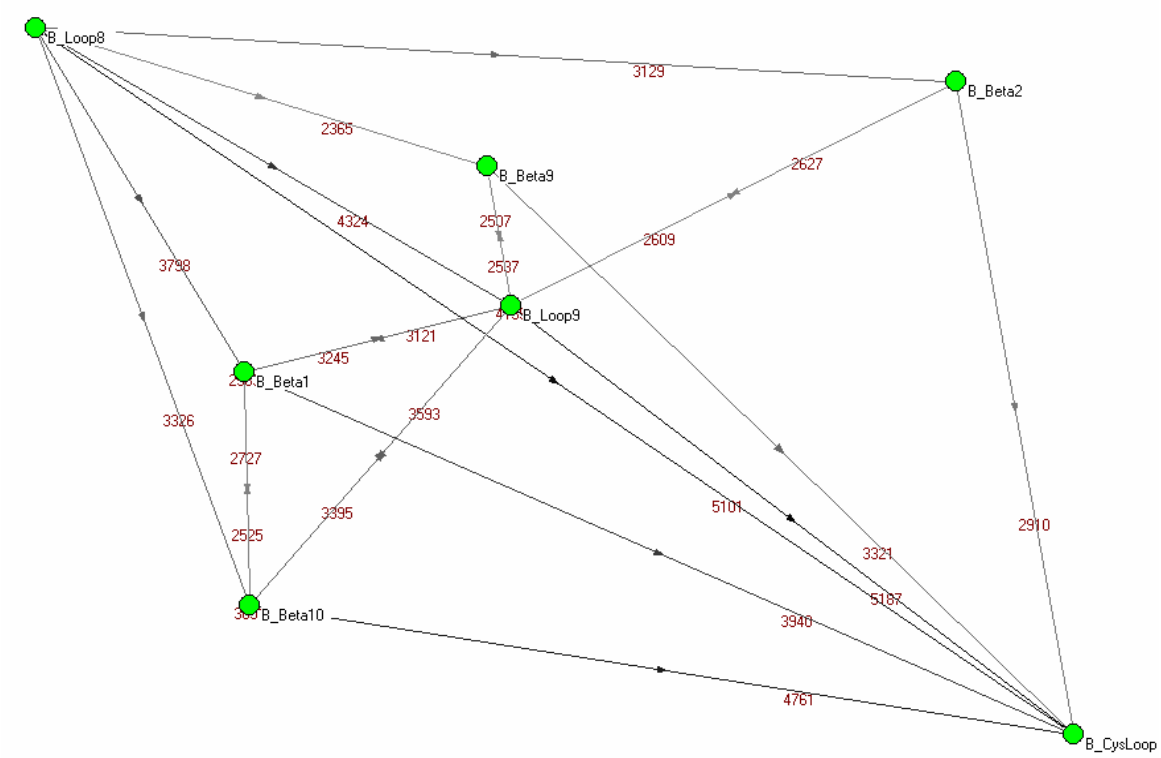

Figure B.31. Graphic representation of the most visited paths which start from the Loop B of Beta subunit of LBD of nAChR and go to the Cys Loop of the same subunit

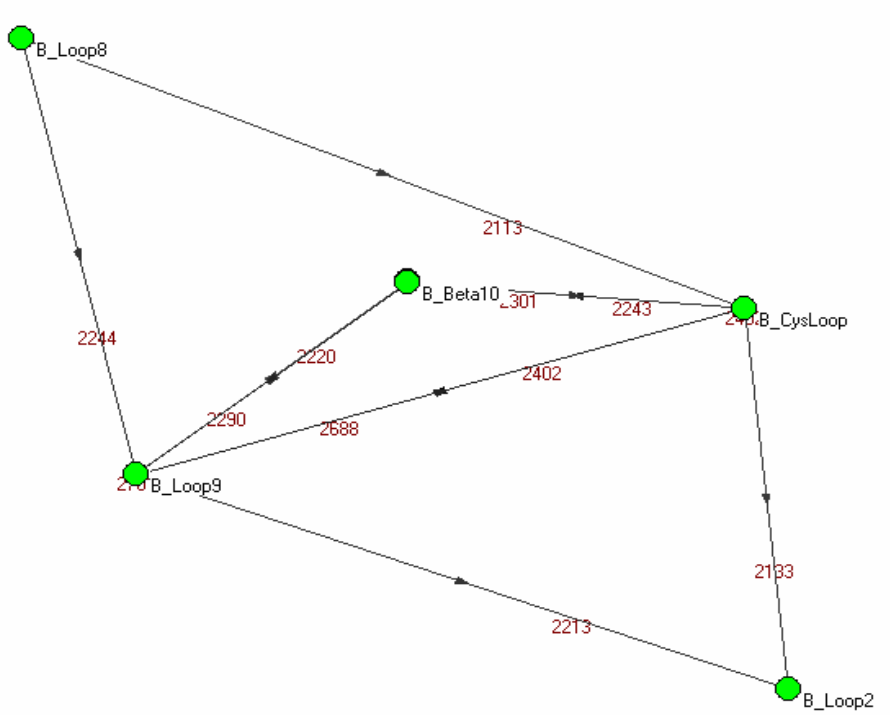

Figure B.32. Graphic representation of the most visited paths which start from the Loop B of Beta subunit of LBD of nAChR and go to the Loop 2 of the same subunit.

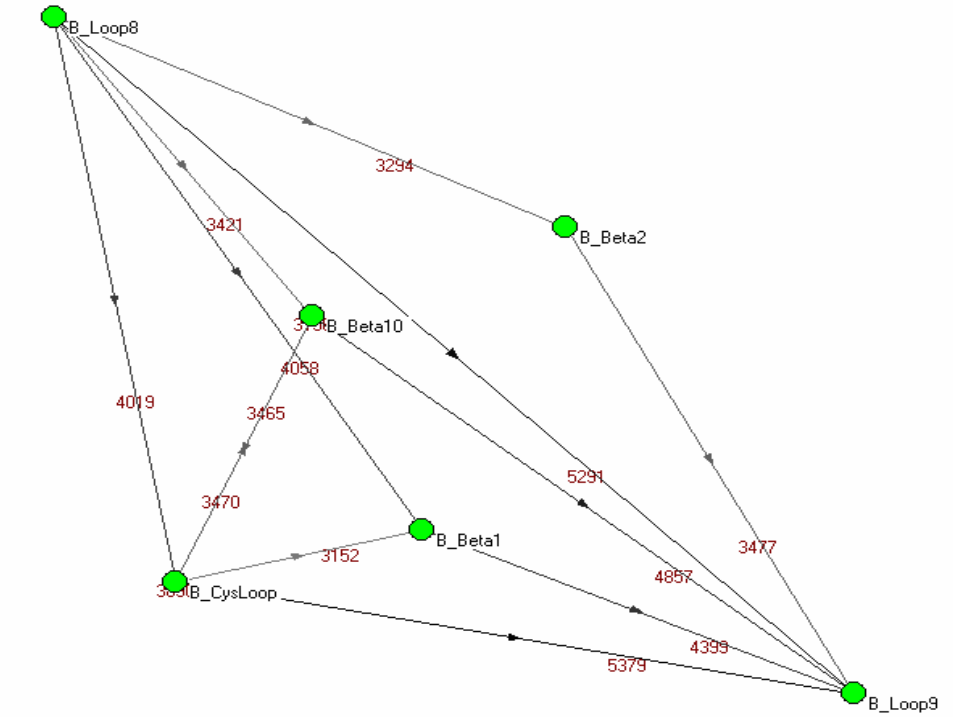

Figure B.33. Graphic representation of the most visited paths which start from the Loop B of Beta subunit of LBD of nAChR and go to the Loop 9 of the same subunit

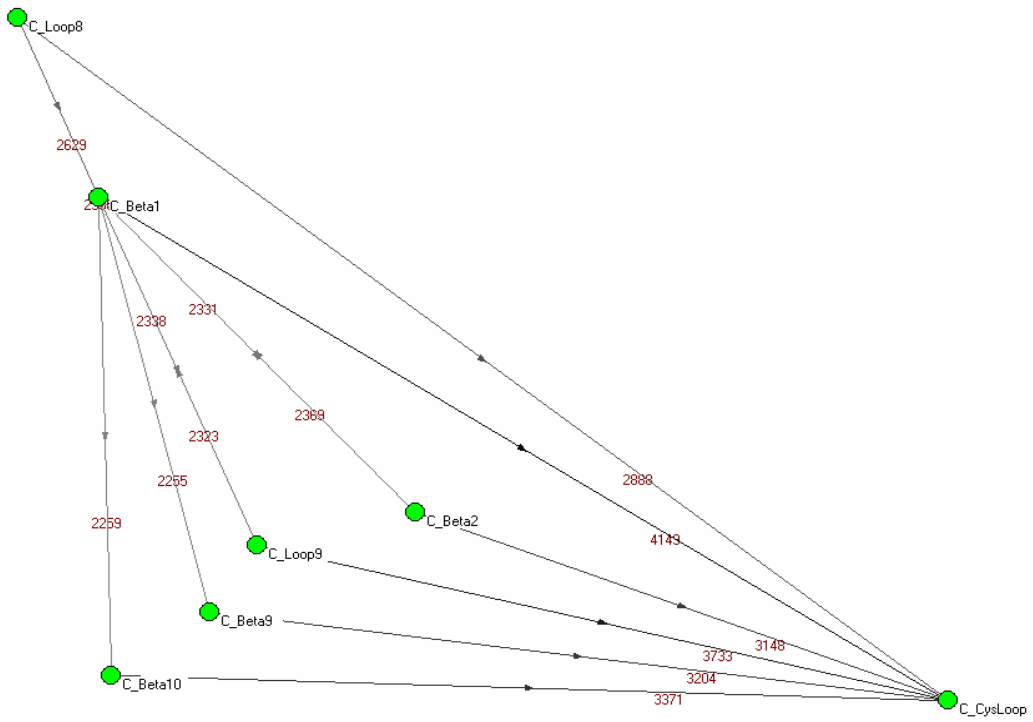

Figure B.34. Graphic representation of the most visited paths which start from the Loop B of Delta subunit of LBD of nAChR and go to the Cys Loop of the same subunit

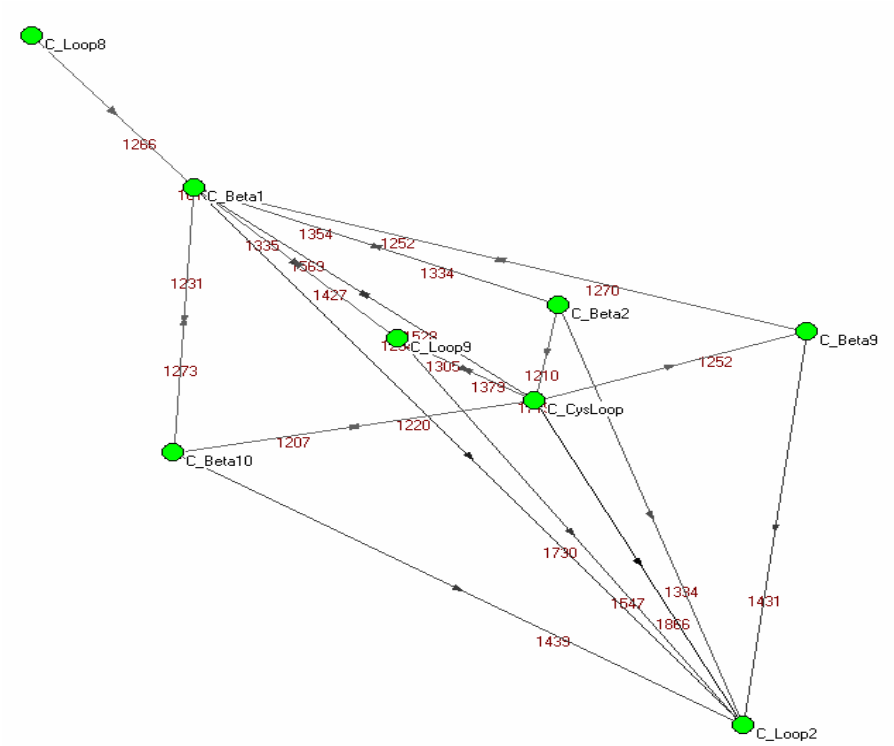

Figure B.35. Graphic representation of the most visited paths which start from the Loop B of Delta subunit of LBD of nAChR and go to the Loop 2 of the same subunit

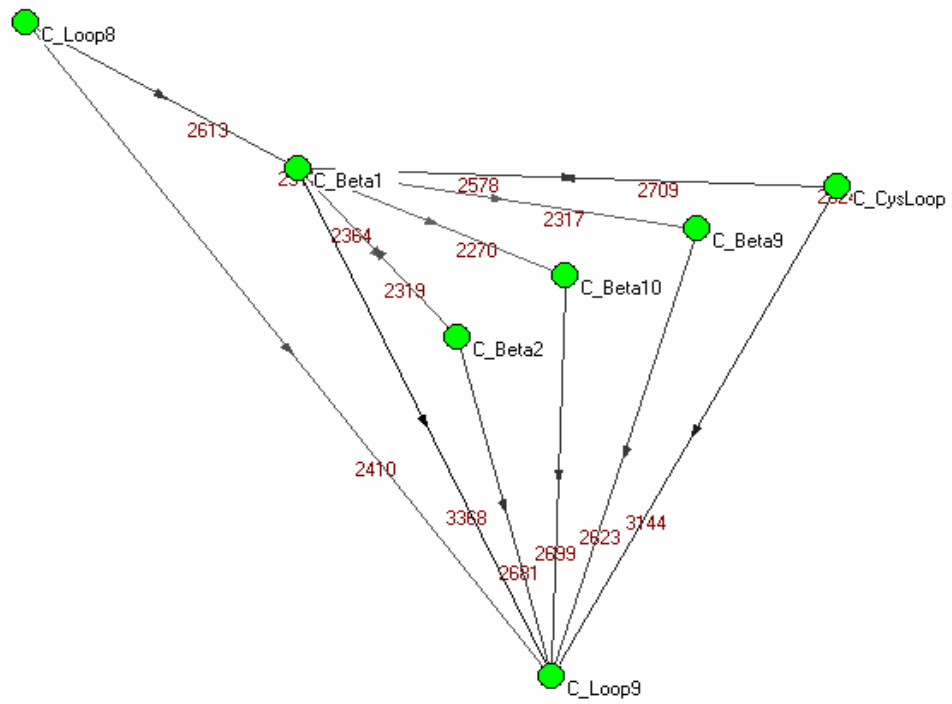

Figure B.36. Graphic representation of the most visited paths which start from the Loop B of Delta subunit of LBD of nAChR and go to the Loop 9 of the same subunit

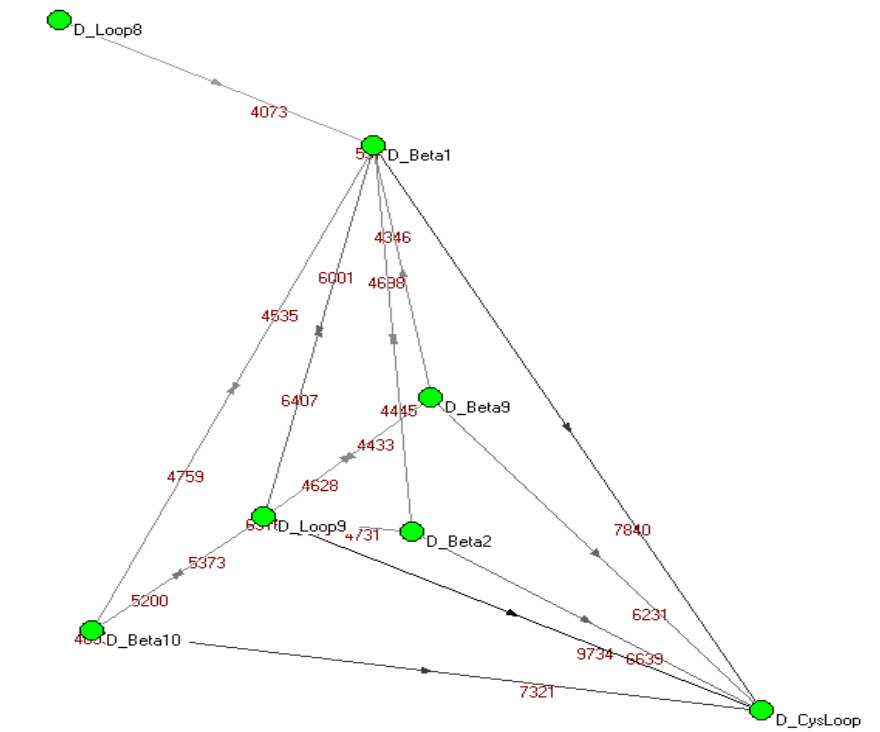

Figure B.37. Graphic representation of the most visited paths which start from the Loop B of Alpha-Delta subunit of LBD of nAChR and go to the Cys Loop of the same subunit

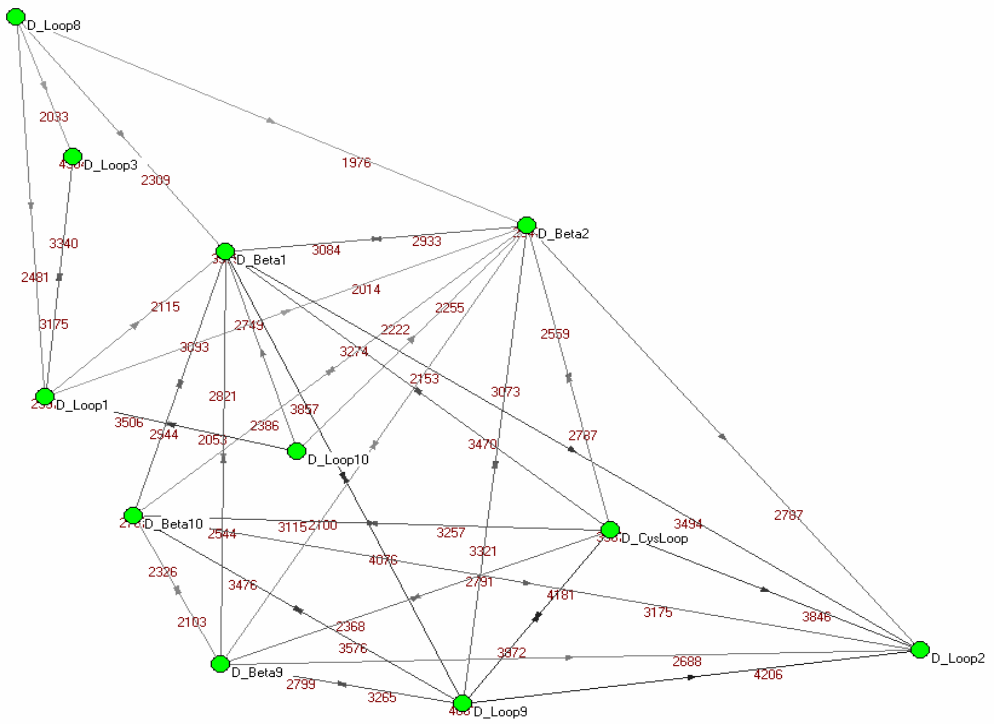

Figure B.38. Graphic representation of the most visited paths which start from the Loop B of Alpha-Delta subunit of LBD of nAChR and go to the Loop 2 of the same subunit

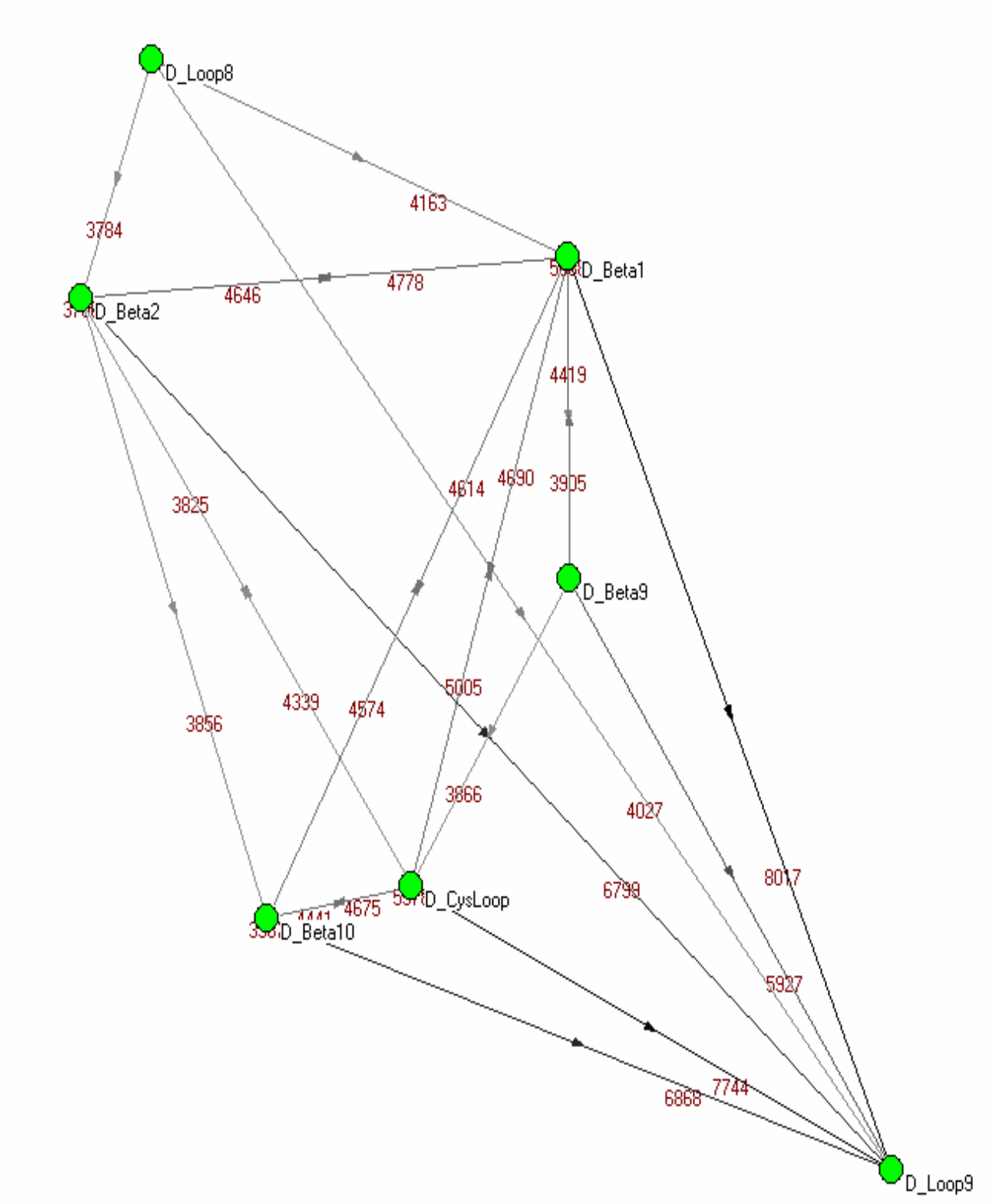

Figure B.39. Graphic representation of the most visited paths which start from the Loop B of Alpha-Delta subunit of LBD of nAChR and go to the Loop 9 of the same subunit

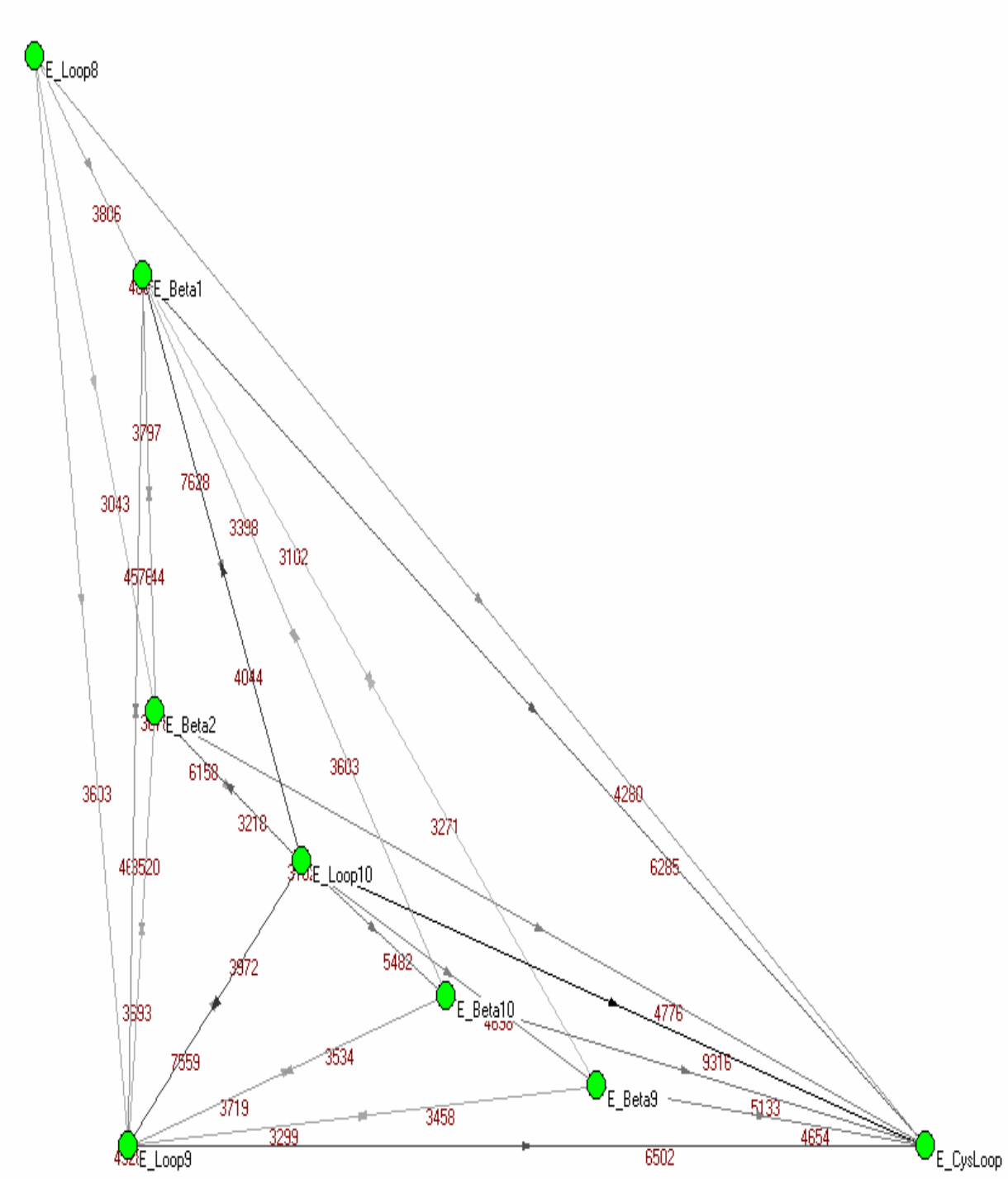

Figure B.40. Graphic representation of the most visited paths which start from the Loop B of Gamma subunit of LBD of nAChR and go to the Cys Loop of the same subunit

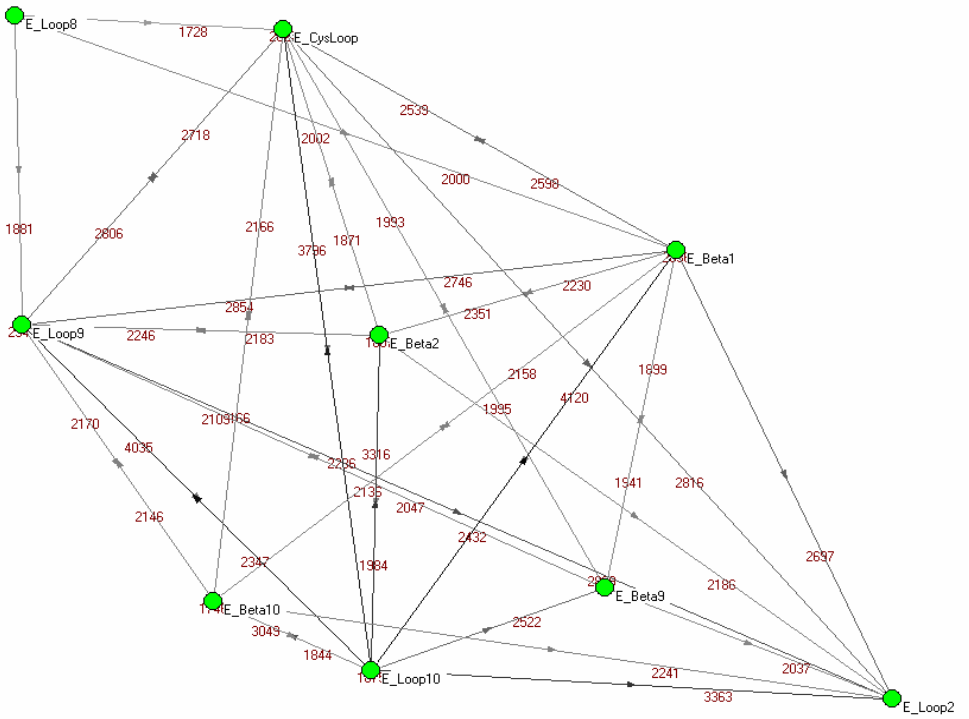

Figure B.41. Graphic representation of the most visited paths which start from the Loop B of Gamma subunit of LBD of nAChR and go to the Loop 2 of the same subunit

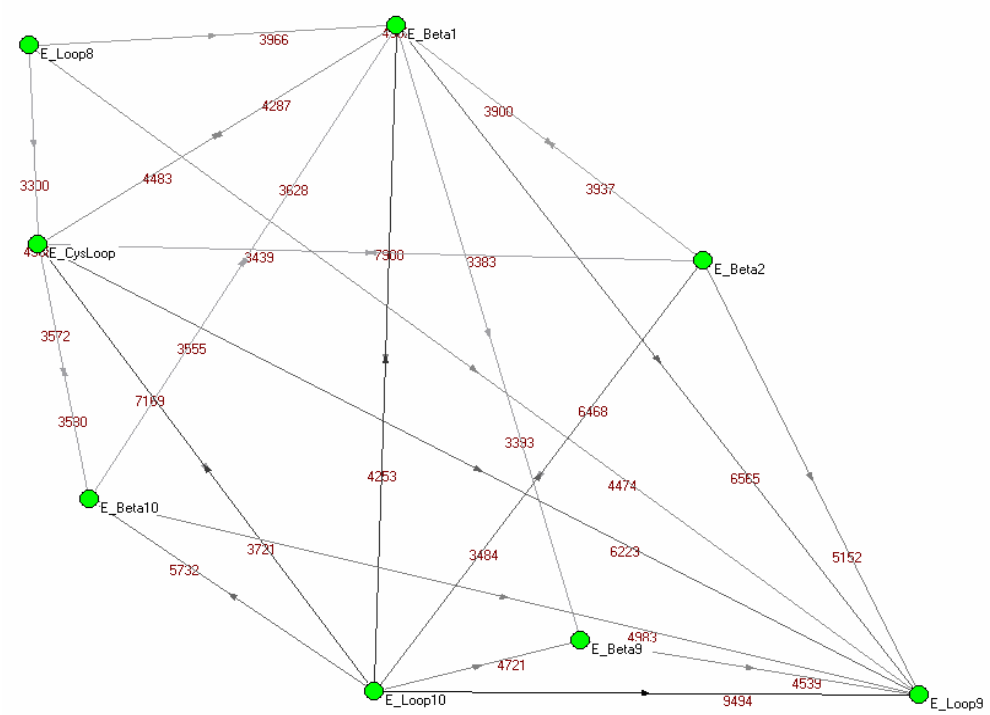

Figure B.42. Graphic representation of the most visited paths which start from the Loop B of Gamma subunit of LBD of nAChR and go to the Loop 9 of the same subunit

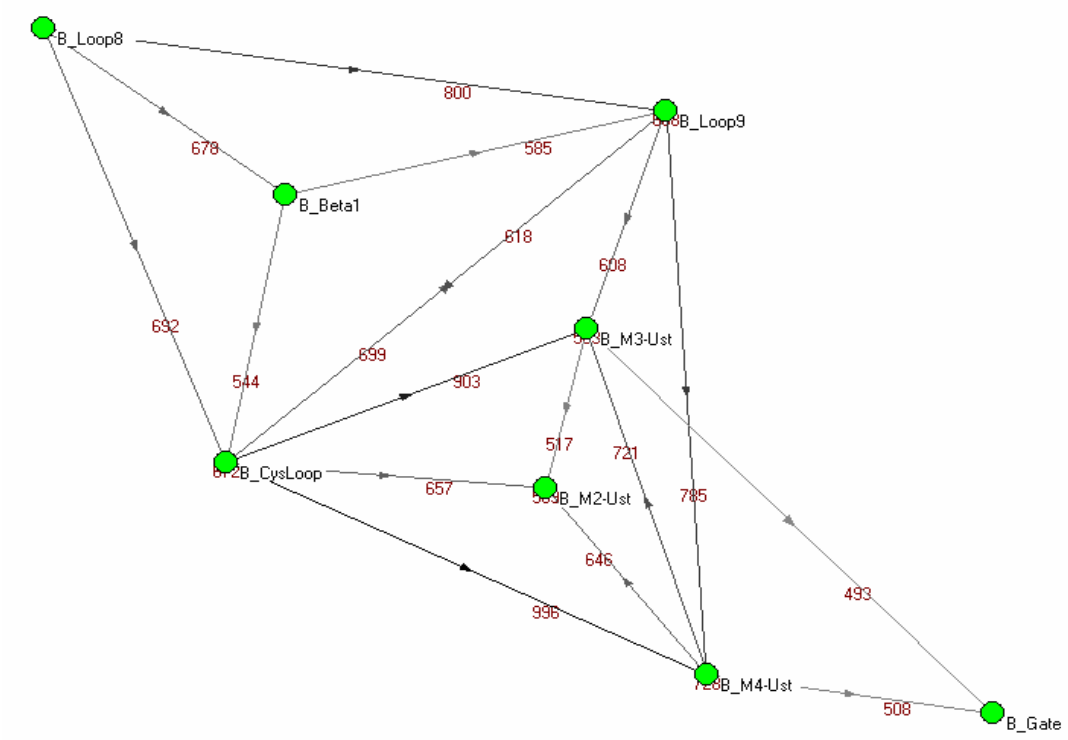

Figure B.43. Graphic representation of the most used and shortest paths which start from the Loop B of Beta subunit of nAChR and go to the Gate of the same subunit

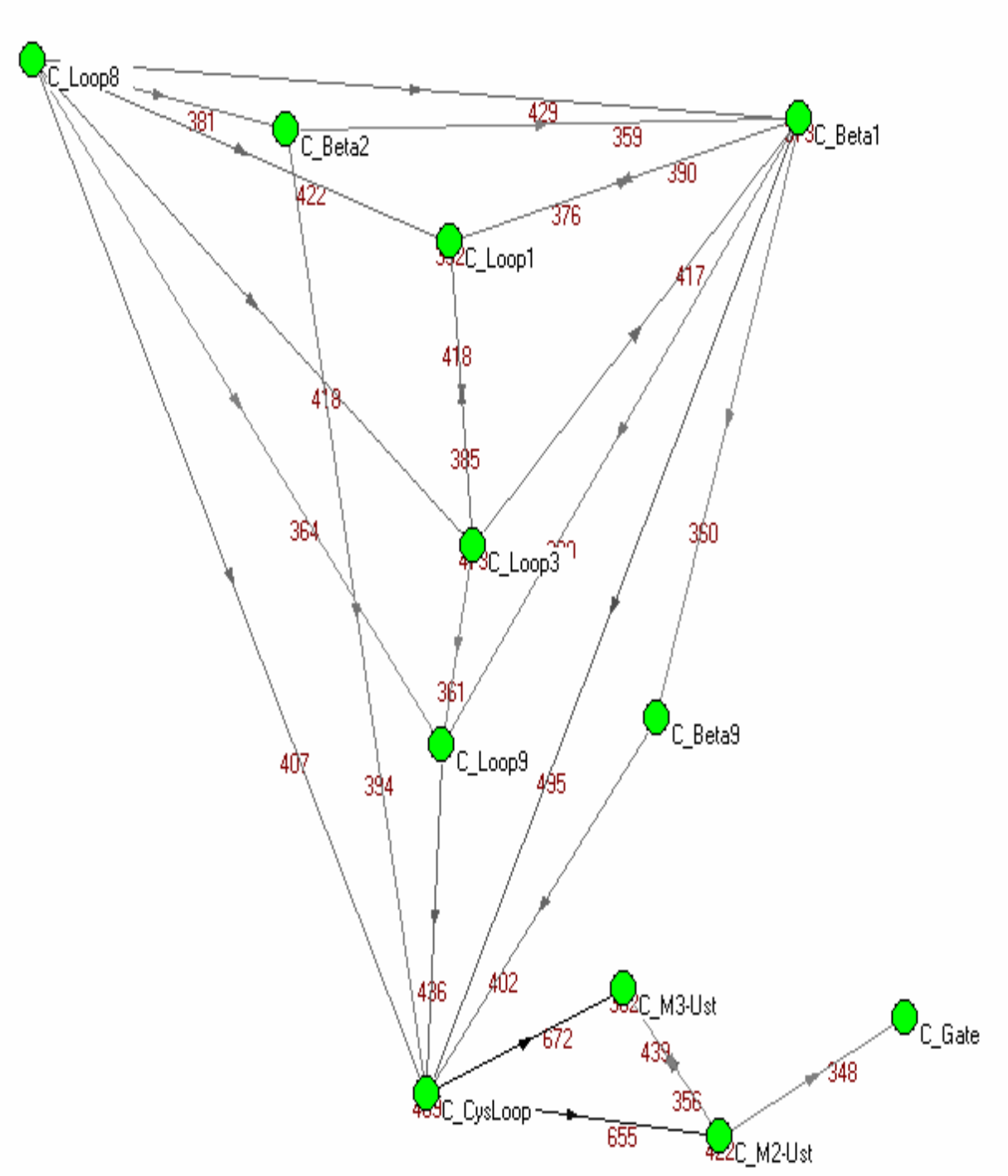

Figure B.44. Graphic representation of the most used and shortest paths which start from the Loop B of Delta subunit of nAChR and go to the Gate of the same subunit

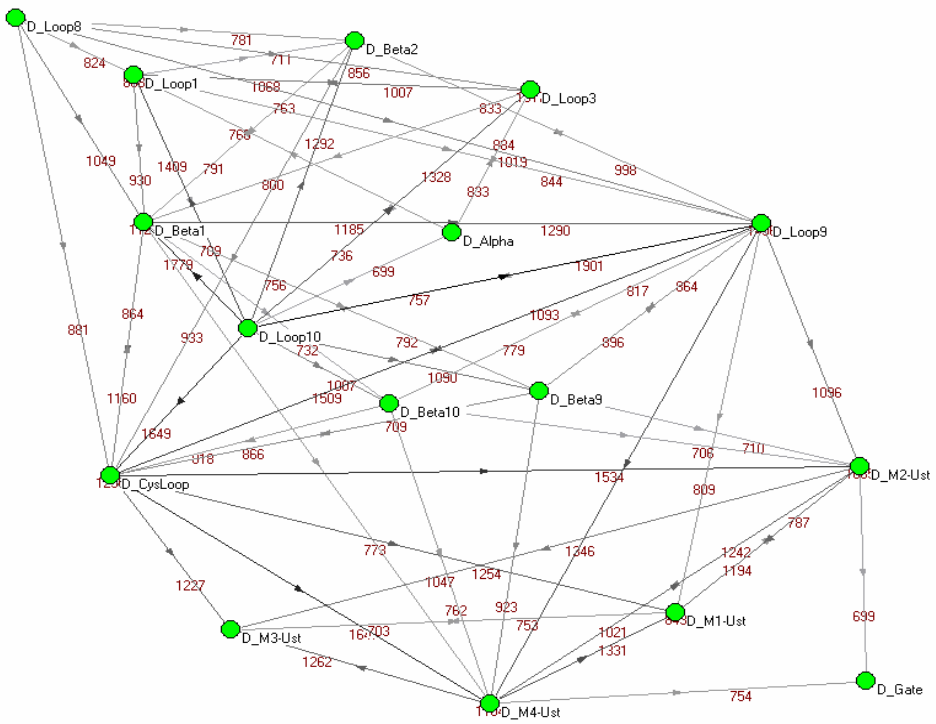

Figure B.45. Graphic representation of the most used and shortest paths which start from the Loop B of Alpha-Delta subunit of nAChR and go to the Gate of the same subunit

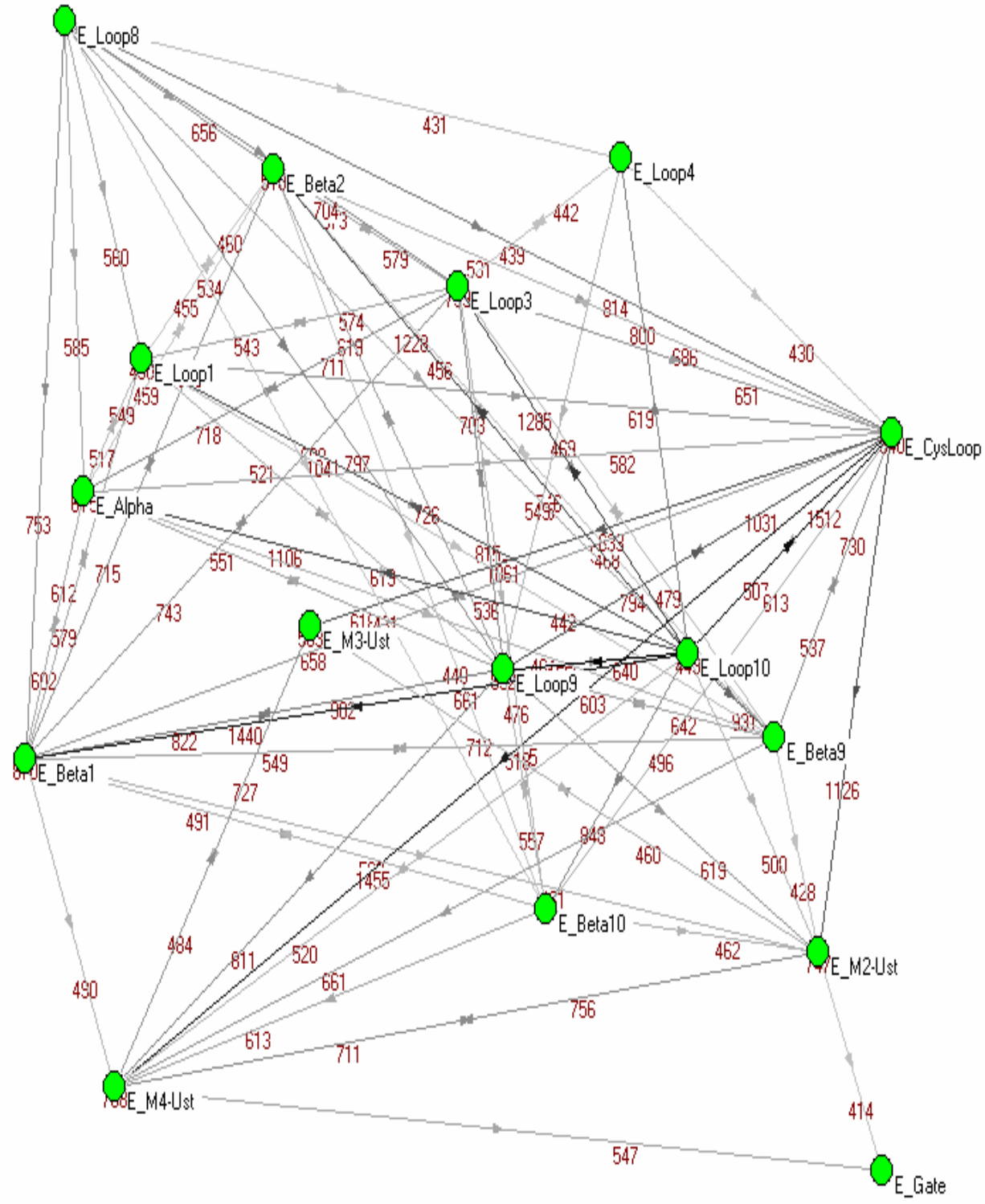

Figure B.46. Graphic representation of the most used and shortest paths which start from the Loop B of Gamma subunit of nAChR and go to the Gate of the same subunit.

5. REFERENCES

1. Barrantes, F. J., "Modulation of nicotinic acetylcholine receptor function through the outer and middle rings of transmembrane domain", Curr Opin Drug Discov Devel., Vol. 6, No. 5, pp. 620-632, September 2003.

2. Schapira, M., R. Abagyan and M. Totrov, "Structural model of nicotinic acetylcholine receptor is isotypes bound to acetylcholine and nicotine", BMC Structural Biology, Vol. 2, 2002.

3. Unwin, N., A. Miyazawa, J. Li and Y. Fujiyoshi, "Activation of the Nicotinic Acetylcholine Receptor Involves a Switch in Conformation of the Alpha Subunits", JMB, Vol. 319, pp. 1165-1176, 2002.

4. Karlin, A., "Emerging structure of the nicotinic acetylcholine receptors", Nat Rev Neurosci., Vol. 3, No. 2, pp. 102-114, February 2002.

5. Lester, H. A., M. I. Dibas, D. S. Dahan, J. F. Leite and D. A. Dougherty, "Cys-loop receptors: new twists and turns", Trends in Neurosciences, Vol. 27, pp. 329-336, 2004.

6. Barrantes, F. J., "Structural studies of the acetylcholine receptor in the transmembrane environment", Current Science, Vol. 81, pp. 983-991, 2001.

7. Unwin, N., "Refined Structure of the Nicotinic Acetylcholine Receptor at 4 A Resolution", J. Mol. Biol., Vol. 346, pp. 967-989, March 2005.

8. Brejc, K., W. J. V. Dijk, R. V. Klaassen, M. Schuurmans, J. V. D. Oost, A. B. Smitt and T. K. Sixma,"Crystal structure of an Ach-binding protein reveals the ligand-binding domain of nicotinic receptors", Nature, Vol. 411, pp. 269-276, 2001.

9. Miyazawa, A., Y. Fujiyoshi and N. Unwin, "Structure and Gating Mechanism of the Acetylcholine Receptor Pore", Nature, Vol. 423, pp. 949-955, June 2003.

10. Bouzat, C., F. Gumilar, G. Spitsmaul, H. L. Wang, D. Reyes, S. B. Hansen, P. Taylor and S. M. Sine, "Coupling of agonist binding to channel gating in an Ach-binding protein linked to an ion channel", Nature, Vol. 430, pp. 896-900, 2004.

11. De Planque, M. R. R., D. T. S. Rijkers, J. I. Fletcher, R. M. J. Liskamp and F. Separovic, "The alphaM1 segment of the nicotinic acetylcholine receptor exhibits conformational flexibility in a membrane environment", BBA, Vol. 1665, pp. 40-47, October 2004.

12. De Almeida, R. F. M., L. M. S. Loura, M. Prieto, A. Watts, A. Fedorov and F. J. Barrantes, "Cholesterol Modulates the Organization of the alphaM4 Transmembrane Domain of the Muscle Nicotinic Acetylcholine Receptor", Biophysical Journal, Vol. 86, pp. 2261-2272, 2004.

13. Unwin, N., "Structure and action of the nicotinic acetylcholine receptor explored by electron microscopy", FEBS Letters, Vol. 555, pp. 91-95, August 2003.

14. Cheng, X., B. Lu, B. Grant, R. J. Law and J. A. McCammon, "Channel Opening Motion of alpha7 Nicotinic Acetylcholine Receptor as Suggested by Normal Mode Analysis", J. Mol. Biol., Vol. 355, pp. 310-324, January 2006.

15. Martin, A. C., J. L. Mercado, L. V. Rojas, M. G. McNamee and J. A. Lasalde-Dominicci, "Trytophan Substitutions at Lipid-exposed Positions of the Gamma M3 Transmembrane Domain Increase the Macroscopic Ionic Current Response of the Torpedo californica Nicotinic Acetylcholine Receptor", The Journal of Membrane Biology, Vol. 183, pp. 61-70, 2001.

16. Quiram, P. A., K. Ohno, M. Milone, M. C. Patterson, N. J. Pruitt, J. M. Brengman, S. M. Sine and A. G. Engel, "Mutation causing congenital myasthenia reveals acetylcholine receptor beta/delta subunit interaction essential for assembly", The Journal of Clinical Investigation, Vol. 104, pp. 1403-1410, 1999.

17. Salamone, F. and M. Zhou, "Aberrations in Nicotinic Acetylcholine Receptor Structure, Function, and Expression", McGill Journal of Medicine, Vol. 5, pp. 90-97, 2000.

18. Blanton, M. P. and J. B. Cohen, “Identifying the lipid-protein interface of the Torpedo nicotinic acetylcholine receptor: secondary structure implications.”, Biochemistry, Vol. 10, pp. 2859-2872, 1994.

19. De Rosa, M. J., D. Rayes, G. Spitzmaul and C. Bouzat, “Nicotinic receptor M3 transmembrane domain: Position 8' contributes to channel gating”, Molecular Pharmacology, Vol. 62, No. 2, pp. 406-414, August 2002.

20. Bouzat, C., F. Barrantes and S. Sine, “Nicotinic Receptor Fourth Transmembrane Domain Hydrogen Bonding by Conserved Threonine Contributes to Channel Gating Kinetics”, The Journel of General Physiology (JGP), Vol. 115, pp. 663-671, 2000.

21. Williamson, P. T. F., B. H. Meier and A. Watts, “Structural and functional studies of the Nicotinic acetylcholine receptor by solid-state NMR”, Eur Biophys J., Vol. 33, pp. 247-254, 2004.

22. Senes, A., B. I. Ubarretxena and D. M. Engelman , “The Calpha ---H…O hydrogen bond: a determinant of stability and specifity in transmembrane helix interactions.”, Proc Natl Acad Sci U S A., Vol. 98, No. 16, pp. 9056-9061, July 2001.

23. Auchbach, A. L., T. D. Bailey and A. Mitra, “Structural Dynamics of the M4 Transmembrane Segment during Acetylcholine Receptor Gating”, Structure, Vol. 12, pp. 1909-1918, 2004.

24. Tamamizu, S., G. R. Guzman, J. Santiago, L. V. Rojas, M. G. McNamee and J. A. L. Dominicci, “Functional Effects of Periodic Tryptophan Substitutions in the alpha M4 Transmembrane Domain of the Torpedo californica Nicotinic Acetylcholine Receptor”, Biochemistry, Vol. 39, pp. 4666-4673, April 2000.

25. Kash, T. L., A. Jenkins, J. C. Kelley, J. R. Trudell and N. L. Harrison, “Coupling of agonist binding to channel gating in the GABAA receptor”, Nature, Vol. 421, pp. 272-275, January 2003.

26. Castillo, M., J. Mulet, J. A. Bernal, M. Criado, F. Sala and S. Sala, "Improved gating of a chimeric alpha7-5HT3A receptor upon mutations at the M2-M3 extracellular loop", FEBS Letters, Vol. 580, pp. 256-260, January 2006.

27. Lee, W. Y. and S. M. Sine, "Principle pathway coupling agonist binding to channel gating in nicotinic receptors", Nature, Vol. 438, pp. 243-247, 2005.

28. Taly, A., M. Delarue, T. Grutter, M. Nilges, N. Le Novere and P. J.Corringer, "Normal Mode Analysis Suggests a Quaternary Twist Model for the Nicotinic Receptor Gating Mechanism", Biophysical Journal, Vol. 88, pp. 3954-3965, June 2005.

29. Xu, Y., F. J. Barrantes, X. Luo, K. Chen, J. Shen and H. Jiang, "Conformational Dynamics of the Nicotinic Acetylcholine Receptor Channel: A 35-ns Molecular Dynamics Simulation Study", JACS, Vol. 127, pp. 1291-1299, January 2005.

30. Hung, A., K. Tai and M. S. P. Sansom, "Molecular Dynamics Simulation of the M2 helices within the Nicotinic Acetylcholine Receptor Transmembrane Domain: Structure and Collective Motions", Biophysical Journal, Vol. 88, No. 5, pp. 3321-3333, May 2005.

31. Law, R. J., R. H. Henchman and J. A. McCammon, "A gating mechanism proposed from a simulation of a human alpha7 nicotinic acetylcholine recepotr", PNAS, Vol. 102 No. 19, pp. 6813-6818, May 2005.

32. Bahar I. "Dynamics of Proteins and Biomolecular Complexes: Inferring Functional Motions From Structure", Reviews in Chemical Engineering, Vol. 15,No. 4, pp. 319-347, 1999.

33. Katz, B. "Nerve, Muscle and Synapse", McGraw Hill, New York, 1966.

34. Bahar, I., A. R. Atilgan, S. R. Durell, R. L. Jernigan, M. C. Demirel and O. Keskin, "Anisotropy of Fluctuation Dynamics of Proteins with and Elastic Network Model", Biophysical Journal, Vol. 80, pp. 505-515, 2001.

35. Smart, O. S., J. M. Goodfellow and B. A. Wallace, “The Pore Dimensions of Gramicidin A”, Biophysical Journal, Vol. 65, pp. 2455-2460, 1993.

36. Landau, M., I. Mayrose, Y. Rosenberg, F. Glaser, E. Martz, T. Pupko and N. Ben-Tal, “ConSurf: identification of functional regions in proteins by surface-mapping of phylogenetic information.”, Bioinformatics, Vol. 19, pp. 163-164, 2003.

37. Landau, M., I. Mayrose, Y. Rosenberg, F. Glaser, E. Martz, T. Pupko and N. Ben-Tal, “ConSurf 2005: the projection of evolutionary conservation scores of residues on protein structures”, Nucleic Acids Research, Vol. 33W, pp. 299-302, 2005.

38. Kass, I. and A. Horovitz, “Mapping Pathways of Allosteric Communication in GroEL by Analysis of Correlated Mutations”, Proteins: Structure, Function, and Gentics, Vol. 48, pp. 611-617, April 2002.

39. Karadağ, S., "Gating mechanism in nicotinic acetylcholine receptor channel", Boğaziçi University, MS Thesis, 2006.

40. Batagelj, V. and A. Mrvar, “Pajek - Program for Large Network Analysis”, Connections, Vol. 21, No. 2, pp. 47-57, 1998.

41. Bahar, I., A .R. Atılgan, M. C. Demirel and B. Erman, “Vibrational dynamics of folded proteins: significance of slow and fast motions in relation to function and stability”, Physical Review Letters, Vol. 80, No. 10, pp. 2733-2736, 1998.

42. Bahar I. “Dynamics of Proteins and Biomolecular Complexes: Inferring Functional Motions From Structure”, Reviews in Chemical Engineering, Vol. 15,No. 4, pp. 319-347, 1999

43. Humphrey, W., A. Dalke and K. Schulten, “VMD - Visual Molecular Dynamics”, J. Molec. Graphics, Vol. 14, pp. 33-38, 1996.

44. Chenna, R., H. Sugawara, T. Koike, R. Lopez, T. J. Gibson, D. G. Higgins and J. D. Thompson, “Multiple sequence alignment with the Clustal series of programs”, Nucleic Acids Research, Vol. 31, No. 13, pp. 3497-3500, 2003.

45. Gasteiger, E., A. Gattiker, C. Hoogland, I. Ivanyi, R. D. Appel and A. Bairoch, "ExPASy: the proteomics server for in-depth protein knowledge and analysis", Nucleic Acids Research, Vol. 31, No. 13, pp. 3784-3788, 2003.

46. Pazos, F., M. H. Citterich, G. Ausiello and A. Valencia, "Correlated Mutations Contain Information About Protein-protein Interactions", J. Mol. Biol., Vol. 271, pp. 511-523, August 1997.

47. Jimenez, R. P., R. G. Ruiz, A. P. Morreale, B. I. Molero and J. M. S. Ruiz, "A simple tool to explore the distance distribution of correlated mutations in proteins", Biophysical Chemistry, Vol. 119, pp. 240-246, 2005.

48. Giraudat J., C. Montecucco, R. Bisson and J. P. Changeux, "Transmembrane topology of acetylcholine receptor subunits probed with photoreactive phospholips.", Biochemistry, Vol. 24, No. 13, pp. 3121-3127, 1985.